

**Dissertation zur Erlangung des Doktorgrades
der Fakultät für Chemie und Pharmazie
der Ludwig-Maximilians-Universität München**

***Arabidopsis* small molecule glucosyltransferase UGT76B1
conjugates both ILA and SA and is essential for the root-
driven control of defense marker genes in leaves**

Rafał Paweł Maksym

aus

Gorzów Wielkopolski, Polen

2017

Erklärung

Diese Dissertation wurde im Sinne von § 7 der Promotionsordnung vom
von Herrn PD Dr. Anton R. Schäffner betreut.

Eidesstattliche Versicherung

Diese Dissertation wurde eigenständig und ohne unerlaubte Hilfe erarbeitet.

München, 30.10.2017

.....
(Rafał Paweł Maksym)

Dissertation eingereicht am 30.10.2017

1. Gutachter: PD Dr. Anton Rudolf Schäffner

2. Gutachter: Prof. Dr. Jörg Durner

Mündliche Prüfung am 22.03.2018

ABSTRACT

Plants as sessile organisms evolved different, sophisticated mechanisms to defend themselves against plethora of environmental stress factors. Pathogen defense is regulated by the mostly antagonistic salicylic acid (SA)- and jasmonic acid (JA)-mediated signaling pathways. The small molecule glucosyltransferase UGT76B1 was identified as a regulator of SA-JA crosstalk, positively stimulating SA-dependent defense, whereas suppressing JA pathway. UGT76B1 is able to glucosylate SA and a new signaling molecule, isoleucic acid (ILA). Thus, SA glucosylation could be catalyzed by UGT76B1 in addition to the previously identified SA glucosyltransferases UGT74F1 and UGT74F2.

Therefore, lines with impaired expression of *UGT74F1*, *UGT74F2* and *UGT76B1* were applied to study whether UGT76B1 can be integrated in the homeostasis of SA and its conjugates. SA glucosides were not reduced in single *ugt76b1* mutants in three different accessions Col-0, *Ler* and Ws-4 as it was previously shown for the Ws-4-based mutant *ugt74f1 amiugt74f2*. In the Ws-4 background, the introgression of *ugt76b1-3* into *ugt74f1 amiugt74f2* led to a strong repression of SA glucoside levels indicating that all three enzymes are involved in SA glucosylation. The root growth inhibition by exogenously added SA was employed as another assay to study the involvement of UGTs in SA glucosylation, since this reaction can be regarded as an inactivation of the inhibitor. *ugt74f1-1*, *ugt74f2-1* and *ugt74f1 amiugt74f2* were not differently affected than wild type, whereas *ugt76b1* single mutants demonstrated stronger root growth inhibition than wild type. The latter was strongly enhanced by the introgression of *ugt74f1 amiugt74f2*. Thus, UGT76B1 might have a specific role in SA conjugation in roots, although again there is an interaction with the two other glucosyltransferases.

ILA is known to stimulate SA-mediated defense and the abundance of ILA conjugate is positively related with UGT76B1 expression. However, the endogenous abundance of ILA aglycon has never been determined and monitored in response to environmental stresses. An optimized GC-MS based method demonstrated that ILA was dependent on *UGT76B1* expression level in contrast to its chemically closely related compound LA (leucic acid). Both compounds showed also a different accumulation during the infection with *Pseudomonas syringae* and during the growth and development, suggesting their distinct role in plants.

Exogenously applied ILA was shown to inhibit root growth in a concentration-dependent manner. Nevertheless, the mechanism behind this process is still not known. Therefore, two

different screening approaches involving root growth response of T-DNA insertion lines and *A. thaliana* accessions were used in this project. The analysis of 159 *Arabidopsis* accessions revealed a region on the chromosome 1 as being weakly associated with root growth response to ILA. Further sequence analysis suggested that polymorphisms in *SRX* gene that is involved in regulation of intracellular ROS levels may cause ILA hypersensitivity. The role of ROS in ILA-mediated root growth inhibition was also supported by one T-DNA insertion line. Furthermore, the study on T-DNA insertion lines suggested that the ABC transporter PDR3/ABCG31 is involved in ILA export.

To assess whether the relatively high expression of *UGT76B1* in root has an impact on shoot defense status, reciprocal grafting experiments of *ugt76b1* and Col-0 were employed. This approach clearly demonstrated that UGT76B1 is essential for a root-driven control of SA-dependent defense marker genes in leaves.

CONTENTS

ABSTRACT	I
ABBREVIATIONS	VII
1. INTRODUCTION	1
1.1. Plant defense response to pathogens	1
1.1.1. SA-mediated pathway in plant defense response	2
1.1.1.1. Regulation of cytosolic SA levels	5
1.1.1.2. Regulation of SA-mediated defense by elicitors	7
1.1.2. JA/ET-mediated pathway in plant defense response	7
1.1.3. Antagonistic interaction between SA- and JA/ET-mediated pathways	9
1.2. Plant UDP-glycosyltransferases (UGTs)	10
1.2.1. Reactions catalyzed by UGTs	11
1.2.2. Plant glucosyltransferases and stress response	12
1.2.2.1. UGT76B1 impacts SA- and JA-mediated defenses	12
1.2.2.2. <i>Arabidopsis thaliana</i> UGTs involved in SA conjugation	13
1.3. Aim of this work	15
2. RESULTS	16
2.1 Salicylic acid as an <i>in vivo</i> substrate of UGT76B1	16
2.1.1. <i>ugt76b1</i> knock-out mutants show different abundance of free and conjugated salicylic acid	16
2.1.2. Triple mutant of <i>ugt74f1 amiugt74f2 ugt76b1</i> provides the evidence that UGT76B1 participates in SA conjugation.	17
2.1.3. <i>ugt74f1</i> , <i>ugt74f2</i> and <i>ugt76b1</i> mutants root growth inhibition in presence of salicylic acid	19
2.1.4. Do <i>UGT74F1</i> , <i>UGT74F2</i> and <i>UGT76B1</i> compensate each other for SA glucosylation?	23
2.1.5. Is <i>UG74F1</i> -CDS driven by <i>UGT76B1</i> regulatory regions able to complement <i>ugt76b1-1</i> phenotype?	27
2.1.6. Analysis of sequence divergences between Col-0, Ws-4 and <i>Ler</i> in UGT76B1 region	29
2.2. ILA as an <i>in vivo</i> substrate of UGT76B1	32
2.2.1. Simultaneous quantification of isoleucic, leucic and valic acid	32
2.2.1.1 Detection of isoleucic acid, leucic acid and valic acid in plant extracts	32
2.2.2. UGT76B1 recombinant protein glucosylates ILA and LA <i>in vitro</i>	36
2.2.3. ILA as an <i>in vivo</i> substrate of UGT76B1	36
2.2.3.1. <i>UGT76B1</i> expression negatively affects ILA abundance in the above- and below-ground tissues	37
2.2.3.2. Isoleucic and leucic acid abundance is affected during the plant growth and development	37
2.2.4. ILA and LA are differently affected by the biotrophic pathogen <i>P. syringae</i>	39
2.2.5. ILA as a ubiquitous compound in plants	40

2.3. Genetic screen for identification of genes involved in 2-hydroxy-3-methyl-pentanoic (ILA) acid sensitivity	42
2.3.1 Genome-wide association study for genes affected by exogenous ILA	42
2.3.1.1. Spatial expression pattern of GWAS associated genes	46
2.3.1.2. Correlation of single nucleotide polymorphism with ILA root growth response	47
2.3.1.3. The physiological function of genes located in the SRX region	48
2.3.2. T-DNA insertion mutants screen for ILA resistant lines	49
2.3.2.1. Mutant lines showing reduced root growth sensitivity in the presence of ILA	50
2.3.2.3. Spatial expression of genes, whose mutants show increased ILA resistance	56
2.3.2.4. The response of ILA resistant mutants to exogenously applied plant hormones	57
2.3.2.4.1. Root growth response of ILA-resistant mutants to salicylic acid	59
2.3.2.4.2. Root growth response of ILA-resistant mutants to jasmonic acid	61
2.3.2.4.3. Root growth response of ILA-resistant mutants to auxin	61
2.3.2.4.4. Common pattern of ILA-resistant mutants displaying wild-type response to exogenously applied hormones	62
2.3.2.4.5. Common pattern of ILA-resistant lines displaying a different response to exogenously applied hormones than wild-type	64
2.3.2.5. SALK_014957 (<i>PDR3</i>) shows the lowest root growth inhibition in presence of ILA	66
2.3.2.5.1. Known functions of <i>PLEIOTROPHIC DRUG RESISTANCE (PDR3)</i>	66
2.3.3. T-DNA mutant lines displaying hypersensitive response to ILA	69
2.4. Is the high expression of <i>UGT76B1</i> in root pivotal for its effect in aboveground organs?	69
3. DISCUSSION	73
3.1 Is SA an in vivo substrate of <i>UGT76B1</i>?	73
3.1.1. Glucosyltransferases contributing to SA conjugation in <i>A. thaliana</i>	73
3.1.2. SA and its conjugates are distinctly accumulated in Col-0, Ler and Ws-4 wild-type plants	77
3.2. The role of ILA and its impact on <i>A. thaliana</i> root growth	80
3.2.1. ILA as an <i>in vivo</i> substrate of <i>UGT76B1</i>	80
3.2.2. ILA and LA are differently involved in plant defense to <i>P. syringae</i>	81
3.2.3. Possible scenarios for ILA action in the <i>A. thaliana</i> roots	83
3.2.3.1. ROS is potentially involved in ILA dependent root growth inhibition	83
3.2.3.2. <i>PDR3</i> is potentially involved in ILA transport	86
3.2.3.3. Potential perspectives for evaluating the impact of ILA on <i>A. thaliana</i> roots	87
3.3. Root expression of <i>UGT76B1</i> modulates <i>PR1</i>, <i>PR2</i>, <i>PR5</i> transcripts abundance in the shoot	90
4. MATERIALS AND METHODS	97
4.1. Materials	97

4.1.1. Chemicals	97
4.1.2. Media	97
4.1.3. Bacterial strains	97
4.1.4. Vectors	98
4.1.5. Antibiotics	98
4.1.6. Primers	98
4.1.6.1. Primers used for genotyping of SALK T-DNA insertion lines	98
4.1.6.2. Primers used for RT-qPCR	100
4.1.6.3. Primers used for UGT76B1 - UGT74F1 hybrid construct	101
4.1.6.3.1. Primers used for production of UGT76B1 - UGT74F1 hybrid construct	101
4.1.6.3.2. Primers used for verification of UGT76B1 - UGT74F1 hybrid construct	101
4.1.6.3. Primers used for amplifying and sequencing of <i>UGT76B1</i> regulatory regions to compare Col-0, <i>Ler</i> and Ws-4 ecotypes	101
4.1.7. Plant material	102
4.2. Methods	103
4.2.1. Plant growth conditions	103
4.2.2. Seedlings grown on solid medium	104
4.2.2.1. Growth conditions applied for T-DNA insertion lines screen for ILA insensitivity	104
4.2.2.2. Growth conditions applied for <i>Arabidopsis</i> accessions screen	105
4.2.3. Treatment with a chemical SA analogue BTH	105
4.2.4. <i>Arabidopsis</i> infection with <i>P. syringae</i>	105
4.2.5. Preparation of reciprocal graftings of <i>ugt76b1</i> and Col-0	106
4.2.6. Generation of hybrid construct composed of <i>UG74F1</i> -CDS and <i>UGT76B1</i> regulatory regions for complementation of <i>ugt76b1-1</i> loss-of-function mutant	107
4.2.6.1. Heat shock transformation of <i>E. coli</i>	108
4.2.6.2. Electroporation of competent <i>Agrobacterium tumefaciens</i> cells	109
4.2.6.3. Plant transformation with <i>Agrobacterium tumefaciens</i>	109
4.2.6.4. Selection of the homozygous lines	109
4.2.7. Genotyping of SALK T-DNA insertion lines	110
4.2.8. Preparation of plant genomic DNA	110
4.2.8.1. CTAB DNA Miniprep	110
4.2.9. Separation nucleic acid by agarose gel	111
4.2.10. Extraction of PCR products from agarose gel	111
4.2.11. Plasmid extraction	111
4.2.12. Total RNA isolation	111
4.2.13. Reverse Transcription Polymerase Chain Reaction (RT-PCR)	112
4.2.14. Quantitative real time polymerase chain reaction (RT-qPCR)	112
4.2.15. DNA sequencing	113
4.2.16. Determination of SA and SA glucose conjugates	113
4.2.17. GC-MS based method for VA, LA and ILA determination in the plant tissues	113
4.2.18. <i>In vitro</i> analysis of the activity of UGT6B1 towards ILA and LA	115

4.2.19. Bioinformatics analyses	116
5. REFERENCES	117
6. SUPPLEMENTARY DATA	139
6.1. Supplementary figures	139
6.2. Supplementary tables	154
CURRICULUM VITAE	157
ACKNOWLEDGEMENTS	159

ABBREVIATIONS

μ M	Micromole
BCAA	Branched Chain Amino Acid
BSTFA	N,O-Bis(trimethylsilyl)trifluoroacetamide
BTH	Benzothiadiazole
cDNA	complementary DNA
DNA	Deoxyribonucleic Acid
dNTPs	Deoxynucleotide-5'-triphosphates
DW	Dry weight
ET	Ethylene
ETI	Effector-Triggered Immunity
ETS	Effector Triggered Susceptibility
FW	Fresh weight
g	Gram
GWAS	Genome-wide association study
HR	hypersensitive response
IAA	Indole-3-acetic acid (auxin)
ILA	Isoleucic acid
JA	Jasmonic acid
LA	Leucic acid
MeJA	Methyl jasmonate
MeSA	Methyl salicylate
MeSAG	Methylsalicylate <i>O</i> - β -glucoside
min	minute
MS	Murashige and Skoog
ng	nanogram
OE	overexpression
PAMP	Pathogen-Associated Molecular Pattern
PCR	Polymerase chain reaction
PRR	Pattern-Recognition Receptors
PTI	PAMP-Triggered Immunity
ROS	Reactive Oxygen Species
rpm	revolutions per minute

ABBREVIATIONS

RT-PCR	Reverse Transcription-PCR
RT-qPCR	Real-time quantitative PCR
SA	Salicylic acid
SAG	SA <i>O</i> - β -glucoside
SAGT	SA glucosyltransferases
SGE	SA glucose ester
T-DNA	Transfer-DNA
UGT	UDP-glycosyltransferase
VA	Valic acid

1. INTRODUCTION

1.1. Plant defense response to pathogens

Plants during all growth and developmental stages are exposed to a vast number of harmful pathogens and pests such as viruses, bacteria, fungi, nematodes or insect herbivores. Plant pathogens are generally divided into necrotrophs and biotrophs. Necrotrophs first destroy the host cells frequently using phytotoxins for this purpose and then derive nutrients from the dead plant tissues. The other group of pathogens named as biotrophs feed on the living host tissues; fungi frequently use specialized feeding structures such as haustoria, which enable to penetrate plant cells without disrupting them (Dangl and Jones, 2001; Pieterse *et al.*, 2009). Biotrophic pathogens can be further divided virulent and avirulent strains. Avirulent pathogens carry a single dominant avirulence gene, which enables the host to recognize the attacker and initiate ETI-mediated responses (see also below). Therefore, the type of the response when the host shows the resistance towards the pathogen is called incompatible plant-pathogen interaction. The virulent pathogen causes a compatible plant-pathogen interaction (Glazebrook, 2005).

Plants, unlike mammals lack the mobile defense cells and adaptive immune system. Instead they evolved an array of different defense mechanisms, relying on the innate immunity of each cell and on systemic signals from infection site. Plant defense response against pathogens is facilitated by a two-branched innate immune system. The first line is based on the recognition of the conserved microbial determinants, called pathogen-associated molecular patterns (PAMPs) *via* pattern-recognition receptors (PRRs), which subsequently initiate PAMP-triggered immunity (PTI) (Jones and Dangl, 2006; Pieterse *et al.*, 2009). All known PRRs are surface localized and are either receptor-like kinases or receptor-like proteins (Macho and Zipfel, 2014). In *Arabidopsis thaliana* PRRs such as FLS2, EFR, Lym1 and Lym3, CeBip and CERK1 are capable of detecting flg22, elongation factor TU, peptidoglycan and chitin, respectively (Gomez-Gomez, Bauer and Boller, 2001; Kunze *et al.*, 2004; Miya *et al.*, 2007; Willmann *et al.*, 2011). In order to overcome the PTI-mediated plant immunity, pathogens acquired during the evolution virulence effectors that are directly secreted into the host cell to suppress PTI, causing effector triggered susceptibility (ETS). In turn, plants established the secondary immune response called effector-triggered immunity (ETI), which acts largely inside the cell and is based on the recognition of the virulence effectors by specific receptor (R) proteins (Jones and Dangl, 2006). Recognition of the

effector through the ETI is very effective due to the SA- and reactive oxygen species (ROS)-mediated hypersensitive (HR) cell death at the infection side, which prohibits the spread of the biotrophic pathogens. PTI- and ETI-mediated defenses demonstrate a substantial response overlap. The common set of the responses include alterations in the plant cell wall by lignin synthesis, production of antimicrobial secondary metabolites and accumulation of pathogenesis-related (PR) proteins (Pieterse *et al.*, 2009). The need to fine-tune defense response relevant for the attacker requires a plethora of downstream responses to PTI and ETI, which are tightly regulated by the signaling pathways depending on the attacker life style. Two antagonistic hormonal pathways play the key role in this process and are responsible for regulation of the defense genes expression. Therefore, depending on the type of pathogen plants can activate separate defense pathways. Salicylic acid (SA) pathway mediates the response against biotrophic pathogens, whereas jasmonic acid/ethylene (JA/ET) pathway is involved in the responses to necrotrophic pathogens and chewing insects. Both pathways are essential for modulating plant defense response to different environmental stresses (Dodds and Rathjen, 2010; Thakur and Sohal, 2013; Bektas and Eulgem, 2015).

1.1.1. SA-mediated pathway in plant defense response

Salicylic acid (2-hydroxy benzoic acid) belongs to the group of phenolic compounds and plays a pivotal role in plant defense response to biotrophic pathogens. This was shown by a number of studies demonstrating that plants deficient in SA signaling display enhanced susceptibility to biotrophs (Van Wees and Glazebrook, 2003).

There are two SA synthesis pathways; namely ISOCHORISMATE SYNTHASE 1 (ICS1), known also as SALICYLIC ACID INDUCTION DEFICIENT 2 (SID2) and PHENYLALANINE AMMONIA LYASE (PAL) (Fig. 1). Both pathways utilize chorismate, the end product of the shikimate pathway as SA precursor (Garcion *et al.*, 2008). ICS1 pathway is presumed to be highly important for stress-induced SA biosynthesis, which was proven for *ics1* mutant that accumulated 5% - 10% of wild-type SA levels upon the infection or UV stress (Nawrath and Métraux, 1999; Dewdney *et al.*, 2000; Wildermuth *et al.*, 2001). The biosynthesis of SA is initiated during PTI and ETI upon detection of PAMPs or pathogen effectors, respectively (Mishina, 2007). Subsequently, the lipase-like protein ENHANCED DISEASE SUSCEPTIBILITY 1 (EDS1) together with PHYTOALEXIN DEFICIENT 4 (PAD4) act upstream SA biosynthesis during PTI and ETI. Both components are known to be essential for activation and amplification SA-mediated defense response (Glazebrook, 2005).

Moreover, Ca^{2+} and calmodulin are also known as the regulators acting upstream SA. Both components are capable of promoting SA synthesis and SA-mediated defense, but also prevent over-accumulation of SA, which could have deleterious effects in unstressed conditions (Du *et al.*, 2009; Cheval *et al.*, 2013; Zhang *et al.*, 2014). Several transcription factors have also been reported to positively regulate *ICS1* expression (Dempsey and Klessig, 2017). This includes CALMODULIN-BINDING PROTEIN 60g (CBP60g) and its homolog SAR DEFICIENT 1 (SARD1) (Zhang *et al.*, 2010; Wang *et al.*, 2011), WRKY28 (Verk, Bol and Linthorst, 2011), teosinte branched 1/cycloidea/PCF 8 and 9 (TCP8, TCP9) (Wang *et al.*, 2015), NTM-like 9 (NTL9) (Zheng *et al.*, 2015) and TCP21 (Lopez *et al.*, 2015).

Signaling downstream SA predominantly depends on NONEXPRESSOR OF PR GENES1 (NPR1). NPR1 is known as a master regulator of SA pathway responsible for activating a large set of defense genes in response to SA (Fu and Dong, 2013). NPR1 is located in the cytoplasm of the unchallenged cells in form of the oligomeric complex, stabilized through disulfide bonds between conserved cysteines. Stress triggered SA produced upon the infection triggers the cellular redox changes and elicits the reduction of the cysteine, which results in the release of monomeric NPR1. On the other hand, functional regulation of NPR1 is also mediated by the direct binding of SA. During the last years number of SA interacting proteins was identified. However, none of them fulfilled the criteria for SA immune signal receptor (Seyfferth and Tsuda, 2014). Only NPR1 together and its paralogs NPR3 and NPR4 were proven to function as SA receptors (Fu *et al.*, 2012; Wu *et al.*, 2012; Kaldorf and Naseem, 2013). The interactions of NPR3 and NPR4 with NPR1 are directly regulated by SA (Fu *et al.*, 2012), however NPR1 can also bind SA independently from its paralogs (Wu *et al.*, 2012). Upon SA monomers of NPR1 are translocated to the nucleus where *via* interaction with TGA transcription factors facilitate the expression of *PATHOGENESIS-RELATED (PR)* genes, such as *PR1*, *PR2*, *PR5* (Dong, 2004; Pajerowska-Mukhtar *et al.*, 2013). All three *PR* genes are known as the SA pathway marker genes. The antimicrobial function of *PR1*, in contrast to *PR2* and *PR5* is still not fully elucidated (van Loon *et al.*, 2006; Oide *et al.*, 2013; Liu *et al.*, 2016). However, SA signaling can also function in an NPR1-independent manner (Kachroo *et al.*, 2001; An and Mou, 2011; Janda and Ruelland, 2015). For instance, ETI mediated defense is known to be still active in *npr1* loss-of-function mutant, whereas impaired in NahG (gene that encodes bacterial salicylate hydroxylase) expressing lines (An and Mou, 2011). The NPR1-independent SA marker genes induction may be accomplished *via* members of WHIRLY (WHY) transcription factor family, which bind single-stranded DNA in an NPR1-independent way (Vlot and Dempsey, 2009). Salicylic acid plays also an

essential role in HR development. SA acts synergistically with ROS to drive the HR by facilitating H_2O_2 accumulation during the oxidative burst triggered by avirulent pathogens during ETI, which leads to cell death at the infection site (Simon *et al.*, 2014). This in consequence inhibits pathogen spread to the uninfected tissues. Systemic Acquired Resistance (SAR) is another important aspect of SA action in plant defense response. Several studies demonstrated accumulation of SA and elevated levels of the *PR* genes in systemic uninfected tissues, which was triggered by the infection in developmentally older leaves (Vlot and Dempsey, 2009; An and Mou, 2011). The methyl derivative of SA is considered to play the crucial role in SAR establishment (see also 1.1.1.1.), however it has been also shown that a mobile SAR signal moved from the infection side before increased SA levels could be detected (Rasmussen *et al.*, 1991; Smith *et al.*, 1991). Furthermore, SA except being highly important for plant defense response was also shown to play a role in flowering and thermogenesis (Vlot and Dempsey, 2009).

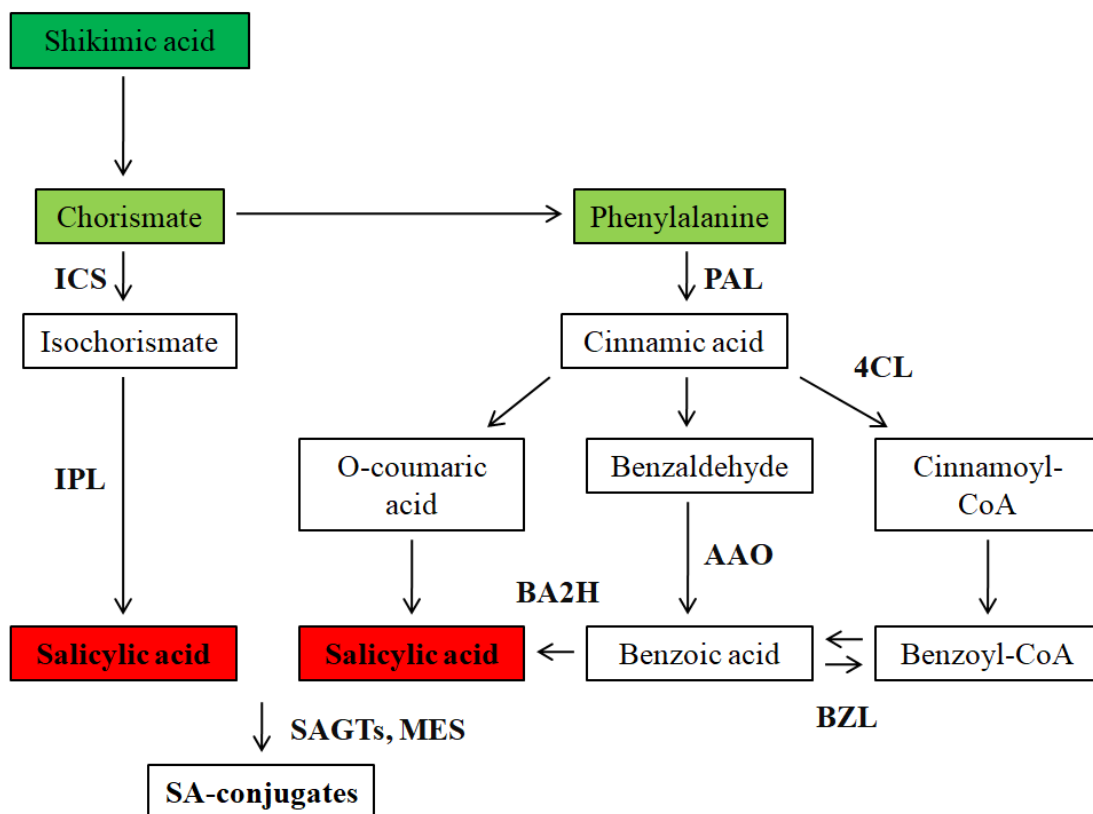


Figure 1. Biosynthesis of salicylic acid.

Abbreviations: 4CL, CoA ligase; AAO, aldehyde oxidase; BA2H, benzoic acid-2-hydroxylase; BZL, benzoyl-CoA ligase; ICS, isochorismate synthase; IPL, isochorismate pyruvate lyase; MT, methyltransferase; PAL, phenylalanine ammonia lyase; SAGTs, Salicylic acid glucosyltransferases; SA, Salicylic acid. Adapted and simplified from Vlot and Dempsey, 2009; Dempsey *et al.*, 2011.

1.1.1.1. Regulation of cytosolic SA levels

The role of SA in plant immunity depends on the interplay between its free and conjugated forms. After being synthesized in the chloroplasts SA is transported by EDS5, a chloroplast envelope-localized member of the multidrug and toxin (MATE) transporter family to the cytosol, where it acts as a signaling molecule during the stress responses. In the cytoplasm salicylic acid undergoes different modifications (Fig. 2), which in general lead to its inactivation (Dempsey and Klessig, 2017). Most of the stress-produced SA is conjugated by SA glucosyltransferases (SAGT) (see also 1.2.2.1.) into SA *O*- β -glucoside (SAG), whereas small amounts are converted into SA glucose ester (SGE). Both derivatives are the inactive form of salicylic acid (Vlot and Dempsey, 2009). During the further steps SAG is transported to the vacuole where it may be stored in its inactive form that can be converted back to SA aglycon (Dean *et al.*, 2003; Dean and Mills, 2004; Dean *et al.*, 2005). SGE likely does not enter the vacuole because it has been shown that the vacuolar ABC transporter and H1 antiporter will only transport glucosylated substrates that possess a negative charge, whereas SGE due to the glucosylation on the carboxylic acid group would not possess the negative charge (Dean and Delaney, 2008). A significant portion of SA is also converted into methyl salicylate (MeSA) and its glucose-derivative methylsalicylate *O*- β -glucoside (MeSAG), both compounds belong to inactive forms of SA. In *Arabidopsis* BA/SA CARBOXYL METHYLTRANSFERASE 1 (BSTM1) catalyzes the conversion of free SA into SA methyl ester (Song *et al.*, 2008; Dempsey *et al.*, 2011). MeSA is implicated in several aspects of signaling, however the most important role of MeSA is its function as a mobile phloem signal for SAR establishment, which has been demonstrated for tobacco, potato and *Arabidopsis* (Park *et al.*, 2008; Dempsey *et al.*, 2011; Liu *et al.*, 2011). However, the presence of MeSA is not essential for SAR (Attaran *et al.*, 2009). The role of MeSAG is not fully elucidated, however most probably it functions as a non-volatile storage form of MeSA (Dempsey *et al.*, 2011). UGT74F2 (AtSGT1) is active towards MeSA and is capable of synthesizing MeSAG *in vitro*. However, *in vivo* it cannot be excluded that BSTM1 or other methyltransferase might produce MeSAG from SAG (Song *et al.*, 2008; Dempsey *et al.*, 2011). Amino acid conjugation can also impact the properties of hormones, thus impact the particular hormone signaling pathway. For instance, conjugation of jasmonic acid (JA) to JA-Ile activates the hormone (Fonseca *et al.*, 2009). In contrast, conjugation of auxin (IAA) to amino acids inactivates this hormone (Woodward and Bartel, 2005). Salicyloyl-L-aspartate (SA-Asp) is a dominant stable SA-AA conjugate. Moreover only this SA amino acid conjugate could be detected in plants (Dempsey *et al.*, 2011). Enhanced expression of acyl-adenylate/thioester-

forming enzyme (GH3.5), involved in amino acid conjugation to SA and IAA (Staswick *et al.*, 2005) was reported to trigger enhanced SA accumulation and pathogen resistance (Park *et al.*, 2007a). Thus, proposing GH3.5 as a positive regulator of SA signaling (Vlot and Dempsey, 2009). On the other hand, exogenous application of SA-Asp did not result in enhanced expression of *PR1* marker gene. This, may suggest that conjugation to SA-Asp similarly like IAA-Asp is likely to be targeted for catabolism (Woodward and Bartel, 2005). Therefore, the role of aspartic acid conjugation to SA still remains to be determined. In *Arabidopsis*, flavonoids, glucosinolates, brassinosteroids, hydroxyjasmonate and SA can be sulfonated *in vitro* by SOT sulphotransferases (Klein and Papenbrock, 2004; Baek *et al.*, 2010). The overexpression of *SOT12* was demonstrated to increase the resistance against *P. syringae*. On the other hand, sulfonated SA could not be detected in plants and *in vitro* reactions required a very high concentration of the substrate in order to enable the detection of sulfonated SA (Baek *et al.*, 2010). Therefore, the direct effect of SA sulfonation on plant defense is currently not substantiated. SA can also be converted to dihydroxybenzoates (DHBAs), which can also occur in non-enzymatic way due to the fact that SA can scavenge hydroxyl radicals (Dempsey *et al.*, 2011). The biological function of DHBs in *Arabidopsis* is currently not fully substantiated. However, 2,5-DHBA has been demonstrated to strongly increase during the infection (Belles *et al.*, 2006) and exogenously supplied 2,3-DHBA was a weak inducer of *PR1* expression as compared with SA (Bartsch *et al.*, 2010).

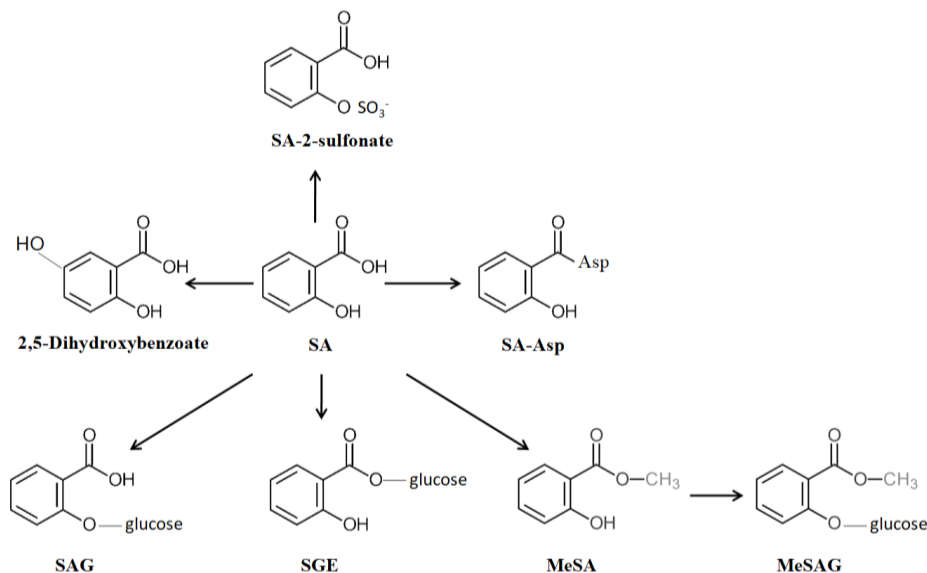


Figure 2. Salicylic acid and its derivatives existing in plants.

Abbreviations: SA, salicylic acid; SAG, SA *O*- β -glucoside; SGE, SA glucose ester; MeSA, methyl salicylate; MeSAG, methylsalicylate *O*- β -glucoside; SA-Asp, Salicyloyl-L-aspartic acid. All modifications except SA-2-sulfonate have been detected in plants including *Arabidopsis*. Adapted and simplified from Vlot and Dempsey, 2009; Dempsey *et al.*, 2011

1.1.1.2. Regulation of SA-mediated defense by elicitors

The term elicitor is commonly used for compounds stimulating plant defense. 2, 6-dichloroisonicotinic acid (INA) and benzothiadiazole (BTH) are known as functional analogs of SA. Both compounds belong to the group of constitutive defense response activators. This includes *PR* marker genes upregulation and SAR establishment. Both INA and BTH activate SA-response mechanisms by functioning as SA agonists with targets downstream from SA accumulation (Bektas and Eulgem, 2015). Several other compounds, such as 3,5-dichloroanthranilic acid (DCA) (Knoth *et al.*, 2009), probenazole (PBZ) (Umemura *et al.*, 2009), tiadinil (TDL), N-cyanomethyl-2-chloroisonicotinamide (NCI) or 3-chloro-1-methyl-1H-pyrazole-5-carboxylic acid (CMPA) (Yasuda, 2007) were also reported to belong to constitutive defense response activators.

The second group of elicitors encompasses compounds impacting plant defense *via* priming. Priming is defined as a mechanism which leads to a physiological state that enables plants to respond more rapidly and efficiently to the environmental conditions (Aranega-Bou *et al.*, 2014). Compounds such as β -aminobutyric acid (BABA), azelaic acid (AzA) or pipercolic acid (Pip) were demonstrated to prime the defense response (Návarová *et al.*, 2012; Shah and Zeier, 2013; Vogel-Adghough *et al.*, 2013; Gao and Zhu, 2015; Baccelli and Mauch-Mani, 2016; Bernsdorff *et al.*, 2016). Isoleucic acid (ILA) was also identified as a immune modulating compound (von Saint Paul *et al.*, 2011). It was demonstrated that exogenously applied ILA can upregulate expression of the *PR1* marker gene to a similar level like the one observed in *ugt76b1* mutant line, which shows enhanced resistance to *Pseudomonas* (see also 1.2.2.). Interestingly, ILA treatment did not trigger the downregulation of JA marker genes, which even showed a tendency for upregulation. However, a similar phenotype was observed for hexanoic acid, which is considered as a broad-spectrum natural inducer (Scalschi *et al.*, 2013). Currently the role of ILA in defense response is not fully elucidated, however most possibly it functions as a competitive inhibitor in SA conjugation (Bauer and Zhang, personal communication). Further aspect of ILA function/action in *Arabidopsis* will be discussed in the next chapters of this dissertation.

1.1.2. JA/ET-mediated pathway in plant defense response

Jasmonic acid and ethylene pathways are known to act in a synergistic manner in defense response to necrotrophic pathogens. JA is a lipid-derived compound that belongs to the oxylipin family. Jasmonic acid biosynthesis from its precursor α -linoleic acid starts in the

chloroplasts (Fig. 3A). Enzymes such as 13-lipoxygenase (13-LOX), 13-allene oxidase (13-AOS) and allene oxide cyclase (AOC) participate in the synthesis of OPDA. This compound is then transported to the peroxisomes, where JA synthesis is completed. JA in its free form is then released to the cytoplasm where it is conjugated. There are many conjugation forms of JA, such as JA-Ile, Me-JA, JA-ACC, JA-Glc and 12-HSO₄-JA. However, only JA-Ile and Me-JA are known to be the active forms of jasmonic acid (Miersch *et al.*, 2006; Acosta and Farmer, 2010). Stress-induced JA is conjugated to JA-Ile by JASMONATE RESISTANT (JAR1). Isoleucine conjugated JA can bind to the F-box protein CORONATINE INSENSITIVE 1 (COI1), which is a critical component of the JA receptor (Wasternack and Xie, 2010). COI1 acts in complex with E3-ligase SKP1-Cullin-F-box (SCF) and leads to the ubiquitination and subsequent proteasomal degradation of JAZ proteins, which relieves jasmonate-inducible genes from the suppression (Sheard *et al.*, 2010). In unchallenged conditions JAZ proteins in order to repress the expression of JA-mediated genes recruit co-repressors, such as TOPLESS (TPL) or TPL-related proteins (TRPs), which is achieved through NOVEL INTERACTOR OF JAZ (NINJA) (Pauwels *et al.*, 2010; Kazan and Manners, 2013). There are two branches of JA signaling, namely MYC and ERF branch. MYC branch is associated with the wound-response and is thought to contribute to defense against insect herbivores. This branch controls the expression of the JA marker gene *VEGETATIVE STORAGE PROTEIN2 (VSP2)* (Chen *et al.*, 2012). ERF branch mediates the defense towards necrotrophic pathogens and involves ETHYLENE RESPONSE FACTOR 1 (ERF1) and OCTADECANOIC ACID RESPONSIVE ARABIDOPSIS AP2 59 (ORA59) that control the expression of *PLANT DEFENSIN1.2 (PDF1.2)*, which is known to be regulated by ET pathway (Verhage *et al.*, 2011). Ethylene is a gaseous hormone synthesized from Met. ET is known to possess a profound role during plant growth and development. It regulates seed germination, seedling growth, leaf and petal abscission, organ senescence, but also pathogen response (Schaller and Kieber, 2012). Five identified ethylene receptors in *Arabidopsis* are localized in the endoplasmic reticulum and can be divided into two subgroups, ETHYLENE RESPONSE1 (ETR1) and ETHYLENE RESPONSE SENSOR1 (ERS1) (Moussatche and Klee, 2004). Upon the necrotrophic pathogen EIN3/EIL1 is a key integration node whose activation requires both JA and ET and is responsible for induction of the expression of downstream defense genes *ERF1*, *ORA59* and *PDF1.2* (Zhu *et al.*, 2011). In the plant defense response ET acts positively on the ERF branch of the JA-mediated pathway, however negative towards wounding inducible MYC branch (Derksen *et al.*, 2013).

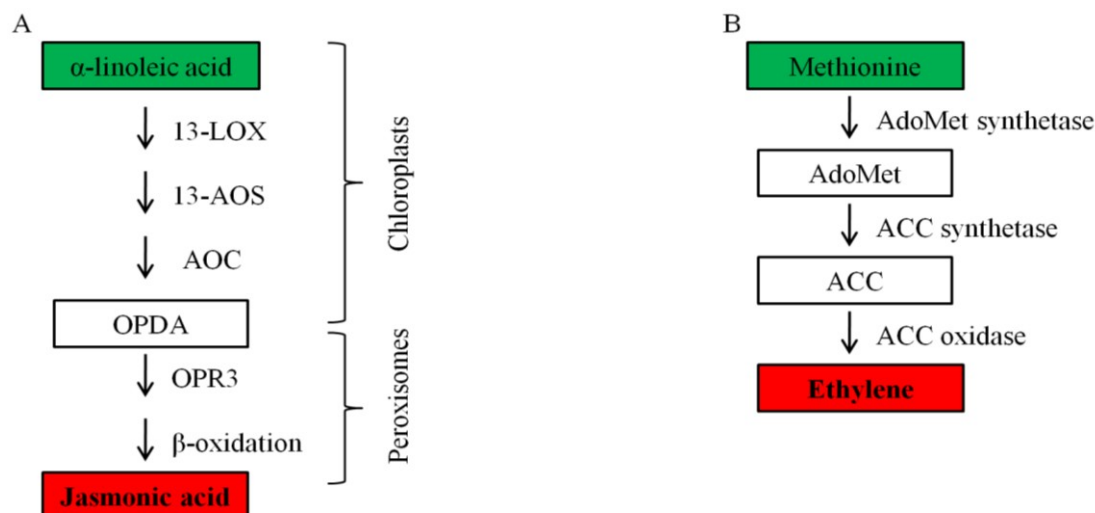


Figure 3. Biosynthesis of jasmonic acid and ethylene

Biosynthesis of Jasmonic acid (A) and Ethylene (B). Abbreviations: (A) 13-LOX, 13- lipoxygenase; 13-AOS, 13-allene oxidesynthase; AOC, allene oxide cyclase; OPR3, OPDA-reductase 3; OPDA, cis-(+)-12-oxo-phytodienoic acid; (B) AdoMet, S-adenyl-methionine; ACC, 1-aminocyclopropane-1-carboxylic acid. Adapted from Schaller and Kieber, 2002; Miersch *et al.*, 2006.

1.1.3. Antagonistic interaction between SA- and JA/ET-mediated pathways

The extensive cross-communication between hormone signaling pathways enables plants to fine-tune the defense response accordingly to the pathogen. The relationship between SA and JA/ET mediated pathway is predominantly antagonistic, however some reports demonstrated that these two pathways may cooperate with each other (Jones and Dangl, 2006). A number of studies demonstrated that the suppression of the JA-mediated pathway by SA is mostly regulated at the transcriptional level (Caarls *et al.*, 2015). NPR1 as a master regulator of SA-mediated defense response is involved in salicylate antagonism against the JA/ET pathways in *Arabidopsis* (Spoel *et al.*, 2003; Spoel *et al.*, 2007). Nuclear NPR1 is responsible for expression of transcription factors such as *GRXs*, *WKRYs* and *TGAs*. For instance, the overexpression of *GRX480* blocks induction of *PDF1.2* by JA, and the overexpression of *GRX13* enhances the susceptibility to necrotrophic pathogens, whereas group II *GRXs*, *ROXY* are able to suppress *ORA59* (Ndamukong *et al.*, 2007; La Camera *et al.*, 2011; Zander *et al.*, 2011). Moreover, Zander *et al.* (2014) showed that *TGAs* can directly stimulate *ORA59* upon ACC treatment or suppress it upon SA. *WRKY* transcription factor family is known for playing an important role in antagonistic relationship between salicylate- and jasmonate-mediated defenses. *WRKY33*, *WRKY41*, *WRKY50*, *WRKY51*, *WRKY62* and *WRKY70* are known to be involved in SA/JA crosstalk by suppression of the JA response (Li *et al.*, 2004; Higashi *et al.*, 2008; Kim *et al.*, 2008; Gao *et al.*, 2011; Birkenbihl *et al.*, 2012). Among them,

WRKY70, WRKY50 and WRKY51 demonstrated an NPR1-independent manner in suppressing the JA-mediated pathway (Gao *et al.*, 2011).

The suppression of SA pathway by JA pathway was also reported. *Pseudomonas* in order to benefit from the antagonistic relationship between SA- and JA-mediated pathways, secrete JA-Ile mimic coronatin (COR) to reduce disease resistance. COR stimulates three homologous NAC transcription factor genes, *ANAC019*, *ANAC055* and *ANAC072*. These transcription factors were shown to inhibit the SA accumulation by repressing *ICS1* and activating *BSMT1* (Zheng *et al.*, 2012).

Furthermore, a novel player in SA/JA cross-talk has been recently identified in our laboratory (von Saint Paul *et al.*, 2011). Small molecule glucosyltransferase UGT76B1 was demonstrated to negatively impact SA-, however positively JA-mediated defense response (see also 1.2.2.1. and 1.2.2.2.).

1.2. Plant UDP-glycosyltransferases (UGTs)

Plants synthesize several thousands of different low-molecular-weight compounds, which are defined as plant secondary metabolites. The strong diversity of these compounds arises *via* the modification by adding glycosyl-, carboxyl-, methyl- and hydroxyl-groups by glycosyltransferases, acyltransferases, methyltransferases and cytochrome P450 monooxygenases, respectively. Glycosylation belongs to the most common modification of the secondary metabolites. UDP-glycosyltransferases (UGTs) catalyze the transfer of a carbohydrate moiety from activated donor to the acceptor molecule (Fig. 4), thereby regulating the activity, stability, solubility or subcellular localization of the glycosylated molecule. Plant UGTs, except being involved in the synthesis of secondary metabolites have also a great importance in regulating the activity of signaling molecules and defense compounds. Furthermore, pathogens produce toxins that are secreted into the host cells to overcome plant defense mechanisms; however glycosylation can inactivate these compounds. For instance, sugar conjugation effectively neutralizes xenobiotics such as herbicides *in vitro* (Jones and Vogt, 2001; Bowles *et al.*, 2006). There are 122 UGTs isoforms in *A. thaliana*, whose genes are scattered across all of the five *Arabidopsis* chromosomes. The length of amino acid sequences of *Arabidopsis* UGTs vary from 435 to 507. The overall sequences similarity between *Arabidopsis* UGTs varies strongly and ranges from ~30% up to ~90% identity; however despite this divergence nine conserved motifs are present in all *Arabidopsis* UGTs. The fifth conserved motif separates UGTs into amino- and carboxy-terminal regions,

which are responsible for recognition and binding of aglycon and nucleotide sugar substrates, respectively. The amino-terminal region due to its function in binding of the highly diverse substrates varies strongly in contrast to the carboxy-terminal regions of *A. thaliana* UGTs (Li *et al.*, 2001).

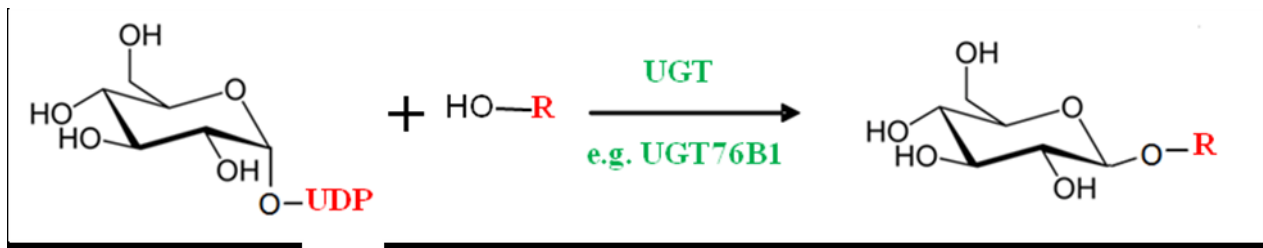


Figure 4. Reaction catalyzed by glucosyltransferases

Adapted from (Zhang, 2013).

1.2.1. Reactions catalyzed by UGTs

UDP-glucose is a typical activated sugar donor of plant UGTs, however UDP-rhamnose, UDP-galactose, UDP-xylose, UDP-glucuronic acid were also identified as being accepted by plant UGTs. Known acceptor molecules belong to hormones, secondary metabolites or biotic compounds (e.g. toxins). The conjugation of a carbohydrate may lead to the formation of a range of glycosylated molecules, such as glucose esters and *O*- β -glucosides, cyanogenic glucosides or glucosinolates. Moreover, some of the aglycons, such as flavonols are capable of accepting more than a one sugar. A single or multiple glycosylation of the acceptor molecule can occur at -OH, -COOH, -NH₂, -SH, or C-C groups (Lim and Bowles, 2004; Bowles *et al.*, 2006). In plants most probably glucosylation occurs in the cytosol, which has been suggested by the sequence studies demonstrating that none of the analyzed plant glycosyltransferases possessed a signal sequence, nor membrane-spanning or targeting signals (Li *et al.*, 2001). This is in contrast to the mammalian UGTs. Mammalian UDP-glycosyltransferases catalyze the conjugation of a variety endo- and exogenous aglycon substrates with glucuronic acid using UDP-glucuronic acid. These glycosyltransferases have a signaling sequence involved in translocation into rough endoplasmic reticulum. However, it is not excluded that these enzymes function is the cytosol as well (Radominska-Pandya *et al.*, 1999).

1.2.2. Plant glucosyltransferases and stress response

A number of plant UGTs are highly expressed upon biotic and abiotic stimuli. This indicates the importance of these enzymes in response to stress. Moreover, the expression of some glycosyltransferases is enhanced during both biotic and abiotic stress conditions (von Saint Paul *et al.*, 2011). The role of plant glycosyltransferases in defense to biotic stresses is substantiated for several UGTs. For instance, Poppenberger *et al.* (2003) introduced UGT73C5/DOGT1 as deoxynivalenol and 15-acetyl-deoxynivalenol glucose conjugating enzyme, which inactivates this compound. Deoxynivalenol is a mycotoxin produced by *Fusarium*, which accumulates in the leaves of infected plants and presumably impacts negatively defense gene expression. In this case, glucosylation blocks the toxic activity of this compound, thus positively impacting the defense response. Recently another UGT has been also identified as essential for *Arabidopsis* defense towards fungus pathogen. Langenbach *et al.* (2013) assigned UGT84A2/BRT1 driven glucosylation of sinapic acid with post-invasion resistance of *Arabidopsis* to its nonhost pathogen *Phakopsora pachyrhizi*. Several reports also associated the defense response to the biotrophic pathogen *P. syringae* with the activity of UGTs. The loss-of-function mutants of *ugt73b3* and *ugt73b5* exhibited decreased resistance to *Pseudomonas syringae avrRpm1*, whereas wild-type response to *Pseudomonas syringae DC3000* virulent line. Similarly, the transcript levels of *UGT73B3* and *UGT73B5* were only affected by the avirulent strain suggesting that the expression of the corresponding UGT genes is necessary during HR (Langlois-Meurinne *et al.*, 2005). Further studies on these two glucosyltransferases revealed their dual function during the defense response to *Pseudomonas*. At the early stages of the infection *UGT73B3* and *UGT73B5* play a role in redox status established during the HR, thus redox perturbations are possibly responsible for the decreased resistance to *P. syringae AvrRpm1* reported for *ugt73b3* and *ugt73b5* mutants. Whereas, the high expression of *UGT73B3* and *UGT73B5* during the late phase of the infection was associated with regulation and detoxification of endogenous secondary metabolites such as camalexin (Simon *et al.*, 2014). Furthermore, UGTs may also directly impact SA-mediated defense pathway by utilizing SA as the substrate.

1.2.2.1. UGT76B1 impacts SA- and JA-mediated defenses

UGT76B1 is a top stress induced small molecule glucosyltransferase, which was previously identified in our laboratory as a novel player in the SA/JA cross-talk. UGT76B1 suppress SA marker genes, such as *PR1*, *EDS1* and *PAD4*, whereas positively stimulates JA marker genes

PDF1.2, *VSP2* and *LOX2*. Moreover, the expression of a known regulator of SA/JA cross-talk *WRKY70* was also negatively correlated with expression of *UGT76B1*. Thus, *UGT76B1* may downregulate *WRKY70* which might be involved in the suppression of JA pathway. Accordingly, *ugt76b1* loss-of-function mutant demonstrated increased resistance to the biotrophic *P. syringae* infection, whereas *UGT76B1* overexpression line demonstrated increased susceptibility. The resistance to the necrotrophic pathogen *A. brassiciola* revealed the opposite phenotype; *ugt76b1* was less resistant, whereas *UGT76B1* overexpression led to reduced susceptibility (von Saint Paul *et al.*, 2011; Zhang, 2013). However, von Saint Paul *et al.* (2011) claimed *UGT76B1* as not being an SA conjugating enzyme *in vivo*, since the levels of glucose-conjugated SA increased in *ugt76b1-1* mutant.

1.2.2.2. *Arabidopsis thaliana* UGTs involved in SA conjugation

Salicylic acid mediated defense can be directly impacted by UGTs. It is known that most of produced SA is glucose-conjugated by a pathogen-inducible SA glucosyltransferases (Vlot and Dempsey, 2009). In *Arabidopsis* *UGT74F1*, *UGT74F2*, *UGT75B1* and *UGT76B1* can recognize SA as the substrate *in vitro* (Lim *et al.*, 2002; von Saint Paul *et al.*, 2011; Noutoshi *et al.*, 2012; Li *et al.*, 2015; Thompson *et al.*, 2017). Among them *UGT74F1* and *UGT76B1* were shown to produce SAG *in vitro*. At the same time, *UGT74F2* is capable of producing both SAG and SGE, however predominantly SGE (Lim *et al.*, 2002; Li *et al.*, 2015; Thompson *et al.*, 2017). Furthermore, *in vitro* *UGT74F1* displays a tenfold higher specific activity for SAG formation than *UGT74F2* does for its primary product SGE (Thompson *et al.*, 2017), whereas *UGT76B1* was demonstrated to synthesize SAG *in vitro* with similar activity as *UGT74F1* (Noutoshi *et al.*, 2012). However, *UGT4F2* showed higher activity towards anthranilate, benzoic acid and nicotinate than SA *in vitro* (Li *et al.*, 2015). Additionally, ILA, which is also known as the substrate of *UGT76B1* (von Saint Paul *et al.*, 2011) is able to significantly inhibit SAG formation by *UGT76B1* *in vitro* (Noutoshi *et al.*, 2012).

In vivo both *UGT74F1* and *UGT74F2* were shown to impact SA/SA glucose conjugates homeostasis by utilizing SA as the substrate. For instance, Dean and Delaney (2008) examined the abundance of SAG and SGE in *Arabidopsis ugt74f1* and *ugt74f2* mutant lines upon exogenously applied [7-¹⁴C]-SA. In *ugt74f1* mutant six hours post [7-¹⁴C]-SA application SAG could not be detected, whereas the levels of SGE were comparable to the wild-type; after twelve hours an increase of SGE and very low levels of SAG were detected.

However, the presence of SAG in *ugt74f1* might be due to the activity of UGT74F2 (Dean and Delaney, 2008). At the same time in the single mutant of *ugt74f2* SGE could not be detected upon [7-¹⁴C]-SA treatment. Therefore, this proves that both UGT74F1 and UGT74F2 are active towards SA *in vivo*. Song (2006) reported the increase of *UGT74F2* (*AtSGT1*) expression upon *P. syringae* and SA treatment, which associates UGT74F2 with the defense response. Moreover Song *et al.* (2008) demonstrated that overexpression *UGT74F2* leads to the enhanced susceptibility to *P. syringae*. This phenotype was attributed to the decreased level of SA aglycon and in consequence reduced and delayed expression of *PR1* marker gene upon the infection, compared to the wild type. In line with the reduced feedback of SA biosynthesis, SA glucosides (SAG, SGE) were also reduced (Song *et al.*, 2008). Li *et al.* (2015) also suggested that UGT74F2 is involved in stress-induced SA conjugation. This was demonstrated by strongly reduced levels of SGE upon *Pseudomonas* infection in a *ugt74f2* knockdown line. Noutoshi *et al.* (2012) observed increased resistance of *ugt76b1* and *ugt74f1*, and consistently of *ugt74f1 ugt76b1* double mutant. The resistances to *P. syringae* of these mutants were correlated with the amounts of free SA; namely highest for *ugt74f1 ugt76b1* and lowest for *ugt74f1*. Therefore, both UGT76B1 and UGT74F1 were proposed as SAG forming enzymes in *Arabidopsis* (Noutoshi *et al.*, 2012).

1.3. Aim of this work

Based on previous results from Wei Zhang and Veronica von Saint Paul UGT76B1 and ILA were demonstrated to play an important role in SA- and JA-mediated defense response. The principal goal of this work was to extend the current knowledge on UGT76B1 and ILA action.

The first aim was to elucidate the role of UGT76B1 as a probable *in vivo* SA conjugating enzyme in *Arabidopsis thaliana*. This involved detailed investigation of both below- and aboveground tissues of single and multiple *ugt* mutant lines in terms of abundance of free and glucose-conjugated SA, marker genes expression as well as growth response to exogenously applied SA.

The second aim was addressed to ILA function and was divided into two projects. In the first project (in cooperation with Dr. Andrea Ghirardo, Helmholtz Zentrum München, Research Unit Environmental Simulation) a GC-MS based method was applied to elucidate the impact of UGT76B1 on endogenous levels of ILA and a closely related 2-HA, LA. Furthermore, this project was also extended into the examination of how ILA and LA behave during plant growth and development and response to *Pseudomonas*. The goal of the second project was to elucidate the mechanism responsible for ILA-driven root growth inhibition. Here two different strategies were applied. The first used the natural genetic variance of Swedish *Arabidopsis thaliana* accessions to identify the regions of the genome involved in response to exogenous ILA (in cooperation with Dr. Arthur Korte, GMI Vienna). In the second strategy homozygous T-DNA insertion lines were screened for ILA root growth insensitivity.

The third aim was to explore if a high expression of *UGT76B1* in the root is essential for the UGT76B1-dependent upregulation of SA *PR* marker genes in the rosette tissues. Therefore, reciprocal grafting experiments of *ugt76b1* and Col-0 were employed and were further analyzed by RT-qPCR.

2. RESULTS

2.1 Salicylic acid as an *in vivo* substrate of UGT76B1

2.1.1. *ugt76b1* knock-out mutants show different abundance of free and conjugated salicylic acid

Previously, UGT76B1 was characterized as a regulator of SA-JA crosstalk showing a high activity towards isoleucic acid (ILA). The *in vivo* elevated levels of SA glucose conjugate in *ugt76b1-1* indicated that UGT76B1 is less likely to contribute in SA conjugation, although it also showed SA-glucosylating activity *in vitro* (von Saint Paul *et al.*, 2011). However, Noutoshi *et al.* (2012) also demonstrated that UGT76B1 conjugates salicylic acid *in vitro* with an activity comparable to UGT74F1 that is known as an enzyme producing SAG (2-*O*- β -D glucosylbenzoic acid). Moreover, *in vivo* study carried out by Noutoshi *et al.* (2012) demonstrated similarly increased levels of free SA, whereas decreased levels of glucose-conjugated SA in *ugt76b1* and in *ugt74f1*. However, it is also worth mentioning that Noutoshi *et al.* (2012) used mutants in Ws-4, whereas Saint Paul *et al.* (2011) had characterized mainly the Col-0 allele of *ugt76b1* (*ugt76b1-1*).

Therefore, *ugt76b1* knock-outs in three *A. thaliana* accessions, *ugt76b1-1* (Col-0), *ugt76b1-1* (*Ler*) and *ugt76b1-3* (Ws-4), were used to elucidate, if a different background could be responsible for distinct accumulation of free and conjugated SA. The determination of free SA showed that Col-0, *Ler* and Ws-4 wild-types accumulate similar levels of SA aglycon. At the same time only *Ler* and Ws-4 displayed similarly increased levels of SA conjugates, if compared to SA in its free form (five- and sixfold, respectively), whereas Col-0 ecotype showed almost elevenfold higher abundance of SA conjugates (Fig. 5). The measurement of *ugt76b1* loss-of-function mutants showed that *ugt76b1-1*, *ugt76b1-2* and *ugt76b1-3* present similar ratio of SA glucose conjugates to SA aglycon. Interestingly, comparisons with the respective wild-types showed that *ugt76b1-1* and *ugt76b1-2* present an increase of free and conjugated SA, whereas, *ugt76b1-3* does not differ from its wild-type (Fig 5). However, *ugt76b1-1* demonstrated a stronger response than *ugt76b1-2*, which was manifested by a higher upregulation of SA and its glucose conjugates.

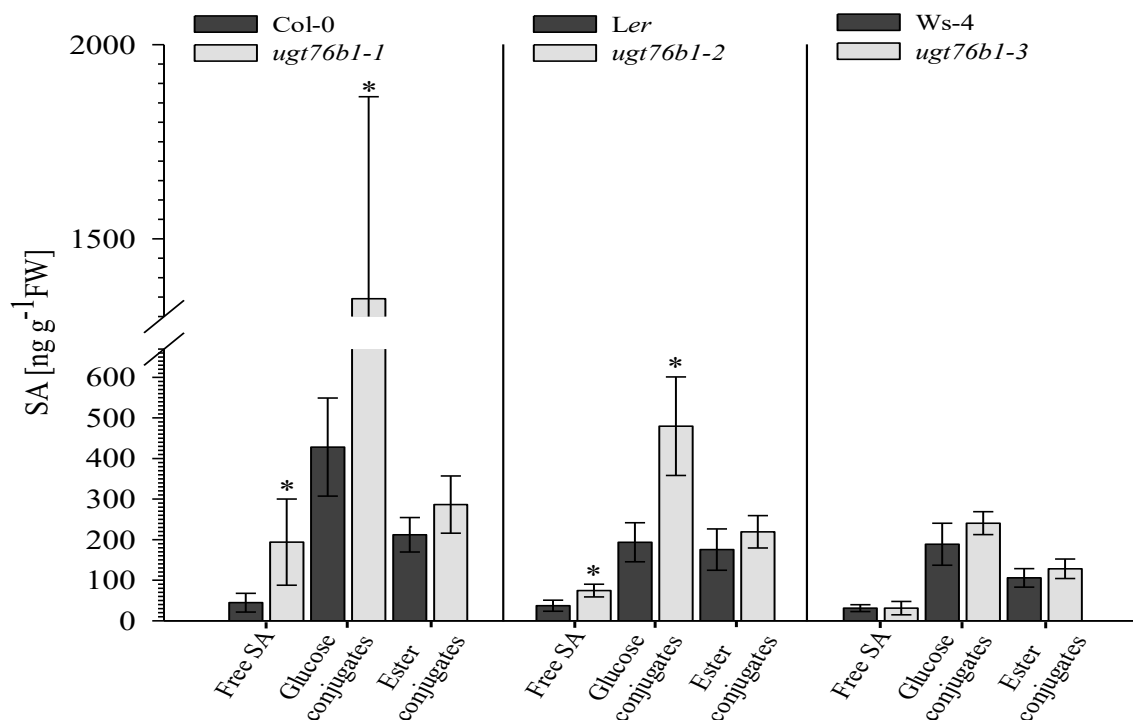


Figure 5. Free and conjugated SA in four-week-old *Arabidopsis thaliana* plants of *ugt76b1-1*, *ugt76b1-2* and *ugt76b1-3* along with their respective wild-types.

Abundance of free and conjugated SA in *ugt76b1* mutant leaves of Col-0, Ler and Ws-4 background. Plants were grown in short day conditions (10 h light and 14 h darkness) for four weeks. Bars represent arithmetic means and standard deviations from three replicates. Asterisks indicate significance of the difference to the wild-type line; *P < 0.05.

2.1.2. Triple mutant of *ugt74f1 amiugt74f2 ugt76b1* provides the evidence that UGT76B1 participates in SA conjugation.

To further assess the role of UGT76B1 in salicylic acid conjugation, other mutants affecting potential SA-glucosylating enzymes, UGT74F1 and UGT74F2, were introgressed and SA/SA glucose conjugates levels were determined. All experiments involving *ugt* multiple mutants due to the unavailability of Col-0 allele were performed with mutants in Ws-4 background. The introduction of *ugt76b1* loss-of-function mutant to *ugt74f1 amiugt74f2* double mutant (knock-out and knock-down, respectively; (Yin, 2010) triggered more than sixfold reduction of the SA glucose conjugate in four-week-old rosettes of such a triple mutant, if compared to the wild-type control (Fig. 6). Previous measurement of SA/SA-conjugates in *ugt74f1 amiugt74f2* double mutant (Yin, 2010) demonstrated not affected levels of free and conjugated SA, if compared to the wild-type. Similarly, *ugt76b1-3* did not show a reduction of SA glucosylation (Fig. 5). Therefore, these three results clearly indicate that UGT76B1, UGT74F1 and UGT74F2 in concert play a crucial role in SA glucosylation. Moreover, a

slight reduction of salicylic acid ester conjugates and a minor increase of salicylic acid in its free form were observed as well (Fig. 6).

For further verification of the role of UGT76B1, UGT74F1 and UGT74F2 in SA conjugation stress-dependent changes in salicylic acid and its conjugates in *ugt74f1 amiugt74f2 ugt76b1* were examined. Elevated level of SA that is triggered by biotrophic pathogens or by exogenous chemical treatment (e.g. SA or its analog benzothiadiazole - BTH) is conjugated in the wild-type to presumably attenuate the response. Moreover, it has been previously shown that SA increases strongly and is conjugated within the 48 hours post BTH treatment (Messner and Schäffner, personal communication). Here, mutant plants lacking enzymes conjugating SA were treated with BTH 24 h prior harvest in order to monitor early time point changes in the abundance of free and conjugated SA. In plants lacking SA-conjugating enzymes BTH treatment triggered a very strong accumulation of SA aglycon, which was not further glucosylated, compared to the mock treated control (Fig. 7). At the same time wild-type plants did not show enhanced accumulation of SA aglycon as well as its glucose conjugates, which is known to occur 48 hours after BTH treatment (Messner and Schäffner, personal communication). Therefore, this result demonstrated that the repression of SA glucosyltransferases increases the sensitivity of mutant plants and triggers a rapid accumulation of the SA aglycon.

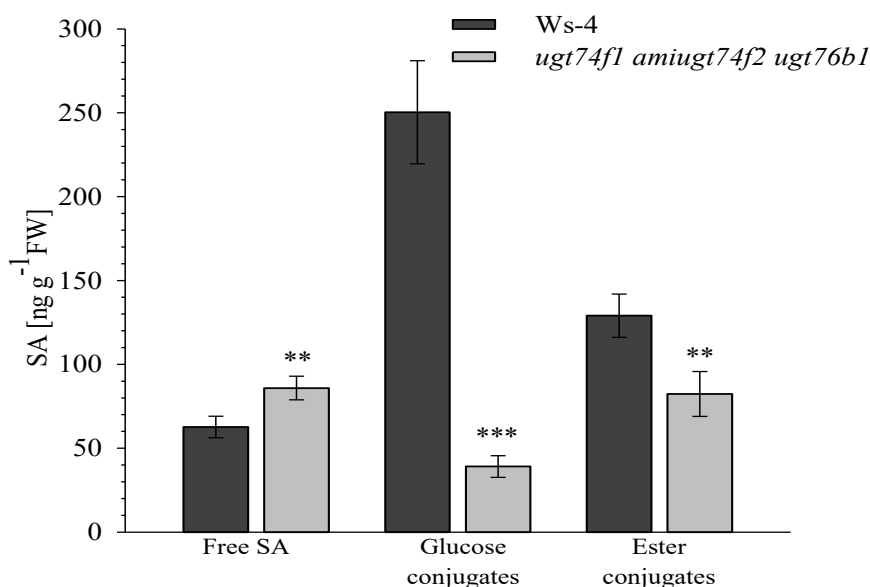


Figure 6. Free and conjugated SA in 4-week-old *Arabidopsis thaliana* plants of the wild-type and *ugt74f1 amiugt74f2 ugt76b1*-3.

Abundance of free and conjugated SA in rosettes of *ugt74f1 amiugt74f2 ugt76b1* mutant. Plants were grown in short day conditions (14 h light and 10 h darkness) for four weeks. Bars represent arithmetic means and standard deviations from four replicates. Asterisks indicate significance of the difference to the wild-type line (Ws-4); **P < 0.01, ***P < 0.001.

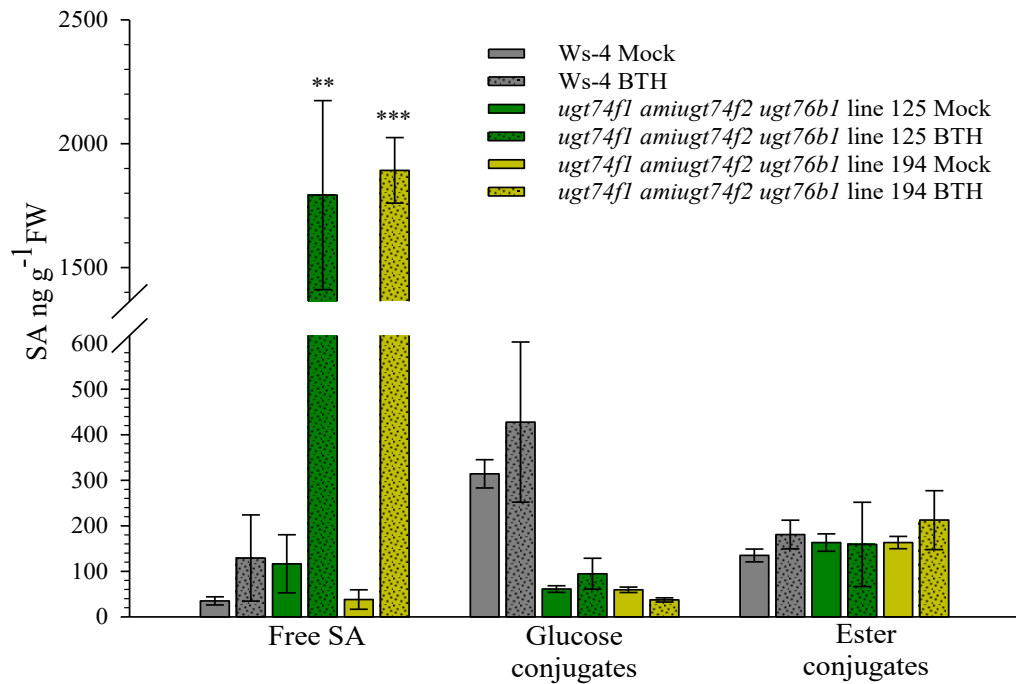


Figure 7. Free and conjugated SA in wild-type plants and *ugt74f1 amiugt74f2 ugt76b1-3* mutants in response BTH treatment.

Abundance of free SA, SA glucose and ester conjugates in rosettes of *ugt74f1 amiugt74f2 ugt76b1* mutants. Plants were grown in short day conditions (10 h light and 14 h darkness) for four weeks and harvested 24 h post 1 mM BTH treatment. Bars represent arithmetic means and standard deviations from three replicates. Asterisks indicate significance of the difference to the mock treated samples; ** $P < 0.01$, *** $P < 0.001$.

2.1.3. *ugt74f1*, *ugt74f2* and *ugt76b1* mutants root growth inhibition in presence of salicylic acid

The above study clearly indicated that UGT76B1 has a remarkable impact on SA conjugation *in vivo*. Exogenous application of SA in the concentrations corresponding with the endogenous stress signaling levels (10 μM – 100 μM) inhibits the root growth (Wildermuth and Jones, 2009). As already described, conjugation impacts negatively the activity of SA. Thus, glucosylation could possibly repress SA inhibitory effect on the root growth, whereas the lack of or hindered SA conjugation could be responsible for an enhanced root growth inhibition. Therefore, plants lacking enzymes putatively involved in SA conjugation (UGT74F1, UGT74F2 and UGT76B1) were grown on $\frac{1}{2}$ MS media containing 20 μM SA (Fig. 8A and 8C) and 40 μM SA (Fig. 8B and 8D). *ugt76b1* loss-of-function mutants displayed higher root growth susceptibility than their wild-types (Ws-4 and Col-0 ecotype). Moreover, *ugt76b1* mutants showed also higher root growth inhibition than mutants of two other SA conjugating enzymes: UGT74F1 and UGT74F2 (Fig. 8A-D), which were not

affected differently from their wild-types. Thus, this demonstrates that independently from the accession UGT76B1 plays a crucial role in the root growth response to the exogenous SA. This experiment also pointed out that Wassilewskija accession behaves differently than Columbia, due to its higher root growth susceptibility, which was more pronounced on plates containing 40 μ M SA (Fig. 8B and 8D).

Since plants lacking *UGT76B1* expression exhibited increased root growth inhibition in presence of salicylic acid, it has been also examined if its over-expression will show the opposite phenotype. Indeed, *UGT76B1-OE-7* demonstrated lower root growth inhibition in presence of SA in media (Fig. 9).

To further explore the importance of UGT76B1 in SA-suppressed root growth *ugt74f1 amiugt74f2* double mutants as well as *ugt74f1 amiugt74f2 ugt76b1* triple mutant were grown on media containing SA. This experiment provided another evidence for UGT76B1 as a crucial player in salicylic acid conjugation. Plants of *ugt74f1 amiugt74f2* double mutant grown on 30 μ M salicylic acid displayed wild-type root growth response. At the same time, *ugt74f1 amiugt74f2 ugt76b1* showed a nearly complete inhibition of germination (Fig. 10). Such a hypersensitive response displayed by triple mutant (Fig. 10D) may also indicate the fact that there is no other UGT that is able to detoxify SA from the media.

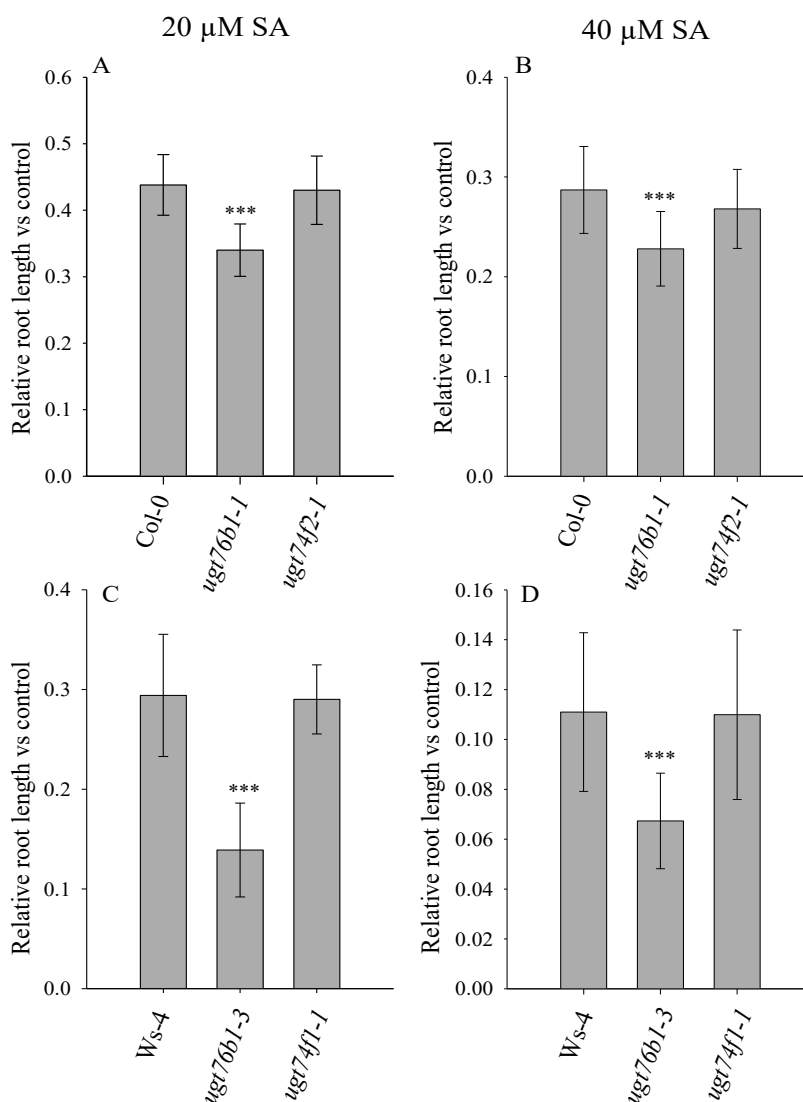


Figure 8. *ugt76b1* knock-out mutants display the highest root growth inhibition in presence of SA.

Col-0, *ugt76b1-1* and *ugt74f2-1* grown on plates with 20 μ M SA (A) and 40 μ M SA (B). Ws-4, *ugt76b1-3* and *ugt74f1-1* grown on plates with 20 μ M SA (C) and 40 μ M SA (D). Plants were grown in long day conditions (16 h light, 8 h darkness) on square vertical plates for nine days. Roots lengths were calculated using ImageJ software and then related to the parallelly grown controls (Gelrite plates without SA). Asterisks indicate the significance of the difference between the genotypes; ***P < 0.001. (D) did not meet the requirements for statistical test, therefore statistical analysis was based on ranks. (A) n= 48-54, (B) n= 40-46, (C) n= 21-29, (D) n= 36-48

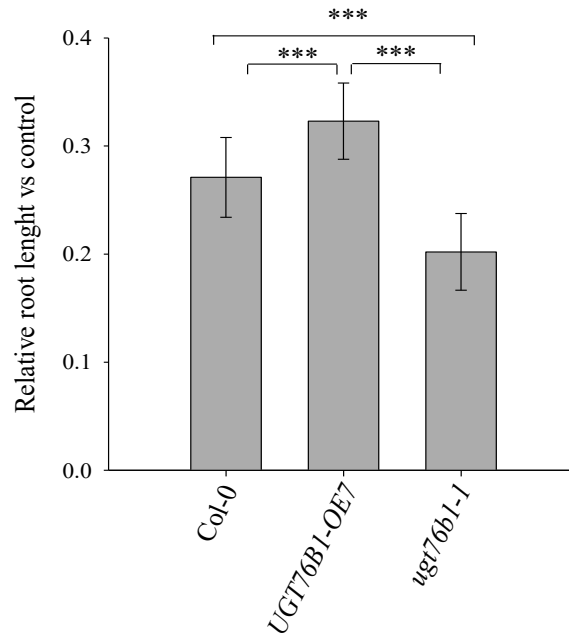


Figure 9. *UGT76B1-OE7* shows a lower root growth inhibition in presence of SA.

Asterisks indicate the significance of the difference to the control (plate without SA). Plants were grown in long day conditions (16 h light, 8 h darkness) on square vertical plates for eight days on $\frac{1}{2}$ MS media containing 40 μ M SA. Roots lengths were calculated using ImageJ software and then related to the parallelly grown controls (Gelrite plates without SA). Asterisks indicate the significance of the difference between the genotypes; ***P < 0.001 n= 17-21

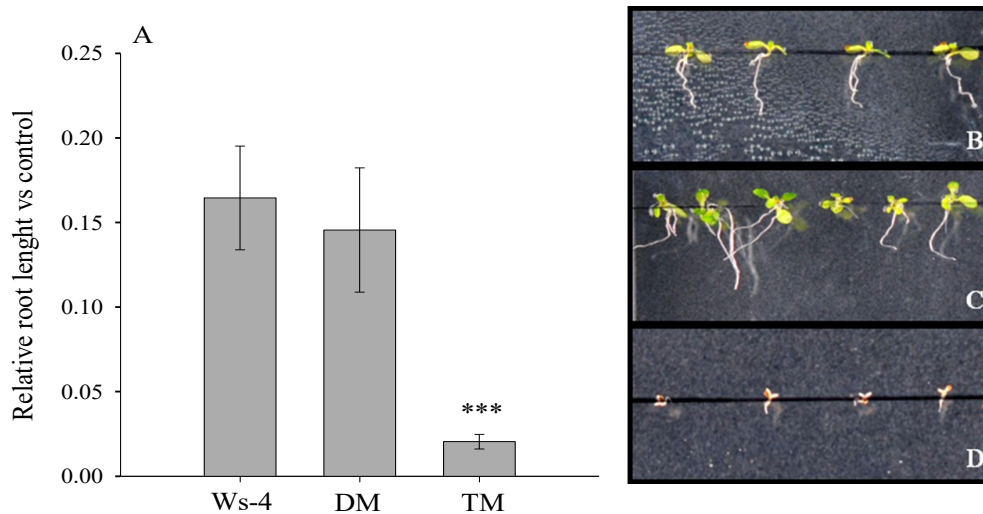


Figure 10. *ugt74f1 amiugt74f2 ugt76b1* shows root growth hypersensitivity in presence of SA.

Abbreviations: DM, double mutant of *ugt74f1 amiugt74f2*; TM, triple mutant of *ugt74f1 amiugt74f2 ugt76b1*. (A) Relative root length of Ws-4, *ugt74f1 amiugt74f2* and *ugt74f1 amiugt74f2 ugt76b1*. (B), (C) and (D) demonstrate how 30 μ M SA affects growth of Ws-40, *ugt74f1 amiugt74f2* and *ugt74f1 amiugt74f2 ugt76b1*, respectively. Plants were grown in long day conditions (16 h light, 8 h darkness) on square vertical plates for nine days on $\frac{1}{2}$ MS media containing 30 μ M SA. Roots lengths were calculated using ImageJ software and then related to the parallelly grown controls (Gelrite plates without SA). Asterisks indicate the significance of the difference between the genotypes; ***P < 0.001. n= 16-21

2.1.4. Do *UGT74F1*, *UGT74F2* and *UGT76B1* compensate each other for SA glucosylation?

Previous experiments have shown that *UGT76B1* is active towards SA *in vivo*, thus the potential redundancy with two other SA-conjugating enzymes was further examined. In this study different combinations of mutants lacking one or two out of the three above mentioned UGTs were used to monitor the expression of the remaining gene/s by RT-qPCR (in cooperation with Sibylle Bauer, BIOP, Helmholtz Zentrum München). Due to the lack of all the mutants in the same background it was necessary to implement both Col-0 and Ws-4 accessions. The following mutants in Col-0 background were involved in this study: *ugt76b1-1*, *ugt74f2-1*, *ugt74f2 ugt76b1*, and in Ws-4 background: *ugt76b1-3*, *ugt74f1-1*, *ugt74f1 amiugt74f2* were used. Only moderated changes could be detected in expression of *UGT74F1* (Fig. 11A) and *UGT74F2* (Fig. 11B). The most pronounced difference was the downregulation of *UGT76B1* expression in *ugt74f2-1* (Fig. 11C). The second highest expression change is the upregulation of *UGT76B1* in *ugt74f1 amiugt74f2* double mutant (Fig. 11C), which could suggest that *UGT76B1* compensates for SA conjugation when two other SA glucosyltransferases are missing or downregulated. Moreover, *UGT74F1* demonstrated a slight upregulation only in *ugt76b1-1* mutant line (Fig. 11A), whereas *UGT74F2* expression was moderately increased in *ugt76b1-1* and *ugt74f1-1* (Fig. 11B).

In order to further explore this issue, analogous measurements involving BTH-treated *ugt76b1-1*, *ugt74f2-1*, *ugt74f2 ugt76b1*, *ugt76b1-3*, *ugt74f1-1* and *ugt74f1 amiugt74f2* were performed. The goal of this experiment was to determine whether the application of the stress conditions could enhance the potential compensation for SA conjugation. This demonstrated that *UGT74F1* and *UGT74F2* did not show higher activation in the tested mutants than their wild-type controls (Fig. 12A-B). Only *UGT76B1* (Fig. 12C) displayed enhanced expression in *ugt74f1 amiugt74f2* double mutant. However, BTH did not trigger a higher upregulation of *UGT76B1* than previously recorded in untreated *ugt74f1 amiugt74f2* double mutant. Nonetheless, this is the second evidence demonstrating that the repression of two other known SA glucosyltransferases is responsible for enhanced expression of *UGT76B1*. This could also be the evidence for a different manner of action of these two glucosyltransferases. Moreover, in *ugt74f1 amiugt74f2* double mutant and *ugt74f1 amiugt74f2 ugt76b1* triple mutant *BSTMI1*, an SA methyltransferase was up-regulated to a similar extent (Fig. 12D). This would indicate its dependency on *UGT74F1* and *UGT74F2*, since its expression was below the detection

limit in Ws-4 and Col-0 wild-types and close to the detection limit in *ugt76b1-1* and *ugt74f2-1*.

Additionally, both *UGT74F1* and *UGT74F2* displayed the same expression levels in Col-0 and Ws-4, whereas *UGT76B1* was up-regulated in Col-0 compared with Ws-4 in untreated conditions (Fig. 11D). On the other hand, *UGT76B1* expression is induced upon BTH treatment to the same levels like in Col-0 (Fig. 12E). Therefore, demonstrating Ws-4 *UGT76B1* as being higher inducible in stress conditions, thus providing another argument for a different behavior of *UGT76B1* in Col-0 and Ws-4 alleles.

Since *UGT74F1* and *UGT74F2* did not display enhanced expression in the *ugt* mutants post BTH treatment may indicate a different manner of their action than *UGT76B1*. This hypothesis was further explored by measuring the impact of BTH on SA-glucoylating UGTs. BTH treatment triggered only a very weak increase of the expression of *UGT74F1*, at the same time *UGT74F2* was moderately upregulated (Fig. 13A). The examination of *UGT76B1* revealed a very strong upregulation, at a similar extent as the highly responsive *PR1* marker gene (Fig. 13B). Therefore, in contrast to *UGT76B1*, the action of *UGT74F1* and *UGT74F2* could mostly rely on their basal expression levels.

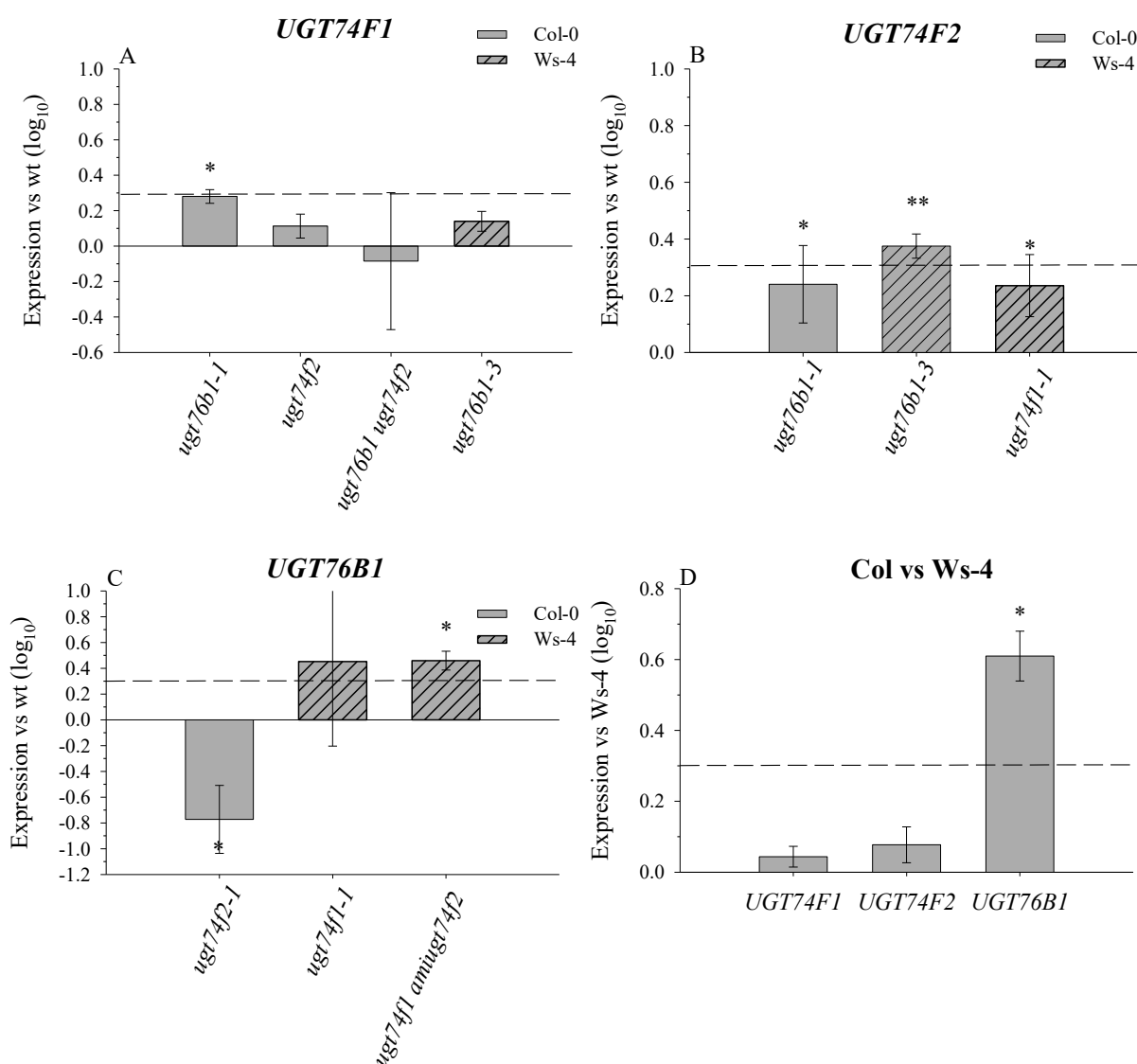


Figure 11. Comparison of the expression levels of *UGT74F1*, *UGT74F2* and *UGT76B1* in different *ugt* mutants.

Expression of *UGT74F1* (A), *UGT74F2* (B) and *UGT76B1* (C) in *ugt* mutants. Panel D shows the difference between Columbia and Wassilewskija in expression of *UGT74F1*, *UGT74F2* and *UGT76B1*. Plants were grown for four weeks in short day conditions (10 h light, 14 h darkness). Expression levels were normalized to *UBIQUITIN5* and *S16*. Dashed lines indicate a twofold expression change. Bars represent arithmetic means and standard deviations from log₁₀ transformed data of three replicates. Asterisks indicate significance of the difference to the adequate wild-type line (A-C) and to Ws-4 (D); *P < 0.05 **P < 0.01.

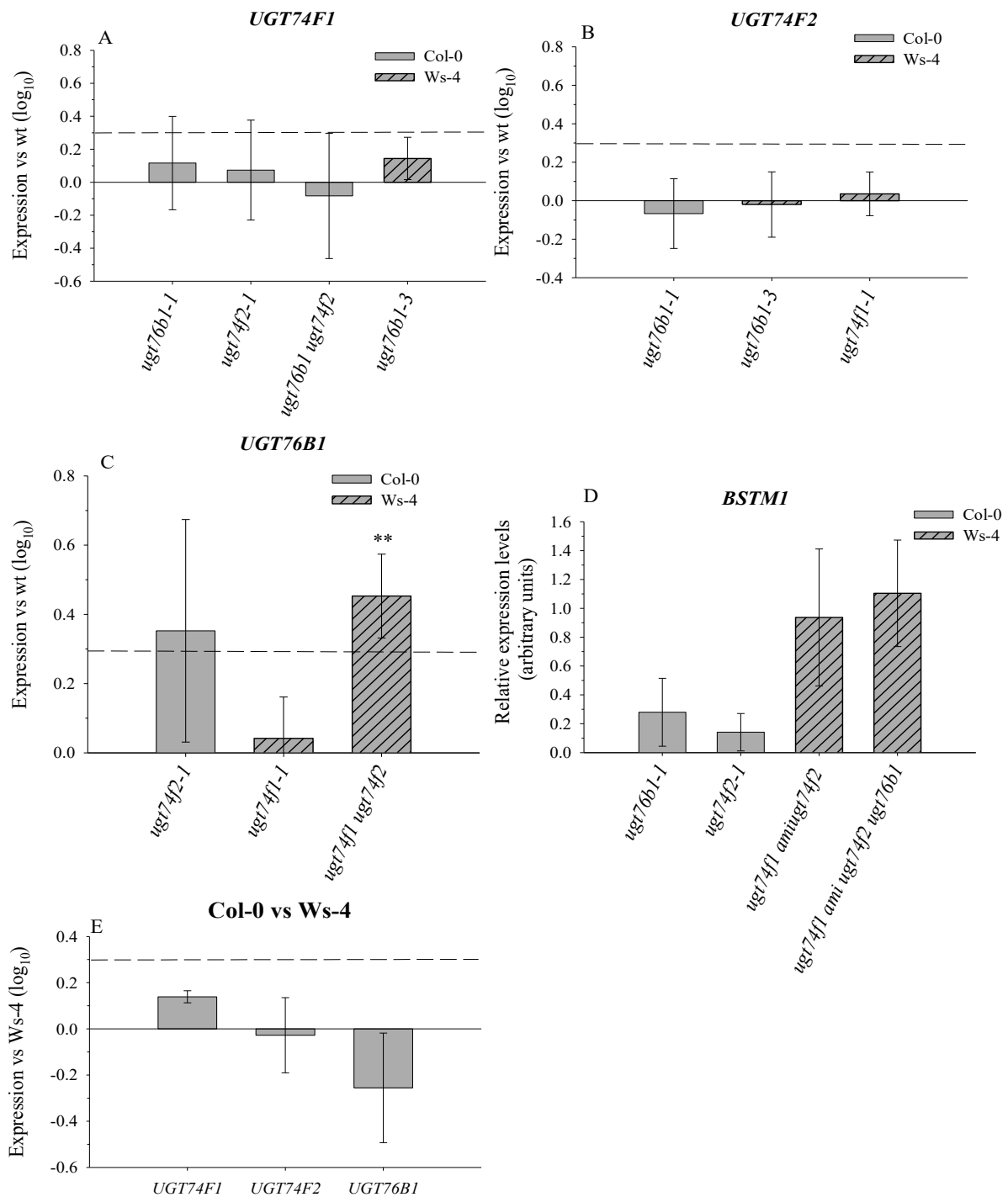


Figure 12. The expression levels of *UGT74F1*, *UGT74F2*, *UGT76B1* and *BSTM1* in BTH-treated *ugt* mutants.

Expression of *UGT74F1* (A), *UGT74F2* (B), *UGT76B1* (C) and *BSTM1* (D) in *ugt* mutants 24 h post BTH treatment. Expression levels of *BSTM1* were undetectable in control (wild-type) plants, thus Figure (D) demonstrates relative expression to reference genes (*S16* and *UBQ5*); expression of *BSTM1* was not detected in control plants. Figure (E) shows the difference between Columbia and Wassilewskija in expression of *UGT74F1*, *UGT74F2* and *UGT76B1*. Plants were grown for four weeks in short day conditions (10 h light, 14 h darkness). Expression levels were normalized to *UBIQUITIN5* and *S16*. Dashed lines indicate the twofold expression change. Bars represent arithmetic means and standard deviations from log₁₀ transformed data of three replicates. Asterisks indicate significance of the difference to the adequate wild-type line (A-C) and to Ws-4 (E); *P < 0.05.

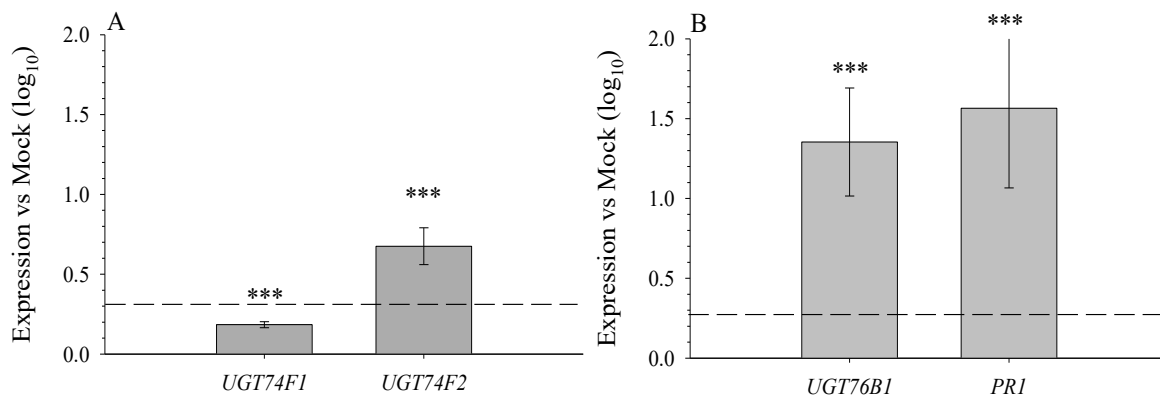


Figure 13. *UGT74F1*, *UGT74F2*, *UGT76B1* and *PRI* expression in Col-0 upon BTH treatment.

Expression of *UGT74F1*, *UGT74F2* (A) and *UGT76B1*, *PRI* (B) in Col-0 24 h post BTH treatment. Plants were grown and BTH sprayed together, RT-qPCRs for (A) and (B) were performed separately. Plants were grown for four weeks in short day conditions (10 h light, 14 h darkness). Expression levels were normalized to *UBIQUITIN5* and *SI6*. Dashed lines indicate the twofold expression change. Bars represent arithmetic means and standard deviations from log₁₀ transformed data of three replicates. Asterisks indicate significance of the difference to the Mock treated samples; ***P < 0.001.

2.1.5. Is *UGT74F1*-CDS driven by *UGT76B1* regulatory regions able to complement *ugt76b1-1* phenotype?

To further assess whether SA glucosylation by *UGT76B1* is its main role, a hybrid construct composed of the *UGT74F1* CDS fused with *UGT76B1* 5' and 3' regulatory regions (Fig. 14) was introduced into *ugt76b1-1* loss-of-function mutant. If the glucosylation of SA is the main role of *UGT76B1* the introduction of a known *in vivo* glucosyltransferase such as *UGT74F1* driven by the native *UGT76B1* regulatory regions should complement the phenotype of *ugt76b1* loss-of-function mutant.



Figure 14. Scheme of *UGT76B1* - *UGT74F1* hybrid construct *UGT76B1*_{pro}:*UGT74F1*_{cds}:*UGT76B1*_{3'-UTR}

A preliminary RT-qPCR analysis of such a hybrid complementation line demonstrated that *UGT74F1* CDS driven by *UGT76B1* regulatory regions is able to complement the changes in gene expression observed in *ugt76b1-1* (Fig. 15). This was demonstrated by the downregulation of the expression of *PRI*, *PR2*, *PR5*, *At1g04600* and *At2g33080*. Nevertheless, to confirm or deny this pilot result it will be necessary to apply more transgenic lines in the future study. Moreover, future studies should also examine whether a hybrid

complementation line can complement *ugt76b1* dependent enhanced resistance to biotrophs, accelerated senescence or elevated levels of SA and its conjugate.

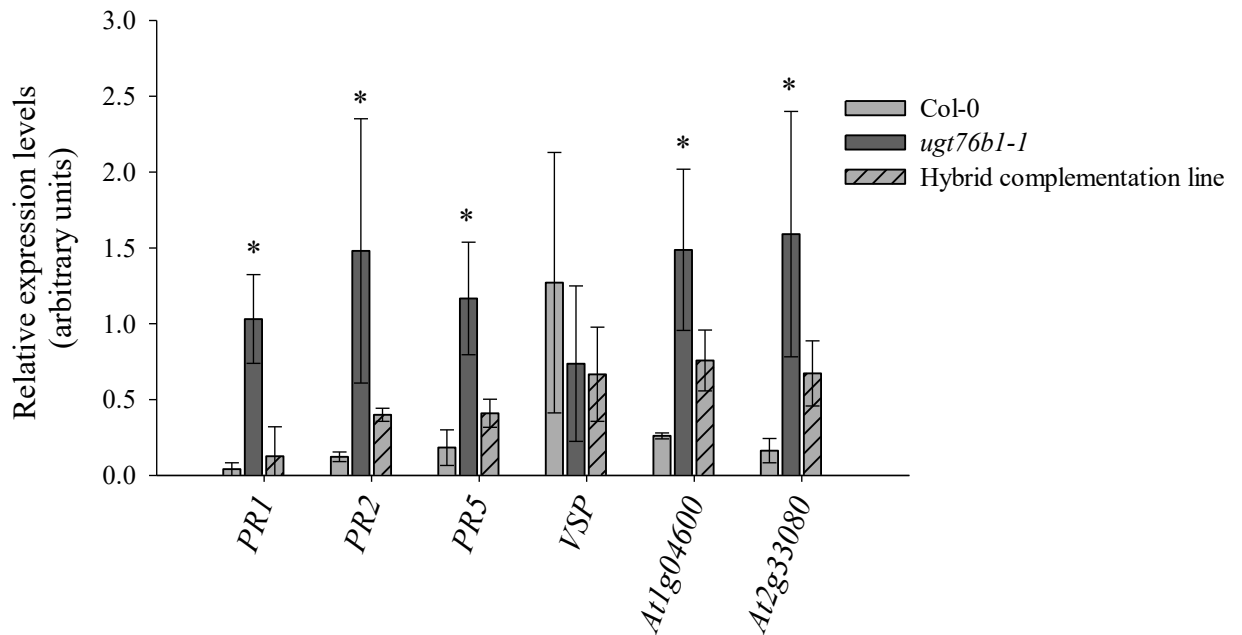


Figure 15. Marker genes expression in Col-0, *ugt76b1-1* and *ugt76b1-1* hybrid complemented line.

The expression of: *PR1*, *PR2*, *PR5*, *VSP*, *At1g04600*, *At2g33080* in Col-0, *ugt76b1-1* in a hybrid complementation line. Expression levels were normalized to *UBIQUITIN5* and *SI6*. Plants were grown for 4 weeks in short day conditions (10 h light, 14 h darkness). Bars represent arithmetic means and standard deviations from three replicates. Asterisks indicate significance of the difference to the Col-0 plants; $P < 0.05$.

Collectively this study confirmed that UGT76B1 utilizes SA as a substrate in Ws-4 ecotype. This was confirmed in aboveground tissues by the determination of SA and SA conjugates in *ugt74f1 amiugt74f2 ugt76b1* triple mutant. The root growth assay also substantiated the importance of UGT76B1 in SA conjugation in belowground, moreover it also demonstrated a potentially different role of UGT76B1 in this process. The role of UGT76B1 as an SA-conjugating enzyme in Col-0 ecotype cannot be fully confirmed at the moment. This is due to the lack of a full set of the mutants in this background. However, previous *in vitro* tests, root growth inhibition assay applied in this study and the pilot experiment with hybrid complemented line indicated that most possibly UGT76B1 conjugates SA also in Col-0 ecotype.

2.1.6. Analysis of sequence divergences between Col-0, Ws-4 and Ler in UGT76B1 region

Due to the fact of a different ratio of free and conjugated SA in Col-0 (Fig. 5), potential variations in the nucleotide sequences in *UGT76B1* region of Col-0, *Ler* and *Ws-4* alleles were examined. This analysis revealed that both 5'- and 3'-regulatory regions as well as *UGT76B1* coding sequence of *Ws-4* and *Ler* share a high level of similarity and differ from the Col-0 allele.

Nucleotide sequence analysis of 5'-UTR *UGT76B1* promoter region showed a relatively high number of single nucleotide polymorphisms (SNP) and deletions, which in most cases are shared by *Ws-4* and *Ler* accessions (Suppl. Fig. 1). Moreover, two big deletions encompassing 121 bp and 24 bp, are shared by *Ws-4* and *Ler* ecotypes (Fig. 16A). To further investigate the regions of *UGT76B1* promoter that are not present in *Ws-4* and *Ler in silico* search for *cis*-regulatory elements was performed. PlantCARE search engine (Lescot *et al.*, 2002) pointed out that the deleted region encompasses *cis*-regulatory regions such as CAAT-box and TATA-box (Fig 16B).

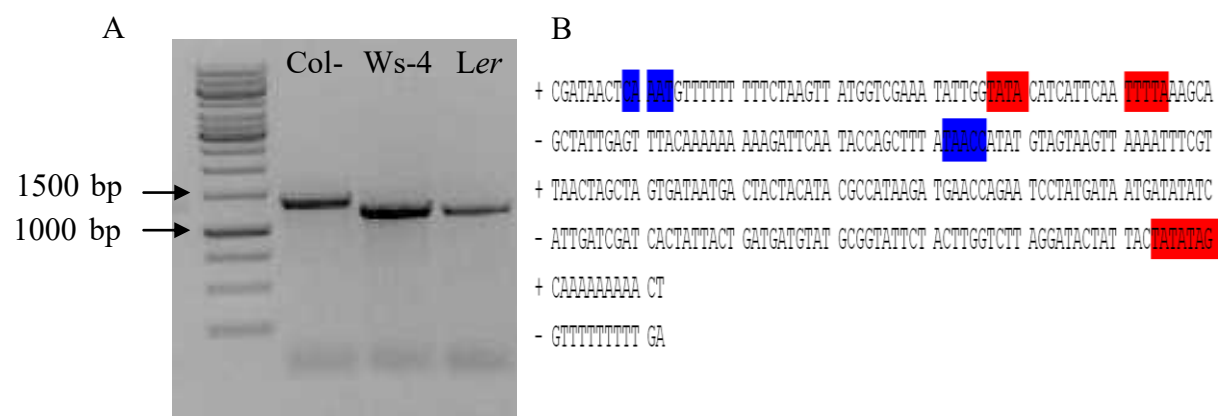


Figure 16. Comparison of the 5'-UTR region of *UGT76B1* in Col-0, Ws-4 and *Ler*.

(A) 1% agarose gel of the PCR amplified promoter region of *UGT76B1* of Col-0, *Ws-4* and *Ler* ecotypes. Shorter PCR products of the *Ws-4* and *Ler* promoter amplification confirm the presence of the deletions. Primers: 76B1_F-1200; 76B1_R150 (B) The double-stranded fragment of the *UGT76B1* promoter, present in the Col-0 promoter at - 482 bp to - 637 bp relative to the start codon, which is lost in *Ler* and *Ws-4* ecotypes with marked *cis*-regulatory regions; CAAT-box - blue, TATA-box - red. The presence of a TATA element on the minus strand may be related to an antisense gene expression (i.e. reverse to *UGT76B1*).

Further investigation of the *UGT76B1* promoter showed the presence of 19 mutations specific only for *Ws-4*, compared to Col-0 and *Ler* alleles (Table 1 and Suppl. Fig. 1). The analysis of

cis-regulatory elements (PlantCARE, Lescot *et al.*, 2002) demonstrated that the A deletion at the position -1129 and C-T substitution at the position -1133 up-stream of the start codon in the Ws-4 allele is responsible for the absence of an ATCT-motif (AATCTAAACT), located -1129 and -1139 bp up-stream of the Col-0 start codon (Suppl. Fig. 1-2). This motif belongs to the light-responsive elements (LREs), which are conserved DNA modules, mediating light-dependent gene activation (Desai and Hu, 2008; Roy *et al.*, 2012).

The analysis of the coding region of *UGT76B1* demonstrated a great sequence similarity between Ws-4 and *Ler* ecotypes. This was shown by the nine, exactly the same substitutions in *UGT76B1* coding sequence in Ws-4 and *Ler*, compared to Col-0 (Suppl. Fig. 3), which in consequence leads to the substitution of five amino acids (Fig. 17).

The 3'-UTR *UGT76B1* region of Ws-4 and *Ler* also significantly differ from the Col-0 ecotype. Based on publically available sequences a deletion of around 5.5 kb in Ws-4 and *Ler* was found (<http://1001genomes.org>, 09/2015). Its presence was first confirmed by PCR. For this purpose primers flanking the missing fragment were applied, which resulted in amplification of the product in Ws-4 and *Ler* (Fig. 18), thus confirming the presence of the deletion. Simultaneously, the analogous PCR, where Col-0 template was applied demonstrated that due to the fragment length it was not possible to obtain the product under the same PCR conditions (Fig. 18). The presence of the deletion was also confirmed by sequencing (Suppl. Fig. 4).

Table 1. Mutations in *UGT76B1* promoter region of Ws-4 allele.

The *Ler* sequence harbors nucleotides identical 5 the position relative to the start codon differs due to other changes in the promoter. Positions are indicated relative to the start codon of the Col-0 allele.

Position up-stream the start codon in Col-0 [bp]	Mutation in Ws-4	Position up-stream the start codon in Col-0 [bp]	Mutation in Ws-4
-997	C - T substitution	-1092	T -> G substitution
-1025	A deletion	-1093-1094	AA deletion
-1034	C deletion	-1097	A -> T substitution
-1040	T deletion	-1099	A -> T substitution
-1051	C deletion	-1109	A -> C substitution
-1064	T - C substitution	-1112	T deletion
-1066-1067	A C deletion	-1121	A -> T substitution
-1069	C - G substitution	-1129	A deletion
-1073	A deletion	-1133	C ->T substitution
-1090	A deletion		

```

Col METRETKPVI FLFPPLQGH LNPMPQLANI FFNRGFSITVIHTEFN SPNSSNFPHFTFVSI PDSLSE PESYPDVIEIL HDLNSKCVAPFGDCLK LISE EPTAACVIV DALWYFTHDLTE
Ws METRETKPVI FLFPPLQGH LNPMPQLANI FFNRGFSITVIHTKFN SPNSSNFPHFSFVSI PDSLSE PESYPDVIEIL HDLNSKCVAPFGDCLK LISE EPTAACVIV DALWYFTHDLTE

Col KFNFPRI VLRVTNLSAFVAFSKFHVLRREKGYLSLQETKADSPVPEL PYLRMKDLPWFQTEDPRSGDKLQIGVMKSLKSSSGIIFNAIEDLETDQLDEARIEFPVPLFCIGPFHRYVSASS
Ws KFNFPRI VLRVTNLSAFVAFSKFHVLRREKGYLSLQETKADSPVPEL PYLRMKDLPWFQTEDPRSGDKLQIGVMKSLKSSSGIIFNAIEDLETDQLDEARIEFPVPLFCIGPFHRYVSASS

Col SLLLAHDMTCLSWLDKQATNSVIYASLGSIASIDSEFLEI AWGLRNSNQPFLLWVVRPGLIHGKEWIEILPKGFIENLEGRGKIVKWA PQPEVLAHRATGGFLTHCGWNSTLEGICEAIP
Ws SLLLAHDMTCLSWLDKQATNSVIYASLGSIASIDSEFLEI AWGLRNSNQPFLLWVVRPGLIHGKEWIEILPKGFITKNLEGRCKIVKWA PQPEVLAHRATGGFLTHCGWNSTLEGICEAIP

Col MICRPSFGDQRVNARYINDVWKIGLHLENKVERLVIENAVR TLMTSSEGE EIRKRIMP KETVEQCLKLGSSFRNLENLIAYILSF
Ws MICRPSFGDQRVNARYINDVWKIGLHLENKVERLVIENAVR TLMTSSEGE EIRKRIMP KETVEQCLKLGSSFRNLENLIAYILSF

```

Figure 17. Alignment of UGT76B1 protein sequence of Col-0 and Ws-4 accessions.

Differences in amino acid sequence are marked in the red color. Nucleotide sequences derived from <http://1001genomes.org> (09/2015).

Further examination of the 3'-UTR of *UGT76B1* in Ws-4 and *Ler* indicated two genes (At3g11350, At3g11370) located downstream of *UGT76B1* in Col-0, which are lost due to the deletion in Ws-4 and *Ler*. They are encoding currently uncharacterized genes: a *PENTATRICOPEPTIDE REPEAT (PPR) SUPERFAMILY PROTEIN* and a *CYSTEINE /HISTIDINE-RICH C1 DOMAIN FAMILY PROTEIN*, respectively (Berardini *et al.*, 2015). Additionally, a similar comparison of the two other potential SA glucosyltransferases showed a very high level of similarity of *UGT74F1* coding sequence of Columbia, Landsberg *erecta* and Wassilewskija ecotypes. However, one mutation could be detected. The T to C substitution in the coding region of Wassilewskija accession (Suppl. Fig. 5) leads to the Leu to Pro substitution in *UGT74F1*. Nevertheless, due to the poor quality of the published sequences further analysis of *UGT74F1* and *UGT74F2* cannot be accomplished at this time point. Collectively, this study demonstrated that the accumulation of conjugated SA varies between the ecotypes. *Ler* and Ws-4 wild-type plants demonstrated a similar ratio of SA conjugates to SA aglycon, at the same time Col-0 this ratio was much higher. Moreover, since the SA in its free form was present at a similar level in all three ecotypes it indicates a potentially different activity of SA-conjugating enzymes in Col-0. However, the analysis of the *ugt76b1* loss-of-function mutants demonstrated that both Col-0 and *Ler* knock-outs respond in a similar way, which was shown by the increased abundance of SA-aglycon and SA conjugates. Although in a quantitatively different manner that was demonstrated by much higher levels of SA and SA conjugates in *ugt76b1-1* than in *ugt76b1-2*. In contrast to the other two alleles, in *ugt76b1-3* the glucosylation of SA does not seem to be affected.

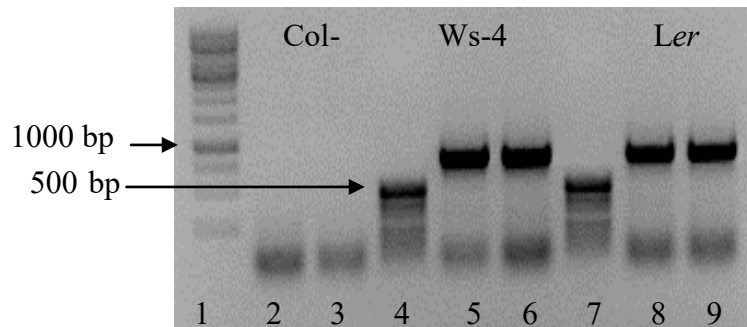


Figure 18. Deletion in 3'-UTR region of *UGT76B1* in *Ws-4* and *Ler*.

1% agarose gel of the PCR amplified products of the 3'-UTR region of *UGT76B1* of Col-0, *Ws-4* and *Ler* ecotypes. Primers: *UGT76B1_F1230*, *UGT76B1_R7600*. (1) 1 kb DNA Ladder, (2,3) Col-0, (4,7) pUC/MspI DNA Ladder, (5,6) *Ws-4*, (8,9) *Ler*. PCR with primers flanking the deletion led to the amplification of the product of about 800 bp in lanes 5, 6, 8, 9.

2.2. ILA as an *in vivo* substrate of *UGT76B1*

2.2.1. Simultaneous quantification of isoleucic, leucic and valic acid

In mammals, isoleucic acid (ILA), leucic acid (LA) and valic acid (VA) are described as the α -hydroxy acid degradation products of isoleucine (Ile), leucine (Leu) and valine (Val), respectively (Mamer and Reimer, 1992; Podebrad *et al.*, 1997). Isoleucic acid as a plant compound was first identified by von Saint Paul *et al.* (2011). Moreover, ILA was described as a small molecule, which actively impacts plant defense response (Zhang 2013, von Saint Paul *et al.*, 2011). Therefore, to further explore the role of ILA and other BCAA α -hydroxy acid derivatives an efficient GC-MS based method for simultaneous quantification of isoleucic acid (2-hydroxy-3-methylpentanoic acid), leucic acid (2-hydroxyisocaproic acid) and valic acid (2-hydroxy-3-methylbutyric acid) was developed.

2.2.1.1 Detection of isoleucic acid, leucic acid and valic acid in plant extracts

GC-MS analysis requires high sample volatility; therefore derivatization is a commonly applied method to render the compounds to be sufficiently volatile. In this study VA, LA and ILA standards were derivatized with BSTFA (N-bis (trimethyl-silyl) trifluoro-acetamide) containing 1% TMCS (trimethylchlorosilane) to their trimethyl silyl esters (Fig. 19 A-C). The quantification of ILA and LA was achieved in Single Ion Mode (SIM) by measuring the m/z 159.1 ($C_8H_{19}OSi$), after loss (dissociation reaction) of $C_4H_9O_2Si$ (m/z 117) from the parental ion m/z 276 ($C_{12}H_{28}O_3Si_2$). Whereas the quantification of VA by measuring m/z 145, after loss (dissociation reaction) of m/z 117 from the parental ion m/z 262. The efficiency of

derivatization was tested in separate reactions of the pure standards of VA, LA and ILA dissolved at 100 ng/ μ L BSTFA/TMCS. The abundance of each compound of interest was determined after 15, 30, 60 and 120 minutes of derivatization (Fig. 20A). This demonstrated that within the first 15 min VA, LA and ILA are rapidly derivatized to their trimethyl silyl esters, but the abundance was further slightly increasing when extending the incubation time. Therefore, all subsequent analyzes have been perceived by a 120-min-long derivatization step. Extracts from the freeze-dried *A. thaliana* rosette leaves have been used for development and validation of the method. Prior to extraction plant material was freeze-dried, without negatively impacting the stability of isoleucic acid (Fig. 20B). The metabolites of interest were extracted using 80% methanol, already pre-mixed with the first standard, 2-hydroxyhexanoic acid. The second standard, 4-nitrophenol was added prior to derivatization. It was demonstrated that the applied internal standards do not co-elute with VA, LA and ILA (Supp. Fig. 6). Moreover, 4-nitrophenol has not been detected in plant extracts, whereas 2-hydroxyhexanoic acid exists in a concentration, which is close to its limit of detection (Fig. 20 C-D). Metabolites including 2-HAs were concentrated and partially purified from other, co-extracted molecules negatively impacting detection and quantification by separation on a weak anion exchange column. The method was further validated to determine the concentration of all three BCAA derivatives in four-week-old *A. thaliana* (Fig. 20F-G) (SIM chromatogram of two-week-old *A. thaliana* - Suppl. Fig. 6). Both, ILA and LA could be simultaneously detected and quantified, yet at very different levels (Fig. 20F-G). The VA abundance could not be determined due to its levels below the detection limit. Nevertheless, the position based on the pure standard elution time of VA is indicated by asterisk (Fig. 20G). Method sensitivity was examined by spiking ILA standard into the plant extract at the following final concentrations: 0.05 ng/ μ L; 0.1 ng/ μ L; 0.15 ng/ μ L; 0.2 ng/ μ L; 0.25 ng/ μ L; 0.3 ng/ μ L; 0.5 ng/ μ L; 1 ng/ μ L; 5 ng/ μ L; 10 ng/ μ L (Fig. 20E). This demonstrated that even slight variations of ILA abundance can be monitored by this method. The limits of detection (LOD) of ILA and LA in *A. thaliana* extracts are 2.13×10^{-2} ng/ μ L and 5.6×10^{-4} ng/ μ L, respectively.

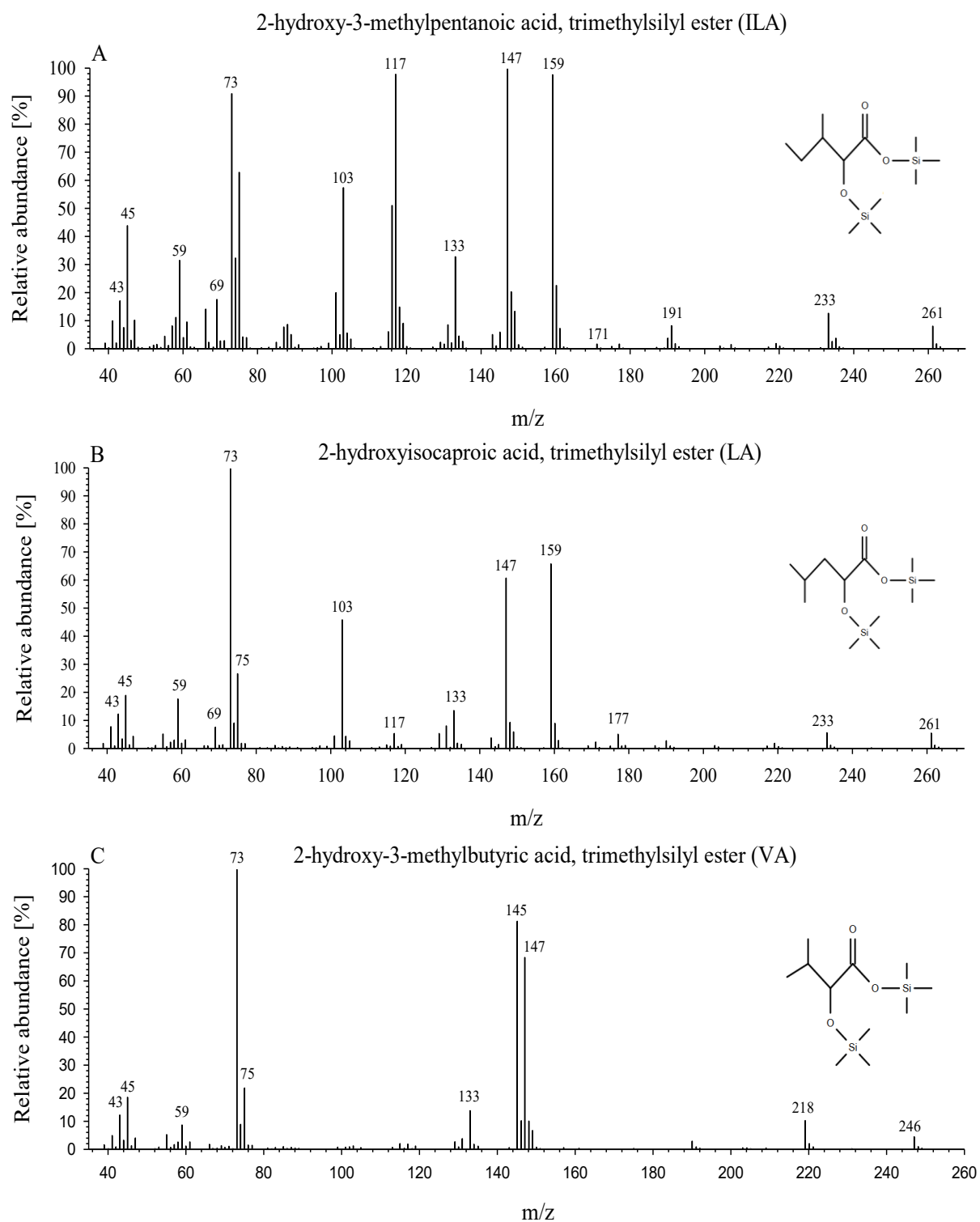


Figure 19. Mass of spectrum isoleucic (ILA), leucic (LA) and valic (VA) acid.

Mass spectrum for the trimethylsilyl derivatives products for ILA (A), LA (B) and VA (C).

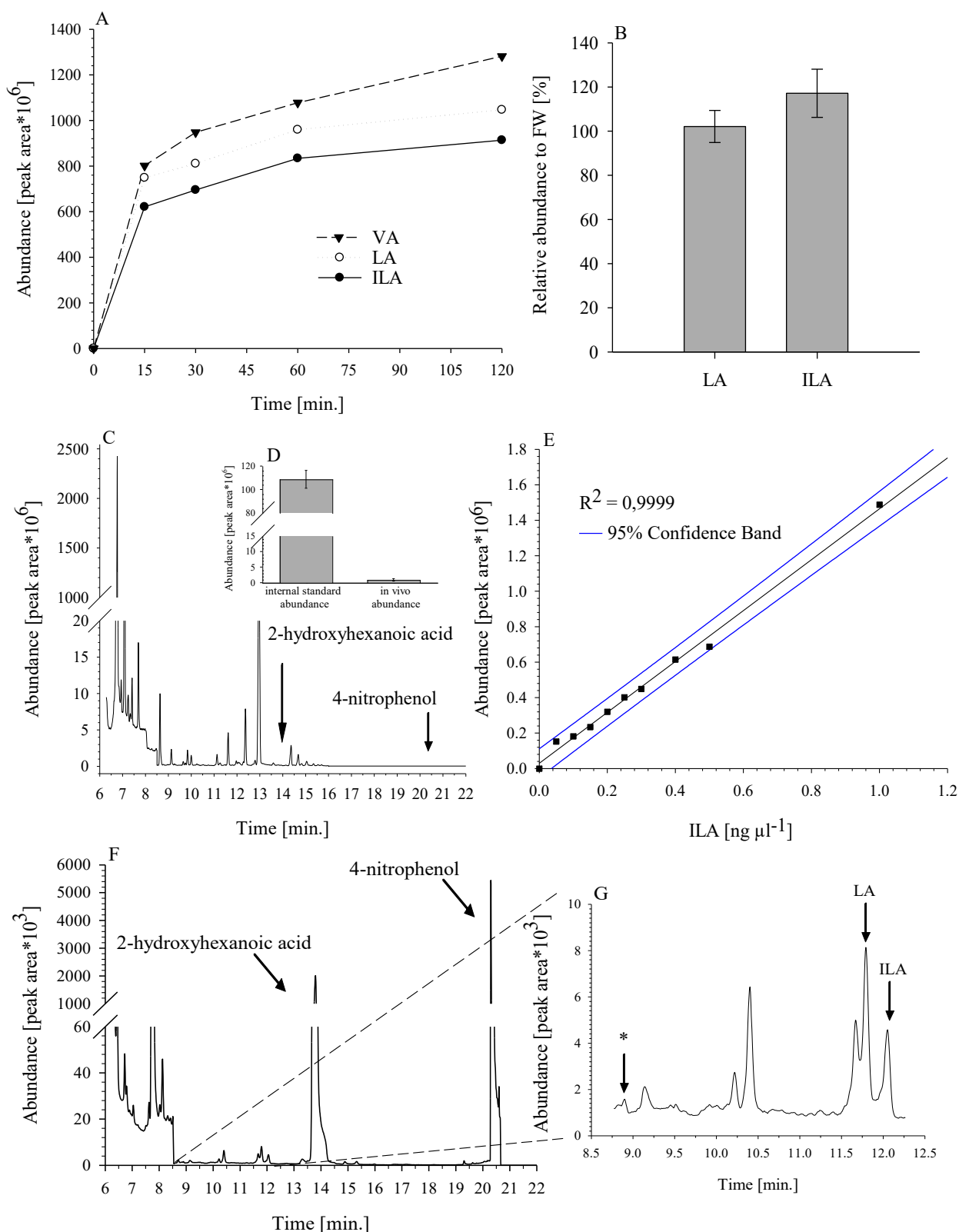


Figure 20. Optimization of detection method for VA, LA and ILA.

(A) Time dependent derivatization of VA, LA, and ILA. (B) Impact of freeze-drying of plant material on LA and ILA. Plant material was harvested, grinded in liquid N₂, then split into equal batches from which one directly used for metabolite extraction and the second one was lyophilized prior metabolite extraction. The measured levels of LA and ILA were related to FW. Bars represent arithmetic means and standard errors from three replicates. Legend continues on the next page.

(C) SIM chromatogram of *A. thaliana* extract, arrows indicate the positions where internal standards would elute, if they were spiked in. (D) Endogenous levels of 2-hydroxyhexanoic acid in comparison to the internal standard concentration. Bars represent arithmetic means and standard errors from three replicates. (E) Calibration curve of ILA (F) SIM chromatogram of LA and ILA. (*) indicates the probable position of the VA peak.

2.2.2. UGT76B1 recombinant protein glucosylates ILA and LA *in vitro*

To elucidate the ability of UGT76B to glucosylate both ILA and LA, its activity to conjugate these two compounds was tested *in vitro* and determined by the aglycon decrease. A two hours incubation of UGT76B1 recombinant protein in presence of UDP-glucose and ILA as the substrate resulted in 64% decrease of the aglycon (Fig 21A). In the analogous reaction involving LA as the substrate, only a moderated decrease of the aglycon could be detected (Fig. 21B). This demonstrated that both ILA and LA are accepted by UGT76B1 *in vitro*, nevertheless ILA seems to be converted to its conjugated form more efficiently than LA.

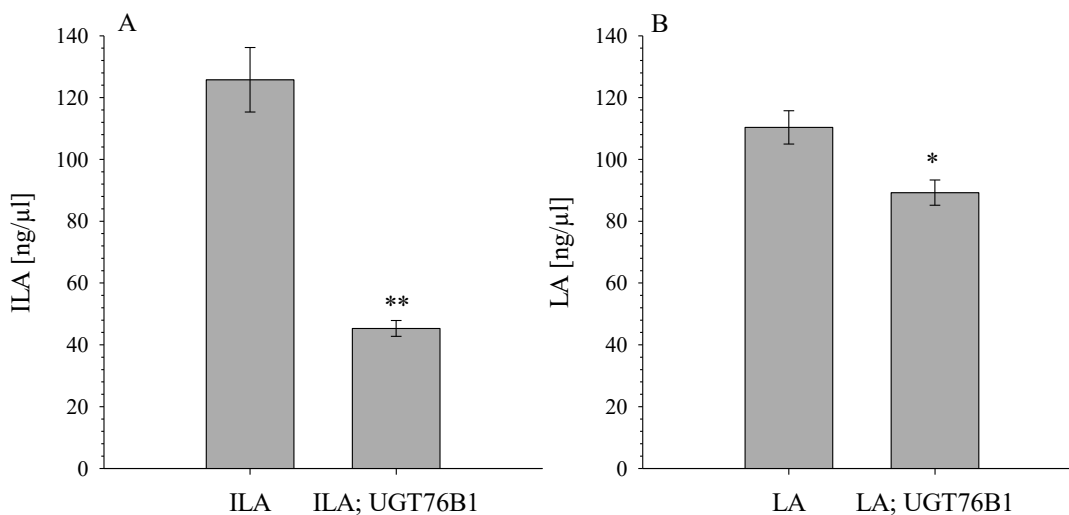


Figure 21. UGT76B1 is able to conjugate both ILA and LA *in vitro*.

The decrease of UGT76B1 substrates: (A) ILA and (B) LA (in ILA equivalents) after two hours of *in vitro* conjugation reaction (for conditions see methods). Bars represent arithmetic means and standard errors obtained from three replicates. Asterisks indicate significance of the difference to the control (reaction mix without UGT76B1 recombinant protein); *P value < 0.05; **P value < 0.01.

2.2.3. ILA as an *in vivo* substrate of UGT76B1

ILA glucoside abundance in the leaves had been shown to be correlated with the level of *UGT76B1* expression (von Saint Paul *et al.*, 2011). Previously, it had been also demonstrated in our laboratory that *UGT76B1* displays the highest expression level in the root. In aboveground tissues the expression of *UGT76B1* is decreased and depends on the age –

reaching the highest level in very young leaves, whereas showing a strong reduction in four-week-old plants (von Saint Paul *et al.*, 2011). To further assess whether ILA is an *in vivo* substrate of UGT76B1 the abundance of the aglycon in *ugt76b1-1* and *UGT76B1-OE7* as well as in Col-0 plants was determined. Furthermore, in this study the expression pattern of *UGT76B1* and the developmental stage were also taken into the account.

2.2.3.1. *UGT76B1* expression negatively affects ILA abundance in the above- and below-ground tissues

Rosettes and roots of plate grown *A. thaliana* seedlings were used in this study. The determination of ILA aglycon showed that its abundance is correlated with the expression of *UGT76B1*. Elevated levels of free ILA were detected in *ugt76b1-1*, whereas decreased levels in *UGT76B1-OE7* in the shoot (Fig. 22A) as well as in the root tissues (Fig. 22B). Therefore, it may suggest ILA as an *in vivo* substrate of UGT76B1. Furthermore, higher levels of ILA were observed in the root, compared to the leaf tissues. At the same time, LA was not affected in the *ugt76b1-1* and *UGT76B1-OE7* lines (Fig. 22C-D). However, similarly like ILA, leucic acid also showed elevated levels in the roots.

2.2.3.2. Isoleucic and leucic acid abundance is affected during the plant growth and development

Since the expression of *UGT76B1* in the aboveground tissues is affected by the age (von Saint Paul *et al.*, 2011), it was determined, if ILA also shows the tendency to vary during plant growth and development. Indeed, rosettes of two-week-old soil grown *A. thaliana* displayed the highest level of ILA, whereas ILA decreased in three-week-old plants and did not further change in four-week-old plants (Fig. 23A). Moreover, two-week-old *A. thaliana* plants displayed the most pronounced increase of unconjugated ILA in *ugt76b1-1* in comparison to *UGT76B1-OE7* and Col-0. The previously observed correlation between ILA abundance and *UGT76B1* expression was only slightly visible in the third and fourth week of the plant growth. The abundance of LA was also determined and interestingly it showed a different correlation (Fig. 23B). LA abundance, in contrast to ILA, displayed a positive correlation with *A. thaliana* age, presenting the highest level in four-week-old, whereas the lowest in two-week-old plants.

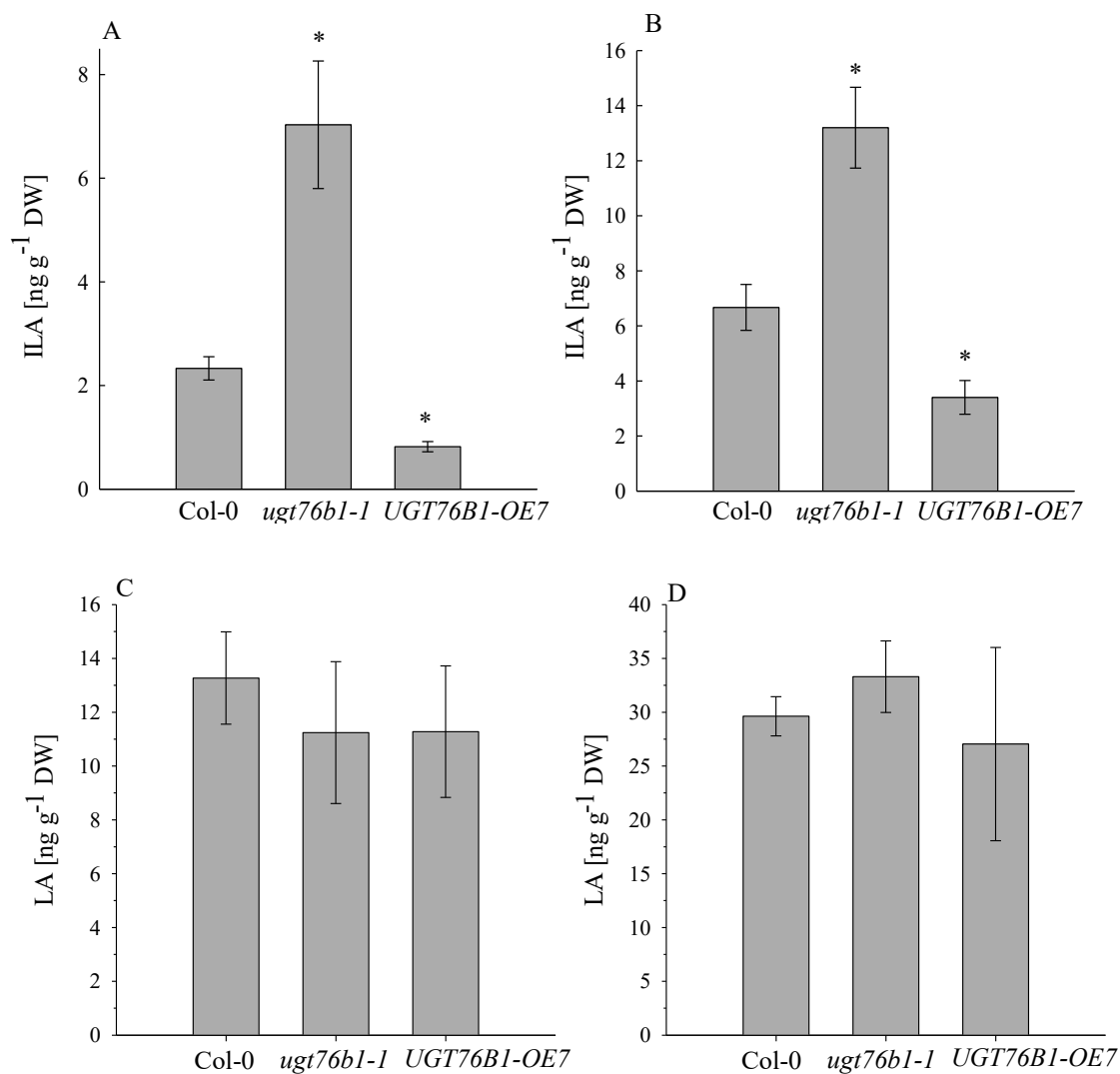


Figure 22. The abundance of unconjugated ILA and LA in above- and below-ground tissues in three-week-old seedlings of Col-0, *ugt76b1-1* and *UGT76B1-OE7*.

Levels of free ILA in the shoot (A) and in the root (B) and free LA (in ILA equivalents) in the shoot (C) and in the root (D) in three-week-old plants (Col-0, *ugt76b1-1* and *UGT76B1-OE7*) grown on Gelrite plates in short day conditions (10 h light, 14 h darkness). Bars represent arithmetic means and standard errors obtained from four replicates. Asterisks indicate significance of the difference to Col-0; *P value < 0.05.

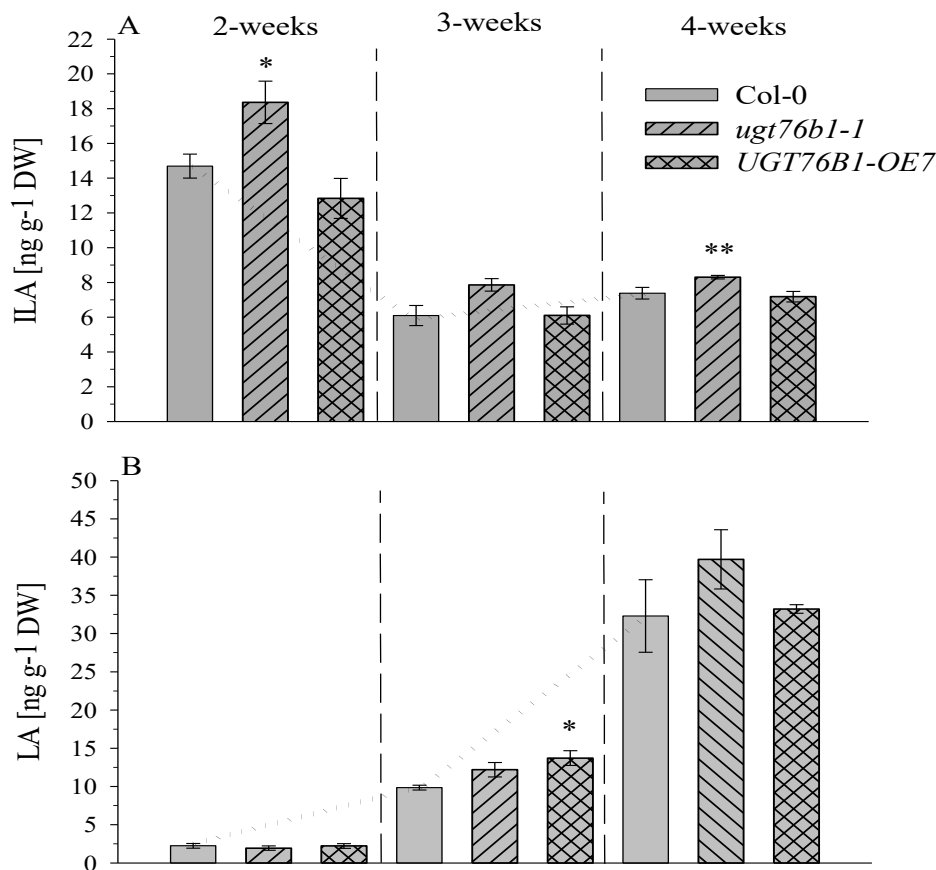


Figure 23. ILA and LA abundance during plant growth and development.

Levels of free ILA (A) and LA (in ILA equivalents) (B) in leaves of two-, three- and four-week old plants (Col-0, *ugt76b1-1* and *UGT76B1-OE7*). Plants were grown on soil in short day conditions (10 h light, 14 h darkness). Bars represent arithmetic means and standard errors obtained from four biological replicates. Asterisks indicate significance of the difference to Col-0; *P value < 0.05; **P value < 0.01. Dotted lines indicate the age dependent changes of ILA and LA abundance.

2.2.4. ILA and LA are differently affected by the biotrophic pathogen *P. syringae*

Previously it was demonstrated that isoleucic acid positively impacts plant defense (von Saint Paul *et al.*, 2011). Therefore, the impact of a biotrophic pathogen on endogenous ILA level was further explored. Infection with *P. syringae avrRpm1* (Fig. 24A) and *P. syringae DC3000* (Fig. 24C) triggered a decrease of ILA abundance in Col-0 plants. Interestingly, the same response could be observed in *ugt76b1-1* mutant plants, which indicates that the decrease of ILA in response to *P. syringae* occurs independently from UGT76B1. In contrast to ILA, the chemically very similar compound, LA was not affected by *P. syringae* in plants of wild-type and *ugt76b1-1* (Fig. 24B and 24D).

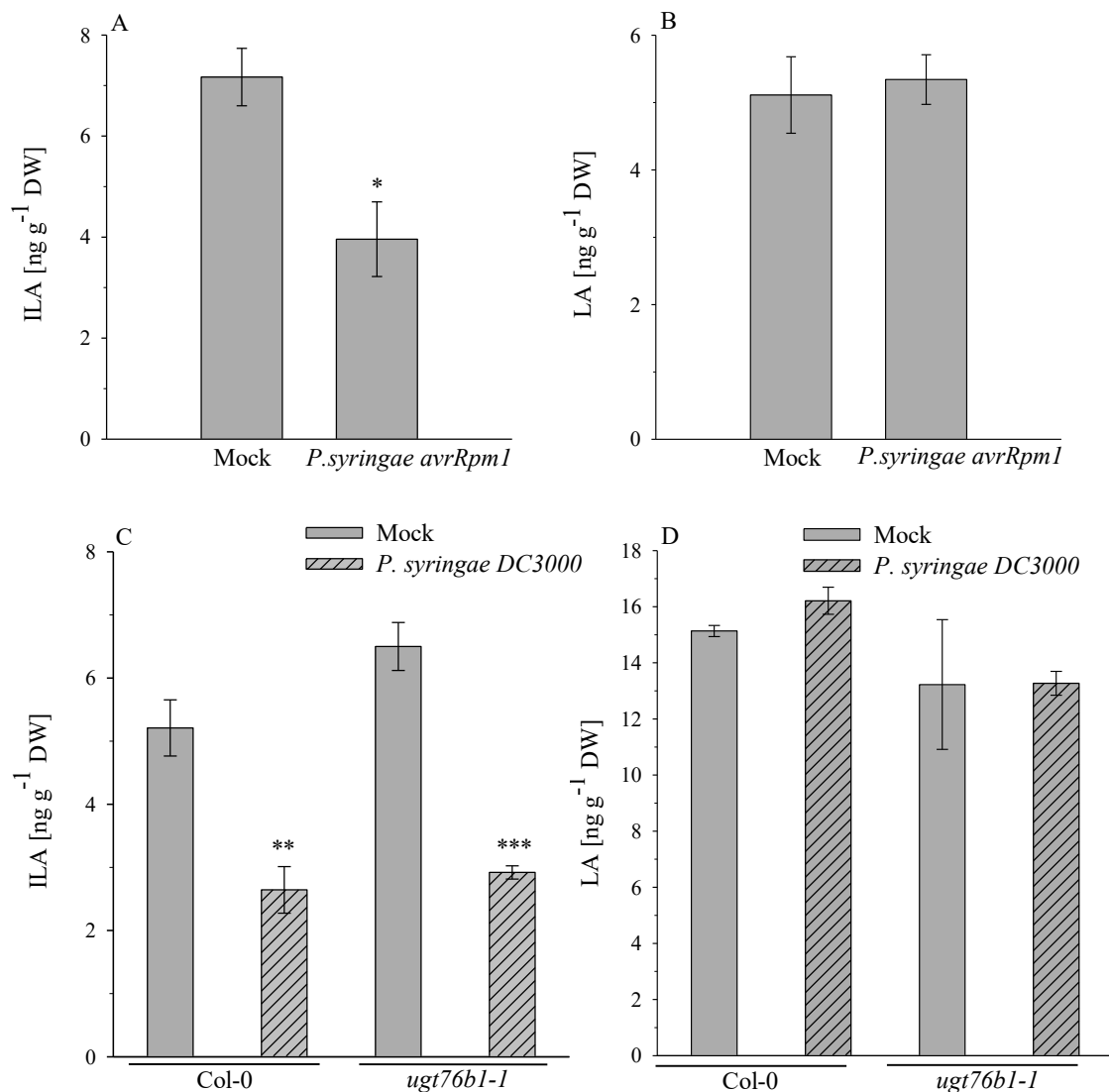


Figure 24. ILA and LA abundance in response to *P. syringae* infection.

Levels of free ILA (A) and LA (in ILA equivalents) (B) in four-week Col-0 24 h post *P. syringae avrRpm1* infection. Levels of free ILA (C) and LA (in ILA equivalents) (D) in plants of four-week Col-0 and *ugt76b1-1* 24 h post *P. syringae DC3000*. For both experiments plants were grown on soil in short day conditions (10 h light, 14 h darkness). Bars represent arithmetic means and standard errors obtained from four replicates. Asterisks indicate significance of the difference to the mock treated control; **P value < 0.01; ***P value < 0.001.

2.2.5. ILA as a ubiquitous compound in plants

Previous infection studies demonstrated that ILA plays a role in promoting defense response to the biotrophic pathogens in *A. thaliana* (von Saint Paul *et al.*, 2011). Therefore different monocot and dicots plants were examined whether they also contain ILA. Moreover, the abundance of the two other 2-HA derivatives, VA, and LA was examined as well. All three α -hydroxy acids could be simultaneously detected only in *Populus x canadensis*, *Hordeum vulgare* and *Solanum lycopersicum* (Fig. 25-26). The quantification of 2-HAs demonstrated

that ILA in contrast to the other molecules of interest is a prevalently existing compound in plants and was detected in all examined species (Fig. 26A-C). Therefore, taking into the account the impact of ILA on the defense response observed in *Arabidopsis*, this may suggests that ILA could have a common function as a resistance modulator also in other plant species.

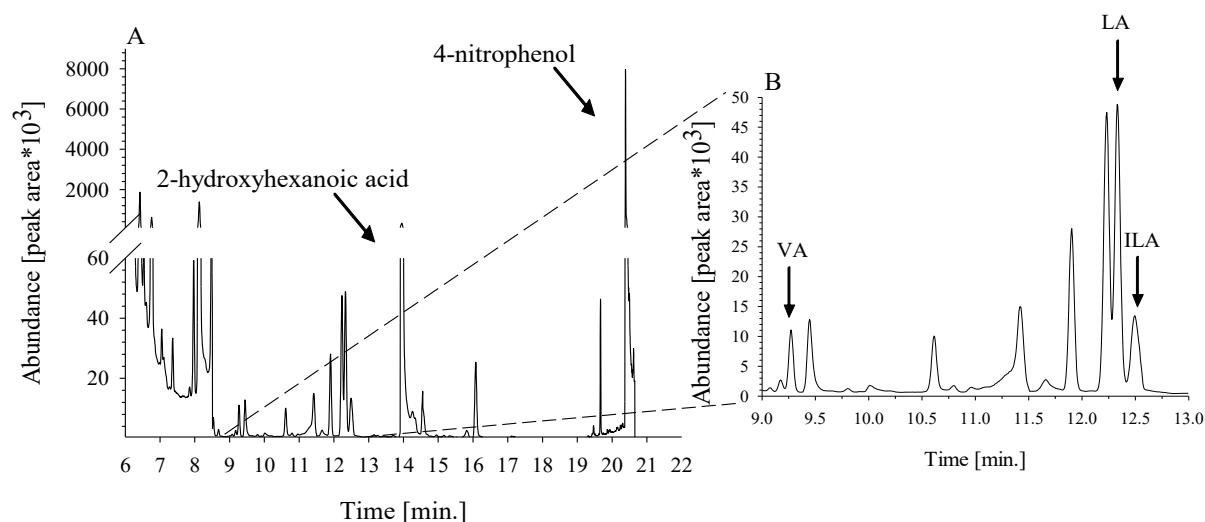


Figure 25. Simultaneous detection of VA, LA, and ILA in *Populus x canescens* extracts.

(A, B) SIM chromatogram of VA, LA and ILA in poplar.

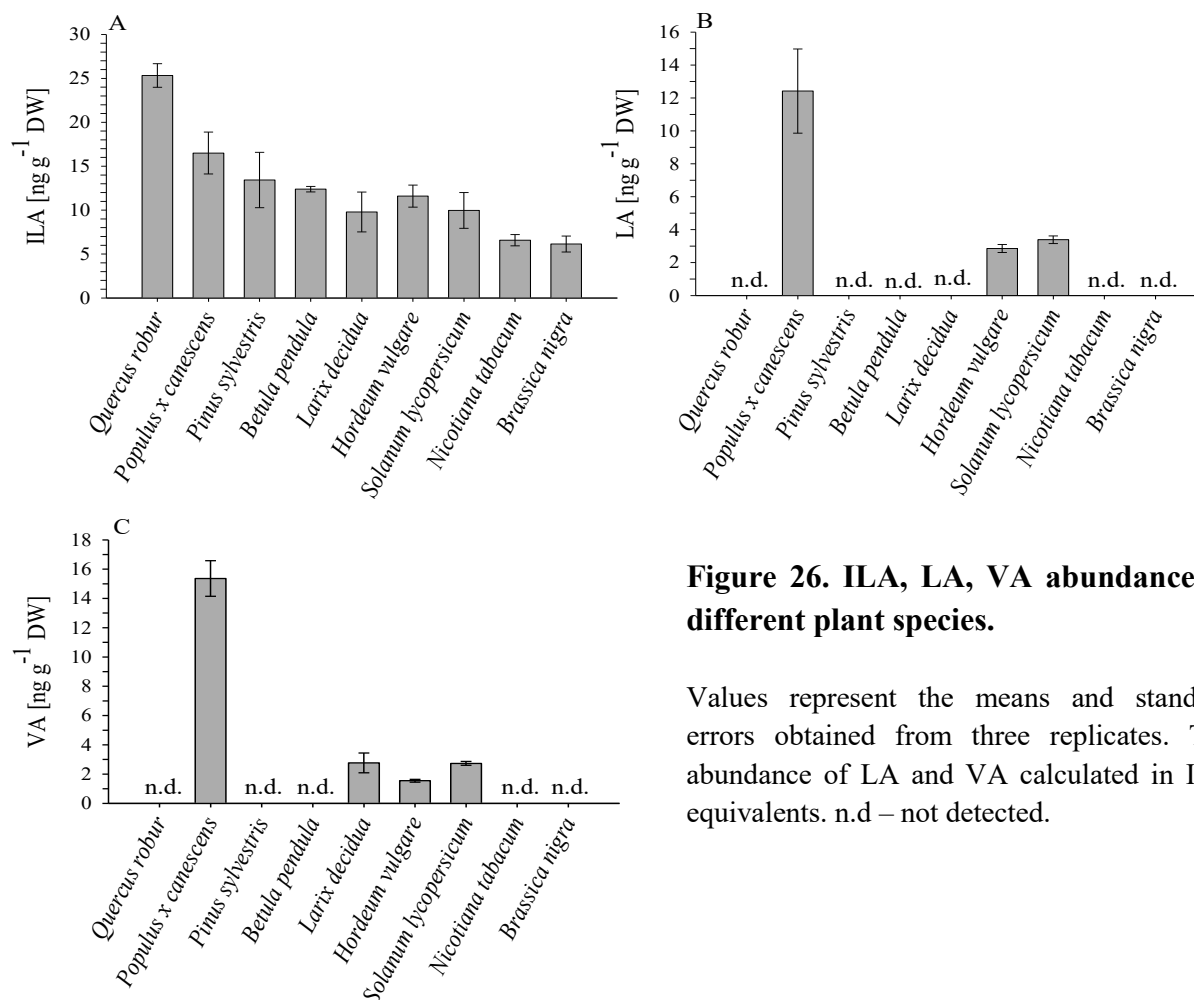


Figure 26. ILA, LA, VA abundance in different plant species.

Values represent the means and standard errors obtained from three replicates. The abundance of LA and VA calculated in ILA equivalents. n.d – not detected.

2.3. Genetic screen for identification of genes involved in 2-hydroxy-3-methyl-pentanoic (ILA) acid sensitivity

It was demonstrated that exogenous ILA application can positively impact defense, whereas it negatively affects *Arabidopsis* root growth. Although the first aspect is already partially explored, the way how ILA influences root growth remains still unclear. Von Saint Paul *et al.* (2011) demonstrated a positive correlation of *UGT76B1* expression and enhanced root growth resistance. Nevertheless, it is still not known how ILA is perceived and which pathway or pathways are influenced by its action. To address this issue the ability of ILA to inhibit root growth was applied in two different types of genetic screens. Genome-wide association study (GWAS), which uses the natural sequence variation in the population of different ecotypes to associate the regions in the genome with the particular trait, i.e. here with the resistance to the compound inhibiting root growth. Altered sensitivity towards ILA could indicate and identify loci or genes, which are related to perception and/or metabolism of ILA. In the second screen, the root growth response of T-DNA insertion mutants in the presence of ILA has been monitored for increased root growth resistance and preliminary for hypersensitivity.

2.3.1 Genome-wide association study for genes affected by exogenous ILA

A population of 179 *A. thaliana* Swedish accessions (received from Magnus Nordborg, GMI Vienna) was grown on $\frac{1}{2}$ MS media containing 500 μ M ILA to determine the potential regions in the genome that may contain genes involved in the root growth response to exogenous ILA (Long *et al.*, 2013). The accession for which both control and ILA-treated plants germinated were used in further steps (Supplementary Table 1). Additionally, due to the lack of good quality sequencing data, two other accessions were excluded from further analysis. Following this requirements, 159 natural accessions were included in association mapping. *UGT76B1-OE7*, the line displaying reduced root growth susceptibility in presence of ILA was applied as the reference in this study. Root lengths of each accession were first normalized among each growth plate to the reference line (same for control and ILA plates) in order to eliminate possible plate-specific, not treatment-dependent root growth variations. Finally GWAS input dataset was prepared as the ratio of ILA-treated to untreated plants (analysis done by Arthur Korte, GMI Vienna). The whole population of *A. thaliana* accessions implemented in this study displayed root growth inhibition in the presence of ILA. Moreover, among the studied population a very high diversity of root growth response could be observed (Fig. 27).

In the population of 159 *A. thaliana* natural accessions implemented in this study there are roughly 3.7×10^6 segregating SNPs. The appropriate GWAS analysis was preceded by the association analysis of control ($\frac{1}{2}$ MS grown plants) and treatment (500 μ M ILA grown plants) conditions, separately. These additional steps could lead to identification of potential false associations that might have occurred due to the growth conditions. GWAS for control growth conditions did not show any significant hits (Fig. 28A). For treatment conditions (500 μ M ILA), no obvious peak could be observed (Fig. 28B). The genome-wide association for ILA-grown plants related to untreated control enabled to identify one hit at position 11132605 on chromosome 1 (Fig. 28C). Although the identified plot does not reach the permutation threshold (black, dashed line), due to its morphology it should not be excluded as invalid. Moreover, a similar situation was observed for some of the genes responsible for flowering time (Seren *et al.*, 2012). Figure 28D shows linkage disequilibrium structure of the leading SNP at the position 11132605.

Zooming into the associated region (Fig. 29) and taking into the account that the potential genes of interest could be located in the range from 20 kb down-stream to 20 kb up-stream of the leading SNP, revealed seven candidate genes (Table 2) that might be considered as being involved in response to ILA.

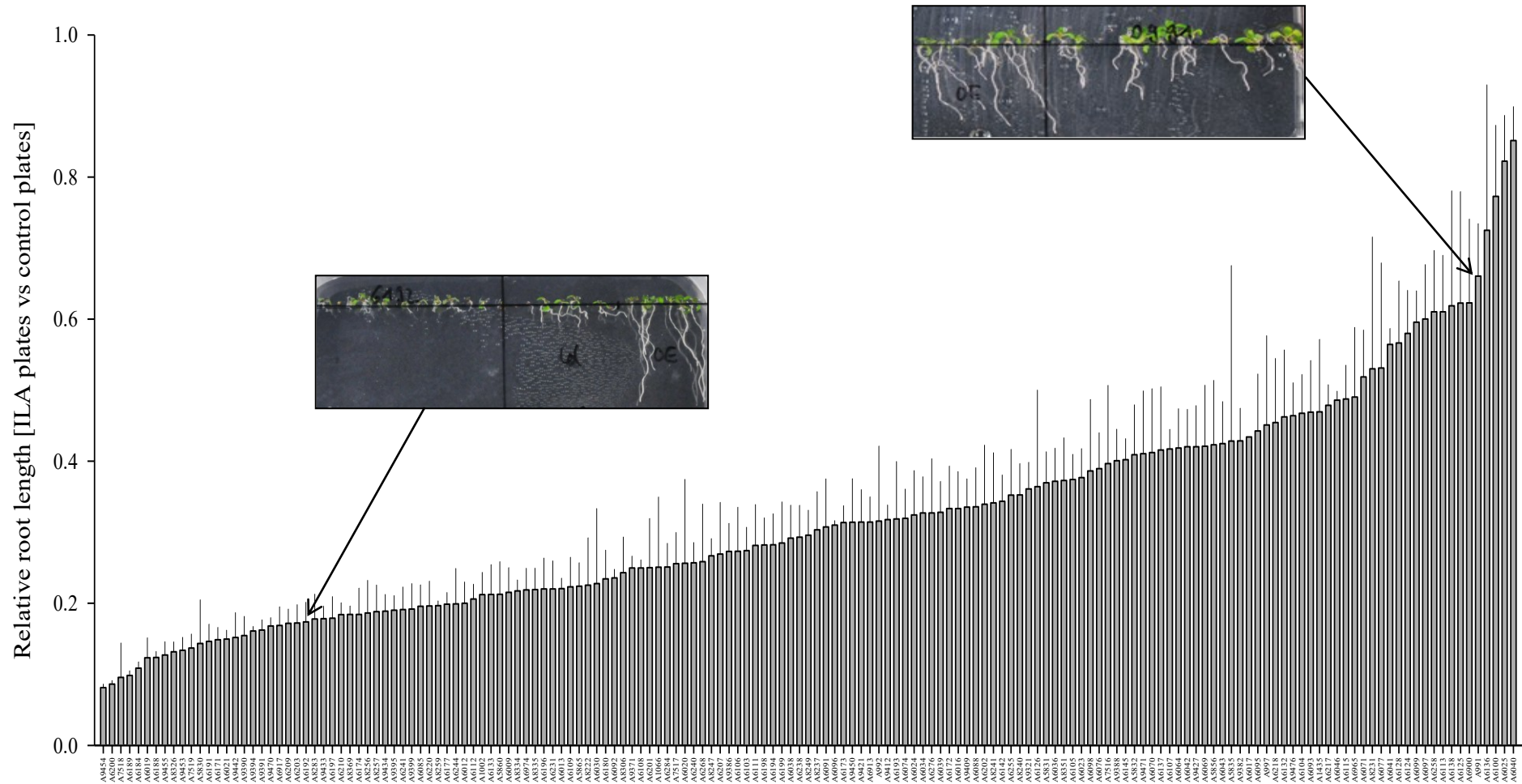


Figure 27. Differential root growth inhibition among 161 natural *A. thaliana* accessions in presence of ILA.

Plants were grown seven days on vertical square plates in long day conditions (16 h light and 8 h darkness). Root lengths were calculated using ImageJ software and normalized to the reference line on each plate, then related to the control plants grown in parallel on ½ MS plates without ILA.

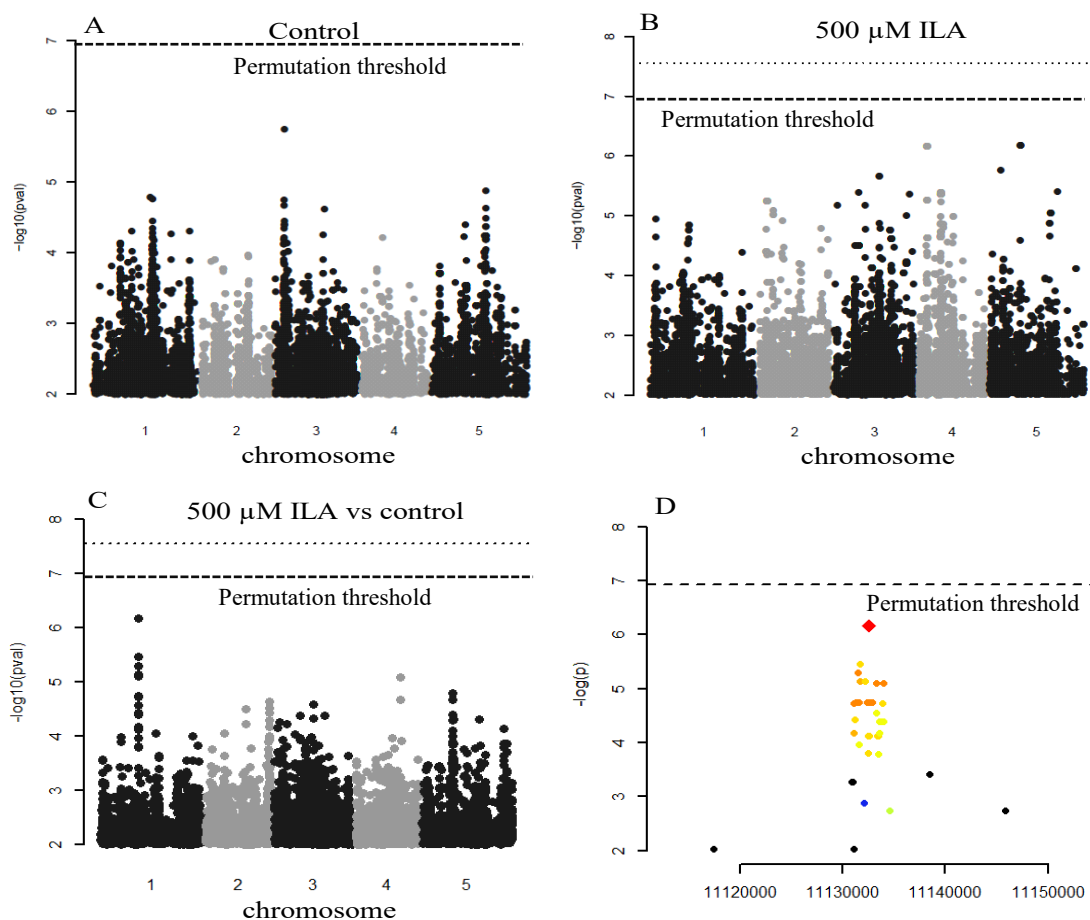


Figure 28. Genome-wide association study for genes responsible for ILA-sensitive root growth.

GWAS of 159 *A. thaliana* accessions. (A) GWAS for control conditions (B) GWAS for ILA treatment conditions (C) GWAS for ILA vs. control conditions (D) The structure of the leading SNP. Plants were grown seven days on vertical square plates in long day conditions (16 h light and 8 h darkness). Root lengths were calculated using ImageJ software and normalized to reference line on each plate, then related to the control plants grown on $\frac{1}{2}$ MS plates without ILA. A dashed line shows the 5% FDR threshold.

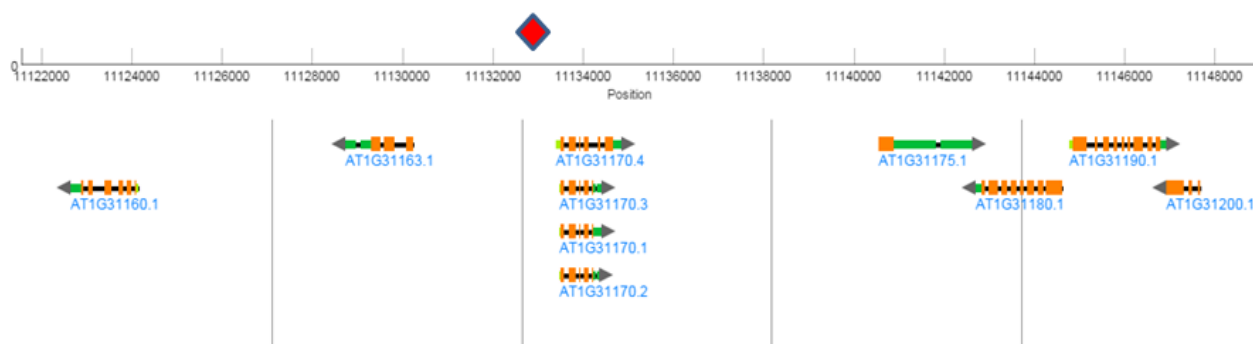


Figure 29. Region of chromosome 1 with genes potentially affecting ILA sensitivity.

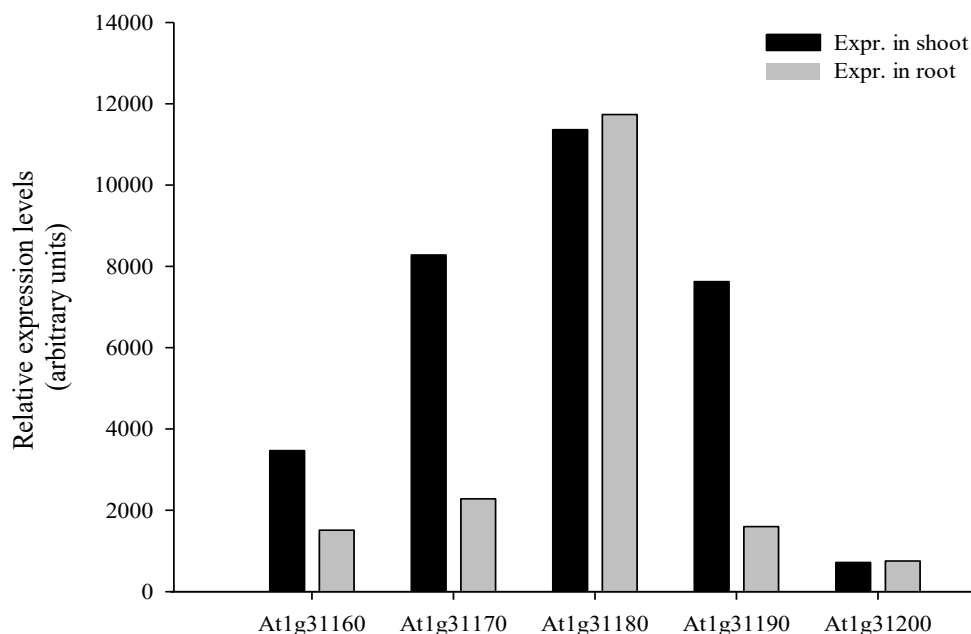
An overview of the GWAS associated region of chromosome 1. Leading SNP at position 11132605 is marked as a red/blue square.

Table 2. GWAS genes potentially involved in ILA response.

AGI code	Annotation (TAIR)
At1g31160	<i>HINT2 - HISTIDINE TRIAD NUCLEOTIDE-BINDING 2</i>
At1g31163	<i>F-box associated ubiquitination effector family protein</i>
At1g31170	<i>SRX - SULFIREDOXIN</i>
At1g31175	Unknown protein
At1g31180	<i>IMD3 - ISOPROPYLMALATE DEHYDROGENASE 3</i>
At1g31190	<i>IMPL1 - MYO-INOSITOL MONOPHOSPHATASE LIKE 1</i>
At1g31200	<i>PP2-A9 - PHLOEM PROTEIN 2-A9</i>

2.3.1.1. Spatial expression pattern of GWAS associated genes

Since the ILA GWAS was based on the root growth inhibition, it was examined if the associated genes are expressed in the root tissues. Public microarray data (dataset available for five out of seven genes of interest) indicated that two GWAS genes are expressed at least at the same level in the root and the shoot: *IMD3* (At1g31180) and *PP2-A9* (At1g31200). The other three genes: *HINT2* (At1g31160), *SRX* (At1g31170) and *IMPL1* (At1g31190) display higher expression in the shoot than in the belowground tissues (Fig. 30).

**Figure 30. Expression of *HINT2*, *SRX*, *ATIMD3*, *HINT2*, *ATPP2-A9* in the root.**

Relative expression of *HINT2* (At1g31160), *SRX* (At1g31170) *ATIMD3* (At1g31180), *IMPL1* (At1g31190), *ATPP2-A9* (At1g31200) in the root and in the shoot. Expression data derived from Genevestigator, ATH1 Genome Array (<https://genevestigator.com/gv/02/2016>).

2.3.1.2. Correlation of single nucleotide polymorphism with ILA root growth response

For a more detailed investigation of the GWAS-associated region, the top 10 resistant as well as the top 10 susceptible accessions were aligned in order to identify and localize SNPs potentially responsible for different root growth response to ILA. Alignment of the whole GWAS region showed that the coding sequence of *SRX* (AT1G31170) displays the expected correlation between nucleotide polymorphism and root growth response to ILA (Fig. 31). This could be explained by the fact that *SRX* is localized in the closest neighborhood to analyzed GWAS peak. Further examination of the GWAS region did not show a similar correlation for the other genes.

Having a closer look on the detected SNPs and their position, it appeared that seven out of eight SNPs are located in the intron and are not involved in potential cryptic splice sites (Fig. 31A). The SNP No. (1) is a wobble in the *SRX* open reading frame without affecting the encoded amino acid serine. Mutations that result in synonymous codon substitutions are so called silent SNPs. Kimchi-Sarfaty *et al.* (2007) demonstrated that silent SNP can influence protein folding and in consequence its function, which was proven by changed substrate specificity of a P-glycoprotein. Further analysis of the identified SNPs revealed that SNP No. (8) (Fig. 31A) is potentially responsible for the loss of donor splicing site, which occurs due to the A to G substitution in the group of accessions with the increased sensitivity to ILA. This substitution was predicted to eliminate the catalytic A residue required for the cleavage of the donor site of the third intron of *SRX* gene in the susceptible accessions (Fig. 31B). As a consequence of this mutation *SRX* may not be expressed in the correct way.

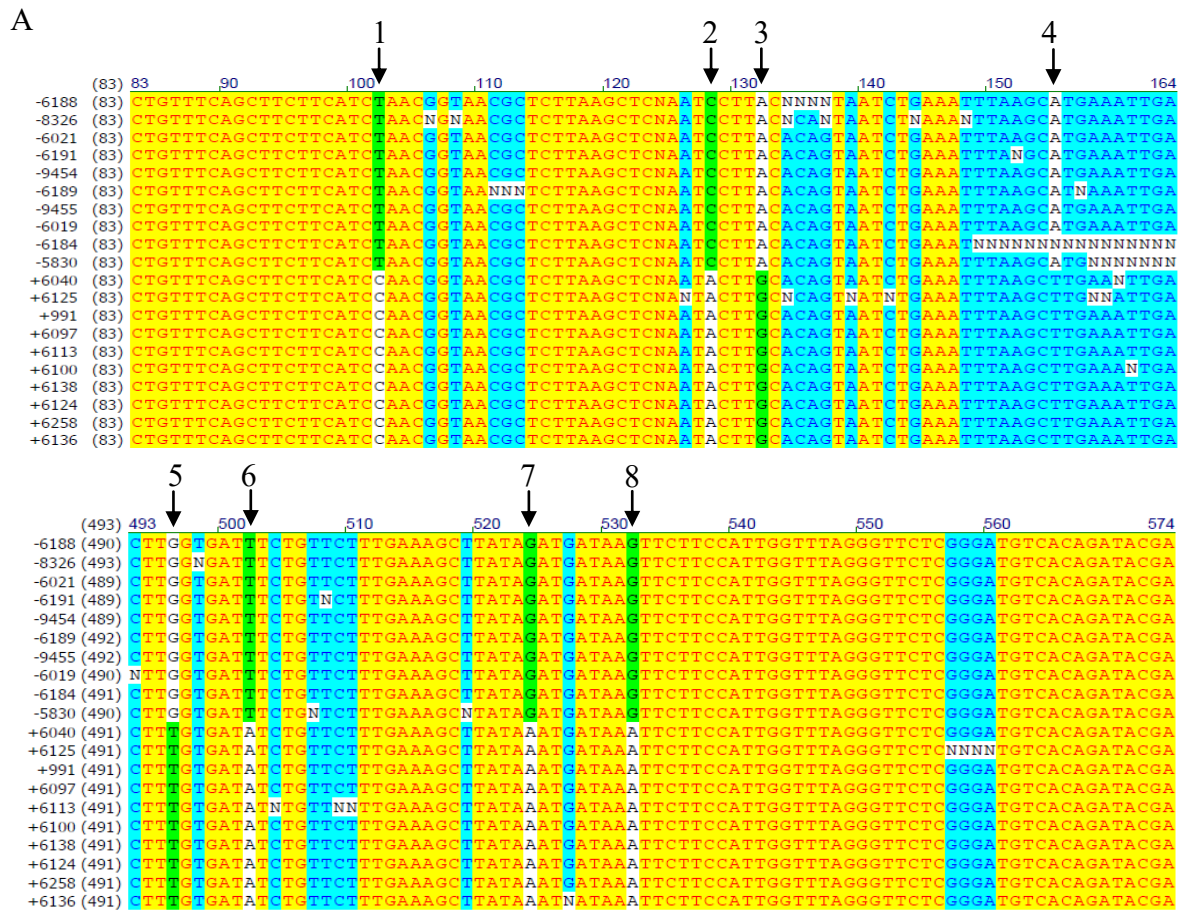


Figure 31. SNPs of the top resistant and the top susceptible accessions in the coding sequence of *SRX* (AT1G31170).

(A) Alignment (fragment) of the fragments of *SRX* coding sequence containing identified SNPs (1-8). The top susceptible accessions are marked with (-), whereas the top resistant ones with (+). Sequence data derived from 1001 genomes project webpage (<http://1001genomes.org>, 02/2016). (B) Analysis of the donor splice sites in ILA-resistant lines. The donor splice site marked in grey color is lost due to an A to G substitution (SNP No. 8) in ILA-hypersensitive accessions. For the full alignment where the lost donor splice site is visible see Suppl. Fig. 8. Analysis performed by NetGene2 v.2.4 (<http://www.cbs.dtu.dk/services/NetGene2/>) (Hebsgaard *et al.*, 1996).

2.3.1.3. The physiological function of genes located in the *SRX* region

IMD3 (At1g31180) is the one out of three isoforms of isopropylmalate dehydrogenases involved in synthesis of the branched chain amino acid leucine (Binder, 2010). Knock-out of

atimd1 shows reduced levels of leucine and the C4 to C8 glucosinolates, whereas *imd2* and *atimd3* display reduction in leucine abundance with no impact on glucosinolates profile (He *et al.*, 2011). Furthermore, preliminary results showed that *imd3* T-DNA insertion may mutant show increased root growth inhibition in presence of 500 μ M ILA. Thus involvement of the GWAS-associated gene in the branched-chain amino acid metabolism proposed *IMD3* for being a potentially important candidate. *SRX* (At1g31170) was reported to have an antioxidative function and it acts as a sulfinic acid reducer in yeasts and *Arabidopsis* and its expression positively correlates with the resistance to ROS (Iglesias-Baena *et al.*, 2010; Chi *et al.*, 2012; Puerto-Galan *et al.*, 2015). Furthermore, Chi *et al.* (2012) demonstrated a novel function of *SRX* that can also acts as the nuclease in mitochondria and chloroplasts and is possibly involved in DNA repair processes in these organelles. *IMPL1* (At1g31190) is involved in inositol and galactosephosphate metabolism in chloroplasts, nevertheless its direct involvement has not been determined.

The physiological functions of the other four associated genes (At1g31160, At1g31163, At1g31175, and At1g31200) have not been determined. Therefore their potential involvement in the root growth resistance in the presence of ILA remains as an open question, which may be addressed by a future study.

2.3.2. T-DNA insertion mutants screen for ILA resistant lines

A. thaliana T-DNA insertion mutants are broadly used in different screening assays. This type of the screen provides a relatively easy way to identify the gene or group of the genes responsible for the observed phenotype. The main question for this study was related to the mechanism of ILA perception and the way how it affects root growth. Applying loss-of-function mutant lines in the ILA insensitivity screen could easily point the genes encoding the potential ILA receptor or elements of the different pathways, which are affected by ILA (e.g. transporters).

In this study, 10 000 homozygous SALK T-DNA insertion mutants from collections 27951, 27952, 27941, 27942 (Nottingham Arabidopsis Stock Centre; (Scholl *et al.*, 2000)) were grown on 24-well plates with media containing 500 μ M ILA (see Methods). The lines have been screened for a root growth resistance, similar to that presented by *UGT76B1-OE7*, which has been reported as ILA-resistant line (von Saint Paul *et al.*, 2011). The applied growth conditions enable to distinguish ILA-susceptible from ILA-resistant lines (Fig. 32).

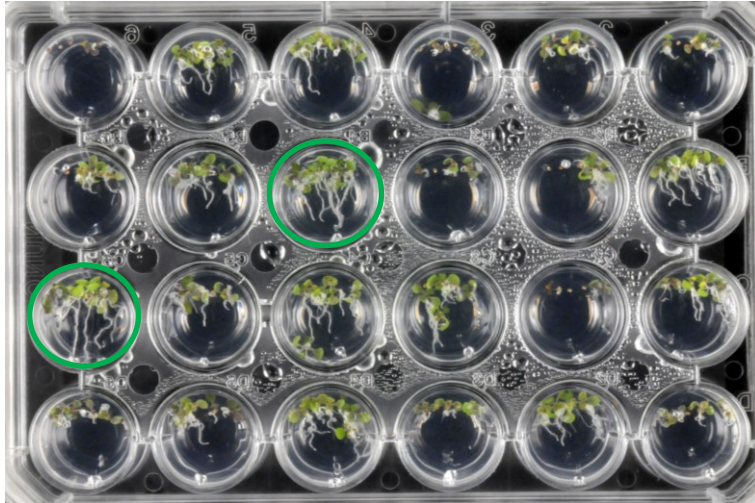


Figure 32. Example of a microtiter screening plate.

Twenty four-well plates were employed for the screening; in each well five to six seeds of a T-DNA insertion line were planted. Plants marked with a green circle were identified and further confirmed as ILA resistant (SALK_017821 – second row; SALK_029488 – third row). Plants were grown for five days in long day conditions (16 h light and 8 h darkness) on Gelrite plates containing 500 μ M ILA (see Methods).

2.3.2.1. Mutant lines showing reduced root growth sensitivity in the presence of ILA

Among 10 000 screened lines around 100 displayed a reduced root growth susceptibility in presence of 500 μ M ILA in media. These candidate mutants were re-screened confirming 46 mutants displaying lower root growth susceptibility than Col-0 plants. All 46 mutants were genotyped, which revealed a group of 26 homozygous T-DNA insertion lines. Mutants that displayed reduced susceptibility to ILA are listed in Table 3, whereas the root growth in the presence of 500 μ M ILA is presented in Supplementary Figure 9. Although nine out of 26 mutants possess the T-DNA insertion in 5'-UTR region they were not excluded from further consideration.

Table 3. Mutant lines showing reduced root growth sensitivity in the presence of ILA.

SALK	AGI	Annotation (TAIR)	Insertion
SALK_006676	At3g51080	<i>GATA6 - GATA TRANSCRIPTION FACTOR 6</i>	CDS-Exon
SALK_007071	At5g63950	<i>CHR24 - CHROMATIN REMODELING 24</i>	CDS-Exon
SALK_012541	At1g73020	<i>DUF590 - Protein of unknown function</i>	CDS-Intron
SALK_014957	At2g29940	<i>PDR3 - ATP-BINDING CASSETTE G31</i>	300-UTR5
SALK_017675	At1g48720	Unknown protein	300-UTR5
SALK_017821	At5g11110	<i>SPS2F - Protein with putative sucrose-phosphate synthase activity</i>	CDS-Intron
SALK_028137	At4g26190	<i>HAD - Haloacid dehalogenase-like hydrolase superfamily protein</i>	CDS-Exon
SALK_029488	At4g12440	<i>APT4 - ADENINE PHOSPHORIBOSYL TRANSFERASE 4</i>	CDS-Intron
SALK_031785	At3g61220	<i>SDR1- SHORT-CHAIN DEHYDROGENASE/REDUCTASE 1</i>	CDS-Intron
SALK_032256	At2g31240	<i>TPR-like - Tetratricopeptide repeat-like superfamily protein</i>	300-UTR5
SALK_040808	At1g61810	<i>BGLU45 - BETA-GLUCOSIDASE 45</i>	CDS-Intron
SALK_043037	At2g01500	<i>HOS9 - HIGH EXPRESSION OF OSMOTICALLY RESPONSIVE GENE 9</i>	1000-UTR5
SALK_053562	At4g09160	<i>SEC14 - Cytosolic factor family protein / phosphoglyceride transfer family protein</i>	300-UTR5
SALK_059101	At1g34460	<i>CYC3 - CYCLIN 3</i>	CDS-Intron
SALK_079374	At3g60410	<i>DUF1639 - Protein of unknown function</i>	300-UTR5

RESULTS

SALK_083322	At1g60040	<i>AGL49 - AGAMOUS-LIKE 49</i>	300-UTR5
SALK_095998	At1g29830	<i>Magnesium transporter CorA-like family protein</i>	CDS-Intron
SALK_103278	At4g32105	<i>Beta-1,3-N-Acetylglucosaminyltransferase family protein</i>	CDS-Exon
SALK_109443	At4g36850	<i>PQ-loop repeat family protein / transmembrane family protein</i>	CDS-Exon
SALK_110864	At3g46630	<i>DUF3223 - Protein of unknown function</i>	1000-UTR5
SALK_118494	At1g04370	<i>ERF14- ETHYLENE-RESPONSIVE ELEMENT BINDING FACTOR 14</i>	CDS-Exon
SALK_123629	At4g35640	<i>SERAT3;2 - CYTOSOLIC SERINE O-ACETYLTRANSFERASE</i>	1000-UTR5
SALK_124100	At3g28690	<i>Protein kinase superfamily protein</i>	CDS-Intron
SALK_138593	At3g56240	<i>CCH - COPPER CHAPERONE</i>	CDS-Intron
SALK_148617	At4g12410	<i>SAUR35 - SMALL AUXIN UPREGULATED RNA 35</i>	1000-UTR5
SALK_150594	At1g08800	<i>DUF593 - Protein of unknown function</i>	CDS-Exon

2.3.2.2. Classification of the mutant lines showing reduced root growth sensitivity in the presence of ILA

A relatively high number of the mutants raised the question whether there is a functional connection between the genes whose mutants displayed increased resistance towards ILA. Therefore, to obtain the linkage to any process, these genes were further categorized for GO term enrichment ($P < 0.05$) (Virtual Plant 1.3, <http://virtualplant.bio.nyu.edu>) in cellular component (Table 4), biological process (Table 5) and molecular function (Table 6).

Table 4. GO terms for cellular component.

Cellular component	AGI code	Gene (TAIR)
Chloroplast	At3g46630	<i>DUF3223</i>
	At3g56240	<i>CCH</i>
	At3g60410	<i>DUF1639</i>
	At4g09160	<i>SEC14</i>
Endomembrane system	At1g08800	<i>DUF593</i>
	At1g29830	<i>CorA-like family protein</i>
	At1g61810	<i>BGLU45</i>
	At4g32105	<i>Beta-1,3-N-Acetylglucosaminyltransferase family protein</i>
Membrane	At1g29830	<i>CorA-like family protein</i>
	At4g32105	<i>Beta-1,3-N-Acetylglucosaminyltransferase family protein</i>
	At4g36850	<i>PQ-loop repeat family protein</i>
Plasma Membrane	At3g28690	<i>Protein kinase superfamily protein</i>
	At3g61220	<i>SDR1</i>
	At5g11110	<i>SPS2F</i>
Nucleus	At1g04370	<i>ERF14</i>
	At2g01500	<i>HOS9</i>
Cellular component	At1g48720	Unknown protein
	At4g26190	<i>HAD superfamily protein</i>
Cytoplasm Cytosol	At2g31240	<i>TPR like superfamily protein</i>
	At4g35640	<i>SERAT3;2</i>

Table 5. GO terms for biological process.

Biological process	AGI code	Gene (TAIR)
Cellular process	At1g04370	<i>ERF14</i>
	At1g61810	<i>BGLU45</i>
	At2g01500	<i>HOS9</i>
	At2g29940	<i>PDR3</i>
	At3g28690	<i>Protein kinase superfamily protein</i>
	At3g56240	<i>CCH</i>
	At4g12440	<i>APT4</i>
	At4g32105	<i>Beta-1,3-N-Acetylglucosaminyltransferase family protein</i>
	At4g35640	<i>SERAT3;2</i>
	At5g11110	<i>SPS2F</i>
Response to stimulus	At1g04370	<i>ERF14</i>
	At2g01500	<i>HOS9</i>
	At3g51080	<i>GATA6</i>
	At3g56240	<i>CCH</i>
	At3g61220	<i>SDRI</i>
	At4g12410	<i>SAUR35</i>
	At5g63950	<i>CHR24</i>
Metabolic process	At1g61810	<i>BGLU45</i>
	At3g28690	<i>Protein kinase superfamily protein</i>
	At4g12440	<i>APT4</i>
	At4g32105	<i>Beta-1,3-N-Acetylglucosaminyltransferase family protein</i>
	At4g35640	<i>SERAT3;2</i>
	At5g11110	<i>SPS2F</i>
Biological regulation	At1g04370	<i>ERF14</i>
	At1g34460	<i>CYC3</i>
	At1g60040	<i>AGL49</i>
	At3g56240	<i>CCH</i>
Developmental process	At2g01500	<i>HOS9</i>
	At3g56240	<i>CCH</i>
Establishment of localization	At2g29940	<i>PDR3</i>
	At3g56240	<i>CCH</i>
Growth	At2g01500	<i>HOS9</i>
Reproduction	At2g01500	<i>HOS9</i>

Table 6. GO terms for molecular function

Molecular function	AGI code	Gene (TAIR)
Catalytic activity	At1g61810	<i>BGLU45</i>
	At2g29940	<i>PDR3</i>
	At3g28690	<i>Protein kinase superfamily protein</i>
	At3g61220	<i>SDR1</i>
	At4g12440	<i>APT4</i>
	At4g32105	<i>Beta-1,3-N-Acetylglucosaminyltransferase family protein</i>
	At4g35640	<i>SERAT3;2</i>
	At5g11110	<i>SPS2F</i>
	At5g63950	<i>CHR24</i>
Binding	At1g04370	<i>ERF14</i>
	At1g60040	<i>AGL49</i>
	At1g61810	<i>BGLU45</i>
	At3g28690	<i>Protein kinase superfamily protein</i>
	At3g56240	<i>CCH</i>
	At5g63950	<i>CHR24</i>
Transcription factor activity	At1g04370	<i>ERF14</i>
	At1g60040	<i>AGL49</i>
	At2g01500	<i>HOS9</i>
	At3g51080	<i>GATA6</i>
Transporter activity	At1g29830	<i>CorA-like family protein</i>
	At2g29940	<i>PDR3</i>
Enzyme regulator activity	At1g34460	<i>CYC3</i>
Chaperone activity	At3g56240	<i>CCH</i>

The above annotation did not identify a clear cluster, which was especially visible for the GO terms for cellular localization. The other two criteria showed a slight enrichment in cellular process, response to stimulus and metabolic process in GO terms for biological process, whereas GO terms for molecular function displayed moderated enrichment in catalytic activity and binding.

2.3.2.3. Spatial expression of genes, whose mutants show increased ILA resistance

The T-DNA insertion screen was based on the root morphology, thus ILA-responsive genes were examined if they belong to root-specific or root-expressed genes. Using the public microarray data (dataset available for 21 out of 26 genes of interest) it has been determined that fifteen genes displayed comparable expression in root as well as in aboveground tissues (At1g48720, At1g61810, At1g73020, At2g01500, At1g60040, At2g31240, At4g12440, At4g26190, At4g32105, At5g63950, At4g12410, At1g34460, At3g56240, At4g09160, At3g60410). Three genes showed enhanced expression in shoot than in root (At3g46630, At3g61220, At2g29940) and three at least twofold higher expression in the root than in shoot (At1g08800, At3g28690, At5g11110) (Fig. 33).

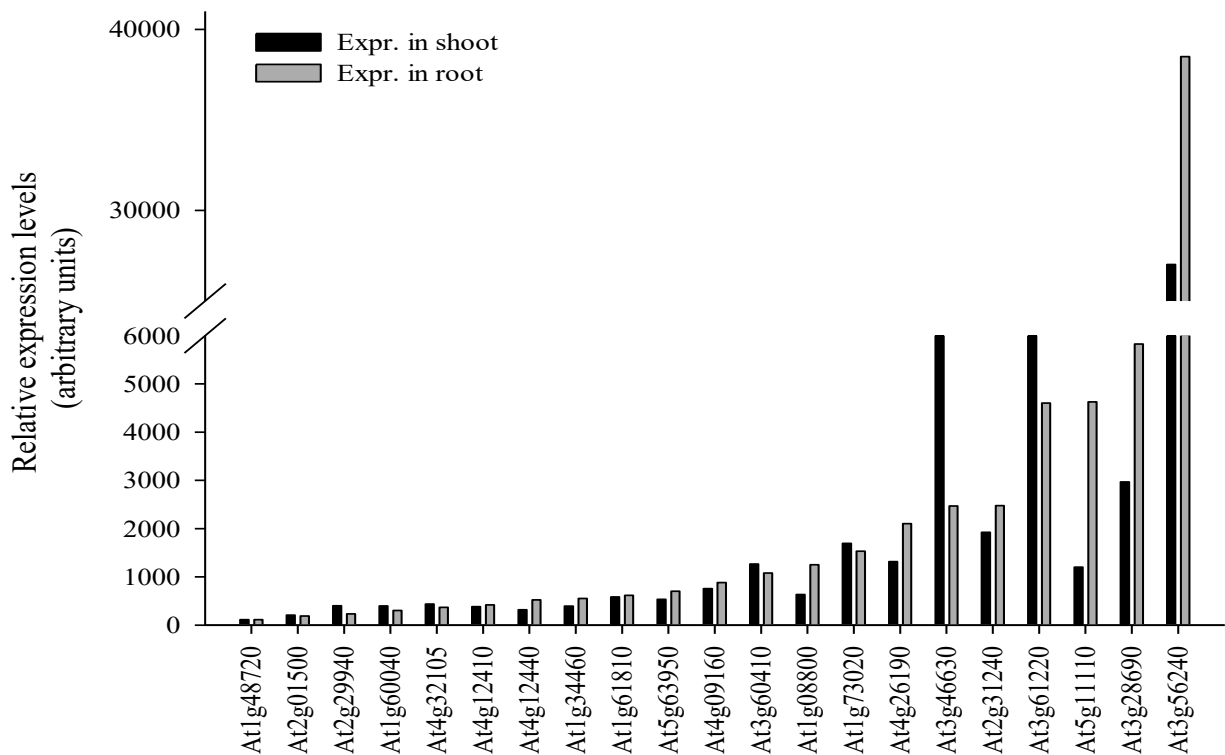


Figure 33. Expression levels in root and shoot of genes, whose mutants show enhanced root growth resistance to ILA.

Expression data derived from Genevestigator ([https:// genevestigator.com/gv/](https://genevestigator.com/gv/), 02/2016).

This comparison demonstrated that the genes from ILA-resistance screening do not belong to the root-specific genes and are in the most cases expressed at a similar level in both below- and above-ground tissues.

2.3.2.4. The response of ILA resistant mutants to exogenously applied plant hormones

To elucidate a potential linkage or a shared response pattern between ILA and the hormonal pathways, ILA-resistant mutants were examined to determine the root growth response in presence of plant hormones; SA, Me-JA, IAA (Fig. 34A-D).

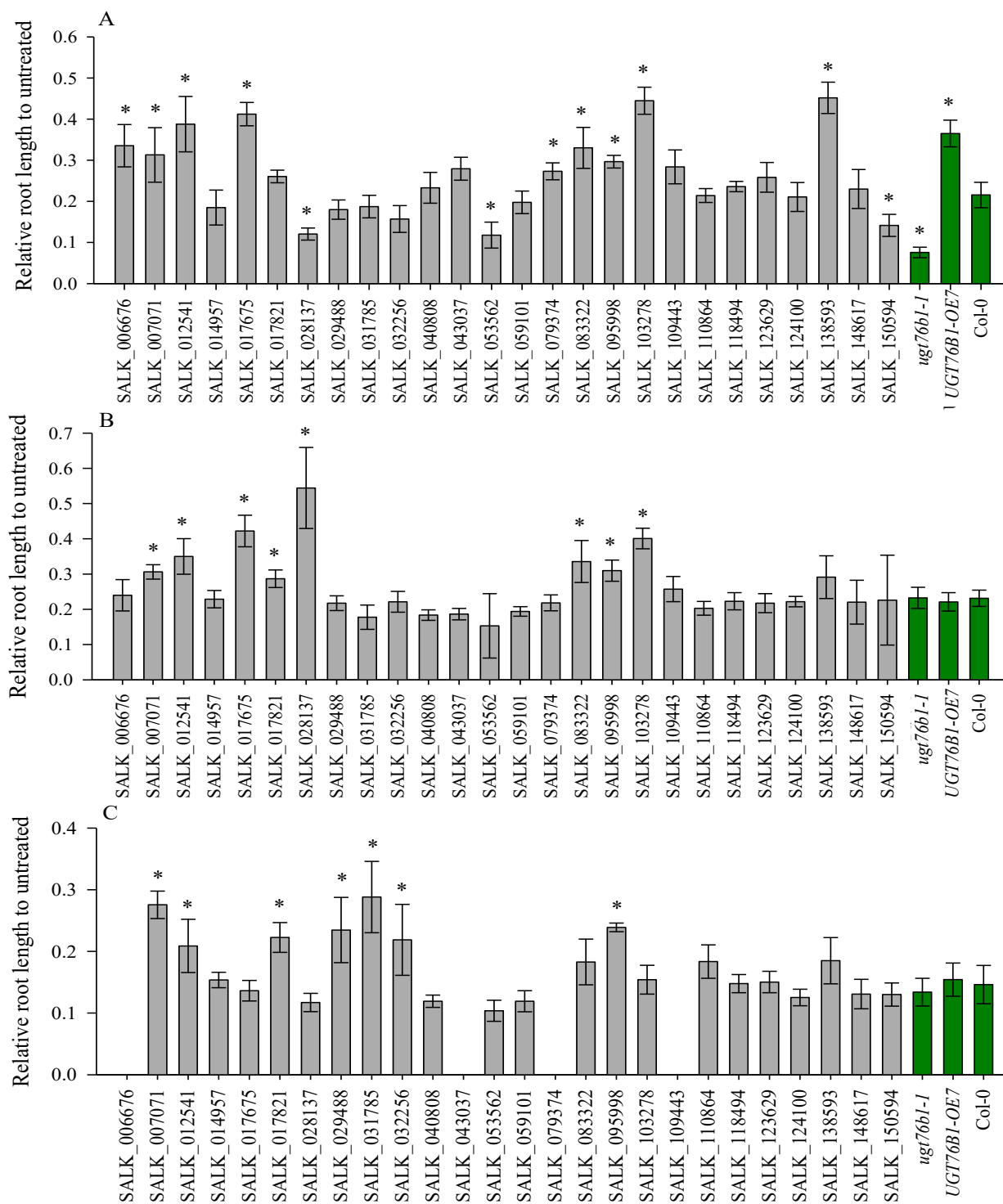


Figure 34. Root growth response of ILA-resistant mutants to exogenous hormones.

Figure continues on the next page.

D

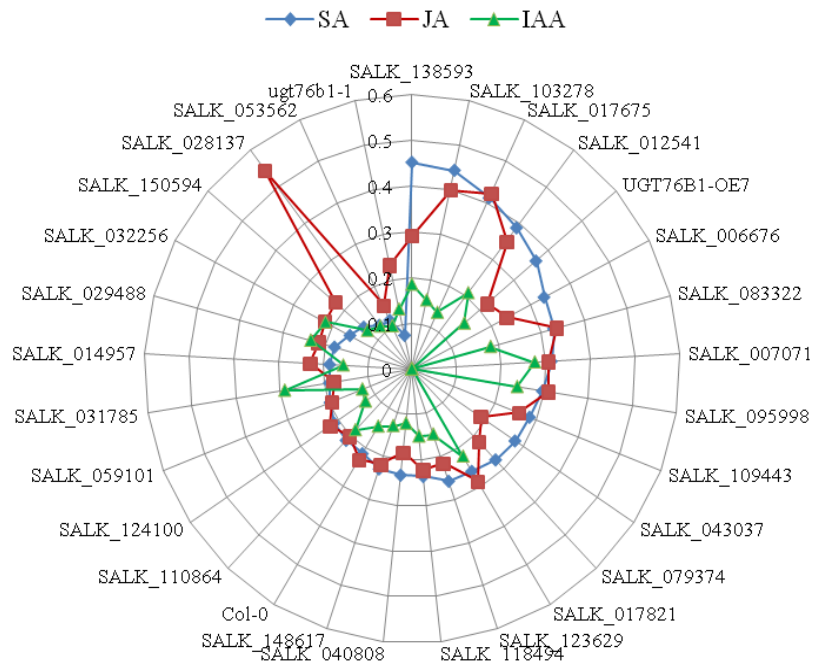


Figure 34. Root growth response of ILA-resistant mutants to exogenous hormones.

Plants have been grown for 8 days in long day conditions (16 h light, 8 h darkness) on square vertical plates containing hormones: (A) 50 μM SA, (B) 50 μM Me-JA, (C) 1 μM IAA; data for SALK_006676, SALK_043037, SALK_079374, SALK_109443 not available. (D) radar plot providing a global overview to all applied hormones. Root lengths were calculated using ImageJ software and then related to the parallelly grown, controls (Gelrite plates without hormones). Asterisks indicate the significance of the difference to Col-0; * $P < 0.05$ ($n = 4-12$)

It has been previously shown that ILA positively impacts the SA-mediated pathway; therefore, it was potentially interesting, whether the ILA-resistant mutant lines would also share a similar phenotype, when grown in the presence of exogenous salicylic acid. Jasmonic acid was applied due to its antagonistic relationship with SA-mediated pathway and the different mechanism of *A. thaliana* root growth inhibition. IAA, except playing a key role in plant growth and development, was also demonstrated to negatively impact SA biosynthesis and signaling, whereas positively JA/ET-mediated pathway (Seilaniantz *et al.*, 2007). Nevertheless, it was reported that both SA and JA can inhibit root growth via the impact on auxin. Salicylic acid inhibits root growth in the concentration range between 10 μM – 100 μM , which is most probably in relevance to its levels achieved during the stress conditions. SA treatment triggers the reduction of cell elongation that is achieved through a negative impact on auxin in the root tips (Wildermuth and Jones, 2009), which occurs via a positive impact of SA on auxin-inhibiting AUX/IAA proteins (Wang *et al.*, 2007). Methyl jasmonate can also inhibit the root growth through the cross-talk with auxin. This occurs via MYC2 transcription factor that binds to *PLT1* and *PLT2* promoters and suppresses their expression. Both *PLT1* and *PLT2* are essential in auxin-mediated root development (Chen *et al.*, 2011;

Yang *et al.*, 2017). Additionally, Me-JA was reported to negatively affect auxin transport (Sun *et al.*, 2011). On the other hand, Me-JA-dependent root growth inhibition could be also based on its inhibitory effect on cell division (Yan *et al.*, 2007). Exogenously applied excess concentrations of auxin can also suppress root growth by impacting negatively on cell elongation (Overvoorde *et al.*, 2017). Therefore, knowing the mechanism how SA, Me-JA and IAA affect the root growth and possible common responses for ILA-resistant mutants can provide a functional linkage for the mechanism of root growth inhibition by ILA.

2.3.2.4.1. Root growth response of ILA-resistant mutants to salicylic acid

Salicylic acid, in contrast to the other two hormones, affected the root growth of the ILA-resistant lines in most divergent way, if compared to the other hormones (Fig. 34). Additionally, this root growth inhibition assay provided an independent evidence for *UGT76B1-OE7* line as being more resistant to exogenous SA. In presence of exogenously applied salicylic acid twelve mutants displayed a different than wild-type root growth phenotype. Nine ILA-resistant lines showed enhanced resistance to SA. From this group five lines were not statistically different from *UGT76B1-OE7* (SALK_017675, SALK_012541, SALK_007071, SALK_083322, and SALK_006676); two lines displayed even a higher resistance than *UGT76B1-OE7* (SALK_138593, SALK_103278). At the same time two lines were more resistant than Col-0 (SALK_079374 and SALK_095998), whereas more susceptible than the *UGT76B1-OE7*. The last identified group is composed of three T-DNA insertion lines that displayed more sensitive root growth than Col-0 (SALK_150594, SALK_028137, and SALK_053562) (Fig. 34A, D)

Among the group of nine SA and ILA co-resistant three lines, SALK_017675, SALK_012541 and SALK_079374 are the mutants of proteins of unknown function. Thus, this could be the first report demonstrating common elements involved in the response to exogenous ILA and SA in *A. thaliana*. SALK_007071 is the mutant of *CHROMATIN REMODELING 24* (*CHR24*) and it has been described as being γ -irradiation and UV-C sensitive (Shaked *et al.*, 2006). It has been also reported that UV-C treated *A. thaliana* and tobacco plants display increased emission of both Me-JA and Me-SA (Yao *et al.*, 2011). SALK_138593 is the *COPPER CHAPERONE* (*CCH*) mutant, which together with *ATX1* are the two chaperons responsible for copper homeostasis in *A. thaliana* (Shin *et al.*, 2012). It has been reported that excess Cu^{2+} in media impacts the root growth architecture by cytokinin and auxin accumulation as well as increased lignin deposition, cell death and reduction in mitotic

activity (Lequeux *et al.*, 2010). Additionally, Shin *et al.* (2012) indicated that only *ATX* but not *CCH* is responsible for changes in root growth in copper excess or deficient conditions, suggesting its distinct properties and functions in plants. Among the SA and ILA resistant lines there is also another mutant line that shows a functional connection to metal ion homeostasis. SALK_095998 is the *MAGNESIUM TRANSPORTER CORA-LIKE FAMILY PROTEIN* mutant. This particular member of this family is not well characterized and it is functionally annotated to transmembrane ion transport (Lamesch *et al.*, 2012). SALK_103278 is a mutant of β -1, 3-N-ACETYLGLUCOSE-AMINYLTRANSFERASE family protein, a poorly characterized protein. Tohge *et al.* (2005) reported its slight upregulation in a *PAPI/MYB75* over-expression line. *PAPI/MYB75* is known for its positive impact on JA-dependent anthocyanin synthesis (Boter *et al.*, 2015). SALK_006676 is a mutant of *GATA6*, a member of transcription factor family implicated in response to light and signals from circadian clock (Manfield *et al.*, 2006). It is worth mentioning that BCAA degradation depends on the circadian clock (Binder, 2010). Therefore, this could be speculated as a potentially interesting linkage between ILA and *gata6* loss-of-function mutant. The last mutant line that displayed simultaneously increased resistance to SA and ILA is SALK_083322, a mutant of *AGL4*. This gene is highly expressed in the female gametophyte and developing seeds (Bemer *et al.*, 2010). Thus, based on the functional annotation of *AGL4* its role in the resistance towards ILA and SA cannot be predicted at this stage of the study.

The last group of SA-responsive contains mutant lines that showed opposite sensitivity to SA and to ILA. SALK_053562, a T-DNA insertion line of *SEC14*. *SEC14* is a phospholipid transfer protein involved in modulation of *N. benthamiana* defense response against *R. solanacearum*. It has been demonstrated that silencing the *SEC14* gene reduce the accumulation of JA and JA-Ile. Moreover *SEC14* has a negative impact on *N. benthamiana* SA marker gene *PR1-a* (Kiba *et al.*, 2014). SALK_053562 line possess the T-DNA insertion line in the promoter region, thus even the enhanced expression of this gene should not be excluded. Nevertheless, the involvement of this gene in plant defense response indicates this gene as a potentially interesting candidate for the future studies. Two last SA-susceptible mutants do not possess a well-studied function. SALK_150594, mutant of *DUF593*, is a highly conserved domain in flowering plants that has been identified as a myosin binding domain, thus implicating this protein in vesicle transport (Peremyslov *et al.*, 2013). SALK_028137, is the mutant of *HALOACID DEHYDROGENASE-LIKE HYDROLASE SUPERFAMILY (HAD)*. Its function in *Arabidopsis* is not explored at the moment and it is

only known that in yeasts this family of proteins is dominated by putative phosphatases (Kuznetsova *et al.*, 2015).

2.3.2.4.2. Root growth response of ILA-resistant mutants to jasmonic acid

In presence of exogenous jasmonic acid (Fig. 34B, D), eight mutant lines demonstrated a co-resistance to ILA and Me-JA (SALK_017675, SALK_012541, SALK_017821, SALK_083322, SALK_103278, SALK_007071, SALK_095998, SALK_028137). Furthermore four lines shared the resistant phenotype with SA treated mutant lines (SALK_083322, SALK_103278, SALK_007071, and SALK_095998). In contrast to salicylic acid treatment, susceptible phenotype has not been observed. Interestingly, one mutant line displayed root growth resistance to JA, whereas susceptibility to exogenous SA (SALK_028137).

SALK_017675 and SALK_012541 are mutants of genes of unknown function, thus predicting their role in root growth response to applied stimuli is not possible. SALK_017821 is a mutant line of *SUCROSE-PHOSPHATE SYNTHASE (SPS2F)*. Sucrose is known to possess both metabolic and signaling function in plants (Wind *et al.*, 2010). It has been reported that sucrose is involved in hormone mediated anthocyanin biosynthesis by inducing the expression of *PAP1/MYB75*, which positively impacts the JA-dependent anthocyanin biosynthesis (Teng *et al.*, 2005; Tohge *et al.*, 2005). This could suggest that the resistance to ILA is negatively correlated with the JA pathway activity.

2.3.2.4.3. Root growth response of ILA-resistant mutants to auxin

Auxin treatment revealed increased resistance of seven mutant lines (Fig. 34C, D), from which three were specific for IAA (SALK_029488, SALK_031785, SALK_032256), three shared resistance with SA and Me-JA (SALK_095998, SALK_012541, SALK_007071) and one with Me-JA (SALK_017821).

SALK_029488, mutant of *ADENINE PHOSPHORIBOSYL TRANSFERASE 4 (APT4)* is one out of five members of the enzyme family responsible for inactivation of cytokinin, through interconversion of cytokinin nucleobase (active form) into its nucleotide form (inactive form). It has been confirmed *in vitro* that *APT4* together with *APT1* and *APT5* possess catalytic activity towards cytokinin *in vitro*. On the other hand, the physiological role of *APT2*–*APT5* in cytokinin metabolism could not be confirmed (Zhang *et al.*, 2013). SALK_031785, the

mutant of *SHORT CHAIN DEHYDROGENASE/ REDUCTASE 1 (SDR1)*; *SDR1* has been described as the pepper ortholog of *CaMNR* that is catalyzing the menthone reduction to neomenthol, which has antimicrobial functions in pepper and *A. thaliana* (Choi *et al.*, 2008; Hwang *et al.*, 2012). Choi *et al.* (2008) also reported the increased susceptibility to *P. syringae* as well as the decreased expression of *PRI* in *sdr1* mutant, indicating the requirement of this gene in response to hemi-biotrophs. SALK_032256 is the mutant of TPR-like protein with annotated function in pollen germination (Wang *et al.*, 2008). Additionally, the insertion in this line is localized in the promoter region, therefore its expression could be affected in a different manner, similarly, like it has been observed for SALK_014957 (see chapter 2.3.2.5.).

2.3.2.4.4. Common pattern of ILA-resistant mutants displaying wild-type response to exogenously applied hormones

The group of the mutants, whose root growth was not differently affected by exogenous hormone application, might be highly important. The wild-type response to SA, Me-JA and IAA could point out that the mutated genes are specifically involved in ILA response. Among the evaluated mutant population, thirteen displayed wild-type response to salicylic acid (Fig. 34A, D), nineteen to methyl jasmonate (Fig. 34B, D) and thirteen to auxin (Fig. 34C, D). Comparison of these three groups led to the identification of eight mutants showing simultaneously wild-type response to applied hormonal stimuli (Fig. 35). Interestingly, SALK_014957 (*PDR3*) showed the lowest root growth inhibition in the presence of ILA among all T-DNA insertion lines implemented in this study (see chapter 2.3.2.5.). *ERF14* (SALK_118494) has been previously described as a positive regulator of JA/ET-mediated responses, playing a non-redundant role in defense against the fungal pathogen *Fusarium oxysporum* (Mcgrath *et al.*, 2005; Onate-Sanchez *et al.*, 2006). The presence of a mutant of a positive JA/ET pathway regulator in the group of ILA resistant mutants could be interesting if taking into the account the preliminary results of the screen for ILA hypersensitive lines. Among the potentially ILA-hypersensitive mutants, a mutant of the negative JA regulation complex (*tpr1*; AT1G80490) has been found (Suppl. Table 2). In this complex the TPL/TPR co-repressors target NINJA, which interacts with JAZ proteins (Pauwels and Goossens, 2011). Therefore, this is a very interesting connection and it could propose that ILA resistance is negatively correlated with JA pathway activity. *CYC3* (SALK_059101) belongs to B1-type cyclins, known for the regulation of mitosis phase transition. Ruzicka *et al.* (2009) reported the reduction of *CYCB1; 1* expression in presence of exogenous cytokinin, indicating that

cytokinin treatment can modulate the root growth *via* mitotic activity disruption. Moreover in presence of excess Cu^{2+} , the enriched pool of cytokinin together with decreased mitotic activity has been reported as well and proposed as one of the mechanism for root growth inhibition (Lequeux *et al.*, 2010). Thus, it could lead to two different conclusions, explaining enhanced tolerance of *cyc3* mutant to exogenous IAA in the media. IAA application could trigger cytokinin accumulation in the root and inhibit its growth *via* mitotic activity disruption. Nevertheless, this would also affect other members of B1-type cyclin family. Therefore, the situation observed in single *cyc3* mutant would rather suggest the direct impact of IAA on CYC3 and its functions. SALK_124100, mutant of At3g28690 has been described as a miRNA regulated gene related to the dark-induced leaf senescence (Huo *et al.*, 2015). One of the reasons for the dark-induced senescence is the reduction of photosynthesis and subsequent carbon starvation (Liesch and Keech, 2016). This fact may be speculated as a potential link to BCAA degradation, which is enhanced during the carbon starvation conditions (Binder, 2010). *BGLU45* (SALK_040808) together with *BGLU46* impacts lignin biosynthesis in *A. thaliana* (Chapelle *et al.*, 2012). Three last mutants assigned to the wild-type responsive group: SALK_110864, SALK_148617 and SALK_123629 have the T-DNA insertion localized in promoter region, which could even trigger an upregulation of those genes, which has been already observed (see also chapter 2.3.2.5.1.).

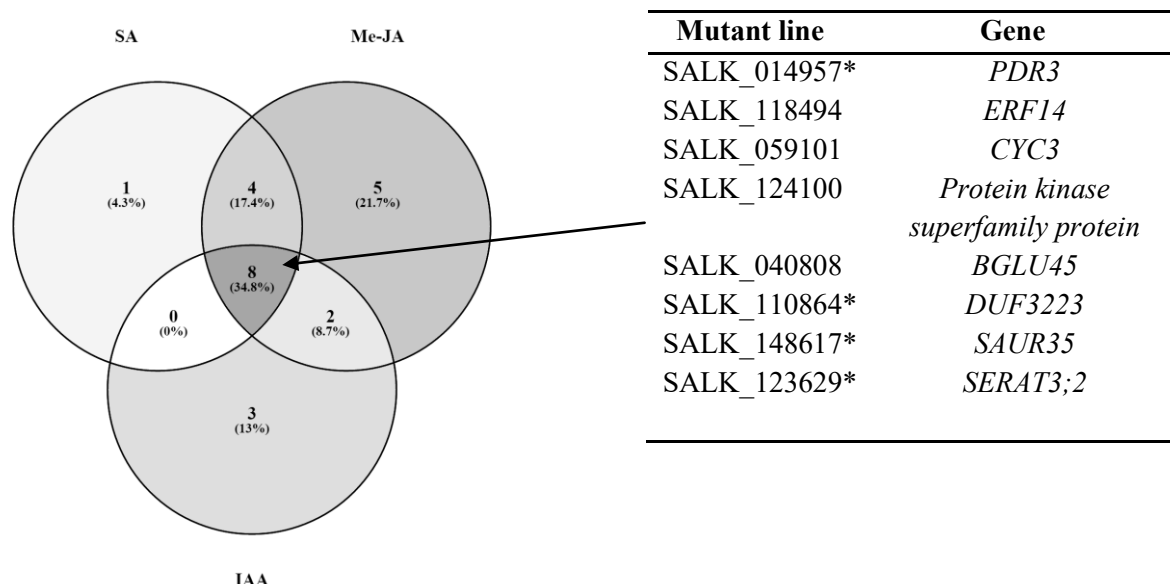


Figure 35. T-DNA insertion mutants showing wild-type root growth response in presence of SA, Me-JA and IAA.

In lines marked with (*) the T-DNA insertion is located in the promoter region, thus they are probably not a loss-of-function alleles and may show elevated or residual expression.

2.3.2.4.5. Common pattern of ILA-resistant lines displaying a different response to exogenously applied hormones than wild-type

Mutant lines showing different root growth response in presence of SA, Me-JA and IAA have been grouped according to shared *vs.* different root growth phenotype. When comparing all mutant lines that displayed enhanced root growth resistance three lines were resistant to all applied hormones and three lines displayed resistance to SA and Me-JA. Three lines were specific for SA (SALK_138593, SALK_079374, SALK_006676) and two for IAA resistance (SALK_032256, SALK_031785, SALK_029488), whereas one line was resistant to Me-JA (SALK_028137). At the same time also one line showed simultaneous resistance to Me-JA and IAA (SALK_017821) (Fig. 36).

The common response pattern to SA and Me-JA is rather surprising due to the fact of a different mechanism of root growth inhibition. Nevertheless, the products of these genes could influence the resistance to SA, Me-JA and ILA indirectly. On the other hand, the group of three lines resistant to all applied hormones and ILA could suggest the presence of a common element that is affected by the applied molecules, or their involvement in the transport of these compounds into the cell.

Due to the antagonistic relationship of SA- and JA-mediated pathways, the SA-sensitive and Me-JA-resistant lines were examined for the overlap as well. This pointed a one T-DNA line (Fig. 37). Nevertheless, the currently known function of this gene (see chapter 2.3.2.4.1) encoding a putative hydrolase does not provide a linkage to the SA-JA crosstalk or to the root growth and development

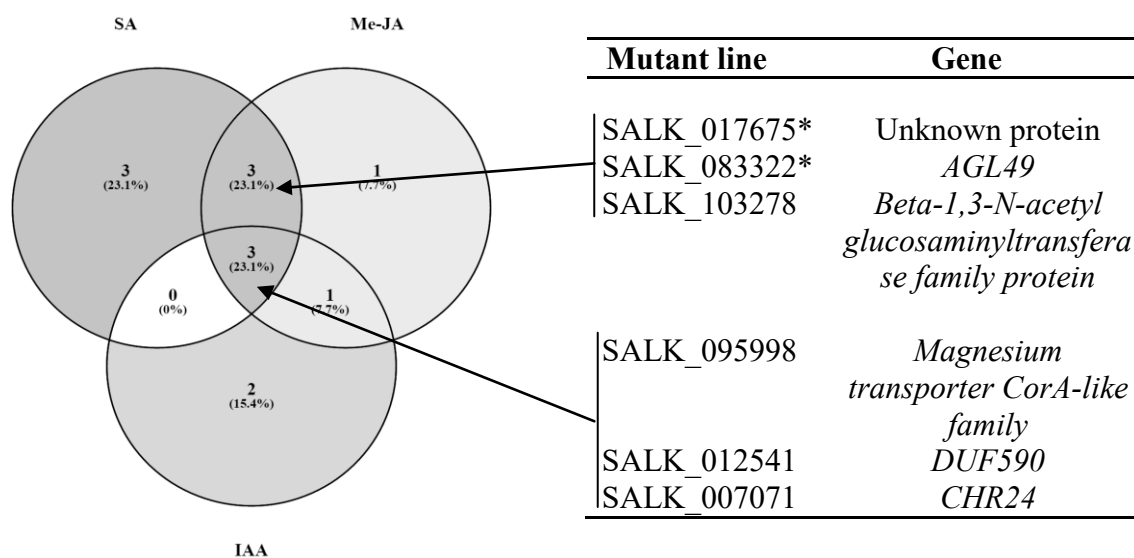


Figure 36. T-DNA insertion mutants showing enhanced root growth resistance in presence of SA, Me-JA and IAA.

In lines marked with (*) the T-DNA insertion is located in the promoter region.

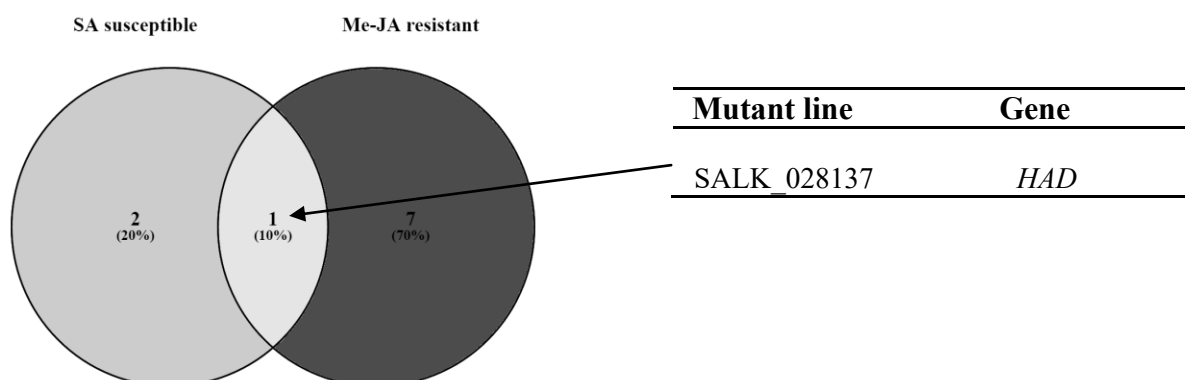


Figure 37. T-DNA insertion mutants showing different root growth response to exogenous SA and Me-JA.

2.3.2.5. SALK_014957 (*PDR3*) shows the lowest root growth inhibition in presence of ILA

Among 10 000 screened T-DNA insertion lines, SALK_014957 displayed the highest root growth resistance in presence of 500 μ M ILA (similar to *UGT76B1-OE-7*) (Fig. 38A). Further experiments including higher ILA concentrations (1.25 mM ILA and 1.5 mM ILA) showed that SALK_014957 still displayed a less susceptible root growth phenotype than Col-0 plants (Fig. 38B). This fact indicates a linkage between *PDR3* function in *A. thaliana* and exogenously applied ILA.

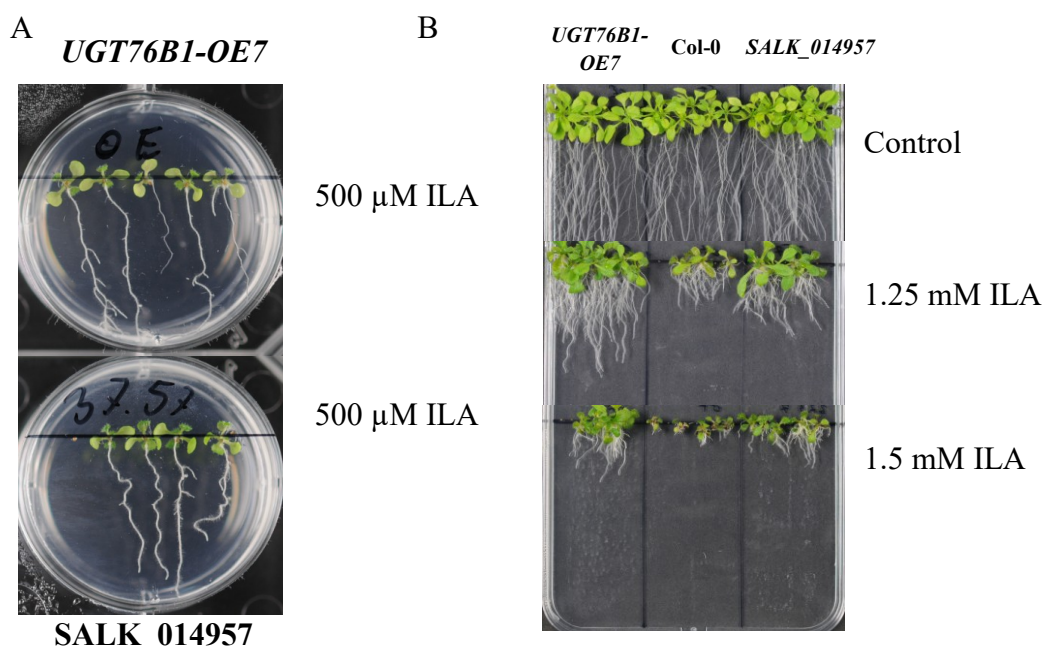


Figure 38. Root growth resistance of SALK_014957 line in presence of exogenous ILA.

Root growth response to ILA of SALK_014957, *UGT76B1-OE*, and Col-0. (A) Plants grown on 6-well, vertical plates in long day conditions (16 h light, 8 h darkness) for 7 days. (B) Plants grown on vertical plates in long day conditions (16 h light, 8 h darkness) for 14 days.

2.3.2.5.1. Known functions of *PLEIOTROPHIC DRUG RESISTANCE (PDR3)*

PDR3, the gene hit in the SALK_014957 line encodes an ABC transporter. ATP-binding cassette (ABC) transporters constitute a very large protein family present in all living organisms. ABC transporters function as ATP-driven pumps and are composed of two hydrophobic transmembrane domains (TMD) and two cytosolic nucleotide-binding domains (NBD) or nucleotide binding folds, which are organized in different orders (TMD-NBD or NBD-TMD) in two or in single coding units (Martinoia *et al.*, 2002; Kang *et al.*, 2011). ABC transporters are predominantly involved in the directional transport of substrates from the

cytosol to the extracellular space or into vacuoles. However it is known that plant ABC transporters are able to act in the opposite direction as well (Shitan *et al.*, 2003).

In *A. thaliana* ABC transporters are classified in nine subfamilies. *PDR3* belongs to the largest ABC transporter family, the ABCG subfamily, which is present only in plants and fungi. It has also a characteristic, reverse organization of domains - the nucleotide binding domain (NBD) precedes the transmembrane domain (TMD) (Crouzet *et al.*, 2006; Kang *et al.*, 2011). In *A. thaliana* *PDR3* has been reported to participate in the deposition of the steryl glycosides on the pollen coat (Choi *et al.*, 2014). Recently, it has been demonstrated that *PDR3* together with three other members of ABCG subfamily are involved in ABA transport from the endosperm to the embryo (Ko *et al.*, 2014). Kang *et al.* (2014) reported that *PDR3* together with ABCG25 export ABA from the endosperm, whereas ABCG30 and ABCG40 are involved in its import into the embryo.

To evaluate the possible connections of ILA action in *A. thaliana* and *PDR3*, SALK_014957 line has been further investigated. The T-DNA insertion is located in the promoter region of the *PDR3* gene, thus it might not lead to loss-of-function mutation. Therefore, the expression of *PDR3* in SALK_014957 was measured. This analysis demonstrated that the expression of *PDR3* gene is strongly upregulated in the insertion line (Fig. 39A). This result together with the previously determined enhanced resistance to ILA may potentially indicate that *PDR3* is involved in ILA transport. Nevertheless, this hypothesis needs to be further substantiated. ILA was previously described as a modulator of plant defense (von Saint Paul *et al.*, 2011). For this reason it was examined, whether the upregulation of *PDR3* can impact plant defense against biotrophic pathogen. Nevertheless, infection study pointed out that *PDR3* did not affect *P. syringae* DC3000 growth in a different manner than the wild-type (Fig. 39B). *PDR3* may also be involved in the regulation of endogenous ILA levels. However, its determination in the shoot of SALK_014957 line revealed wild-type levels of ILA (Fig. 39C). RT-qPCR measurement of *PRI*, *FMO1* and *SAG13*, genes up-regulated in *ugt76b1-1* and *PDF1.2*, which shows downregulation as well as *UGT76B1* that is active towards ILA were not affected in SALK_014957 line, if compared to Col-0 (Fig. 39D).

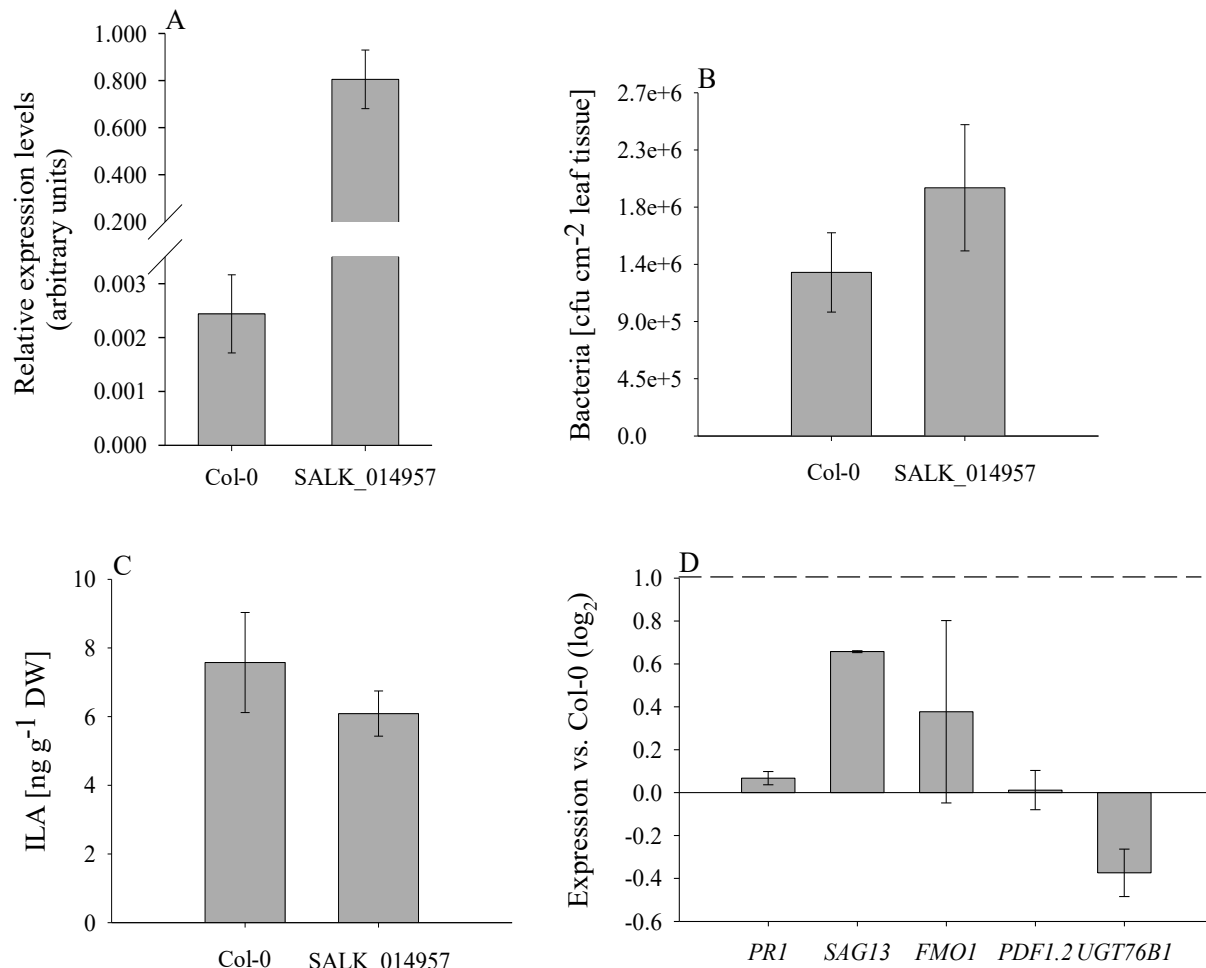


Figure 39. The influence of *PDR3* on plant defense, ILA abundance and marker genes expression.

(A) The expression of *PDR3* in SALK_014957 line in the root. Data presents arithmetic means and standard deviations of three replicates. Expression levels were normalized to *UBIQUITIN5* and *S16*. Plants were grown for two weeks in long day conditions (16 h light, 8 h darkness). Asterisks indicate the significance of the difference to Col-0; *** $P < 0.001$. (B) Response of Col-0 and SALK_014957 line to biotrophic pathogen. Plants were infiltrated with *P. syringae DC3000* (OD 600nm = 0.001), treated leaves were harvested three days post infection. Data presents arithmetic means and standard deviations of three replicates. (C) Abundance of free ILA in Col-0 and SALK_014957 line in whole rosettes. Data presents arithmetic means and standard errors of four replicates. (D) Expression of *PRI*, *SAG13*, *FMO1*, *PDF1.2* and *UGT76B1* in SALK_014957 line. Data presents arithmetic means and standard deviations of three replicates of log₂ transformed data related to Col-0. Expression levels were normalized to *UBIQUITIN5* and *S16*. For B, C and D plants were grown for four weeks in short day conditions (10 h light, 14 h darkness).

The above results indicate that it is less likely that *PDR3* directly impacts on ILA action in *Arabidopsis* leaves. However, the increased expression level of *PDR3* in the SALK_014957 line, together with enhanced root growth resistance in presence of exogenous ILA indicates *PDR3* as being potentially involved in ILA export.

2.3.3. T-DNA mutant lines displaying hypersensitive response to ILA

The screening plates with T-DNA insertion were applied for preliminary identification of mutants displaying hypersensitive root growth response in presence of ILA. In this approach mutants lacking elements of pathways involved in ILA degradation/detoxification process are expected to appear. Moreover the elements of ILA perception mechanism could also be included in the group of mutants displaying enhanced root growth inhibition in the presence of exogenous ILA. This approach identified 293 candidate genes (Supp. Table 2), whose mutants displayed root hypersensitivity; therefore this group of mutants should be considered in the future study. Furthermore, this preliminary screening provided an interesting additional overlap with JA-mediated pathway. Whereas *ERF14* known as the positive regulator of JA pathway has been identified as ILA-resistant line (see above), a mutant of the negative regulator (*TPRI*) has been identified as ILA-hypersensitive. Thus, it could be speculated that the resistance to ILA is negatively correlated with JA pathway-mediated responses. However, this overlap cannot be further substantiated at this stage of the study and stays as an opened question for the future research.

2.4. Is the high expression of *UGT76B1* in root pivotal for its effect in aboveground organs?

Previous work revealed that *UGT76B1* displays the highest expression in root and in very young leaves, whereas in older leaves it is strongly reduced (von Saint Paul, 2011). Interestingly, the upregulation of salicylic acid marker genes *PR1*, *PR2* and *PR5* in *ugt76b1-1* and the enhanced resistance to the (hemi-)biotrophic pathogen *P. syringae* was analyzed in four to five-week old *A. thaliana* leaf tissue, while so far the function in root tissue had not been addressed. One could even hypothesize that the strong expression in root endodermal cells impacts the response or defense status in leaves. To further explore this possibility, the grafting method was applied. Thereby chimeric plants are established by physical joining roots and the aerial part of defined, different genotypes at the hypocotyl. In this study hetero-grafts composed of *ugt76b1-1* scion and Col-0 rootstock as well as the opposite combination were applied, whereas as a control homo-grafts of *ugt76b1-1* and Col-0 were fused. Obtaining grafted plants is preceded by a severe wounding, thus very young, one-week-old plants have been used in order to repress the possible influence from this event upon later analysis. In addition, homo-grafts were essential to monitor if the wounding can impact the expression of studied genes. Nevertheless, early growth stage and in consequence small hypocotyl diameter

lowers the efficiency of the method. A second issue negatively impacting the efficiency is a frequently recorded wounding-induced formation of adventitious roots, i.e. roots that are initiated by the scion at the hypocotyl; thus, they override the grafting strategy. Examples of correct and aberrant grafting union are presented in Fig. 40A. In contrast, Fig. 40B shows plants that due to the aberrant union development were excluded from further measurements.



Figure 40. Examples of correct and aberrant grafting unions

Four-week-old, chimeric *A. thaliana* plants showing correct (A) and aberrant (B) development of the grafting union. Formed grafting unions are indicated by the arrows. For plant growth conditions see methods.

Whole rosettes of four-week-old grafted plants were used to monitor the expression of *PR1*, *PR2* and *PR5* marker genes by RT-qPCR. Homo-grafts of *ugt76b1-1* shoot and *ugt76b1-1* root (ko/ko) displayed the already known upregulation of *PR1*, *PR2* and *PR5* marker genes in comparison to Col-0 homo-grafts (WT/WT). This shows that grafting as well as applied growth conditions do not disturb previously reported enhanced expression of *PR1*, *PR2* and *PR5* in *ugt76b1-1* in the shoot. Further examination of chimeric plants (Fig. 41A-C) composed of *ugt76b1-1* shoot and Col-0 root (ko/WT) demonstrated a change in expression of *PR* marker genes. Introducing Col-0 root to *ugt76b1-1* rosette abolished the upregulation of *PR1*, *PR2* and *PR5* in knock-out aboveground tissues to the level displayed by wild-type plants. This provides a clear evidence for the presence of the root-derived signal that impacts *PR* genes expression and its activity is negatively correlated with *UGT76B1* expression in the root. The opposite grafting combination composed of Col-0 rosette and *ugt76b1-1* root (WT/ko) presented an intermediate stage. WT/ko plants showed a slight upregulation of *PR1*,

PR2 and *PR5*. The detected expression is not significantly different from *ugt76b1-1* homo-grafts, although at the same time it is not statistically different from Col-0 homo-grafts as well.

The lack of *PR* gene induction after introducing Col-0 root to *ugt76b1-1* shoot obviously indicates that the root plays a pivotal role in modulating *UGT76B1*-dependent expression of *PR1*, *PR2* and *PR5* in aboveground tissues. However, *ugt76b1-1* root introduced to Col-0 shoot showed only a tendency for upregulation of *PR* marker genes.

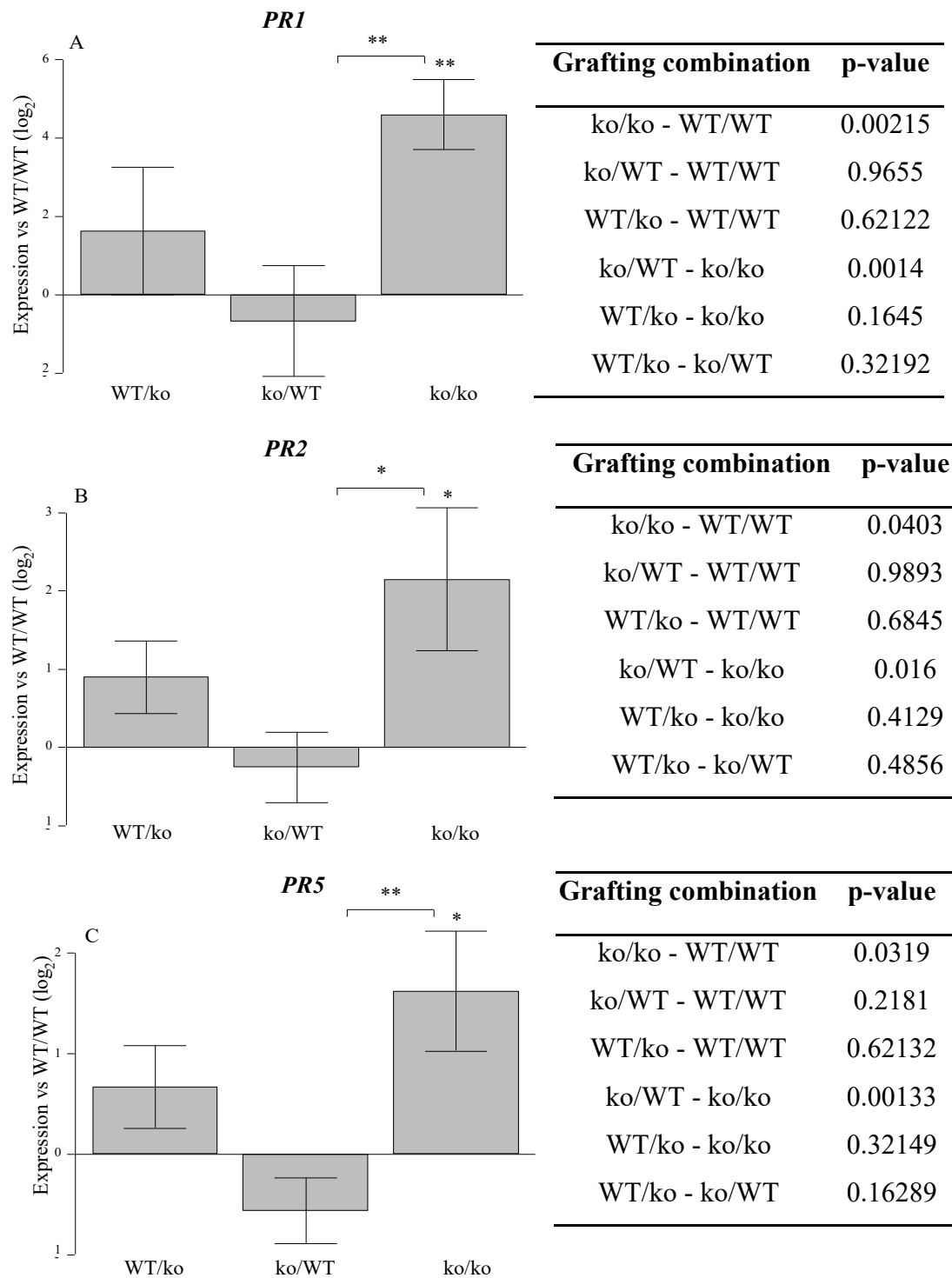


Figure 41. Expression of *PR1*, *PR2* and *PR5* marker genes in grafted *A. thaliana* plants.

Gene expression of *PR1* (A), *PR2* (B), *PR5* (C) in homo- and hetero-grafts of *ugt76b1-1* and Col-0. WT/ko – Col-0 shoot and *ugt76b1-1* root; ko/WT - *ugt76b1-1* shoot and Col-0 root; ko/ko homo-graft of *ugt76b1-1*. Plants were grown for four weeks, for conditions see methods. Expression levels were normalized to *UBIQUITIN5* and *S16*. Arithmetic means and standard errors from \log_2 transformed data from three independent experiments. Asterisks above the bars indicate significance of the difference to the WT/WT homo-grafts, the significant differences between grafting combinations are marked by lines; ** $P < 0.01$, * $P < 0.05$ (paired ANOVA equal variance).

3. DISCUSSION

3.1 Is SA an *in vivo* substrate of UGT76B1?

3.1.1. Glucosyltransferases contributing to SA conjugation in *A. thaliana*

There are many enzymes identified as being active towards SA that convert salicylic acid to its inactive forms such as: SA *O*- β -glucoside (SAG), salicyloyl glucose ester (SGE), methylsalicylate (MeSA), methyl salicylate *O*- β -glucoside (MeSAG) or dihydroxybenzoates (DHBA) (Vlot and Dempsey, 2009). UGT76B1 was identified as a regulator of SA-JA cross-talk, negatively impacting the SA pathway, whereas positively affecting JA-mediated responses. *In vitro* it showed glucosyltransferase activity for ILA and SA, however the activity of UGT76B1 towards both substrates has not been further characterized in terms of enzyme kinetics. *In vivo*, increased level of conjugated SA in *ugt76b1-1* indicated that UGT76B1 is less likely contributing to SA conjugation (von Saint Paul *et al.*, 2011). Surprisingly, Noutoshi *et al.* (2012) introduced UGT76B1 as being involved in SAG synthesis *in vitro* and *in vivo*, which was demonstrated by the reduced SAG content in *ugt76b1-3*, similar to *ugt74f1*. However, Noutoshi applied mutants in Ws-4 accession, whereas von Saint Paul *et al.* (2011) characterized the Col-0 allele *ugt76b1-1*. In this work the previous studies were extended in order to further substantiate the role of UGT76B1 as well as of UGT74F1 and UGT74F2 in SA conjugation. Therefore, determination of SA/SA-conjugates, expression studies and root growth resistance were applied. Due to the lack of the full set of mutants in one genetic background some comparisons involved both Col-0 and Ws-4 ecotypes, however this was not applicable for the multiple mutants. It is also necessary to underline that the analytical methods applied in this study differs from the other reports in terms of the detection of SA in its conjugated form. The HPLC-based method applied in our laboratory (von Saint Paul *et al.*, 2011; Yin, 2010; Messner and Schöffner) did not discriminate SAG and SGE, therefore this analyte will be named as SA glucosides. The other key reports cited in this work (Dean and Delaney, 2008; Noutoshi *et al.*, 2012; Li *et al.*, 2015; Thompson *et al.*, 2017) applied analytical methods that enable distinguishing SAG from SGE.

A simultaneous comparison of SA and SA glucosides abundances in *ugt76b1* loss-of-function mutants in Col-0, *Ler* and Ws-4 background showed that Ws-4 allele *ugt76b1-3* contained wild-type levels of SA and SA glucosides, whereas the other alleles had enhanced levels (Fig. 5). Therefore, since SA glucosides are formed in all three mutants at least at the wild-type level, these results do not indicate the involvement of UGT76B1 in SA glucosylation in any

of the analyzed accessions. In *Arabidopsis* UGT74F1 and UGT74F2 were shown to glucosylate SA *in vitro* (Lim *et al.*, 2002; Li *et al.*, 2015; Thompson *et al.*, 2017). *In vitro* UGT74F2 synthesized mainly SGE and weakly SAG, whereas UGT74F1 only SAG. UGT74F2 demonstrated a much weaker activity towards SA (tenfold), compared to UGT74F1 (Thompson *et al.*, 2017). However, UGT4F2 showed higher activity towards anthranilate, benzoic acid and nicotinate than SA *in vitro* (Li *et al.*, 2015). Dean and Delaney (2008) monitored SAG and SGE abundance *in vivo* in mutants with affected expression of *UGT74F1* and *UGT74F2*. Treatment with exogenous [7-14C]SA resulted in decrease of SAG in *ugt74f1-1* and a lack of SGE formation in *ugt74f2-1*, compared to the corresponding wild-types. Moreover, *ugt74f2-1* mutant line showed reduced levels of SA, SAG and SGE upon *Pseudomonas* infection (Li *et al.*, 2015). On the other hand, two studies previously conducted in our laboratory indicated that the role of UGT74F1 and UGT74F2 in SA conjugation may potentially be less essential, than previously anticipated (Yin, 2010). Messner and Schöffner (personal communication) detected an increase of SA glucosides in *UGT74F1* and *UGT74F2* overexpression lines, therefore demonstrating that UGT74F1 and UGT74F2 may also accept SA as the substrate *in vivo*. Nonetheless, the analysis of untreated and BTH-treated *ugt74f1-1* (Ws-4) loss-of-function mutant and *ugt74f2-1* (Col-0) splice knock-down mutant indicated that neither *ugt74f1-1* nor *ugt74f2-1* led to a decrease of SA glucosides, if compared to the corresponding wild-types. Furthermore, Yin (2010) showed that a *ugt74f1 amiugt74f2* (Ws-4) double mutant with a strongly suppressed expression of UGT74F2, did not display reduced levels of SA glucosides in both untreated and BTH-sprayed double mutant plants, similar to the observation with *ugt76b1-3* mutants. Nevertheless, Yin (2010) could not fully exclude the residual activity of amiRNA-silenced *UGT74F2* as being responsible for the wild-type levels of SA conjugates in the double mutant plants. Double mutant chemotype may also suggest a presence of another SA conjugating enzyme. However, wild-type levels of SA and SA glucosides in both *ugt76b1-3* single mutant (Fig. 5) and *ugt74f1 amiugt74f2* double mutant (Yin, 2010) could also suggest that neither UGT76B1 nor UGT74F1 and UGT4F2 are involved in SA conjugation or that the two enzyme groups are complementary to each other. In this work it was demonstrated that the introduction of *ugt76b1-3* into *ugt74f1 amiugt74f2* (Ws-4) mutant triggered a strong decrease of SA conjugates, whereas the SA aglycon was induced (Fig. 6). Moreover, BTH-treated *ugt76b1 ugt74f1 amiugt74f2* triple mutant triggered a very strong accumulation of the free SA without raising SA conjugates levels (Fig. 7). This demonstrated that UGT76B1 is indeed involved in SA conjugation in concert with UGT74F1

and UGT74F2, which could not be previously ascertained by the determination of SA and SA glucosides in single loss-of-function mutants.

The examination of the role of UGT74F1, UGT74F2 and UGT76B1 in glucosylating SA was also extended to the belowground tissues. This was achieved by monitoring the effect of exogenously applied SA on root elongation, which is known to negatively impact *A. thaliana* growth (Rivas-San Vicente and Plasencia, 2011; Zhao *et al.*, 2015). The over-accumulation of the free SA could be triggered either by its enhanced synthesis or hindered conjugation, which most possibly transfers SA to its inactive storage form (Vlot and Dempsey, 2009). Here, UGT76B1 was identified as a crucial player in neutralizing the impact of exogenous SA on the root growth. This was demonstrated by the enhanced reduction of the root growth in the presence of SA in *ugt76b1-1* and *ugt76b1-3*, whereas a wild-type response of simultaneously grown *ugt74f1-1* and *ugt74f2-1* was recorded (Fig. 8). Furthermore, *UGT76B1-OE7* demonstrated increased resistance to SA in the media (Fig. 9). Interestingly, the *ugt74f1 amiugt74f2* double mutant showed wild-type root growth response in presence of SA as well, whereas the *ugt74f1 amiugt74f2 ugt76b1* triple mutant demonstrated hypersensitivity (Fig. 10). This was in agreement with the assumption that UGT76B1 glucosylates SA in the root tissues and is essential for root growth response to exogenously applied SA, but again *UGT74F1/UGT74F2* had an influence on SA sensitivity in a *ugt76b1* background. Since the assays had been performed on SA-containing plates, in addition to root growth inhibition, an impact on germination of the triple mutant cannot be excluded.

The wild-type phenotype observed in single and double mutants together with the reverted chemotype of the *ugt76b1 ugt74f1 amiugt74f2* triple mutant in terms of abundance of SA and SA glucosides may suggest a mutual compensation of UGT74F1, UGT74F2 and UGT76B1. Furthermore, wild-type root growth response to SA of *ugt74f1-1*, *ugt74f2-1* and *ugt74f1-1 amiugt74f2-1* double mutant, whereas hypersensitive response of *ugt74f1 amiugt74f2 ugt76b1* triple mutant also suggests compensation. Gene expression analysis in the rosette tissues revealed a moderately increased mutual expression of *UGT74F1* in *ugt76b1-1* and *UGT74F2* in *ugt76b1-1*, *ugt76b1-3* and *ugt74f1-1* (Fig. 11 A-B) and *UGT76B1* in *ugt74f1 amiugt74f2* double mutant (Fig. 11C), which also indicates compensation. However, due to a distinct spatial expression pattern it is currently not clear how these enzymes may collaborate in this process. *UGT74F1* is expressed in the vascular tissue of roots including closely neighboring cell layers, leaves vascular tissue and flower stalks (Messner, Bauer and Schäffner, personal communication). *UGT74F2* is expressed in patchy way in the leaves and evenly in sepals and

petals and opened flowers, whereas in roots in the cortex and rhizodermis. Moreover, *UGT74F2* is highly expressed in the seeds (Li *et al.*, 2015; Messner and Schöffner, personal communication). *UGT76B1* displays the highest expression in the root, mainly in cortex and endodermis, whereas in the aboveground tissues in very young leaves, hydathodes, sepals, and style (von Saint Paul *et al.*, 2011). Furthermore, except different expression pattern two other differences between *UGT76B1* and *UGT74F1*, *UGT74F2* were recorded. In contrast to *UGT74F1* and *UGT74F2*, *UGT76B1* was shown as being highly inducible in response to environmental conditions. For instance, application of BTH revealed a very weak and moderate response of *UGT74F1* and *UGT74F2* (Fig 13A), whereas a very strong activation of *UGT76B1* (similar to *PR1*) in Col-0 plants (Fig. 13B). Secondly, *UGT74F1* and *UGT74F2* may impact the expression of *BSTM1*, an SA-methyltransferase, which also can contribute to SA conjugation. This was demonstrated by a comparable induction of *BSTM1* in *ugt74f1 amiugt74f2* and *ugt76b1 ugt74f1 amiugt74f2* mutant lines upon BTH treatment (Fig. 12D).

Collectively, this work confirmed the work by Noutoshi *et al.* (2012) that *UGT76B1* is an *in vivo* SA glucosyltransferase in Ws-4 accession. This fact was further substantiated by the analysis of single and multiple mutants of *ugt74f1*, *ugt74f2* and *ugt76b1* in terms of abundance of SA and SA glucosides, root growth response to elevated levels of SA and gene expression analysis. On the other hand, in Col-0 background, the *in vivo* activity of *UGT76B1* towards SA still needs to be confirmed and remains a partially open question, due to the lack of a full set of the mutants in Col-0 background, which should be established along with multiple mutants of *ugt74f1 ugt74f2* and *ugt74f1 ugt74f2 ugt76b1* in Col-0, to properly address this question. Moreover, currently CRISPR/Cas genome editing system provides the opportunity for producing a loss-of-function *ugt74f1 ugt74f2* double mutant, instead of applying an amiRNA silenced line, which may still possess a residual activity of *UGT74F2*. Nevertheless, *in vitro* study on *UGT76B1* SA-dependent glucosylation clearly demonstrated that *UGT76B1* recombinant protein from Col-0 and Ws-4 accession shows activity towards SA (Noutoshi *et al.*, 2012; Zhang, personal communication). Furthermore, future studies have also an opportunity to apply a new useful tool. Its concept is based on the introduction of a known *in vivo* SA glucosyltransferase such as *UGT74F1*, driven by the 5' and 3' regulatory regions of *UGT7B1* into the *ugt76b1-1* mutant (Fig. 14). Therefore, this transgenic situation should complement any function of *UGT76B1* that is related to a *in vivo* activity towards SA, e.g. it might restore the changes of marker genes expression in *ugt76b1-1* loss-of-function mutant, if this is solely or primarily related to *UGT76B1*'s SA glucosylation. Preliminary data

using a transgenic line expressing such a hybrid UGT construct indicated that this scenario could be possible (Fig. 15).

3.1.2. SA and its conjugates are distinctly accumulated in Col-0, Ler and Ws-4 wild-type plants

SA determination revealed that in terms of SA conjugation the Col-0 ecotype behaves differently than Ws-4 and *Ler* accessions, which was manifested by a highly increased SA glucosides abundance in Col-0, if compared with two other ecotypes (Fig. 5). This may be modulated upstream of SA, for instance due to its enhanced synthesis or downstream of SA due its increased conjugation in Col-0. Here, the expression analysis of the three SA-conjugating glucosyltransferases indicated fourfold higher basal expression level of *UGT76B1* in Col-0 than in Ws-4, however indistinguishable levels of *UGT74F1* and *UGT74F2* (Fig. 11D). This could imply *UGT76B1* as being potentially responsible for a higher accumulation of SA glucose conjugates in Col-0 ecotype. It is known that natural genetic variations between the accessions are responsible for a different phenotype among the plants of the same species (see also chapter 2.3.1.). Therefore, the nucleotide sequence of *UGT76B1* coding region and regulatory regions of the three ecotypes were further investigated. This proven that Col-0 differs strongly from Ws-4 and *Ler* accessions. *In silico* analysis of the deleted regions of 5'-UTR of *UGT76B1* are localized at -482 bp to -637 bp relative to the start codon (Fig. 16), which is beyond the core promoter. Therefore, the localization of the TATA-element in this region of the promoter cannot impact the expression level of *UGT76B1*. The second missing *cis*-regulatory element of Ws-4 and *Ler* promoter CAAT-box, which in plants is present in 5' – UTR of the genes involved in light response, circadian clock regulation (Wenkel *et al.*, 2006) and regulation of flowering time (Cai *et al.*, 2007). Interestingly, light and circadian clock have been shown to play an important role in SA-mediated defense response (Roden and Ingle, 2009; C. Zhang *et al.*, 2013). For instance, Griebel and Zeier (2008) demonstrated a positive impact of light on SA and SAG accumulation upon *P. syringae* infection. Furthermore, the location of the analyzed CAAT-box beyond the core promoter should not exclude this sequence motif from the consideration. It was demonstrated that the promoters do not display a consistent location for CAAT elements and for instance in yeasts and humans they are found 80 – 300 bp upstream the transcription start site (Wenkel *et al.*, 2006). Moreover, Testa *et al.* (2005) proven the presence of functional CAAT elements in the distal regions of the human promoters.

This study also revealed a different organization of the 3'-UTR of *UGT76B1* in *Ws-4* and *Ler* which is manifested by a deletion starting 375 bp downstream of the stop codon in *Ws-4* and *Ler UGT76B1* terminators, relative to *Col-0* (Fig. 18, Suppl. Fig. 4). Moreover, this deletion encompasses two genes in *Ler* and *Ws-4*. However, due to the not annotated function their impact on SA/SA glucosides homeostasis cannot be substantiated at the moment. Untranslated gene regions are known to have a very broad function in regulation of gene expression (Barrett *et al.*, Fletcher and Wilton, 2012). Therefore, predicting the effect of the mutations at the 3'-UTR of *UGT76B1* in *Ws-4* and *Ler* cannot be assessed at this stage of the study.

Analysis of *UGT76B1* protein sequence demonstrated five identical amino acid substitutions (AAS) in *Ws-4* and *Ler* compared to *Col-0* (Fig. 17). It is known that AASs located at the active site could block its entrance, alter the substrate specificity, or affect the binding affinity (Teng *et al.*, 2010). A preliminary analysis of the *Col-0* and *Ws-4* protein structure was performed by Phyre2 (Kelley *et al.*, 2015) and SWISS-MODEL (Biasini *et al.*, 2014). Nevertheless, protein structure modeling is based on the homology to already known three dimensional structures, thus application of these methods can only visualize the location of the mutation in a 3D structural context (Kelley *et al.*, 2015). Here, the recently published structure of *UGT74F2* (Thompson, *et al.*, 2017) was used as a template for modeling the structure of *UGT76B1*. The predicted model of *UGT76B1* 3D structure demonstrated that AASs in *Ws-4* and *Ler* are not located in close neighborhood of the substrate-binding protein pocket (Fig. 42). Nevertheless, the protein sequence identity between *UGT76B1* and *UGT74F1* and *UGT74F2* is at a relatively low level, 28.1% and 27.6%, respectively (Suppl. Fig. 10-11) (77% between *UGT74F1* and *UGT74F2* (Thompson *et al.*, 2017)). However, the sequence identity at the level of ~ 30% was proven to provide at least a partially correct model. Thompson *et al.* (2017) compared the crystallized structure of *UGT74F2* to already crystallized homologs. Despite the low sequence conservation the C-terminal domain containing the nucleotide binding site exhibited a very similar structure, whereas the N-terminal domain containing the acceptor binding site showed shifts and rotations.

Additional investigation of *UGT76B1* protein sequence by PROVEAN (Choi and Chan, 2015), a software that predicts whether an amino acid substitution has an impact on the biological function of a protein demonstrated that two AAs at positions 316 and 322 may have a strong impact on the protein (Table 7). However, these substitutions are located in the C-terminal domain (Fig. 42) that is responsible for sugar binding and therefore they should

not impact aglycon binding. Three other AAs are located in the N-terminal domain (Fig. 42) containing acceptor binding site for the aglycon. Although, PROVEAN analysis qualified these substitutions as having neutral impact on protein function their impact should not be fully excluded during future studies.

This study demonstrated the potential reasons for a distinct regulation and/or activity of UGT76B1 in Col-0 than in Ws-4 and *Ler* potentially affecting the homeostasis of SA/SA glucosides in the analyzed accessions. This was concluded from the enhanced expression of *UGT76B1* in Col-0, however undistinguishable levels of *UGT74F1* and *UGT74F2*. On the other hand, future studies should further prove the decisive function of UGT76B1 in this process. This could be easily achieved by complementation of the Ws-4 allele *ugt76b1-3* with a copy of the Col-0 *UGT76B1* gene. Furthermore, a number of studies already demonstrated that Ws-4 ecotype frequently displays a specific phenotype different from Col-0 and *Ler*-0 (Chevalier *et al.*, 2003; Routaboul *et al.*, 2012; Yin *et al.*, 2012; Matsoukas *et al.*, 2013). In addition to the many known differences between these accessions, it was observed that Ws-4 shows a different accumulation of SA glucosides (Fig. 5), lower basal expression of *UGT76B1* (Fig. 11D), however higher induction upon BTH treatment (Fig. 12E), enhanced root growth inhibition in the presence of SA (Fig. 8), smaller rosette size and slightly accelerated flowering time than the Col-0 allele.

Table 7. The potential effect of AASs on UGT76B1 in Ws-4 and *Ler*

Table presents the AASs in UGT76B1 in Ws-4 and *Ler*, compared to Col-0. Variants with a score equal to or below -2.5 are considered as deleterious, whereas variants with a score above -2.5 are considered as neutral. Analysis performed by PROVEAN (<http://provean.jcvi.org> 05/2017).

Substitution	Position	Score	Predicted impact on the protein
Glu -> Lys	44	0.023	Neutral
Thr -> Ser	57	-1.694	Neutral
Ser -> Gly	64	2.703	Neutral
Glu -> Lys	316	-2.554	Deleterious
Gly -> Cys	322	-7.433	Deleterious

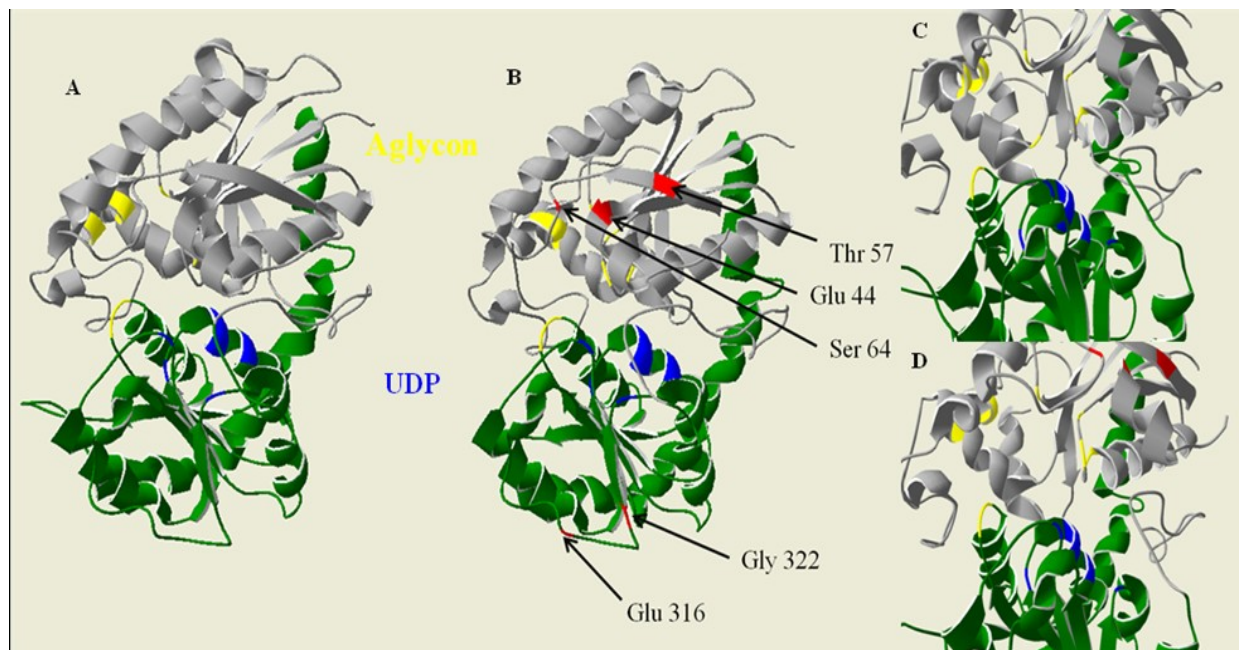


Figure 42. Predicted model of the tertiary structure of UGT76B1 (Col-0).

(A) Tertiary structure of UGT74F2 (Thompson *et al.*, 2017). N-terminal domain (residues 4 to 245) is colored in gray, while C-terminal domain (residues 246 to 447) in green. (B) Predicted model of tertiary structure of UGT76B1 (Col-0). Modeling performed by Phyre2 (www.sbg.bio.ic.ac.uk/~phyre/) (Kelley *et al.*, 2015). Template: c5v2kA, UGT74F2; Confidence: 100%; % of identity: 27%. N-terminal domain (residues 6 to 245) colored in gray, while C-terminal domain (residues 246 to 445) in green. Amino acids substituted in *Ler* and *Ws-4* are marked in red color. In (A), (B), (C) and (D) amino acids marked in yellow color are responsible for aglycon binding, whereas in blue color for binding of UDP-glucose. In UGT76B1 structure amino acids that bind aglycon and carbohydrate (Fig. B and D) are predicted, based on the protein sequence alignment (Suppl. Fig. 11). (C) and (D) close up on protein pockets of UGT74F2 and UGT76B1, respectively.

3.2. The role of ILA and its impact on *A. thaliana* root growth

3.2.1. ILA as an *in vivo* substrate of UGT76B1

A nontargeted metabolomic approach led to the identification of ILA glucoside as being positively correlated with *UGT76B1* expression, thus pointing to ILA as an endogenous substrate of UGT76B1 (von Saint Paul *et al.*, 2011). In the current study, targeted metabolomic approach confirmed the *in vivo* activity of UGT76B1 towards ILA, which was demonstrated by the negative correlation of ILA in its free form with *UGT76B1* expression both in below- and above-ground tissues (Fig. 22). In contrast to ILA, its chemically closely related compound LA is not affected by UGT76B1 *in vivo*, albeit LA is a weak substrate of UGT76B1 *in vitro* (Fig. 21). At the same time, VA could not be detected in *A. thaliana* (Fig. 20F-G; Suppl. Fig. 7). Further studies revealed a very different behavior of ILA and LA, thus possibly pointing to a distinct function of these two chemically similar compounds.

A very intriguing aspect of ILA and LA nature is their reverted accumulation pattern during plant growth and development (Fig. 23). Two-week-old *Arabidopsis* plants demonstrated the highest abundance of ILA, which is reduced in three-week-old plants and not further changed in four-week-old plants. Whereas, LA behaves in the opposite manner; demonstrating lowest abundance in the young *Arabidopsis* and increased in the four-week-old plants. However, LA content in contrast to ILA is further changed in four-week-old plants. It may be speculated that the decrease of ILA and a concomitant increase of LA are possibly associated with growth phase. *UGT76B1* displays an age-dependent expression profile in aboveground tissues, which is enhanced in very young, whereas decreased in older leaves (von Saint Paul *et al.*, 2011). Therefore, this fact could be considered as being correlated with ILA depletion during growth and development. However, the increased conjugation of ILA that could trigger its depletion cannot be excluded without the simultaneous determination of free and conjugated ILA. Nevertheless, the strong increase of LA remains obscure and is less likely to be associated with the *UGT76B1* activity, albeit LA is a weak substrate of *UGT76B1 in vitro* (Fig. 21).

The synthesis of ILA, LA and VA in humans occurs via Ile, Leu and Val degradation (Podebrad *et al.*, 1997). In plants it still has not been confirmed, however it cannot be excluded that the analogous way of BCAA 2-HA derivatives synthesis occurs in plants as well. Yu *et al.* (2013) demonstrated Val as the most abundant BCAA in *Arabidopsis*, whereas Ile and Leu levels were respectively 3 and almost 7 fold lower. Thus, it could be speculated that the levels of ILA, LA and VA are modulated in accordance to their function and are not determined by the particular BCAA availability. On the other hand, the lack of correlation could also indicate a different way of ILA and LA synthesis in plants than in humans. Nevertheless, the current knowledge on the regulation of BCAA degradation is poorly explored. It is only known to be enhanced during the carbohydrate starvation conditions in the darkness (Binder, 2010).

3.2.2. ILA and LA are differently involved in plant defense to *P. syringae*

The first report introducing the potential L-isoleucine derivative ILA as an active compound in plants, demonstrated that its exogenous application stimulates plant defense response against biotrophic pathogen *P. syringae* (von Saint Paul *et al.*, 2011), therefore pointing ILA as a potential modulator of plant immunity.

It has been shown that the levels of BCAAs, if compared to the other amino acids are highly increased upon *P. syringae* infection in *A. thaliana* (Návarová *et al.*, 2012) and *N. tabaccum* (Vogel-Adghough *et al.*, 2013), thus indicating their potential involvement in plant defense response against biotrophic pathogen. Except the broadly described synthesis and degradation pathways of BCAAs (Hagelstein *et al.*, 1997; Campbell *et al.*, 2001; Diebold *et al.*, 2002; Schuster and Binder, 2005; Binder, 2010; Maloney *et al.*, 2010), the physiological role of BCAAs beyond protein biosynthesis stays still obscure. Amino acid-derived molecules are known to be relevant for plant defense response activation. For instance, pipecolic acid (Pip), a Lys catabolite, has been introduced as a crucial regulator of plant immunity in *A. thaliana* (Návarová *et al.*, 2012) and *N. tabaccum* (Vogel-Adghough *et al.*, 2013). Among tested α -hydroxy acids, only ILA, the 2-HA derivative of Ile, displayed significant changes upon *P. syringae* infection (Fig. 24A, C). Simultaneous determination of LA, the 2-HA derivative of Leu, demonstrated that this compound is not affected 24 hours post pathogen infection (Fig. 24B, D). *Arabidopsis* wild-type plants infected with *P. syringae* displayed a decreased content of ILA. It was already shown that both ILA and SA are the *in vivo* substrates of UGT76B1. The role of ILA may be to prevent UGT76B1 from glucosylating SA, therefore enhancing or/and prolonging SA-mediated defense. This mechanism would explain the decrease of ILA upon infection with biotrophic pathogen. On the other hand, one can also speculate that ILA abundance indeed increases at the very early stage of *P. syringae* infection. Von Saint Paul *et al.* (2011) demonstrated that *UGT76B1* reaches the highest expression level eight hours post *Pseudomonas* infection. Furthermore this report also suggested that the high expression of *UGT76B1* within this timeframe might be required for a controlled suppression of SA-dependent defense response. Therefore to further substantiate the role of ILA as a competitive inhibitor of SA glucosylation a time-dependent determination of ILA upon the infection is required. Furthermore, it is also strongly advised to determine the abundance of SA and SA conjugates upon ILA treatment. Thus, if considering the suggested function of ILA as a competitive inhibitor of SA glucosylation, it seems surprising at the first glance that ILA also decreases in *ugt76b1-1* mutant. However, this may indicate an independent from UGT76B1 regulation of ILA abundance. During the further steps post infection ILA may be degraded or not formed, instead of being conjugated, thus explaining its depletion after infection in *ugt76b1-1* mutant. One could also speculate that ILA functions as an inhibitor of UGT74F1 and UGT74F2 dependent SA glucosylation. However, this is not likely, since UGT74F1 *in vitro* activity tests (Noutoshi *et al.*, 2012) indicated that UGT74F1 does not accept ILA as the substrate.

Alternatively, however less possibly, an UGT76B1 independent manner of ILA action may indicate that ILA stimulates SA-mediated defense by interacting directly or indirectly *via* a yet unknown component or signaling cascade, which subsequently triggers ILA inactivation via degradation or conjugation. Furthermore, it cannot be excluded that in *ugt76b1-1* loss-of-function mutant ILA is conjugated by another UGT. Microarray expression profile of *ugt76b1-1* mutant (Zhang, 2013) showed upregulation of three glucosyltransferases: *UGT73B2* (At4g34135), *UGT73B3* (At4g34131) and *UGT71B6* (At3g21780) (4.8, 4.5 and 2.9 fold, respectively). Moreover, *UGT73B3* and *UGT71B6* displayed a slight activation upon ILA treatment (Zhang, 2013). Therefore in future studies a simultaneous determination of ILA and its conjugate should be performed.

So far, the positive impact of ILA on defense in the other plant species was demonstrated in barley (Zhang, 2013). To further explore, if ILA may impact on defense modulation in other plant species, its abundance was determined in different species, including crop plants and trees (Fig. 25-26). This demonstrated the ubiquitous presence of ILA, yet at very different levels. This indicates that ILA has potentially a similar role in modulating the defense response in other species and future studies should be also extended to agricultural plants.

3.2.3. Possible scenarios for ILA action in the *A. thaliana* roots

3.2.3.1. ROS is potentially involved in ILA dependent root growth inhibition

A genome-wide association mapping for loci associated with the increased root growth resistance to exogenous ILA led to the identification of a region on the chromosome 1 containing a set of genes potentially involved in the response to exogenous ILA (Table 2). Sequence comparison of the top ten susceptible and resistant accessions led to A->G polymorphism which was predicted to eliminate the catalytic A residue required for the cleavage of the donor site of the third intron of *SRX* gene in the susceptible accessions (Fig. 31, SNP No. 8). As a consequence, the *SRX* gene would not be correctly expressed. Deregulation of the splice site can have a numerous consequences to RNA processing, such as exon skipping, intron retention, cryptic splicing, leaky splicing or introduction of pseudo-exons into mRNA (Caminsky *et al.*, 2014). Therefore, it is highly possible that the product of the *SRX* gene will be impaired in its function in the accessions demonstrating enhanced root growth susceptibility in the presence of ILA. *SRX* encodes a redox dependent sulfinic acid reductase involved in the regulation of intracellular reactive oxygen species (ROS) levels. The function of *SRX* in regulating ROS abundance has already been confirmed in different

organisms, such as yeasts (Biteau *et al.*, 2003), plants (Iglesias-Baena *et al.*, 2010; Chi *et al.*, 2012; Puerto-Galán *et al.*, 2015) and mammals (Jeong *et al.*, 2006). In order to eliminate the excess levels of hydrogen peroxide the active cysteine 2-Cys peroxiredoxin (2-Cys-Prx) is oxidized into cysteine sulfinic acid (Cys-SO₂H), which inactivates the protein. The inactive 2-Cys-Prx is then reactivated by the reductase activity of SRX (Chi *et al.*, 2012). Puerto-Galán *et al.* (2015) demonstrated both that NADPH thioredoxin reductase C (NTRC) together with SRX play a central role determining the redox status of 2-Cys-Prx. The same study also showed that deficiency of *srx* caused the increase of oxidized form of 2-Cys-Prx. Moreover, two previous studies (Peng *et al.*, 2006; Iglesias-Baena *et al.*, 2010) recorded the increased susceptibility to oxidative stress of the *srx* loss-of-function mutant. Furthermore, Chi *et al.* (2012) reported also a novel activity of SRX, which can act as a nuclease and potentially participate in repair of ROS-triggered DNA damage in chloroplasts and mitochondria. Thus, the ILA dependent root growth inhibition may be associated with the enhanced ROS production. A number of reports already associated ROS production with the response to biotic and abiotic stress factors, which can affect plants in two ways. During the stress ROS can act as a signaling molecule activating response pathways (Mersmann *et al.*, 2010; Shapiguzov *et al.*, 2012; Gilroy *et al.*, 2016). On the other hand, overaccumulation of ROS is toxic to nucleic acids, proteins and lipids and may be responsible for cellular damage (Gill and Tuteja, 2010). Choudhury *et al.* (2016) indicated the presence of a two major ROS sources in plants during the abiotic stress, a signaling and a metabolic ROS. The signaling ROS is generated upon the stress perception and is mediated by calcium or phosphorylation-derived activation of NADPH oxidases, whereas the metabolic ROS abundance increases as a consequence of metabolic activity disruptions during the stress event. Considering the role of *SRX* in ROS homeostasis and the toxicity of its elevated levels, at this stage of the study both, metabolic and signaling ROS should be considered. It could be speculated that a long-term exposure of the roots to ILA may trigger metabolic disruptions initiating the oxidative stress in the root tissues and as a consequence of this event inhibit root growth in *Arabidopsis*. Moreover, oxidative stress was already reported to affect negatively the root growth (Singh *et al.*, 2006; Tsukagoshi, 2012; Martins, Gonçalves and Romano, 2013). Accordingly, ILA-dependent root growth inhibition could be triggered/mediated by oxidative stress. On the other hand, it cannot be excluded that function of ILA is based on triggering signaling ROS production, which is then potentially overaccumulating in susceptible accessions as the consequence of hindered *SRX* function. Previous studies on the aboveground tissues demonstrated the synergistic effect of ILA on SA-mediated defense pathway (Zhang and

Bauer, personal communication). The way how ILA stimulates SA pathway is most possibly based on a competitive inhibition of UGT76B1-dependent SA glucosylation. Thus it may be worth to consider if ILA-mediated root growth inhibition is also dependent on SA, which can be evaluated by planting of SA-deficient mutants (i.e. *NahG* or *sid2*) on plates containing ILA. On the other hand, it has been reported that H₂O₂ bursts precede SA signaling in response to stress (Herrera-Vásquez and Salinas, 2015). Thus, it could be speculated that the manner of ILA action is based on a more direct induction of H₂O₂ that further stimulates the SA-mediated defense. Nevertheless, further studies on this aspect should be preceded by the experimental confirmation of the predicted deviation in the splicing of *SRX*. As the next step it is advised to confirm the involvement of *SRX* in response to exogenous ILA. This may be easily determined by planting the *srx* T-DNA insertion mutant on ILA plate or by complementing a susceptible, *SRX*-deficient accession by a fully functional *SRX* gene.

Moreover, the potential involvement of ROS in ILA-dependent root growth inhibition was also implied in an independent T-DNA insertion line screen for ILA insensitivity. Due to a high number of mutant lines demonstrating an increased resistance towards ILA, a further examination involving application of IAA, SA and Me-JA was performed (Fig. 34A-D), which revealed a cluster composed of the mutants demonstrating wild-type responses to the applied hormones, however enhanced resistance to ILA (Fig. 35). Thus, this phenotype may be considered as being ILA-specific. SALK_05835 is a T-DNA insertion line of SERAT3;2 with the insertion in the promoter region. It has been observed that the T-DNA insertion in the 5'-UTR may enhance the expression of the particular gene. This phenomenon was already observed in this study (Fig. 39A) and was also recently reported for SALK_05835 line (Thatcher *et al.*, 2016). Therefore, the elevated level of SERAT3;2 transcripts may potentially be present in SALK_05835 line as well. SERAT3;2 is involved in cysteine biosynthesis, which may be inferred as a potential linkage to the resistance to ROS. Cys residues are highly important in regulating ROS homeostasis. The elevated expression of the genes involved in Cys synthesis were already linked with the response to ROS (Błaszczuk *et al.*, 2002; Queval and Noctor, 2009; Speiser *et al.*, 2015). Queval and Noctor (2009) associated elevated abundance of ROS with the induction of the chloroplast SERAT2;1 and increased levels of Cys that is used for glutathione synthesis, which is further involved in H₂O₂ detoxification. On the other hand, SERAT3;2 belongs to the cytosolic isoforms of serine acetyltransferase family (Kawashima *et al.*, 2005; Hell and Wirtz, 2011). Nevertheless, Błaszczuk *et al.* (2002) demonstrated that bacterial SERAT proteins targeted to the cytosol of *N. tabaccum* trigger an increased resistance to H₂O₂. Furthermore, Kawashima *et al.* (2005) suggested a specific role

of *SERAT3;2* when plants are subjected to different environmental conditions, therefore its role in response to ILA should not be excluded. Nevertheless, future studies should first experimentally evaluate how the expression of *SERAT2;1* is affected in SALK_05835 line. It might also be examined whether ILA is capable of inducing ROS in the root tissues.

3.2.3.2. PDR3 is potentially involved in ILA transport

SALK_014957, similarly like above discussed insertion line of *SERAT2;1* was identified as a line displaying a wild-type response to the applied hormones, however increased resistance to ILA. SALK_014957, an insertion line of *PLEIOTROPHIC DRUG RESISTANCE 3 (PDR3)* showed a strongly reduced root growth susceptibility to ILA (Fig. 38). The stimulatory effect of ILA on plant defense is already known (von Saint Paul *et al.*, 2011; Zhang, 2013). On the other hand, the examination of the defense response as well as exogenous ILA levels in SALK_014957 line did not reveal a response different from the wild-type (Fig. 39B-C). Furthermore, the expression of the defense marker genes was also not affected in the leaves of SALK_014957 (Fig. 39D). Taking together these results it can be assumed that PDR3 does not impact the endogenous levels of ILA in the aboveground tissues of *A. thaliana*. The expression profiling of *PDR3* in the root tissues revealed a highly elevated level of *PDR3* transcript in SALK_014957 line (Fig. 39A), which is due to the T-DNA insertion located in the promoter region. Based on this result, it can be assumed that the root growth resistance to the exogenous ILA is associated with the enhanced expression level of *PDR3*. This fact was further confirmed by recent studies, which demonstrated an increased root growth susceptibility of *prd3* loss-of-function mutant (Schmiesing, personal communication). Recently PDR3 was reported to be involved in ABA (Kang *et al.*, 2015) and steryl glycosides (Choi *et al.*, 2014) transport. Kang *et al.* (2015) proven that PDR3/ABCG31 together with ABCG25 actively export ABA from the endosperm. Moreover, Kang *et al.*, (2015) localized PDR3 to the plasma membrane of *Arabidopsis* protoplasts. Therefore, taking together the subcellular localization of PDR3 and the positive relation of its expression with resistance to ILA, it can be hypothesized that PDR3 facilitates the export of ILA across the plasma membrane to the apoplast. PDR3 is an ATP-binding cassette (ABC) transporter, a member of ABCG subfamily and is full-size ABC transporter, composed of two transmembrane domains (TMD) and two nucleotide binding (NBD) at the cytosolic side (Kang *et al.*, 2011). ABC transporters are active transporters, where ATP hydrolysis drives a conformational shift in

TMD, which in consequence leads to the translocation of the molecule¹. Here, PDR3 was proposed to function as an isoleucic acid exporter, therefore the inward-facing conformation will have a greater binding affinity for ILA, whereas the outward-facing conformation will show a lower binding affinity in order to release ILA to the apoplast. It still requires experimental analysis whether PDR3 acts as an ILA exporter e.g. using an assay that would monitor ILA flux. Therefore, it may be worth to consider the method used by Kuromori *et al.* (2010) to prove the exporter activity of ABCG25. This would require expressing PDR3 in Sf9 insect cells and monitoring the flux of isotope labeled ILA. Furthermore, since ABCG25 and PDR3 act together in exporting ABA and share the subcellular localization (Kuromori *et al.*, 2010; Kang *et al.*, 2015), it cannot be excluded that these transporters also cooperate in the ILA export. Additionally, the role of ABCG25 in exporting ABA out of the cell was already confirmed (Kuromori and Shinozaki, 2014). Thus, it may be worth to examine, whether ABCG25 is also involved in response to exogenously applied ILA, which can be easily evaluated by recording the root growth response of *abcg25* loss-of-function in presence of ILA.

3.2.3.3. Potential perspectives for evaluating the impact of ILA on *A. thaliana* roots

GWAS are a very promising route for dissecting natural variation by associating phenotypes with genotypes. This method was successfully applied to analyze different traits such as salt tolerance (Baxter *et al.*, 2010), response to heavy metal (Chao *et al.*, 2012) or shade avoidance (Filiault and Maloof, 2012). In this study 159 *A. thaliana* accessions were applied to potentially identify the genes involved in root growth response in the presence of exogenous ILA. This led to the identification of only one GWAS hit at the position 11132605 on chromosome 1, which was slightly below the permutation threshold (Fig. 28C). The associated region on the chromosome 1 contains six other genes potentially involved in the response to exogenous ILA, in addition to the previously discussed *SRX* gene (Table 2). Nevertheless, due to the poor quality of the available sequences, an alignment of the sequences of the top susceptible and top resistant accessions was restricted to *SRX*. Therefore, when considering the extension of the current study it might be worth to examine the root growth in presence of ILA of the mutants whose genes were associated together with *SRX*.

¹ The model of function of ABC transporter is based on so called alternating-access model. In this model binding affinity for the substrate depends on the transporter conformation. Moreover, the direction of the transport is also determined by the binding affinity for the particular molecule to the inward- or outward-facing conformations (Rees *et al.*, 2009).

Thus, a response to ILA different from wild-type would indicate a potential importance of a particular gene in response to ILA. As a further step the regions containing genes potentially involved in ILA response may be sequenced in order to identify any polymorphisms. A preliminary examination of the *imd3* T-DNA insertion mutant showed a slightly reduced root growth in presence of exogenous ILA (data not shown). IMD3 is the isopropylmalate dehydrogenase, which is responsible for an oxidative decarboxylation of 3-isopropylmalate to 4-methyl-2-oxopentanoate that is then transaminated into branched chain amino acid Leu (Binder, 2010). This provides a linkage to the BCAA metabolism and may be highly important. GWAS can easily associate traits driven by a low number of loci with large effect size². Traits with complex architecture may be difficult to study by GWAS. This type of the architecture occurs when a particular trait depends either on many rare variants strongly affecting the phenotype, or on many common variants having a small phenotypic effect (Gibson, 2012; Korte and Farlow, 2013). Here, a relatively low number of 159 Swedish *A. thaliana* accessions had been applied. On the other hand, successful *Arabidopsis* GWAS was previously performed for only 107 accessions (Atwell *et al.*, 2010). Nevertheless, this clearly demonstrates that the particular trait is driven only by a few loci, which is known to increase a phenotypic variance (Korte and Farlow, 2013), thus enabling to obtain a meaningful associations even when applying such a small group of *Arabidopsis* accessions. Therefore, it cannot be excluded that the root growth resistance to ILA has complex architecture. The future application of GWAS as a method for dissecting the root growth response to ILA should involve a different population of *Arabidopsis* accessions. Korte and Farlow (2013) suggested application of geographically distinct accessions, which will maximize the genetic variance. However, application of geographically distant accessions can potentially introduce enhanced genetic heterogeneity, which has a negative impact on finding meaningful associations. Therefore it may be worth to focus on the local populations, similarly like it was performed in this study, which lowers the risk of introducing the heterogeneity. Nevertheless, it is strongly advised to significantly increase the population size.

Clustering the responses of ILA resistant T-DNA mutants to different hormones revealed a group of mutants displaying wild-type response to IAA, SA and Me-JA, however increased resistance to ILA. The potential role of two candidate genes candidates was already described above. This group of the mutants contains other potentially interesting lines. SALK_118494,

² The phenotypic variance between the accessions is determined by the effect size. It demonstrates how strongly the allelic variants differ in the phenotypic effect (Korte and Farlow, 2013; Gibson, 2012).

the mutant line of *ERF-14*, a positive regulator of JA-mediated (Mcgrath *et al.*, 2005; Onate-Sanchez *et al.*, 2006), together with the presence of a mutant of the negative JA regulation complex (*tp1*; AT1G80490) among the hypersensitive candidates may indicate a negative correlation of ILA resistance and JA-mediated pathway (see also chapter 2.3.2.4.4.). This may be evaluated by planting JA-pathway deficient mutants on the plates containing ILA. The other mutant lines may indicate the impact of ILA on sRNA regulated genes. SALK_110864, the T-DNA insertion line of *DUF3223*, recently annotated as a Dicer-like protein (DCL) (<https://www.araport.org> 06/2016) is also potentially interesting for the future studies due to its probable involvement in sRNA synthesis. The importance of sRNAs in response to a vast stress factors has been extensively reported (Matsui *et al.*, 2013; Cao *et al.*, 2016; Huang *et al.*, 2016; Wu *et al.*, 2016). Moreover, the expression of *DUF3223* in SALK_110864 may be enhanced due to the insertion on the promoter region. The contribution of the other mutants annotated in this cluster (lines: SALK_124100, SALK_040808, SALK_148617 and SALK_059101) cannot be excluded, nevertheless due to the lack of the functional connection, their contribution stays as an open question for the future study.

ILA-resistant mutants were also clustered for common responses to IAA, SA and Me-JA (Fig. 36). This can indicate a down-stream response, which is potentially associated with the growth regulation and currently cannot provide a linkage to the processes affected by ILA. Therefore, at this stage of the study this group may be considered as less essential. Taking together, further studies should rather concentrate on the common response to ILA and a particular hormone. Moreover, a very interesting candidate line was associated with the high resistance to the Me-JA (Fig. 37). SALK_028137 displayed enhanced resistance to methyl-jasmonate and ILA, however increased susceptibility to salicylic acid (Fig. 34). This line is a mutant of a HAD superfamily protein and, for instance, in yeasts this family of proteins is dominated by putative phosphatases (Kuznetsova *et al.*, 2015). Moreover, its expression in the root tip (Kerk *et al.*, 2008) and potential involvement in the nutrient uptake (Allen and Dunaway-Mariano, 2010) points this candidate as highly interesting for the future study.

Interestingly, it was observed that only SA treatment revealed susceptible mutants. Except the previously discussed *had* mutant there are two mutant lines demonstrating an increased ILA, however reduced root growth resistance to SA (Fig. 34A). SALK_150594 is a mutant of the protein of unknown function, thus its role in the presented phenotype cannot be assessed, and may potentially trigger the interest for the future study. Another potentially interesting candidate is SALK_053562, a mutant of SEC14, which was recently implied into modulation

of JA-mediated pathway activity (Kiba *et al.*, 2014). However, it is worth underlining that the T-DNA insertion in SALK_053562 line is located in the promoter region, thus it is required to first validate the expression level of *SEC14*.

3.3. Root expression of *UGT76B1* modulates *PR1*, *PR2*, *PR5* transcripts abundance in the shoot

Grafting experiments emphasized that the high expression of *UGT76B1* in the root has a decisive impact on the expression of *PR* genes in the shoot. This phenomenon was demonstrated by the down-regulation of *PR1*, *PR2* and *PR5* marker genes in *ugt76b1-1* rosette after fusion with wild-type root. Surprisingly, the opposite grafting combination (wild-type rosette fused with *ugt76b1-1* root) did not reveal a significantly enhanced expression of *PR* marker genes. However, further examination involving increased number of replicates (performed by Sybille Bauer) showed that *ugt76b1-1* root is indeed able to enhance the expression of *PR* marker genes in the wild-type rosette. Thus, it was demonstrated that the previously reported enhanced resistance of *ugt76b1-1* rosettes (von Saint Paul *et al.*, 2011) is regulated by the belowground tissues.

Past studies on plant defense mechanisms of the aboveground tissues mostly ignored or largely marginalized the role of the root in this process (Erb *et al.*, 2009). However, newest reports manifested the importance and the integral role of the root in the shoot response to the different stress factors (Bezemer and van Dam, 2005; Hasegawa *et al.*, 2011; Nalam *et al.*, 2012; Pieterse *et al.*, 2014; Agut *et al.*, 2016; Groen, 2016). Furthermore, the recently suggested model of the shoot-root-shoot (SRS) loop in the plant defense underlines the importance of the belowground organs in the shoot defense responses (Groen, 2016). This model explains a tight cooperation between the shoot and the root occurring under herbivore or pathogen attack. Leaves send systemic signal such as Glu, citric acid, fatty acids and myo-inositol to the root in response to a biotic stress (Agut *et al.*, 2016). As a response to that, roots may produce and send oxylipins (Nalam *et al.*, 2012) or defensive metabolites such as nicotine (Erb *et al.*, 2009) to the aerial parts. Alternatively roots may recruit beneficial rhizobacteria (Pieterse *et al.*, 2014), which was proven to impact positively defense response to biotrophs. However, the details of mechanisms how the root impacts and modulates the response to biotrophic pathogen are not fully evaluated. Currently it is known that the soil-inhabiting organisms can positively impact the defense response to *P. syringae* by triggering the induced systemic resistance (ISR). This was shown for non-pathogenic rhizobacteria

Pseudomonas fluorescens that increases the resistance to *P. syringae* infection in leaves (Bakker *et al.*, 2007). Lakshmanan *et al.* (2012) also substantiated the presence of a tight cooperation between above- and belowground tissues in defense response upon *P. syringae* infection. Leaf infection with biotrophic pathogen increased the expression of malic acid (MA) transporter, which led to enhanced MA secretion into the rhizosphere and triggered root colonization with *Bacillus subtilis* FB17, which subsequently caused ISR against *P. syringae*. However, in both examples the positive impact of the root on the shoot defense response depends on the recruitment of the rhizosphere-living organisms. Furthermore, rhizobacteria-mediated ISR against *P. syringae* occurs independently from SA (Wees *et al.*, 1997; Van Loon and Bakker, 2006; Pieterse *et al.*, 2014). My study demonstrated a different way, independent from the interaction with the soil-inhabiting bacteria, how the root modulates the shoot defense pathway against biotrophic pathogen. Moreover, this is the first report clearly manifesting that the expression of the *PR1*, *PR2* and *PR5* SA marker genes in the rosette can be modulated by the belowground tissues.

A vast number of molecules such as phytohormones (Zhang and Baldwin, 1997; Hartung *et al.*, 2002; Kohlen *et al.*, 2011; Kazan, 2013; Ko *et al.*, 2014), amino acids (Besnard *et al.*, 2016), peptides (Tabata *et al.*, 2014), proteins (Notaguchi and Okamoto, 2015), carbohydrates (Hammond and White, 2008), RNA species (Kehr and Buhtz, 2008; Bologna and Voinnet, 2014; Notaguchi, Higashiyama and Suzuki, 2015; Thieme *et al.*, 2015) and secondary metabolites (Groen, 2016) are known to participate in the communication between root and shoot. Nevertheless, at this stage of the study role of these compounds in UGT76B1-driven *PR* marker genes expression cannot be substantiated. However, two interesting observations involving ILA and moveable mRNA were recorded.

Previous determination of isoleucic acid abundance demonstrated increased levels of ILA in the belowground tissues in comparison to rosette, aboveground tissue (Fig. 22A-B). Furthermore, it is also known that exogenously applied ILA can trigger the up-regulation of *PR1* marker gene in the wild-type rosette to comparable levels like those reported for *ugt76b1-1* (Zhang, 2013). Therefore, even ILA itself may be considered as the root-to-shoot mobile signaling molecule responsible for root-driven *PR* genes expression modulation. When considering isoleucic acid as a part of the SRS, ILA translocation to the shoot would rather occur after transmission of a signal from the attacked aboveground tissues to the root.

Recently Thieme *et al.* (2015) presented a comprehensive identification of moveable transcripts in *Arabidopsis*. Importantly, mobile transcripts were already associated with phenotypic alterations in the targeted tissues, which was manifested by decreased plants size of *Arabidopsis* and tomato (Haywood *et al.*, 2005) and potato tuber size (Banerjee *et al.*, 2006). This also indicates that mobile mRNAs can produce functional proteins in targeted tissues. Thus, it may be concluded that the mobile mRNAs may act as regulatory RNA in response to stress facilitating the systemic adaptation and defense (Thieme *et al.*, 2015). Therefore, to assess, whether the phenomenon of moveable transcripts could be involved in modulating the root-dependent expression of *PR1*, *PR2* and *PR5* (*PR1* and *PR2* transcripts are not movable) the microarray expression dataset of *ugt76b1-1* leaves (Zhang, 2013) and a dataset of moveable transcripts in *A. thaliana* (Thieme *et al.*, 2015) were compared. Additionally to examine a potential involvement of ILA as a signaling molecule in moveable mRNA-dependent modulation of *PR* genes expression, a microarray dataset for the genes upregulated in leaves upon ILA treatment (Zhang, 2013) was included in this comparison as well. This led to the identification of 115 genes encoding moveable mRNA in *A. thaliana* that are at least twofold upregulated in *ugt76b1-1* mutant leaves. At the same time ILA can positively impact the abundance of 38 moveable transcripts. Interestingly, almost all (34 out of 38) ILA impacted moveable mRNAs exhibited at the same dependence on *UGT76B1* expression (Fig. 43). An analogous comparison of the genes that are at least twofold downregulated in *UGT76B1-OE7*, and at least twofold upregulated post ILA treatment pointed out 4 genes of moveable transcripts. Moreover, these four genes are shared by the group of a 34 (Table 8) moveable transcripts simultaneously upregulated in *ugt76b1-1* and by ILA application. Therefore, ILA may potentially impact moveable mRNAs abundance in a *UGT76B1*-dependent manner, thus being responsible for modulating the expression of *PR1*, *PR2* and *PR5* expression in aboveground tissues. However, when considering the potential involvement of moveable mRNA in *UGT76B1*- and root-dependent modulation of *PR* gene expression, it has to be emphasized that the microarray experiment has been performed using leaf material. Therefore, it is assumed that an upregulation in the leaf could also be related to an import from the root at least for transcripts with low abundance in wild-type or untreated conditions. A closer look on the identified mobile mRNAs revealed that fifteen out of thirty-four transcripts were moved bidirectionally. This number may be considered as enrichment, since in total in *Arabidopsis* only ~24% mRNAs translocate bidirectionally. The same number of mRNA demonstrated the mobility in the shoot-root direction, which corresponds to the overall percentage of the mobile mRNAs translocated in this direction in *Arabidopsis*.

Interestingly, the identified group of mobile transcripts contains also four mRNAs moving exclusively in root-shoot direction (Thieme *et al.*, 2015).

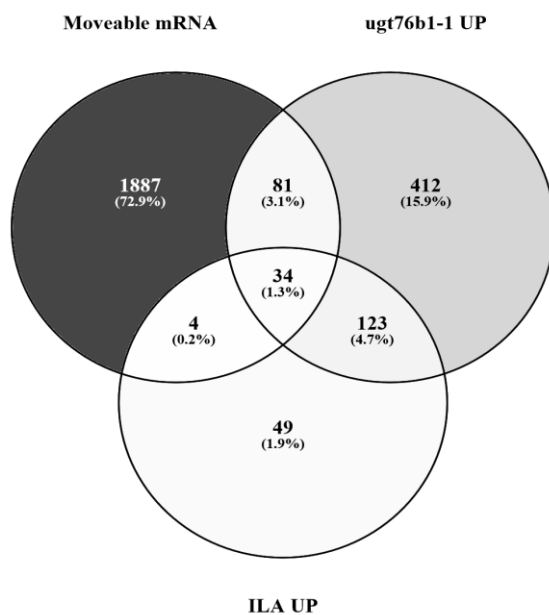


Figure 43. Moveable transcripts in *A. thaliana* positively associated with *ugt76b1-1* and ILA.

Pattern for *ugt76b1-1* and ILA upregulated genes (at least twofold) and genes encoding moveable transcripts in *A. thaliana*. Analysis based on the microarray expression profile of *ugt76b1-1* leaves and Col-0 ILA treated leaves (Zhang, 2013) and moveable mRNA in *Arabidopsis* (Thieme *et al.*, 2015).

For this study mRNAs translocated from the root to the shoot tissues are potentially more relevant, thus further considerations were focused only on this group of transcripts. Moreover, this mobile mRNAs were further screened for transcripts showing high upregulation (at least two \log_2 fold change) in *ugt76b1-1* and upon ILA treatment, whereas low abundance in control plants. Following these restrictions seven genes encoding moveable mRNA were identified (Table 9). Furthermore these genes can be associated with defense response. At3g26830 (*PAD3*) is responsible for camalexin biosynthesis (Böttcher *et al.*, 2009), which accumulation was associated with resistance to necrotrophic and hemibiotrophic fungus. However *PAD3* expression does not affect plant resistance to *Pseudomonas* (Lemarie *et al.*, 2015). At3g50770 (*CML41*) encodes a calmodulin like protein. CMLs together with calmodulin bind Ca^{2+} and are known to be essential for calcium signaling, which is important in response to pathogens and abiotic stress factors (Eulgem *et al.*, 2004; Ranty *et al.*, 2006). Moreover, At1g61800 (*GTP2*) may also be linked to calcium signaling since its expression was strongly upregulated in *cax1 cax3* double mutant under excess P_i (Liu *et al.*, 2011). However, more recent study demonstrated *GTP2* to be involved in acclimation of photosynthesis to increased light conditions (Dyson *et al.*, 2015). At4g14630 (*GLP9*) belongs to 9-hydroxyoctadecatrienoic acid (9-HOT) responsive genes and is strongly upregulated upon *Pseudomonas* virulent and avirulent strain infection (Vellosillo *et al.*, 2007). At4g00700 encodes a *PHOSPHORIBOSYL ANTHRANILATE TRANSFERASE*, a key enzyme in Trp biosynthesis (Pastori *et al.*, 2003). The abundance of Trp is known increase upon

Pseudomonas (*hrp*⁻) avirulent strain (Rojas *et al.*, 2013), which may associate this transcript with defense response. In contrast to the above discussed genes the function of At4g10500 (*DLO1*) is differently related to defense response. *DLO1* was characterized as an enzyme that hydroxylates SA to 2,3-DHBA, thus acting as negative regulator of SA-mediated defense (Zeilmaker *et al.*, 2014). Therefore, it most probably attenuates the defense response after pathogen infection. Furthermore, *DLO1* except being highly upregulated in *ugt76b1-1* and upon ILA treatment showed also a strong downregulation in *UGT76B1-OE7* line, which was not recorded for any other gene in this group (Table 9).

Collectively, two possible scenarios how the root may impact the *PR* marker were suggested in this study. However, prior exploring the role of ILA and mobile mRNAs in this process it is strongly advised to study the role of SA in the root-driven *PR* marker genes expression. This can be achieved by grafting wild-type plants with *ugt76b1 NahG sid2* triple mutant. Although the involvement of ILA or/and mobile mRNA in regulation of this process seems to be promising at the first glance, however, it needs to be further substantiated. Although ILA and moveable transcripts presented a strong relationship (Fig. 43) their simultaneous involvement in root-mediated *PR* marker genes expression in the shoot cannot be confirmed at the moment. Future studies may first concentrate on confirming the involvement of ILA. This would require grafting of *ugt76b1* and a mutant impaired in ILA synthesis. Nevertheless, first the way how ILA is produced in *Arabidopsis* needs to be evaluated.

Currently, the role of the root in the defense response of the shoot is emerging, however until now the function of the root in the shoot defense response against *P. syringae* was restricted to the recruitment of the beneficial rizosphere-inhabiting organisms triggering ISR. This work presented a novel, endogenous, *UGT76B1*-dependent way how the root can regulate the expression of *PR1*, *PR2* and *PR5* defense marker genes.

Table 8. Genes of moveable mRNA dependent on *UGT76B1* expression and ILA.

Genes displaying at least twofold upregulation in *ugt76b1-1* and upon ILA treatment. Genes marked with (*) are simultaneously in the common group for at least twofold downregulated genes in *UGT76B1-OE7* and at least twofold upregulated post ILA treatment.

AGI	Direction of the movement		AGI	Direction of the movement	
	Shoot-Root	Root-Shoot		Shoot-Root	Root-Shoot
At1g06670	+		At3g28580	+	
At1g07900	+		At3g50770	+	+
At1g20970	+		At3g50930	+	+
At1g21240	+		At3g51860	+	+
At1g61800		+	At4g00700	+	+
At1g67810	+		At4g10500*		+
At2g18690	+	+	At4g14630	+	+
At2g28290	+		At4g15610	+	+
At2g32240	+	+	At4g16660	+	+
At2g32680*	+		At4g21120	+	
At2g35980	+		At4g24450		+
At3g04720*	+		At4g27500	+	+
At3g13950*	+		At5g10380	+	
At3g21520	+		At5g16730		+
At3g26470		+	At5g23020	+	+
At3g26830	+	+	At5g39670	+	
At3g28510	+	+	At5g41790	+	+

Table 9. Genes of moveable mRNA that show high induction upon ILA and in *ugt76b1-1*

Genes displaying at least two log₂ fold upregulation in *ugt76b1-1* and upon ILA treatment. At4g10500 shows also strong downregulation in *UGT76B1-OE7*. Transcripts of these genes are expressed at a relatively low level in shoot and are translocated in root-shoot direction. (*) transport occurs exclusively from root to shoot.

AGI	Annotation (TAIR)
At3g28510	<i>P-loop containing nucleoside triphosphate hydrolase superfamily protein</i>
At3g26830	<i>PAD3 - PHYTOALEXIN DEFICIENT 3</i>
At3g50770	<i>CML41- CALMODULIN-LIKE 41</i>
At4g10500*	<i>DLO1 - DMR6-LIKE OXYGENASE 1</i>
At4g00700	<i>PHOSPHORIBOSYL ANTHRANILATE TRANSFERASE</i>
At1g61800*	<i>GPT2 - GLUCOSE-6-PHOSPHATE/PHOSPHATE TRANSLOCATOR 2</i>
At4g14630	<i>GLP9 - GERMIN-LIKE PROTEIN 9</i>

4. MATERIALS AND METHODS

4.1. Materials

4.1.1. Chemicals

Compounds leucic acid (2-hydroxyisocaproic acid), salicylic acid (2-hydroxybenzoic acid), methyl jasmonate (methyl 3-oxo-2-(2-pentenyl) cyclopentaneacetate), valic acid ((S)-(+)-2-hydroxy-3-methylbutyric acid), 2-hydroxyhexanoic acid and 4-nitrophenol were obtained from Sigma-Aldrich (Germany). ILA [(2S, 3S)-2-hydroxy-3-methylpentanoic acid] was from Interchim (France) and IAA (indole-3-acetic acid) from Roth (Germany). BSTFA (N-bis(trimethyl-silyl) trifluoro-acetamide) containing 1% TMCS (trimethylchlorosilane) was obtained from Macherey Nagel (Germany).

4.1.2. Media

NYGA

5 g/L Bactopeptone (Roth, Germany), 3 g/L Yeast Extract (Sigma, Germany), 20 mL/L Glycerol (Roth, Germany), pH=7 adjusted with KOH; for solidified media 18 g/L Agar (Duchefa, The Netherlands)

½ MS

2.2 g/L Murashige & Skoog Medium including vitamins (Duchefa, The Netherlands), 1% (w/v) sucrose, 0.5 % (w/v) Gelrite (Duchefa, The Netherlands), pH=5.7 adjusted with KOH

LB

25 g/L Luria-Bertani (LB) (Duchefa, The Netherlands), 2 mL/L 1N NaOH, for solidified media 12.5 g/L Agar (Duchefa, The Netherlands)

4.1.3. Bacterial strains

Escherichia coli (DH5 α , BL21 (DE3) pLys)

Pseudomonas syringae pv. *tomato* DC3000

Pseudomonas syringae pv. *tomato* DC3000 (*avrRpm1*)

Agrobacterium tumefaciens GV3101 (pMP90)

4.1.4. Vectors

pDNOR221 (Invitrogen, Germany)

pAlligator2Δ35S (Zhang and Schäffner, unpublished)

pBluescript KS(+) (Stratagene, USA)

4.1.5. Antibiotics

Rifampicin was dissolved in methanol. The other antibiotic stock solutions were dissolved in ddH₂O. All antibiotics were stored at -20 °C.

Antibiotics	Stock	Working
	solution (mg/mL)	concentration (µg/mL)
Ampicillin (Roche, Germany)	100	100
Kanamycin (Sigma, Germany)	50	50
Rifampicin (Sigma, Germany)	10	25
Spectinomycin (Sigma, Germany)	10	50
Gentamycin (Roche, Germany)	50	25

4.1.6. Primers

4.1.6.1. Primers used for genotyping of SALK T-DNA insertion lines

Line	AGI	Forward/Reverse	Sequence (5'-3')
SALK_006676	At3g51080	Forward	TATGAATTTTTGCCGGTTGAG
		Reverse	CAGACTCTGACTCCGGTTCTG
SALK_007071	At5g63950	Forward	CGAAAAGAAAAGTGCAGGTTG
		Reverse	TCTGGTGTTTGATTTTCGGTC
SALK_012541	At1g73020	Forward	CCTCCTAGCCGAGTGAGGTAC
		Reverse	CTGAAACTTGACGGCAGAGAG
SALK_014957	At2g29940	Forward	GATTTTCGGAACCTCCATACC
		Reverse	TTCCCAAAAACACTCCACAAG
SALK_017675	At1g48720	Forward	GAATCCCTTAATAACCCACCG
		Reverse	AGGACGTGCAATTGGAGTATG
SALK_017821	At5g11110	Forward	ATCCTATCGGGGAAGCATATG
		Reverse	CCTCAGATCTTCTTGCAGTGG
SALK_028137	At4g26190	Forward	CATCGATCTTGATCCTTCAGC
		Reverse	CTGCTTCTTTGGTTGGAATTG
SALK_029488	At4g12440	Forward	CCCCGACTGTAAAAGATTCC
		Reverse	CGGCCCTAAATAAAGTTTTG

SALK_031785	At3g61220	Forward	CAAGACTAAAACAACGGCGTC
		Reverse	CCCATGGAGGATGATACATTG
SALK_032256	At2g31240	Forward	TAGCAGAACCCATTAATTGCG
		Reverse	ACAACGTTGATGACCTCAAGG
SALK_040808	At1g61810	Forward	AGCATCTTGTGGAATCCTGTG
		Reverse	CATTTGTGACGTTGAACCATG
SALK_043037	At2g01500	Forward	TTCCCATCTCCATTTTGTTC
		Reverse	TTGTTGTTGGAGATGTAGCCC
SALK_053562	At4g09160	Forward	GTCTCTGAATAATCCTCCGCC
		Reverse	CCCTTGGTCTTCTCTAACTTGC
SALK_059101	At1g34460	Forward	TCCGGTGAGTAAAACATCGTC
		Reverse	ACAAAACCTGAACCACGAAACG
SALK_079374	At3g60410	Forward	CAAAGGGAACCTTATTGCCTC
		Reverse	TTCGTTACCTCCTCAATCAC
SALK_083322	At1g60040	Forward	AACCCTTGCACCATCTTTTTC
		Reverse	GGAATTCTTGATTTCGAAGGC
SALK_095998	At1g29830	Forward	CAGTCAAGTGACACCACCATG
		Reverse	TTTATGAAAACGTTTACGCGC
SALK_103278	At4g32105	Forward	CAGTGCGGTCAAAGAATTAGC
		Reverse	GCGCTCATTAAACGTATCAGC
SALK_109443	At4g36850	Forward	TTTGGTGGTTTCAATGGTCTC
		Reverse	TCATTTTCCTCACCCATAATCC
SALK_110864	At3g46630	Forward	GATCCAACCTCGATCTTCCTCC
		Reverse	AGGTCATCGACCACAATCAAG
SALK_118494	At1g04370	Forward	TGTTGTACATTTCCGAAACCC
		Reverse	CAAGGAACCGTTTGAACCTTG
SALK_123629	At4g35640	Forward	TGCTCTTGTGTTGTAATGCGTG
		Reverse	ACAAGATTCAAGGAAGAGCCC
SALK_124100	At3g28690	Forward	CTTTCTGAGCACCTTTGATCG
		Reverse	AGAGTCTCTTCTCGGTGAGGG
SALK_138593	At3g56240	Forward	TGGTACTGCAACAAAACATGTG
		Reverse	TCAAATGACTCAACCCCTGAG
SALK_148617	At4g12410	Forward	CGACTTTTTTCGGATCCTTACC
		Reverse	TGAACATTCAACTAGTGGTTGC
SALK_150594	At1g08800	Forward	ACTGAAGAATGTCCCATGGTG
		Reverse	TACCCAAGATTGGTTTGCTTG
T-DNA primer		Reverse	CTTCAACGTTGCGGTTCTGTCA

4.1.6.2. Primers used for RT-qPCR

Gene	AGI	Forward/Reverse	Sequence (5'-3')
<i>UGT76B1</i>	At3g11340	Forward	TGGAAGATCGGATTGCATT
		Reverse	CCTTCATGGGCATAATCCTC
<i>PR1</i>	At2g14610	Forward	GTGCCAAAGTGAGGTGTAACAA
		Reverse	CGTGTGTATGCATGATCACATC
<i>PR2</i>	At3g57260	Forward	TGGTGTGAGATTCCGGTACA
		Reverse	CATCCCTGAACCTTCCTTGA
<i>PR5</i>	At1g75040	Forward	ATCGGGAGATTGCAAATACG
		Reverse	GCGTAGCTATAGGCGTCAGG
<i>PDF1.2</i>	At5g44420	Forward	CCAAGTGGGACATGGTCAG
		Reverse	ACTTGTGTGCTGGGAAGACA
<i>VSP2</i>	At5g24770	Forward	TTGGCAATATCGGAGATCAAT
		Reverse	GGGACAATGCGATGAAGATAG
<i>SAG13</i>	At2g29350	Forward	TTGCCACCCATTGTAAA
		Reverse	GATTCATGGCTCCTTTGGTT
<i>FMO1</i>	At1g19250	Forward	ATCCCTTTATCCGCTTCCTCAA
		Reverse	CTCTTCTGCGTGCCGTAGTTTC
-	At1g04600	Forward	TTCTCTGTTTCTCGTTCAGAA
		Reverse	TCACTTTTATGCCCATGTTGA
-	At2g33080	Forward	GACGTTTGTGCATCTTCGAA
		Reverse	CTTGGAAGCGTCCCAGATAT
<i>UGT74F1</i>	AT2G43840	Forward	TCATCAGCCGGTTCTGTCCC
		Reverse	ACCATCTCAAAGTAAGCAAGGTGT
<i>UGT74F2</i>	AT2G43820	Forward	AGTTGGAAGTGCATGAGAAT
		Reverse	GATTATGCTGAATGAAAGACG
<i>PDR3</i>	At2g29940	Forward	CAGTGTGGTGGATATGGTTCTATT
		Reverse	CCGTGCCATGAAACAATG
<i>BSTM1</i> ³	AT3G11480	Forward	TGCGTTTGTGAAAGCTCTATG
		Reverse	CTGGTTTGGCCATTGATAAAA
UBQ5	At3g62250	Forward	GGTGCTAAGAAGAGGAAGAAT
		Reverse	CTCCTTCTTCTGGTAAACGT
S16	At5g18380, At2g09990	Forward	TTTACGCCATCCGTCAGAGTAT
		Reverse	TCTGGTAACGAGAACGAGCAC

³ Boachon *et al.* (2014)

4.1.6.3. Primers used for UGT76B1 - UGT74F1 hybrid construct

4.1.6.3.1. Primers used for production of UGT76B1 - UGT74F1 hybrid construct

Primer	Sequence (5'-3')
76B1_PRO_GW_F	GGGGACAAGTTTGTACAAAAAAGCAGGCTCGGTAAA CATAAACCATGT
76B1_PRO_Hy_R	ACATGTCCTCTCATCTTCTCCATTTTTGTTGTGAATTTCT CTC
76B1_PRO-74F1_HyF	GAGAGAAATTCACAACAAAAATGGAGAAGATGAGAGG ACAT
74F1-76B1pA_Hy_R	AACACATATGCATGTGTTTGTATTGATTTGAATTTTT GATACA
74F1 -76B1pA_Hy_F	TATCAAAAATTCAAATCAAATAATGCGGTGTTCTTCTTC T
76B1_CO_GW_R2	GGGGACCACTTTGTACAAGAAAGCTGGGTCTGTGATTT CTGCTTTCTGAT

4.1.6.3.2. Primers used for verification of UGT76B1 - UGT74F1 hybrid construct

Primer	Forward/Reverse	Sequence (5'-3')
M13_F	Forward	GTTTTCCCAGTCACGAC
M13_R	Reverse	AACAGCTATGACCATGATTA
76B1_F-1230	Forward	TTTTGGATCTTCAAAATGA
76B1_F-690	Forward	CTTTTATTGGATATCGTAGC
76B1_R1660	Reverse	AGGATCATAAGATTACGACGTT
74F1_R558	Reverse	ACCATCTCAAAGTAAGCAAGGTGT
74F1_F462	Forward	TCCCATCAAGGATTTGCC

4.1.6.3. Primers used for amplifying and sequencing of *UGT76B1* regulatory regions to compare Col-0, *Ler* and *Ws-4* ecotypes

Primer	Forward/Reverse	Sequence (5'-3')
UGT76B1_F-1200	Forward	GGATCTTCAAATGAAATAGTTT
UGT76B1_R150	Reverse	GAGGGAAATTGGAAGAGTTT
UGT76B1_F1230	Forward	TTTGAAAACAAGGTAGAGAGACT
UGT76B1_R7600	Reverse	TTCTCGACGATTCCTCTTAATAAC
UGT76B1_r150	Reverse	GAGGGAAATTGGAAGAGTTT
Ws_Ler_UGT76B1_r-600	Reverse	GCAAAAAGAAAAGGTCAATG

4.1.7. Plant material

Arabidopsis thaliana ecotypes Col-0, *Ler* and Ws-4 were the genetic background for wild-type plants. The loss-of-function mutants of *ugt76b1-1* (Col-0), *ugt76b1-2* (*Ler*) and *ugt76b1-3* (Ws-4) and overexpression line *UGT76B1-OE7* were obtained from Veronica von Saint Paul (Tab. 10). The double mutant *ugt74f1 amiugt74f2* and the triple mutant *ugt74f1 amiugt74f2 ugt76b1* were produced by Ruohe Yin. *ugt74f1-1* was obtained from INRA-Versailles Genomic Resource Center (<http://www.versailles-grignon.inra.fr>) and *ugt74f2-1* from J. Bender, John Hopkins University. SALK T-DNA insertion lines were obtained from the Nottingham Arabidopsis Stock Center (NASC) (<http://arabidopsis.info>). *Arabidopsis thaliana* Swedish accessions were kindly provided by Dr. Magnus Nordborg and Dr. Arthur Korte (GMI Vienna, Austria). Oak (*Quercus robur*), poplar (*Populus x canescens*), silver birch (*Betula pendula*), Scots pine (*Pinus sylvestris*) and European larch (*Larix deciduas*) were provided by Dr. Andrea Ghirardo (Helmholtz Zentrum München, Research Unit Environmental Simulation). Tobacco (*Nicotiana tabaccum*) and tomato (*Solanum lycopersicum*) were provided by Felicitas Groß and Dr. Imonge Gross (Institute of Biochemical Plant Pathology, Helmholtz Zentrum München).

Table 10. *Arabidopsis* mutant lines applied in this study

AGI	Name	Ecotype	Reference
At3g11340	<i>ugt76b1-1</i>	Col-0	von Saint Paul <i>et al.</i> , 2011
At3g11340	<i>ugt76b1-2</i>	<i>Ler</i>	von Saint Paul <i>et al.</i> , 2011
At3g11340	<i>ugt76b1-3</i>	Ws-4	von Saint Paul <i>et al.</i> , 2011
At3g11340	<i>UGT76B1-OE7</i>	Col-0	von Saint Paul <i>et al.</i> , 2011
At2g43840	<i>ugt74f1-1</i>	Ws-4	Brunaud <i>et al.</i> , 2002
At2g43820	<i>ugt74f2-1</i>	Col-0	Quiel <i>et al.</i> , 2003; Niyogi <i>et al.</i> , 1993
At2g43840, At2g43820	<i>ugt74f1 amiugt74f2</i>	Ws-4	Yin, 2010
At2g43840, At2g43820, At3g11340	<i>ugt74f1 amiugt74f2 ugt76b1</i>	Ws-4	Yin, 2010
At2g43820, At3g11340	<i>ugt74f2 ugt76b1</i>	Col-0	Schäffner, unpublished

4.2. Methods

4.2.1. Plant growth conditions

Arabidopsis plants for SA and SA conjugates determination, expression profiling by RT-qPCR and determination of ILA, LA and VA were grown in soil under a light cycle of 14 h darkness and 10 h with the light intensity $180 \mu\text{mol m}^{-2} \text{s}^{-1}$ at $20 \text{ }^\circ\text{C}$ in the light and at $18 \text{ }^\circ\text{C}$ in the darkness with 75% relative humidity. *Arabidopsis* plants for 2-HAs determination in the roots were grown on square plates containing $\frac{1}{2}$ MS medium with vitamins and grown vertically under the same conditions. Barley (*Hordeum vulgare*), tobacco (*Nicotiana tabacum*) and *Brassica nigra* were grown in soil under a light cycle of 14 h darkness and 10 h with the light intensity $\sim 180 \mu\text{mol m}^{-2} \text{s}^{-1}$ at $20 \text{ }^\circ\text{C}$ in the light and at $18 \text{ }^\circ\text{C}$ in the darkness with 60% relative humidity. Tomato (*Solanum lycopersicum*) plants were grown in soil under a light cycle of 14 h darkness and 10 h with the light intensity $\sim 180 \mu\text{mol m}^{-2} \text{s}^{-1}$ at $29 \text{ }^\circ\text{C}$ in the light (54% relative humidity) and at $18 \text{ }^\circ\text{C}$ in the darkness (72% relative humidity). Tree samples were grown in the different conditions, however optimal for each species. Silver birch (*Betula pendula*), Scots pine (*Pinus sylvestris*), and European larch (*Larix decidua*) were two-year-old plants. Plants were grown outside, in the garden of IMK-IFU in Garmisch-Partenkirchen during the growing season. Summer temperature ranged from $10 \text{ }^\circ\text{C}$ to $30 \text{ }^\circ\text{C}$ and photosynthetic photon flux density (PPFD) from 100 to $1500 \text{ mmol m}^{-2} \text{s}^{-1}$. The samples were collected during the first two weeks of September, after the twigs were enclosed into air-tight cuvettes and flushed with 600 ml min^{-1} of ultra-pure VOC-free synthetic air, containing 385 ppmv of CO_2 . Light intensities were set to a photosynthetic photon flux density (PPFD) of $1000 \text{ mmol m}^{-2} \text{s}^{-1}$ during the light phase. Leaf temperature was kept constant at $30 \text{ }^\circ\text{C}$. Oak (*Quercus robur*) trees originated from North Rhine-Westphalia. Branches of the 3 trees ASB2a, ASB14a and ASB17a from the oak population ‘Asbeck’ (Ghirardo *et al.*, 2012), were grafted onto *Quercus robur* saplings (Schröder, 2010). All the plants were fed for 31 h by four larvae of *Tortrix viridana*. Samples used in this study were not directly touched by larvae. Wild-type grey poplar saplings (hybrid of *Populus tremula* x *P. alba*, syn. *Populus x canescens* were 3-year-old (Ghirardo *et al.*, 2014). Plants were grown and cultivated according to Behnke *et al.*, 2007 and Cinege *et al.*, 2009.

4.2.2. Seedlings grown on solid medium

To sterilize seeds of *Arabidopsis*, seeds were dropped with 80 % ethanol on filter papers in sterile Petri dishes in the sterile hood. Procedure was repeated two times until seeds got completely dry. Then seeds were transferred with the sterile toothpicks to square Petri dishes (120 mm x 120 mm x 17 mm, Greiner bio-one, Germany) containing 50 mL ½ MS medium (Duchefa, The Netherlands) with vitamins (1 % sucrose; 0.5 % (w/v) Gelrite (Duchefa, The Netherlands)). To provide sterile conditions the whole process was performed in the hood. In the next step plates with seeds were transferred into 4 °C for two-day stratification in the darkness. After stratification plates were taken into the growth chamber and were grown in a vertical orientation under a light cycle of 16 h light 8 h darkness cycle with the light intensity of 160 $\mu\text{mol m}^{-2} \text{s}^{-1}$ at 22 °C – 23 °C. This procedure was applied to determine root growth inhibition in presence of SA, Me-JA, IAA and to further examine root growth resistance of SALK_014957 insertion line to ILA.

To observe root growth in response to hormones and ILA, *Arabidopsis* seedlings were grown on ½ MS medium supplemented with ILA, SA, Me-JA and IAA. 100 mM stock solutions of the compounds were prepared in ddH₂O sterilized by membrane filtration using the filters with 0.20 μm pore diameter (DIAFIL, Germany) and then stored at 4 °C. The stock solutions added to ½ MS medium with Gelrite were diluted to a final concentration before use. In order to fully resuspend SA, its stock solution was heated to 60 °C prior application. Additionally, a relatively high concentration of ILA (final concentration 500 μM) triggered a decrease of media pH value, which was responsible for root growth inhibition. Moreover, addition of MES, a commonly applied buffering agent also inhibited root growth. Therefore, media pH was increased to 6.45 by adding KOH, which was lowered after addition of ILA to ~5.7. SA, Me-JA and IAA concentrations applied in this study did not require buffering.

4.2.2.1. Growth conditions applied for T-DNA insertion lines screen for ILA insensitivity

Vapor-phase sterilization with Cl₂ gas was applied in order to simultaneously sterilize large numbers of mutant lines. 0.5 mL collection tubes containing seeds were placed on the rack and moved into 2 L tupperware box. To obtain Cl₂ gas, a glass beaker containing 10 mL of commercial bleach and 0.5 mL 32 % HCl was placed together with seeds inside the tupperware box. Boxes were moved under the fume for 2 h. After the incubation, boxes were opened under the fume and left for 2 h to evaporate the gas. In the next step five seeds of each line were transferred with the sterile toothpick a one well of a twenty four-well microtiter

plate (Greiner bio-one, Germany). Each well contained 2 mL $\frac{1}{2}$ MS medium with vitamins (1 % sucrose; 0.5 % (w/v) Gelrite) and 500 μ M ILA. To provide sterile conditions the whole process was performed in the hood. In the next step plates with seeds were transferred into 4°C for two-day stratification in the darkness. After stratification plates were transferred to the same growth conditions as described in 4.2.2. and were grown for five days.

4.2.2.2. Growth conditions applied for *Arabidopsis* accessions screen

Seeds of *Arabidopsis* accessions were sterilized like explained in 4.2.2.1. Eight up to ten seeds of each accession were transferred with the sterile toothpick to square Petri dishes (120 mm x 120 mm x 17 mm, Greiner bio-one, Germany) containing 50 mL $\frac{1}{2}$ MS medium with vitamins (1 % sucrose; 0.5 % (w/v) Gelrite) and ILA. Each plate contained five accessions and two controls (Col-0 and *UGT76B1-OE7*). Plants for control conditions (plates without ILA) and on ILA plates were planted in the same position on the plate. To provide sterile conditions the whole process was performed in the hood. In the next step plates with seeds were transferred into 4°C for five-day stratification in the darkness. After stratification plates were transferred to the same growth conditions like in 4.2.2. and were grown for seven days.

4.2.3. Treatment with a chemical SA analogue BTH

For BTH application, four-week-old *Arabidopsis* plants were sprayed with 1 mM commercially available BTH (BION, Ciba-Geigy, Germany). Spraying mixture contained 0.01 % Silwet to support entering BTH into the leaves. Plants were covered with a plastic dome for approximately 6 h. Then the lid was half uncovered to let the liquid evaporate and the surface of leaves become dry. Leaves of BTH treated plants and control plants (solution without BTH) were harvested 24 h after treatment and frozen in liquid nitrogen.

4.2.4. *Arabidopsis* infection with *P. syringae*

Pseudomonas syringae pv. *tomato* DC3000 (virulent strain) and *P. syringae* pv. *tomato* DC3000 (avrRpm1) (avirulent strain) were used in this project. Bacteria in -80°C glycerol stock were streaked out onto solid NYGA medium and grown two days at 28°C. Then a single colony was picked and transferred to liquid NYGA medium and grown overnight at 28°C at a shaker speed of 170 rpm with antibiotics (50 mg/L kanamycin and 50 mg/L rifampicin). Bacteria were grown until the late log phase of growth (OD_{600} 0.6 to 1.0). Bacteria were diluted with 10 mM $MgCl_2$ to $OD_{600} = 0.001$ for syringe infiltration or to OD_{600}

= 0.2 for spraying. An $OD_{600} = 0.2$ is approximately 1×10^8 colony-forming units/mL. Solution for spraying contained 0.01 % Silwet to support entering bacteria into the leaves. Control solutions did not contain bacteria. Sprayed plants were used to determine ILA and LA abundance 24 h post bacterial infection. Infiltrated plants were used to quantify bacterial growth. *Arabidopsis* leaves (6th to 11th) were marked by a blunted marker pen, followed by the infiltration using a 1 mL syringe. Infiltrated leaves were harvested 72 h post infection. The leaf discs with an area of 0.20 cm^2 were punched out with a cork borer. Two leaf discs from the individual infected plant were harvested. One biological replicate contained six leaf discs from three plants. Leaf discs were collected in 1.5 mL collection tubes with 500 μL MgCl_2 (10 mM) and 0.01 % Silwet and incubated in shaker in 28 °C for 2 h. 100 μL from each sample were transferred to a 96-well plate and five consecutive 10X serial dilutions were done by transferring 10 μL of bacterial suspension to 90 μL MgCl_2 (10 mM). From each dilution 20 μL were transferred onto solid NYGA media. After incubation for two days in 28 °C colonies (only spots with more than 10 colonies and less than 100) were counted and calculated to the original titer/ cm^2 .

4.2.5. Preparation of reciprocal graftings of *ugt76b1* and Col-0

Grafting protocol was kindly provided by Dr. Alexander Christmann (WZW TUM, Freising). Seeds were planted on round Petri dishes (Greiner bio-one, Germany) supplied with $\frac{1}{2}$ MS medium without vitamins (1 % sucrose; 1 % (w/v) Agar (Fluka)) like demonstrated in Fig. 44 A. After 2-day stratification in the darkness in 4 °C plants were transferred into growth incubator and grown for three to four days in constant light ($50 \mu\text{mol m}^{-2} \text{ s}^{-1}$) at 22 °C. Next, the light intensity was reduced to $10 \mu\text{mol m}^{-2} \text{ s}^{-1}$ for at least two days in order to stimulate hypocotyl elongation. Approximately one-week-old plants were grafted. Seedlings were cut straight and in the middle of the hypocotyls; rootstocks and scions were combined with their cuttings on the agar surface ($\frac{1}{2}$ MS medium without vitamins (Duchefa, The Netherlands) (0.5 % sucrose; 1 % (w/v) Agar (Fluka)) and with the cotyledons placed at the edge of the channel without agar (marked by red circle in Fig. 44 B), which prevents the growing cotyledons from disturbing the graft union. These grafted seedlings were grown under constant light conditions ($10 \mu\text{mol m}^{-2} \text{ s}^{-1}$) in 27 °C (higher temperature promotes callus formation) for one week. Afterwards growth conditions were changed to $50 \mu\text{mol m}^{-2} \text{ s}^{-1}$ light intensity and the light cycle 10 h light and 14 h darkness in 22 °C during the light period and 17 °C during the darkness and plants were grown for one week. In the next step plants were transferred to square Petri dishes (120 mm x 120 mm x 17 mm, Greiner bio-one, Germany)

containing 50 mL $\frac{1}{2}$ MS medium (Duchefa, The Netherlands) without vitamins (without sucrose; 1 % (w/v) Agar (Fluka)). Adventitious roots growing from graft unions were cut. Plants were grown under $50 \mu\text{mol m}^{-2} \text{s}^{-1}$ light intensity and the light cycle 10 h light and 14 h darkness in 22 °C during the light period and 17 °C during the darkness. After one week plants were examined for adventitious roots formation. Growth of adventitious roots from the grafting union indicates a partially independent growth of the shoot; therefore such plants were discarded. If necessary, plants were transferred to the new plates (same growth conditions) and grown for one up to two weeks. For gene expression analysis the whole rosettes were harvested. Further steps involved RNA extraction (4.2.10.), cDNA synthesis (4.2.11.) and RT-qPCR (4.2.12.).

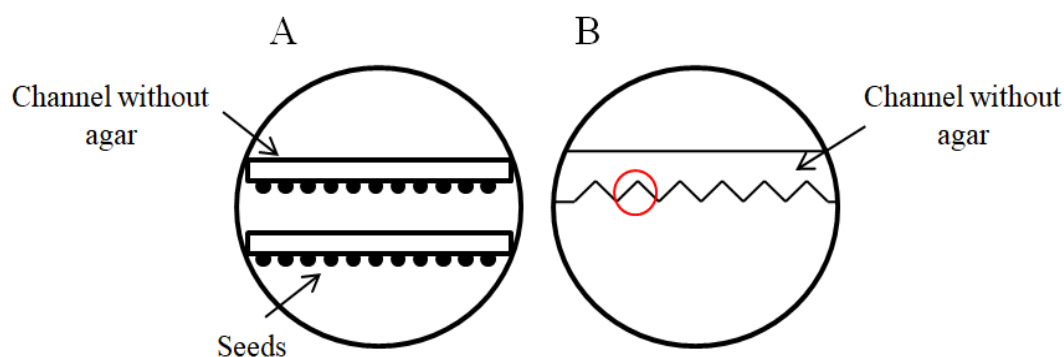


Figure 44. Schematic overview of agar growth plates applied in grafting

(A) Plates used for germination and growth in condition promoting hypocotyl elongation. (B) Plates used during grafting union formation. Placing the scion at the edge (marked with red circle) prevents growing cotyledons from disrupting the union.

4.2.6. Generation of hybrid construct composed of *UG74F1*-CDS and *UGT76B1* regulatory regions for complementation of *ugt76b1-1* loss-of-function mutant

The Gateway™ recombination technology (Invitrogen) was used in this study for cloning the construct composed of *UGT76B1* regulatory regions and *UG74F1*-CDS. To prepare a hybrid construct of *UG74F1*-CDS and *UGT76B1* promoter and terminator primers introducing overlap sequences (20 nucleotides) required for the assembly of adjacent fragments were applied in this study (4.1.6.3.1.). Moreover, to generate the construct suitable for Gateway BP recombination with a donor vector, attB sites were incorporated to the construct by forward *UGT76B1* promoter primer (76B1_Pro_GW_F) and reverse *UGT76B1* terminator primer (76B1_CO_GW_R2). For amplification of the desired fragments from genomic DNA, Phusion® High-Fidelity DNA Polymerase (NEB, Germany) was applied (according to the manual). However, the amplification resulted in obtaining a mixture of correct and incorrect

PCR products. Therefore, PCR products were sub-cloned into pBluescript KS (+) vector (EcoR V). Plasmids were used to transform *E. coli* (DH5 α strain), according to 4.2.6.1. Colony PCR, restriction digest and sequencing were applied to screen for clones carrying the desired fragments. Therefore, plasmids instead of genomic DNA were used as templates for PCR amplification of *UG74F1*-CDS and *UGT76B1* regulatory regions by Phusion® High-Fidelity DNA Polymerase (NEB, Germany). After amplification, PCR products were separated by 1 % agarose gel, extracted from the gel as explained in 4.2.10. and sequenced. Subsequently, purified PCR products in equal molar concentrations (0.5 pM) were assembled by Gibson Assembly kit (NEB) during a 2 h reaction, according to the manufacturer's protocol. In the next step reaction mixture was dried (SpeedVac Concentrator) and resuspended in 10 μ L HPLC-grade water (Merck, Germany). From this mixture 2 μ L were used for Gateway™ recombination technology (Invitrogen). UGT76B1-UGT74F1 hybrid construct was cloned into the destination vector by two steps site-specific recombination reactions. In the first step construct was cloned into pDONOR221 entry vector *via* BP reaction and then transformed into *E. coli* (DH5 α strain), according to 4.2.6.1. Before proceeding to the next step clones were examined by colony PCR, restriction digest and sequencing. Subsequently, construct was cloned into pAlligator2 Δ 35S destination vector *via* LR reaction and transformed into *Agrobacterium* (4.2.6.2.) and then into *ugt76b1-1* loss-of-function line (4.2.6.3.). Compared to the manufacturer's protocol recombination reactions (BP and LR) were scaled-down to 5 μ L, other steps were not changed. Colony PCRs were performed as follows. Single PCR reaction contained: 2 μ L 10x reaction buffer, 2 μ L 2 mM dNTPs, 1 μ L 10 μ M forward primer, 1 μ L 10 μ M reverse primer, 0.1 μ L Taq polymerase (5 U/ μ L), 13.9 μ L HPLC-grade water (Merck, Germany). Single colony was picked by a sterile pistil and dipped in the PCR reaction mix and then transferred to the liquid LB media. The reaction program was as follows: 95 °C for 10 min, followed by 34 cycles of 95 °C for 20 sec, 55 °C for 1 min/kb, 72 °C for 45 sec and final extension 72 °C for 3 min.

4.2.6.1. Heat shock transformation of *E. coli*

An aliquot of competent *E. coli* (DH5 α strain) was thawed on ice and mixed with 100 ng plasmid DNA. Mixture was incubated for 20 min on ice and transferred for 1 min into 42°C water bath and subsequently cooled on ice for 2 min. 950 mL LB medium without antibiotics was added and bacteria were incubated 1 h at 37 °C with gentle agitation. Bacterial suspension was centrifuged at 5000 rpm for 2 min at a room temperature. Bacterial pellet was

resuspended with ~ 100 µL LB medium and transferred to the plates with solid LB medium containing appropriate antibiotics.

4.2.6.2. Electroporation of competent *Agrobacterium tumefaciens* cells

An aliquot of competent *Agrobacterium tumefaciens* GV3101 was thawed on ice and mixed with 100 ng plasmid DNA. This mixture was transferred to a dry, pre-cooled electroporation cuvette (0.1 cm). Electroporation was performed with the BioRad Gene-Pulser; conditions: Capacitance 25 µF, Voltage 1.25 kV and Resistance 400 Ω. After electroporation, 1 mL of LB medium without antibiotics was added to the cuvette; bacterial suspension was transferred to a 1.5 mL collection tube and incubated for 2 h at 28 °C with gentle agitation. Bacteria suspension was centrifuged at 5000 rpm for 2 min at the room temperature. The bacterial pellet was resuspended with ~100 µL LB medium and transferred to the plates with solid LB medium containing appropriate antibiotics; rifampicin and gentamycin for *Agrobacterium tumefaciens* and spectinomycin for pAlligator2Δ35S.

4.2.6.3. Plant transformation with *Agrobacterium tumefaciens*

Floral dip procedure was applied to transform *Arabidopsis thaliana* plants (*ugt76b1-1* in this study). *Arabidopsis* plants were grown in big round pots (approx. 10 – 15 plants per pot) (10 h light 14 h darkness, 22 °C) until flowering stage. A single colony of transformed *Agrobacterium tumefaciens* was transferred to 2 mL LB media with antibiotics (rifampicin, gentamycin for bacteria and spectinomycin for vector) to form a pre-culture. Bacteria were grown overnight (28 °C, 200 rpm). 1 mL of the pre-culture was transferred to 250 mL of LB medium (with the same antibiotics). Bacteria were grown overnight (28°C, 200 rpm) until stationary growth phase (OD₆₀₀ 1.5-1.6). Bacterial cells were harvested by 10 min centrifugation at 4 °C, 5500 x g. Pellet was resuspended in 5 % sucrose solution with 0.05 % Silwet to OD₆₀₀ ~ 0.8. *Arabidopsis* plants were dipped into the bacterial suspension and soaked for 45 sec. Plants were covered with plastic bag to provide high humidity. Plastic bags were removed after 24 h and plants were grown for next 4 – 5 weeks when the first-generation seeds (T0) were harvested.

4.2.6.4. Selection of the homozygous lines

Selection was carried out by a visible marker, using seed coat expressed GFP (pAlligator2Δ35S vector).

4.2.7. Genotyping of SALK T-DNA insertion lines

Primers listed in 4.1.6.1. were used for genotyping of SALK T-DNA insertion lines. Genomic DNA was extracted by Extract-N-AmpTM plant PCR kit (Sigma, Germany) (4.2.8.). Three DNA extracts were done for each SALK line and three PCRs were performed for each extract. (I) PCR with mutant DNA template, left border SALK primer and T-DNA primer. (II) PCR with mutant DNA template, left border SALK primer and right border SALK primer, which was a negative control. (III) PCR with wild-type DNA template, left border SALK primer and right border SALK primer, which was a control reaction. The presence of PCR product in reactions (I) and (III) and no product in (II) pointed homozygous lines. Single PCR reaction contained: 1 μ L template, 2 μ L 10x reaction buffer, 2 μ L 2 mM dNTPs, 1 μ L 10 μ M forward primer, 1 μ L 10 μ M reverse primer, 0.1 μ L Taq polymerase (5 U/ μ L), 12.9 μ L HPLC-grade water (Merck, Germany). The reaction program was as follows: 95 °C for 2 min, followed by 34 cycles of 95 °C for 20 sec, 55 °C for 1 min/kb, 72 °C for 45 sec and final extension 72 °C for 3 min.

4.2.8. Preparation of plant genomic DNA

Two methods were applied to extract genomic DNA from the plant material. Extract-N-AmpTM plant PCR kit (Sigma, Germany) according to the manufacturer's protocol and Cetyltrimethyl ammonium bromide (CTAB) DNA miniprep (4.2.7.1.).

4.2.8.1. CTAB DNA Miniprep

One young leaf pro plant was harvested and transferred to the 1.5 ml collection tube with 250 μ L 2x CTAB buffer (1.4 M NaCl; 100 mM Tris-HCl, pH 8.0; 2 % (w/v) CTAB; 20 mM EDTA, pH 8.0; 1 % (w/v) LPA, Mr 40.000) and was grinded with a pistil, followed by 20 min. incubation in 65 °C. After incubation 200 μ L chloroform/isoamylalcohol (24:1) was added, intensively mixed for ~1 min. and centrifuged at 14000 rpm for 2 min. Approximately 200 μ L of the upper faze was taken to a new 1.5 mL collection tube, next 1 μ L of 1 % (w/v) LPA as a precipitation agent and 96 % ethanol were added. Samples were precipitated for at least 20 min. in -20 °C. Next, samples were centrifuged for 10 min. at 14000 rpm, supernatant was discarded and the pellet was washed with 70 % ethanol. Samples were centrifuged for 5 min. at 14000 rpm, supernatant was discarded. Finally, samples were dried and resuspended in 100 μ L HPLC-grade water (Merck, Germany).

4.2.9. Separation nucleic acid by agarose gel

Nucleic acids were separated by agarose (1 %) gel electrophoresis containing 0.05 µg/mL ethidium bromide in 1x TAE buffer. Each sample was mixed with 6x loading dye buffer and then loaded in the gel. Nucleic acids were visualized by UV light ~20-30 minutes after running the gel.

4.2.10. Extraction of PCR products from agarose gel

QIAquick Gel Extraction Kit (Qiagen) was applied for extracting PCR products from the gel. Samples were separated by 1 % agarose gel electrophoresis. PCR products of appropriate size were cut from the gel under the UV light and transferred into a 2 mL collection tube. The exposure to UV light was reduced to the minimum in order to prevent nucleic acid degradation. Further steps were performed according to the manufacturer's protocol.

4.2.11. Plasmid extraction

Plasmid Miniprep Kit (Qiagen) was used to isolate plasmids from bacterial cells according to the manufacturer's protocol.

4.2.12. Total RNA isolation

Plant leaf material (up to 100 mg) was homogenized in grinding tubes (Ceramic Beads for cell lysis, Genaxxon, Germany) in MP FastPrep-24 Homogenizer for 2 minutes (2 x 1 min). Total RNA was extracted using RNeasy plant mini kit (Qiagen, Germany). Lysis step was modified due to the grinding method and was performed directly in the grinding tubes by adding 600 µL of Qiagen RLT buffer. Further steps were performed according to the manufacturer's protocol. To avoid contamination with genomic DNA, DNase digestion was performed on the column as recommended by the kit manufacturer. The concentration and quality of the RNA extracts were determined by measuring the absorption at 260 nm and 280 nm by Nanodrop ND-1000 spectrophotometer (Kisker-biotech, Germany). Additionally, RNA samples (~ 100 ng) were separated by 1 % agarose gel to examine for eventual RNA degradation.

4.2.13. Reverse Transcription Polymerase Chain Reaction (RT-PCR)

QuantiTect Rev. Transcription Kit (Qiagen, Germany) was applied for the first-strand cDNA transcription from 1 µg total RNA. Reaction was performed according to the manual, including fast elimination of the genomic DNA. In order to rule out contamination with the genomic DNA, for each sample a negative reaction without enzyme was prepared. To examine whether the reaction was successful a PCR with *TUBULIN 9* primers and 1 µL of cDNA was performed. Primers (Forward: 5'-GTACCTTGAAGCTTGCTAATCCTA-3', Reverse: 5'-GTTCTGGACGTTTCATCATCTGTTC-3') for house-keeping gene *TUBULIN 9* were designed to span an intron, thus the genomic DNA contamination could be distinguished by the bigger size of the PCR product, visualized on agarose gel. No band for the negative control (-RT), whereas a band of expected size amplified from the reverse transcription reaction was considered as a proof for successful RNA extraction and cDNA synthesis. Reactions were performed in a Multicycler PTC-200 (Biozym, Germany). Single PCR reaction contained: 1 µL template, 2 µL 10x reaction buffer, 2 µL 2 mM dNTPs, 1 µL 10 µM forward primer, 1 µL 10 µM reverse primer, 0.1 µL Taq polymerase (5 U/µL), 12.9 µL HPLC-grade water (Merck, Germany). The reaction program was as follows: 95 °C for 2 min, followed by 34 cycles of 95 °C for 20 sec, 55 °C for 30 sec, 72 °C for 45 sec and final extension 72 °C for 3 min.

4.2.14. Quantitative real time polymerase chain reaction (RT-qPCR)

The fluorescence dye SYBR Green (Bioline, Germany) that binds to the double stranded DNA was used to monitor genes expression levels in this study. Total RNA was extracted as described in 4.2.10., reverse transcription was performed as described in 4.2.11. For primers see 4.1.6.2. All cDNA templates applied for RT-qPCR were diluted with HPLC-grade water (Merck, Germany) to the ratio of 1:15. Single RT-qPCR contained 4 µL cDNA, 10 µL of SYBR Green Mastermix and 250 µM of each primer in a 20 µL reaction volume. Each sample had two technical replicates. The reactions were loaded into 96 well plates and quantification was performed by a 7500 real time PCR system (Applied Biosystems, Germany). The reaction program was as follows: 95 °C for 10 min initial denaturation, followed by 40 cycles of 95 °C for 15 sec, 55 °C for 15 sec, and 72 °C for 45 sec and a final step of 95 °C for 15 sec, 60 °C for 1 min and 95 °C for 15 sec to collect the melting curve. In this study for all RT-qPCRs *UBQ5* and *S16* were applied as reference genes to normalize the relative abundance of the genes of interest by GeNorm (Vandesompele *et al.*, 2002).

4.2.15. DNA sequencing

To evaluate the nucleotide sequences of the DNA fragments or plasmids samples were sequenced. Mixture containing template in an appropriate concentration and a one primer were prepared according to the manufacturer's protocol. Sequencing was processed by Eurofins MWG GmbH (Germany). Analysis of the sequences was performed by Vector NTI (Thermo Fisher).

4.2.16. Determination of SA and SA glucose conjugates

The measurements of salicylic acid and its glucose conjugates in the rosette tissues were done by Lucia Gößl (Institute of Biochemical Plant Pathology, Helmholtz Zentrum München) according to von Saint Paul *et al.* (2011).

4.2.17. GC-MS based method for VA, LA and ILA determination in the plant tissues

The whole rosettes or roots were used to determine the abundance of VA, LA and ILA in plant tissues. Materials were harvested and immediately frozen in the liquid nitrogen, which was followed by 24 h lyophilisation. 20 mg of a dried plant material was transferred into the grinding tubes (Ceramic Beads for cell lysis, Genaxxon, Germany) and was grinded in MP FastPrep-24 Homogenizer for 2 min (2 x 1 min). Grinding tubes before use were washed twice with dichloromethane (Sigma, Germany) and twice HPLC-grade water (Merck, Germany) to remove contaminants that could disrupt the measurement. After washing grinding tubes were dried by SpeedVac Concentrator. Metabolites were extracted with 1 mL 80 % methanol (pre-cooled to 4 °C) and already pre-mixed with the first internal standard, 2-hydroxyhexanoic acid (Sigma, Germany) (2.5 µg/mL). Extraction buffer was added directly into the grinding tubes, which was followed by 60 min incubation on shaker in 4 °C. The extraction solution was centrifuged for 15 min at 14000 rpm in 4 °C; supernatant was transferred into a fresh 2 mL collection tube and centrifuged for 10 min at 14000 rpm in 4°C. 900 µL of the supernatant was transferred into a fresh 2 mL collection tube. Extracts were dried (SpeedVac Concentrator, Savant) and dissolved in 1 mL 25 mM ammonium acetate (pH 6-7). To fully dissolve the sample, suspension was sonicated for 3 min at setting 50 % (Branson Sonifier Cell Disruptor B15) and incubated on shaker for 5 min in 4 °C. Extracts were purified on SPE weak anion exchange columns (StrataX-AW 30 mg / 1mL, Phenomenex, Germany). Prior applying the sample columns were conditioned with 0.5 mL methanol and equilibrated with 0.5 mL HPLC-grade water (Merck, Germany). After the

sample went through the column two washing steps with 0.5 mL 25 mM ammonium acetate and 0.5 mL methanol were performed. Metabolites were eluted twice with 0.5 mL methanol containing 5 % (v/v) formic acid. Samples were dried (SpeedVac Concentrator, Savant) and dissolved in 200 μ L methanol with second internal standard, 4-nitrophenol (Sigma, Germany) (12.5 ng/ μ L) and transferred to a 250 μ L glass inserts (Restek, Germany (REST-21776) or alternatively Sigma, Germany (29436-U)). Samples were dried (SpeedVac Concentrator), inserts were transferred into glass vials and dissolved with 50 μ L BSTFA (N-bis (trimethylsilyl) trifluoro-acetamide) containing 1 % TMCS (trimethylchlorosilane) (Macherey Nagel, Germany). After incubation in 60 °C for 120 min abundances of VA, LA and ILA were determined by GC-MS. Samples were analyzed with a thermo-desorption unit (TDU, Gerstel, Germany) coupled to a GC-MS instrument (GC type: 7890; MS type: 5975C, both Agilent Technologies, Palo Alto, CA, USA). The TDU was used as injector for the conversion of the sample from liquid to air phase. The TDU-GC-MS was run as follows. One μ L of sample was injected into the TDU in a dedicated glass tube containing the glass insert for liquid injection (both from Gerstel, Germany). Prior to each analysis, tubes and inserts were cleaned with acetone, methanol and water, separately used in ultrasonic bath for 30 min each, and kept in hexane solution overnight. Immediately before analysis, tubes were baked out in oven at 400 °C for 1 h under \sim 80 mL/min N₂ (5.0 gas purity) flow. Samples were vaporized into TDU by quickly rising the temperature from 40 to 270 °C at a rate of 360 °C/min and holding for 0.5 min, The compounds were refocused using a Cryo Injection System (CIS, Gerstel) at -50 °C, then desorbed in splitless mode to 250 °C at a rate of 12 °C/sec and hold for 1.5 min, followed by ramping at 12 °C/sec to 275 °C and holding for 2 min. Separation was achieved by using the Agilent J&W HP-5ms GC column (30 m x 250 μ m x 0.25 μ m) with 1 mL/min constant flow rate of He, and a temperature program of 90 °C for 4 min, followed by ramping at 2 °C/min to 120 °C and holding for 0 min, then 100 °C/min to 300 °C and holding for 5 min. Identification and quantification of VA, LA, ILA and two internal standards (ISDs) (2-hydroxyhexanoic acid and 4-nitrophenol) were achieved by spectra and retention time comparison, and calibration curve obtained from pure standards (Sigma) MS spectra were parallelly acquired in scan (TIC) and in selective ion monitoring (SIM) modes. Scan was performed in the range of 35-300 m/z (threshold: 150; 7.76 scan/sec). SIM parameters were as follows, VA: start time: 6.20 min, ion: 147.0 m/z, dwell: 150 ms; LA: start time: 8.5 min, ion: 145.0 m/z, dwell: 150 ms; ILA: start time: 11.5 min, ion: 159.0 m/z, dwell: 150 ms; 2-hydroxyhexanoic acid: start time: 13.9 min, ion: 173.1 m/z, dwell: 100 ms; 4-nitrophenol: start time: 16.0 min, ion: 196.1 m/z, dwell: 25 ms. MS detector was kept off until 6.20 min

and switched off after 20.65 min until the end of the run to prevent damage from highly occurring abundant compounds. Calibration was achieved by adding 11 different concentrations of ILA (0, 0.05, 0.1, 0.15, 0.2, 0.25, 0.3, 0.5, 1, 5, 10 ng/ μ L) into the same pool of plant extract, in order to take into account the matrix effects potentially occurring in plant material. Each concentration contained a fix concentration of ISDs (both 50 ng/ μ L). Calibration samples were treated in exactly the same way as the sample preparation explained above. Data were background corrected using the mean value obtained from measuring the plant extract at zero point (i.e. addition of 0 ng/ μ L ILA standard solution), to consider the basal levels of ILA occurring in the pooled plant material. Data were always normalized to ISD values of 4-nitrophenol. Standards were prepared independently in triplicate, and each concentration was measured twice. The last two technical replicates were averaged and their means were further used for the calculation of response factors. The standard curve was therefore calculated using the data obtained from the 3 independently created serial dilutions. The resulting MS signal responses were found to be linear ($R^2 > 0.9999$) with an increasing standard concentration. Response factors of VA and LA were calculated based on the matrix-dependent calibration curve of ILA and assuming that the matrix effects occur in the same extend to VA, LA and ILA: serial dilutions of pure standards (0-100 ng/ μ L) of ILA, VA and LA were measured in parallel and the ratios of VA/ILA and LA/ILA were applied to the matrix-dependent response factor of ILA. Limits of detection (LOD) were calculated with 2σ and where 1.290 (ILA), 0.229 (VA) 0.029 (LA) pg/mg DW, referred to *A. thaliana* extracts. The limits of quantification (LOQ) were set to 3 times the respective LOD.

4.2.18. *In vitro* analysis of the activity of UGT6B1 towards ILA and LA

UGT76B1 recombinant protein was produced by Birgit Geist (Institute of Biochemical Plant Pathology, Helmholtz Zentrum München) according to the protocol (Zhang, 2013). To analyze the activity of UGT76B1 towards ILA and LA, UGT76B1 recombinant protein was incubated with aglycon (separate reactions for LA and ILA) and UDP-Glucose. The abundances of remaining, unconjugated aglycons were determined by GC-MS. The reaction mixture was composed of 0.1 M Tris-HCl buffer pH=7.5, 5 mM UDP-Glc, 1 mM aglycon, and ~ 1 μ g protein in 50 μ L. The reaction was incubated for 2 h at 30°C in a water bath and stopped by adding 200 μ L methanol. In the next step mixtures containing methanol were evaporated (SpeedVac Concentrator, Savant) and prepared for the GC-MS measurement (starting from purification on SPE column). For further steps see 4.2.17.

4.2.19. Bioinformatics analyses

The expression levels in root and shoot of the genes associated by T-DNA screen and GWAS were obtained from Genevestigator (<https://genevestigator.com/gv/>). Functions of the T-DNA screen and GWAS associated genes were annotated by TAIR (<https://www.arabidopsis.org/>) and VirtualPlant 1.3 (<http://virtualplant.bio.nyu.edu/cgi-bin/vpweb/>). VirtualPlant 1.3 was also applied for GO term analysis. Nucleotide sequence analysis was performed by Vector NTI (Thermo Fisher, Germany). Amino acid alignment was done by EMBOSS Needle (http://www.ebi.ac.uk/Tools/psa/emboss_needle/). Modeling of the 3D structure of UGT76B1 protein was performed by Phyre2 (<http://www.sbg.bio.ic.ac.uk/phyre2/html/page.cgi?id=index>) and by SWISS-MODEL (<https://swissmodel.expasy.org>). PdbViewer was used to process 3D structure model (<https://spdbv.vital-it.ch>). PROVEAN (<http://provean.jcvi.org> 05/2017) was applied for analysis of the amino acid substitution in UGT76B1. Primers for genotyping SALK T-DNA insertion lines were designed by T-DNA Primer Design (<http://signal.salk.edu/tdnaprimers.2.html>). Figures and statistical analysis were done by SigmaPlot 11.0; for comparing two groups *T*-test was applied, whereas for comparing more than two groups One Way ANOVA test. Venn diagrams were prepared in VENNY 2.1 (<http://bioinfogp.cnb.csic.es/tools/venny/>). Statistical analysis of grafting results was done by Elisabeth Georgii (Institute of Biochemical Plant Pathology, Helmholtz Zentrum München).

5. REFERENCES

- Acosta, I. F., and Farmer, E. E. (2010).** Jasmonates. *The Arabidopsis Book* 8: e0129. 2010.
- Agut, B., Gamir, J., Jaques, J. A., Flors, V. (2016).** Systemic resistance in citrus to *Tetranychus urticae* induced by conspecifics is transmitted by grafting and mediated by mobile amino acids. *Journal of Experimental Botany* 67(19): 5711–5723.
- Allen, K. N. and Dunaway-Mariano, D. (2009).** Markers of fitness in a successful enzyme superfamily. *Current Opinion in Structural Biology* 19(6):658-65.
- An, C. and Mou, Z. (2011).** Salicylic acid and its function in plant immunity. *Journal of Integrative Plant Biology* 53(6): 412–428.
- Aranega-Bou, P., Leyva, M. D. O., Finiti, I. and García-agustín, P. (2014).** Priming of plant resistance by natural compounds. Hexanoic acid as a model. *Frontiers in Plant Science* 5: 488.
- Attaran, E., Zeier, T. E. and Griebel, T. (2009).** Methyl salicylate production and jasmonate signaling are not essential for systemic acquired resistance in *Arabidopsis*. *The Plant Cell* 21(3): 954–971.
- Atwell, S., Huang, Y. S., Vilhjálmsson, B. J., Willems, G., Horton, M., Li, Y., Meng, D., Platt, A., Tarone, A. M., Hu, T. T., Jiang, R., Mulyati, N. W., Zhang, X., Amer, M. A., Baxter, I., Brachi, B., Chory, J., Dean, C., Debieu, M., de Meaux, J., Ecker, J. R., Faure, N., Kniskern, J. M., Jones, J. D. G., Michael, T., Nemri, A., Roux, F., Salt, D. E., Tang, C., Todesco, M., Traw, M. B., Weigel, D., Marjoram, P., Borevitz, J. O., Bergelson, J. and Nordborg, M. (2010).** Genome-wide association study of 107 phenotypes in a common set of *Arabidopsis thaliana* inbred lines. *Nature* 465(7298): 627–631.
- Bacelli, I. and Mauch, B. (2016).** Beta-aminobutyric acid priming of plant defense: the role of ABA and other hormones. *Plant Molecular Biology* 91(6): 703–711.
- Baek, D., Pathange, P., Chung, J., Jiang, J., Gao, L., Oikawa, A., Hirai, M. Y., Saito, K., Pare, P. W. and Shi, H. (2010).** A stress-inducible sulphotransferase sulphonates salicylic acid and confers pathogen resistance in *Arabidopsis*. *Plant Cell and Environment* 33(8):1383-92.
- Bakker, P. A. H. M., Pieterse, C. M. J. and Loon, L. C. Van (2007).** Induced systemic resistance by fluorescent *Pseudomonas spp.* *Phytopathology* 97(2): 239-43.
- Banerjee, A. K., Chatterjee, M., Yu, Y., Suh, S., Miller, W. A. and Hannapel, D. J. (2006).** Dynamics of a mobile RNA of potato involved in a long-distance signaling pathway. *The Plant Cell* 18: 3443–3457.
- Bartsch, M., Bednarek, P., Vivancos, P. D., Schneider, B., Roepenack-lahaye, E. Von, Foyer, C. H., Kombrink, E., Scheel, D. and Parker, J. E. (2010).** Accumulation of isochorismate-derived 2,3-dihydroxybenzoic 3-O-beta-D-xyloside in *Arabidopsis* resistance to pathogens and ageing of leaves. *Journal of Biological Chemistry* 13;285(33): 25654-65.
- Barrett, L. W., Fletcher, S. and Wilton, S. D. (2012).** Regulation of eukaryotic gene

expression by the untranslated gene regions and other non-coding elements. *Cellular and Molecular Life Sciences* 69(21): 3613–3634.

Baxter, I., Brazelton, J. N., Yu, D., Huang, Y. S., Lahner, B., Yakubova, E., Li, Y., Bergelson, J., Borevitz, J. O., Nordborg, M., Vitek, O. and Salt, D. E. (2010). A coastal cline in sodium accumulation in *Arabidopsis thaliana* is driven by natural variation of the sodium transporter AtHKT1;1. *PLOS Genetics* 6(11): e1001193.

Behnke K, Ehling B, Teuber M, Bauerfeind M, Louis S, Hänsch R, Polle A, Bohlmann J, Schnitzler J-P (2007). Transgenic, non-isoprene emitting poplars don't like it hot. *The Plant Journal* 51: 485–99.

Bektas, Y. and Eulgem, T. (2015). Synthetic plant defense elicitors. *Frontiers in Plant Science* 5: 1–17.

Belles, J.M., Garro, R., Pallas, V., Fayos, J., Rodrigo, I., Conejero, V. (2006). Accumulation of gentisic acid as associated with systemic infections but not with the hypersensitive response in plant-pathogen interactions. *Planta* 223: 500–511.

Bemer, M., Heijmans, K., Airoidi, C., Davies, B. and Angenent, G. C. (2010). An atlas of Type I MADS box gene expression during female gametophyte and seed development in *Arabidopsis*. *Plant Physiology* 154(1): 287- 300.

Berardini, T. Z., Reiser, L., Li, D., Mezheritsky, Y., Muller, R., Strait, E. and Huala, E. (2015). The *Arabidopsis* information resource: Making and mining the “gold standard” annotated reference plant genome. *Genesis* 53(8): 474–485.

Bernsdorff, F., Döring, A., Gruner, K., Schuck, S. and Bräutigam, A. (2016). Pipecolic acid orchestrates plant systemic acquired resistance and defense priming *via* salicylic acid-dependent and independent pathways. *The Plant Cell* 28(1):102-29.

Besnard, J., Pratelli, R., Zhao, C., Sonawala, U. and Collakova, E. (2016). UMAMIT14 is an amino acid exporter involved in phloem unloading in *Arabidopsis* roots. *Journal of Experimental Botany* 67(22): 6385–6397.

Bezemer, T. M. and van Dam, N. M. (2005). Linking aboveground and belowground interactions via induced plant defenses. *Trends in Ecology and Evolution* 20(11): 617–624.

Biasini, M., Bienert, S., Waterhouse, A., Arnold, K., Studer, G., Schmidt, T., Kiefer, F., Cassarino, T. G., Bertoni, M., Bordoli, L. and Schwede, T. (2014). SWISS-MODEL : modelling protein tertiary and quaternary structure using evolutionary information. *Nucleic Acids Research* 42: 252–258.

Binder, S. (2010). Branched-chain amino acid metabolism in *Arabidopsis thaliana*. *The Arabidopsis Book* 8(1): 1–14.

Birkenbihl, R. P., Diezel, C. and Somssich, I. E. (2012). Arabidopsis WRKY33 is a key transcriptional regulator of hormonal and metabolic responses toward *Botrytis cinerea* infection. *Plant Physiology* 159(1): 266–285.

Biteau, B., Labarre, J. and Toledano, M. B. (2003). ATP-dependent reduction of cysteine-

sulphinic acid by *S. cerevisiae* sulphiredoxin. *Nature* 425(6961): 980–984.

Błaszczyk, A., Sirko, L., Hawkesford, M. J. and Sirko, A. (2002). Biochemical analysis of transgenic tobacco lines producing bacterial serine acetyltransferase. *Plant Science* 162(4): 589–597.

Boachon, B., Gamir, J., Pastor, V., Erb, M., Dean, J. V., Flors, V. and Mauch-Mani, B. (2014). Role of two UDP-Glycosyltransferases from the L group of arabisopsis in resistance against *Pseudomonas syringae*. *European Journal of Plant Pathology*, 139(4): 707–720.

Bologna, N. G. and Voinnet, O. (2014). The diversity, biogenesis and activities of endogenous silencing small RNAs in *Arabidopsis*. *Annual Review of Plant Biology* 65: 473–503.

Boter, M., Golz, J. F., Giménez-Ibañez, S., Fernandez-Barbero, G., Franco-Zorrilla, J. M. and Solano, R. (2015). FILAMENTOUS FLOWER is a direct target of JAZ3 and modulates responses to jasmonate. *The Plant Cell* 27: 1–15.

Bowles, D., Lim, E., Poppenberger, B. and Vaistij, E. (2006). Glycosyltransferases of lipophilic small molecules. *Annual Review of Plant Biology* 57: 567–597.

Böttcher, C., Westphal, L., Schmotz, C., Prade, E., Scheel, D. and Glawischnig, E. (2009). The multifunctional enzyme CYP71B15 (PHYTOALEXIN DEFICIENT3) converts cysteine-indole-3-acetonitrile to camalexin in the indole-3-acetonitrile metabolic network of *Arabidopsis thaliana*. *Plant Cell* 21(6): 1830–1845.

Brunaud, V., Balzergue, S., Dubreucq, B., Aubourg, S., Samson, F., Chauvin, S., Bechtold, N., Cruaud, C., DeRose, R., Pelletier, G., Lepiniec, L., Caboche, M. and Lecharny, A. (2002). T-DNA integration into the *Arabidopsis* genome depends on sequences of pre-insertion sites. *EMBO Reports* 3(12): 1152–1157.

Caarls, L., Pieterse, C. M. J. and Wees, S. C. M. Van (2015). How salicylic acid takes transcriptional control over jasmonic acid signaling. *Frontiers in Plant Science* 6: 1–11.

Cai, X., Ballif, J., Endo, S., Davis, E., Liang, M., Chen, D. and Dewald, D. (2007). A putative CCAAT-binding transcription factor is a regulator of flowering timing in *Arabidopsis*. *Plant Physiology* 145 (1): 98–105.

La Camera, S., L'Haridon, F., Astier, J., Zander, M., Abou-Mansour, E., Page, G., Thurow, C., Wendehenne, D., Gatz, C., Métraux, J.-P. and Lamotte, O. (2011). The glutaredoxin ATGRXS13 is required to facilitate *Botrytis cinerea* infection of *Arabidopsis thaliana* plants. *Plant Journal* 68(3): 507–519.

Caminsky, N., Mucaki, E. J. and Rogan, P. K. (2015). Interpretation of mRNA splicing mutations in genetic disease: review of the literature and guidelines for information-theoretical analysis. *F1000Research* 18(3): 282.

Campbell, M. A., Patel, J. K., Meyers, J. L., Myrick, L. C. and Gustin, J. L. (2001). Genes encoding for branched-chain amino acid aminotransferase are differentially expressed in plants. *Plant Physiology and Biochemistry* 39(10): 855–860.

- Cao, J.-Y., Xu, Y.-P., Li, W., Li, S.-S., Rahman, H. and Cai, X.-Z. (2016).** Genome-wide identification of Dicer-like, argonaute, and RNA-Dependent rna polymerase gene families in *Brassica* species and functional analyses of their *Arabidopsis* homologs in resistance to *Sclerotinia sclerotiorum*. *Frontiers in Plant Science* 7: 1614.
- Chao, D., Silva, A., Baxter, I., Huang, Y. S., Nordborg, M., Danku, J., Lahner, B., Yakubova, E. and Salt, D. E. (2012).** Genome-Wide Association Studies identify heavy metal ATPase3 as the primary determinant of natural variation in leaf cadmium in *Arabidopsis thaliana*. *PLOS Genetics* 8(9).
- Chapelle, A., Morreel, K., Vanholme, R., Le-Bris, P., Morin, H., Lapierre, C., Boerjan, W., Jouanin, L. and Demont-Caulet, N. (2012).** Impact of the absence of stem-specific β -glucosidases on lignin and monolignols. *Plant Physiology* 160(3): 1204–17.
- Chen, Q., Sun, J., Zhai, Q., Zhou, W., Qi, L., Xu, L., Wang, B., Chen, R., Jiang, H., Qi, J., Li, X., Palme, K. and Li, C. (2011).** The basic helix-loop-helix transcription factor MYC2 directly represses PLETHORA expression during jasmonate-mediated modulation of the root stem cell niche in *Arabidopsis*. *Plant Cell* 23(9): 3335-3352.
- Chen, R., Jiang, H., Li, L., Zhai, Q., Qi, L., Zhou, W., Liu, X. and Li, H. (2012).** The Arabidopsis Mediator Subunit MED25 Differentially Regulates Jasmonate and Abscisic Acid Signaling through Interacting with the MYC2 and ABI5 Transcription Factors. *Plant Cell* 24(7): 2898-916.
- Cheval, C., Aldon, D., Galaud, J. and Ranty, B. (2013).** Biochimica et Biophysica Acta Calcium/calmodulin-mediated regulation of plant immunity. *Molecular Cell Research* 1833(7): 1766–1771.
- Chevalier, F., Pata, M., Nacry, P., Dumas, P. and Rossignol, M. (2003).** Effects of phosphate availability on the root system architecture: large-scale analysis of the natural variation between *Arabidopsis* accessions. *Plant Cell & Environment* 26(11):1839–1850.
- Chi, Y. H., Kim, S. Y., Jung, I. J., Shin, M. R., Jung, Y. J., Park, J. H., Lee, E. S., Maibam, P., Kim, K., Park, J. H., Kim, M. J., Hwang, G. Y. and Lee, S. Y. (2012).** Dual functions of *Arabidopsis* sulfiredoxin: Acting as a redox-dependent sulfinic acid reductase and as a redox-independent nuclease enzyme. *FEBS Letters* 586(19): 3493–3499.
- Cinege G, Louis S, Hänsch R, Schnitzler J-P (2009) Regulation of isoprene synthase promoter by environmental and internal factors. *Plant Molecular Biology* 69: 593–604.
- Choi, H., Ohyama, K., Kim, Y.-Y., Jin, J.-Y., Lee, S. B., Yamaoka, Y., Muranaka, T., Suh, M. C., Fujioka, S. and Lee, Y. (2014).** The role of Arabidopsis ABCG9 and ABCG31 ATP binding cassette transporters in pollen fitness and the deposition of steryl glycosides on the pollen coat. *Plant Cell* 26(1): 310–24.
- Choi, H. W., Lee, B. G., Kim, N. H., Park, Y., Lim, C. W., Song, H. K. and Hwang, B. K. (2008).** A role for a menthone reductase in resistance against microbial pathogens in plants. *Plant physiology* 148(1): 383–401.
- Choi, Y., Chan, A. P. and Craig, T. J. (2015).** Sequence analysis PROVEAN web server: a tool to predict the functional effect of amino acid substitutions and indels. *Bioinformatic*

31(16): 2745–2747.

Choudhury, F. K., Rivero, R. M., Blumwald, E. and Mittler, R. (2016). Reactive oxygen species, abiotic stress and stress combination. pp. 1–12. *The Plant Journal* 90(5): 856–867.

Crouzet, J., Trombik, T., Fraysse, A. S. and Boutry, M. (2006). Organization and function of the plant pleiotropic drug resistance ABC transporter family. *FEBS Letters* 580(4): 1123.

Dangl, J. L. and Jones, J. D. G. (2001). Plant pathogens and integrated defence responses to infection. *Nature* 411: 826–833.

Dean, J. V., Shah, R. P. and Mohammed, L. A. (2003). Formation and vacuolar localization of salicylic acid glucose conjugates in soybean cell suspension cultures. *Physiologia Plantarum* 118(3): 328–336.

Dean, J. V. and Delaney, S. P. (2008). Metabolism of salicylic acid in wild-type, *ugt74f1* and *ugt74f2* glucosyltransferase mutants of *Arabidopsis thaliana*. *Physiologia Plantarum* 132(4): 417–25.

Dean, J. V. and Mills, J. D. (2004). Uptake of salicylic acid 2-*O*- β -D-glucose into soybean tonoplast vesicles. *Physiologia Plantarum*. 120: 603–612.

Dean, J. V., Mohammed, L. A. and Fitzpatrick, T. (2005). The formation, vacuolar localization, and tonoplast transport of salicylic acid glucose conjugates in tobacco cell suspension cultures. *Planta* 221: 287–296.

Dempsey, D. A., Vlot, A. C., Wildermuth, M. C. and Klessig, D. F. (2011). Salicylic Acid Biosynthesis and metabolism. *The Arabidopsis Book* 9: e0156.

Dempsey, M. A. and Klessig, D. F. (2017). How does the multifaceted plant hormone salicylic acid combat disease in plants and are similar mechanisms utilized in humans? *BMC Biology* 15: 23.

Derksen, H., Rampitsch, C. and Daayf, F. (2013). Signaling cross-talk in plant disease resistance. *Plant Science*. 207: 79–87.

Desai, M. and Hu, J. (2008). Light induces peroxisome proliferation in *Arabidopsis* Seedlings through the Photoreceptor Phytochrome A, the transcription factor HY5 HOMOLOG, and the peroxisomal protein PEROXIN11b. *Plant Physiology* 146 (3):1117–1127.

Dewdney, J., Reuber, T. L., Wildermuth, M. C., Devoto, A., Cui, J., Stutius, L. M., Drummond, E. P. and Ausubel, F. M. (2000). Three unique mutants of *Arabidopsis* identify eds loci required for limiting growth of a biotrophic fungal pathogen. *The Plant Journal* 24(2): 205–218.

Diebold, R., Schuster, J., Däschner, K. and Binder, S. (2002). The branched-chain amino acid transaminase gene family in *Arabidopsis* encodes plastid and mitochondrial proteins. *Plant Physiology* 129(2): 540–550.

Dodds, P. N. and Rathjen, J. P. (2010). Plant immunity: towards an integrated view of

plant–pathogen interactions. *Nature* 11(8): 539–548.

Dong, X. (2004). NPR1, all things considered. *Current Opinion in Plant Biology* 7(5): 547-552

Dyson, B. C., Allwood, J. W., Feil, R., Xu, Y. U. N., Miller, M., Bowsher, C. G., Goodacre, R., Lunn, J. E. and Johnson, G. N. (2015). Acclimation of metabolism to light in *A. thaliana*: the glucose 6-phosphate/phosphate translocator GPT2 directs metabolic acclimation. *Plant, Cell & Environment* 38(7):1404–1417.

Du, L., Ali, G. S., Simons, K. A., Hou, J., Yang, T., Reddy, A. S. N. and Poovaiah, B. W. (2009). Ca²⁺/calmodulin regulates salicylic-acid-mediated plant immunity. *Nature* 457:1154-1158

Erb, M., Lenk, C., Erb, M., Lenk, C. and Turlings, T. C. J. (2009). The underestimated role of roots in defense against leaf attackers. *Trends in Plant Science* 14(12):653-9

Eulgem, T., Weigman, V. J., Chang, H.-S., McDowell, J. M., Holub, E. B., Glazebrook, J., Zhu, T. and Dangl, J. L. (2004). Gene Expression Signatures from Three Genetically Separable Resistance Gene Signaling Pathways for Downy Mildew Resistance. *Plant Physiology* 135(2): 1129-1144.

Filiault, D. L. and Maloof, J. N. (2012). A Genome-Wide Association Study identifies variants underlying the *Arabidopsis thaliana* shade avoidance response. *PLOS Genetics* 8(3): e1002589

Fonseca, S., Chico, J. M. and Solano, R. (2009). The jasmonate pathway: the ligand, the receptor and the core signalling module. *Current Opinion in Plant Biology* 12(5):539-47

Fu, Z. Q. and Dong, X. (2013). Systemic Acquired Resistance: turning local infection into global defense. *Annual Review of Plant Biology* 64:839-863.

Fu, Z. Q., Yan, S., Saleh, A., Wang, W., Ruble, J., Oka, N. and Mohan, R. (2012). NPR3 and NPR4 are receptors for the immune signal salicylic acid in plants. *Nature* 486(7402): 228–232.

Gao, Q.-M., Venugopal, S., Navarre, D. and Kachroo, A. (2011). Low oleic acid-derived repression of jasmonic acid-inducible defense responses requires the WRKY50 and WRKY51 proteins. *Plant Physiology* 155(1): 464-476.

Garcion, C., Lohmann, A., Lamodièrre, E., Catinot, J., Buchala, A., Doermann, P. and Métraux, J.-P. (2008). Characterization and biological function of the ISOCHORISMATE SYNTHASE2 gene of *Arabidopsis*. *Plant Physiology* 147(3): 1279–1287.

Gibson, G. (2012). Rare and common variants: twenty arguments. *Nature* 13(2): 135–145.

Gill, S. S. and Tuteja, N. (2010). Reactive oxygen species and antioxidant machinery in abiotic stress tolerance in crop plants. *Plant Physiology et Biochemistry* 48(12): 909–930.

Gilroy, S., Bia, M., Suzuki, N., Górecka, M., Devireddy, A. R. and Mittler, R. (2016). Update on reactive oxygen species and systemic signaling ROS, calcium and electric signals

- key mediators of rapid systemic signaling in plants. *Plant Physiology* 171(3): 1606-1615
- Ghirardo A, Heller W, Fladung M, Schnitzler J-P, Schroeder H (2012).** Function of defensive volatiles in pedunculate oak (*Quercus robur*) is tricked by the moth *Tortrix viridana*. *Plant, Cell & Environment* 35: 2192–2207.
- Ghirardo A, Wright LP, Bi Z, Rosenkranz M, Pulido P, Rodríguez-Concepción M, Niinemets Ü, Brüggemann N, Gershenzon J, Schnitzler J., P. (2014).** Metabolic flux analysis of plastidic isoprenoid biosynthesis in poplar leaves emitting and nonemitting isoprene. *Plant Physiology* 165: 37–51.
- Glazebrook, J. (2005).** Contrasting mechanisms of defense against biotrophic and necrotrophic pathogens. *Annual Review of Phytopathology* 2005(43):205–27.
- Gomez-Gomez, L., Bauer, Z. and Boller, T. (2001).** Both the extracellular leucine-rich repeat domain and the kinase activity of FLS2 are required for flagellin binding and signaling in *Arabidopsis*. *Plant Cell* 13(5):1155–1164.
- Griebel, T. and Zeier, J. (2008).** Light regulation and daytime dependency of inducible plant defenses in *Arabidopsis*: phytochrome signaling controls systemic acquired resistance rather than local defense. *Plant Physiology* 147(2): 790-801.
- Groen, S. C. (2016).** Signalling in systemic plant defence – roots put in hard graft. *Journal of Experimental Botany* 67(19): 5585–5587.
- Hagelstein, P., Sieve, B., Klein, M., Jans, H. and Schultz, G. (1997).** Leucine synthesis in chloroplasts: leucine/isoleucine aminotransferase and valine aminotransferase are different enzymes in spinach chloroplasts. *Journal of Plant Physiology* 150:23–30.
- Hammond, J. P. and White, P. J. (2008).** Sucrose transport in the phloem: integrating root responses to phosphorus starvation. *Journal of Experimental Botany* 59(1): 93–109.
- Hartung, W., Sauter, A. and Hose, E. (2002).** Abscisic acid in the xylem: where does it come from, where does it go to? *Journal of Experimental Botany* 53(366): 27–32.
- Hasegawa, S., Sogabe, Y., Asano, T., Nakagawa, T., Nakamura, H., Kodama, H., Ohta, H., Yamaguchi, K., Mueller, M. J. and Nishiuchi, T. (2011).** Gene expression analysis of wounding-induced root-to-shoot communication in *Arabidopsis thaliana*. *Plant Cell and Environment* 34: 705–716.
- Haywood, V., Yu, T., Huang, N. and Lucas, W. J. (2005).** Phloem long-distance trafficking of GIBBERELLIC ACID-INSENSITIVE RNA regulates leaf development. *The Plant Journal* 42: 49–68
- He, Y., Galant, A., Pang, Q., Strul, J. M., Balogun, S. F., Jez, J. M. and Chen, S. (2011).** Structural and functional evolution of isopropylmalate dehydrogenases in the leucine and glucosinolate pathways of *Arabidopsis thaliana*. *The Journal of Biological Chemistry* 286(33): 28794–28801.
- Hebsgaard, S. M., Korning, P. G., Tolstrup, N., Engelbrecht, J., Rouzé, P. and Brunak, S. (1996).** Splice site prediction in *Arabidopsis thaliana* pre-mRNA by combining local and

global sequence information. *Nucleic Acids Research* 24(17): 3439–3452.

Hell, R. and Wirtz, M. (2011). Molecular biology, biochemistry and cellular physiology of cysteine metabolism in *Arabidopsis thaliana*. *The Arabidopsis Book* e0154. 1–19.

Herrera-Vásquez, A., Salinas, P. and Holuigue, L. (2015). Salicylic acid and reactive oxygen species interplay in the transcriptional control of defense genes expression. *Frontiers in Plant Science* 19(6): 171.

Higashi, K., Ishiga, Y., Inagaki, Y., Toyoda, K., Shiraishi, T. and Ichinose, Y. (2008). Modulation of defense signal transduction by flagellin-induced WRKY41 transcription factor in *Arabidopsis thaliana*. *Molecular Genetics and Genomics* 279(3): 303–312.

Huang, J., Yang, M. and Zhang, X. (2016). The function of small RNAs in plant biotic stress response. *Journal of Integrative Plant Biology* 58(4): 312–327.

Huo, X., Wang, C., Teng, Y. and Liu, X. (2015). Identification of miRNAs associated with dark-induced senescence in *Arabidopsis*. *BMC Plant Biology* 15(1): 266.

Hwang, S. G., Lin, N. C., Hsiao, Y. Y., Kuo, C. H., Chang, P. F., Deng, W. L., Chiang, M. H., Shen, H. L., Chen, C. Y. and Cheng, W. H. (2012). The *Arabidopsis* short-chain dehydrogenase/reductase 3, an ABSCISIC ACID DEFICIENT 2 homolog, is involved in plant defense responses but not in ABA biosynthesis. *Plant Physiology and Biochemistry* 55: 63–73.

Iglesias-Baena, I., Barranco-Medina, S., Lázaro-Payo, A., López-Jaramillo, F. J., Sevilla, F. and Lázaro, J.-J. (2010). Characterization of plant sulfiredoxin and role of sulphinic form of 2-Cys peroxiredoxin. *Journal of Experimental Botany* 61(5): 1509–1521.

Janda, M. and Ruelland, E. (2015). Model Magical mystery tour: Salicylic acid signalling. *Environmental and Experimental Botany* 114: 117–128

Jeong, W., Park, S. J., Chang, T., Lee, D. and Rhee, S. G. (2006). Molecular Mechanism of the reduction of cysteine sulfinic acid of peroxiredoxin to cysteine by mammalian sulfiredoxin. *The Journal of Biological Chemistry* 281(20): 4400–4407.

Jones, J. D. G. and Dangl, J. L. (2006). The plant immune system. *Nature* 444: 323–329

Jones, P. and Vogt, T. (2001). Glycosyltransferases in secondary plant metabolism: tranquilizers and stimulant controllers. *Planta* 213(2): 164–174.

Gao, Q. M., Zhu, S., Kachroo, P., Kachroo, A. (2015). Signal regulators of systemic acquired resistance. *Frontiers in Plant Science* 6: 1–12.

Kachroo, P., Shanklin, J., Shah, J., Whittle, E. J. and Klessig, D. F. (2001). A fatty acid desaturase modulates the activation of defense signaling pathways in plants. *Proceedings of the National Academy of Sciences of the United States of America* 98(16): 9448–53.

Kaltdorf, M. and Naseem, M. (2013). How many salicylic acid receptors does a plant cell need? *Science Signaling* 6(279): 4–6.

- Kang, J., Park, J., Choi, H., Burla, B., Kretschmar, T., Lee, Y. and Martinoia, E. (2011).** Plant ABC Transporters. *The Arabidopsis book* 9p. e0153.
- Kang, J., Yim, S., Choi, H., Kim, A., Lee, K. P., Lopez-Molina, L., Martinoia, E. and Lee, Y. (2015).** Abscisic acid transporters cooperate to control seed germination. *Nature Communications* 6: 8113.
- Kawashima, C. G., Berkowitz, O., Hell, R., Noji, M. and Saito, K. (2005).** Characterization and expression analysis of a serine acetyltransferase gene family involved in a key step of the sulfur assimilation pathway in *Arabidopsis*. *Plant Physiology* 137: 220–230.
- Kazan, K. (2013).** Auxin and the integration of environmental signals into plant root development. *Annals of Botany* 112: 1655–1665.
- Kazan, K. and Manners, J. M. (2013).** MYC2 : The master in action. *Molecular Plant* 6: 686–703.
- Kehr, J. and Buhtz, A. (2008).** Long distance transport and movement of RNA through the phloem. *Journal of Experimental Botany* 59: 85–92.
- Kelley, L. A., Mezulis, S., Yates, C. M., Wass, M. N. and Sternberg, M. J. E. (2015).** The Phyre2 web portal for protein modeling , prediction and analysis. *Nature Protocols* 10(6): 845–858.
- Kerk, D., Templeton, G. and Moorhead, G. B. G. (2008).** Evolutionary radiation pattern of novel protein phosphatases revealed by analysis of protein data from the completely sequenced genomes of humans, green algae, and higher plants. *Plant Physiology* 146(2): 351-367.
- Kiba, A., Galis, I., Hojo, Y., Ohnishi, K., Yoshioka, H. and Hikichi, Y. (2014).** SEC14 phospholipid transfer protein is involved in lipid signaling-mediated plant immune responses in *Nicotiana benthamiana*. *PLOS ONE* 9(5): e981509(5).
- Kim, K.-C., Lai, Z., Fan, B. and Chen, Z. (2008).** Arabidopsis WRKY38 and WRKY62 transcription factors interact with histone deacetylase 19 in basal defense. *Plant Cell* 20(9): 2357–2371.
- Kimchi-Sarfaty, C., Oh J. M., Kim I. W., Sauna Z. E., Calcagno A. M., Ambudkar S. V., Gottesman M. M. (2007).** A “Silent” polymorphism in the MDR 1 gene changes substrate specificity. *Science* 318(5855):1382-3.
- Klein, M. and Papenbrock, J. (2004).** The multi-protein family of *Arabidopsis* sulphotransferases and their relatives in other plant species. *Journal of Experimental Botany* 55(404): 1809–1820.
- Knoth, C., Salus, M. S., Girke, T. and Eulgem, T. (2009).** The synthetic elicitor 3,5-dichloroanthranilic acid induces NPR1-dependent and NPR1-independent mechanisms of disease resistance in *Arabidopsis*. *Plant Physiology* 150(May): 333–347.
- Ko, D., Kang, J., Kiba, T., Park, J., Kojima, M., Do, J., Yoon, K., Kwon, M., Endler, A., Song, W.-Y., Martinoia, E., Sakakibara, H., Lee, Y. (2014).** Arabidopsis ABCG14 is

essential for the root-to-shoot translocation of cytokinin. *Proceedings of the National Academy of Sciences of the United States of America* 111(19):7150-7155.

Kohlen, W., Charnikhova, T., Liu, Q., Bours, R., Domagalska, M. A., Beguerie, S., Verstappen, F., Leyser, O., Bouwmeester, H. and Ruyter-Spira, C. (2011). Strigolactones are transported through the xylem and play a key role in shoot architectural response to phosphate deficiency in nonarbuscular mycorrhizal host *Arabidopsis*. *Plant Physiology* 155(2): 974–987.

Korte, A. and Farlow, A. (2013). The advantages and limitations of trait analysis with GWAS: a review. *Plant Methods* 9: 29.

Kunze, G., Zipfel, C., Robatzek, S., Niehaus, K., Boller, T. and Felix, G. (2004). The N terminus of bacterial elongation factor tu elicits innate immunity in *Arabidopsis* Plants. *Plant Cell* 16: 3496–3507.

Kuromori, T., Miyaji, T., Yabuuchi, H., Shimizu, H., Sugimoto, E. and Kamiya, A. Moriyama, Y., Shinozaki, K. (2010). ABC transporter AtABCG25 is involved in abscisic acid transport and responses. *Proceedings of the National Academy of Sciences of the United States of America* 107(5): 2361–2366.

Kuromori, T., Sugimoto, E. and Shinozaki, K. (2014). Intertissue signal transfer of abscisic acid from vascular cells to guard cells. *Plant Physiology* 164(4): 1587–1592.

Kuznetsova, E., Nocek, B., Brown, G., Makarova, K. S., Flick, R., Wolf, Y. I., Khusnutdinova, A., Evdokimova, E., Jin, K., Tan, K., Hanson, A. D., Hasnain, G., Zallot, R., Crécy-lagard, V. De, Babu, M., Savchenko, A. and Joachimiak, A. (2015). Functional diversity of haloacid dehalogenase superfamily phosphatases from *Saccharomyces cerevisiae*. *Journal of Biological Chemistry* 290(30): 18678–18698.

Lakshmanan, V., Kitto, S. L., Caplan, J. L., Hsueh, Y. and Kearns, D. B. (2012). Microbe-associated molecular patterns-triggered root responses mediate beneficial rhizobacterial recruitment. *Plant Physiology* 160: 1642–1661.

Lamesch, P., Berardini, T. Z., Li, D., Swarbreck, D., Wilks, C., Sasidharan, R., Muller, R., Dreher, K., Alexander, D. L., Garcia-hernandez, M., Karthikeyan, A. S., Lee, C. H., Nelson, W. D., Ploetz, L., Singh, S., Wensel, A. and Huala, E. (2012). The *Arabidopsis* information resource (TAIR): improved gene annotation and new tools. *Nucleic Acids Research* 40: 1202–1210.

Langenbach, C., Campe, R., Schaffrath, U., Goellner, K. and Conrath, U. (2013). UDP-glucosyltransferase UGT84A2/BRT1 is required for *Arabidopsis* nonhost resistance to the Asian soybean rust pathogen *Phakopsora pachyrhizi*. *New Phytologist* 198: 536–545.

Langlois-Meurinne, M., Gachon, C. M. M. and Saindrenan, P. (2005). Pathogen-Responsive Expression of Glycosyltransferase genes UGT73B3 and UGT73B5 is necessary for resistance to *Pseudomonas syringae* pv *tomato*. *Plant Physiology* 139(4): 1890–1901.

Lemarié, S., Robert-Seilaniantz, A., Lariagon, C., Lemoine, J., Marnet, N., Levrel, A., Jubault, M., Manzaneres-Dauleux, M. and Gravot, A. (2015). Camalexin contributes to the partial resistance of *Arabidopsis thaliana* to the biotrophic soilborne protist

Plasmodiophora brassicae. *Frontiers in Plant Science* 21(6):539.

Lequeux, H., Hermans, C., Lutts, S. and Verbruggen, N. (2010). Response to copper excess in *Arabidopsis thaliana*: Impact on the root system architecture, hormone distribution, lignin accumulation and mineral profile. *Plant Physiology and Biochemistry* 48(8): 673–682.

Lescot, M., Déhais, P., Thijs, G., Marchal, K., Moreau, Y., Peer, Y. Van De, Rouzé, P. and Rombauts, S. (2002). PlantCARE, a database of plant cis-acting regulatory elements and a portal to tools for in silico analysis of promoter sequences. *Nucleic Acids Research* 30(1): 325–327.

Li, J., Brader, G. and Palva, E. T. (2004). The WRKY70 transcription factor: a node of convergence for jasmonate-mediated and salicylate-mediated signals in plant defense. *Plant Cell* 16(2): 19–331.

Li, W., Zhang, F., Chang, Y., Zhao, T., Schranz, M. E. and Wang, G. (2015). Nicotinate O -glucosylation is an evolutionarily metabolic trait important for seed germination under stress conditions in *Arabidopsis thaliana*. *Plant Cell* 27(7): 1907-1924.

Li, Y., Baldauf, S., Lim, E. and Bowles, D. J. (2001). Phylogenetic Analysis of the UDP-glycosyltransferase multigene family of *Arabidopsis thaliana*. *Journal of Biological Chemistry* 276(6): 4338–4343.

Liebsch, D. and Keech, O. (2016). Tansley insight dark-induced leaf senescence: new insights into a complex light-dependent regulatory pathway. *New Phytologist* 212: 563–570.

Lim, E. and Bowles, D. J. (2004). A class of plant glycosyltransferases involved in cellular homeostasis. *EMBO Journal* 23(15): 2915–2922.

Lim, E., Doucet, C. J., Li, Y., Elias, L., Worrall, D., Spencer, S. P., Ross, J. and Bowles, D. J. (2002). The activity of *Arabidopsis* glycosyltransferases toward salicylic acid, 4-hydroxybenzoic acid, and other benzoates. *Journal of Biological Chemistry* 277(1): 586–592.

Liu, C., Cheng, F., Sun, Y., Ma, H. and Yang, X. (2016). Structure–function relationship of a novel PR-5 protein with antimicrobial activity from soy hulls. *Journal of Agricultural and Food Chemistry* 64(4): 948–959.

Liu, P., Dahl, C. C. Von and Klessig, D. F. (2011). The extent to which methyl salicylate is required for signaling systemic acquired resistance is dependent on exposure to light after infection. *Plant Physiology* 157(4): 2216-26.

Liu, T.-Y., Aung, K., Tseng, C.-Y., Chang, T.-Y., Chen, Y.-S. and Chiou, T.-J. (2011). Vacuolar Ca²⁺/H⁺ transport activity is required for systemic phosphate homeostasis involving shoot-to-root signaling in *Arabidopsis*. *Plant Physiology* 156(3):1176–1189.

Long, Q., Rabanal, F. A., Meng, D., Huber, C. D., Farlow, A., Platzer, A., Zhang, Q., Vilhjálmsson, B. J., Korte, A., Nizhynska, V., Voronin, V., Korte, P., Sedman, L., Mandáková, T., Lysak M., Seren, U., Hellmann, I., Nordborg, M., (2013). Massive genomic variation and strong selection in *Arabidopsis thaliana* lines from Sweden. *Nature Genetics* 45(8): 884–890.

- Van Loon, L. C. and Bakker, P. A. H. M. (2006).** Induced systemic resistance as a mechanism of disease suppression by rhizobacteria. *PGPR: Biocontrol and Biofertilization* 39–66.
- Loon, L. C., Rep, M. and Pieterse, C. M. J. (2006).** Significance of inducible defense-related proteins in infected plants. *Annual Review of Phytopathology* 44:135-162.
- Lopez, J. A., Sun, Y., Blair, P. B. and Mukhtar, M. S. (2015).** TCP three-way handshake: linking developmental processes with plant immunity. *Trends in Plant Science* 20(4): 238–245.
- Macho, A. P. and Zipfel, C. (2014).** Review Plant PRRs and the activation of innate immune signaling. *Molecular Cell* 54(2): 263–272.
- Maloney, G. S., Kochevenko, A., Tieman, D. M., Tohge, T., Krieger, U., Zamir, D., Taylor, M. G., Fernie, A. R. and Klee, H. J. (2010).** Characterization of the branched-chain amino acid aminotransferase enzyme family in tomato. *Plant Physiology* 153(3): 925–36.
- Orval A. Mamer, O. A., Reimer M. L. J. (1992).** On the Mechanisms of the formation of L-alloisoleucine and the 2-hydroxy-3-methylvaleric acid stereoisomers from L-isoleucine in Maple Syrup Urine Disease patients and in normal humans. *The Journal of Biological Chemistry* 267(5): 22141–22147.
- Manfield, I. W., Devlin, P. F., Jen, C., Westhead, D. R. and Gilmartin, P. M. (2006).** Conservation, convergence, and divergence of light-responsive, circadian-regulated, and tissue-specific expression patterns during evolution of the arabidopsis GATA gene family. *Plant Physiology* 143(2): 941–958.
- Martinoia, E., Klein, M., Geisler, M., Bovet, L., Forestier, C., Kolukisaoglu, Müller-Röber, B. and Schulz, B. (2002).** Multifunctionality of plant ABC transporters: more than just detoxifiers. *Planta* 214(3): 345–355.
- Martins, N., Gonçalves, S. and Romano, A. (2013).** Aluminum inhibits root growth and induces hydrogen peroxide accumulation in *Plantago algarbiensis* and *P. almogravensis* seedlings. *Protoplasma* 250(6):1295-302.
- Matsoukas, I. G., Massiah, A. J. and Thomas, B. (2013).** Starch metabolism and antiflorigenic signals modulate the juvenile-to-adult phase transition in Arabidopsis. *Plant, Cell & Environment* 36(10): 1802–1811.
- Matsui, A., Nguyen, A. H., Nakaminami, K. and Seki, M. (2013).** Arabidopsis non-coding RNA regulation in abiotic stress responses. *International Journal of Molecular Sciences* 14(11): 22642-54.
- Mcgrath, K. C., Dombrecht, B., Manners, J. M., Schenk, P. M., Edgar, C. I., Udvardi, M. K., Kazan, K., Maclean, D. J. and Plant, T. (2005).** Repressor- and activator-type ethylene response factors functioning in jasmonate signaling and disease resistance identified via a genome-wide screen of *Arabidopsis* Transcription factor gene expression. *Plant Physiology* 139(2): 949-59
- Mersmann, S., Bourdais, G., Rietz, S. and Robatzek, S. (2010).** Ethylene Signaling

- Regulates Accumulation of the FLS2 Receptor and Is Required for the Oxidative Burst Contributing to Plant Immunity. *Plant Physiology* 154(1): 391-400.
- Miersch, O., Neumerkel, J., Dippe, M., Stenzel, I., Wasternack, C. and Wasternack, C. (2006).** Hydroxylated jasmonates are commonly occurring metabolites of jasmonic acid and contribute to a partial switch-off in jasmonate signaling. *New Phytologist* 177(1): 114-27.
- Mishina, T. E. (2007).** Pathogen-associated molecular pattern recognition rather than development of tissue necrosis contributes to bacterial induction of systemic acquired resistance in *Arabidopsis*. *Plant Journal* 50(3): 500-13.
- Miya, A., Albert, P., Shinya, T., Desaki, Y., Ichimura, K., Shirasu, K., Narusaka, Y., Kawakami, N., Kaku, H. and Shibuya, N. (2007).** CERK1, a LysM receptor kinase is essential for chitin elicitor signaling in *Arabidopsis*. *Proceedings of the National Academy of Sciences of the United States of America* 104(49): 19613-8.
- Moussatche, P. and Klee, H. J. (2004).** Autophosphorylation activity of the *Arabidopsis* ethylene receptor multigene family. *Journal of Biological Chemistry* 279(47): 48734-41.
- Nalam, V. J., Keeretaweep, J., Sarowar, S. and Shah, J. (2012).** Root-derived oxylipins promote green peach aphid performance on *Arabidopsis* foliage. *Plant Cell* 24(4): 1643-53.
- Návarová, H., Bernsdorff, F., Döring, A.-C. and Zeier, J. (2012).** Pipecolic acid, an endogenous mediator of defense amplification and priming, is a critical regulator of inducible plant immunity. *Plant Cell* 24(12): 5123-41.
- Nawrath, C. and Métraux, J. (1999).** Salicylic acid induction – deficient mutants of *Arabidopsis* express PR-2 and PR-5 and accumulate high levels of camalexin after pathogen inoculation. *Plant Cell* 11(8): 1393-1404.
- Ndamukong, I., Abdallat, A. Al, Thurow, C., Fode, B., Zander, M., Weigel, R. and Gatz, C. (2007).** SA-inducible *Arabidopsis* glutaredoxin interacts with TGA factors and suppresses JA-responsive PDF1.2 transcription. *Plant Journal* 50(1): 128-39.
- Niyogi, K. K., Last, R. L., Fink, G. R. and Keith, B. (1993).** Suppressors of *trp1* fluorescence identify a new *Arabidopsis* gene, TRP4, encoding the anthranilate synthase beta subunit. *Plant Cell* 5(9): 1011-1027.
- Notaguchi, M., Higashiyama, T. and Suzuki, T. (2015).** Identification of mRNAs that move over long distances using an RNA-Seq analysis of *Arabidopsis/Nicotiana benthamiana* heterografts. *Plant & Cell Physiology* 56(2): 311-21.
- Notaguchi, M. and Okamoto, S. (2015).** Dynamics of long-distance signaling via plant vascular tissues. *Frontiers in Plant Science* 6: 161.
- Noutoshi, Y., Okazaki, M., Kida, T., Nishina, Y., Morishita, Y., Ogawa, T., Suzuki, H., Shibata, D., Jikumaru, Y., Hanada, a., Kamiya, Y. and Shirasu, K. (2012).** Novel plant immune-priming compounds identified via high-throughput chemical screening target salicylic acid glucosyltransferases in *Arabidopsis*. *Plant Cell* 24(9): 3795-3804.
- Oide, S., Bejai, S., Staal, J., Guan, N., Kaliff, M. and Dixelius, C. (2013).** A novel role of

PR2 in abscisic acid (ABA) mediated, pathogen- induced callose deposition in *Arabidopsis thaliana*. *New Phytologist* (4): 1187-99.

Onate-Sanchez, L., Anderson, J. P., Young, J. and Singh, K. B. (2006). AtERF14, a member of the ERF family of transcription factors, plays a nonredundant role in plant defense. *Plant Physiology* 143(1): 400–409.

Orval A. Mamer and Mark L. J. Reimer (1992). On the mechanisms of the formation of l-alloisoleucine and the 2-hydroxy-3-methylvaleric acid stereoisomers from L-Isoleucine in maple syrup urined disease patients and in norma humans. *Journal of Biological Chemistry* 267: 22141–22147.

Overvoorde, P., Fukaki, H. and Beeckman, T. (2017). Auxin Control of Root Development. *Cold Spring Harbor Perspectives in Biology* 2(6): a001537.

Pajeroska-Mukhtar, K. M., Emerine, D. K. and Mukhtar, M. S. (2013). Tell me more: roles of NPRs in plant immunity. *Trends in Plant Science* 18(7): 402–411.

Park, J., Park, J., Kim, Y., Staswick, P. E., Jeon, J., Yun, J., Kim, S., Kim, J., Lee, Y. and Park, C. (2007). GH3-mediated auxin homeostasis links growth regulation with stress adaptation response in *Arabidopsis*. *Journal of Biological Chemistry* 282(13): 10036-46.

Park, S., Kaimoyo, E., Kumar, D., Mosher, S. and Klessig, D. F. (2008). Methyl salicylate is a critical mobile signal for plant systemic acquired resistance. *Science* 318(5847): 113-6.

Pastori, G. M., Kiddle, G., Antoniw, J., Bernard, S., Veljovic-Jovanovic, S., Verrier, P. J., Noctor, G. and Foyer, C. H. (2003). Leaf vitamin C contents modulate plant defense transcripts and regulate genes that control development through hormone signaling. *Plant Cell* 15(4): 939–951.

Pauwels, L., Barbero, G. F., Geerinck, J., Tilleman, S., Grunewald, W., Pérez, A. C., Chico, J. M., Bossche, R. Vanden, Sewell, J., Gil, E., García-Casado, G., Witters, E., Inzé, D., Long, J. A., De Jaeger, G., Solano, R. and Goossens, A. (2010). NINJA connects the co-repressor TOPLESS to jasmonate signalling. *Nature* 464(7289): 788–91.

Pauwels, L. and Goossens, A. (2011). The JAZ Proteins: a crucial interface in the jasmonate signaling cascade. *Plant Cell* 23(9): 3089-100.

Peng, X., Liu, X. P., Liu, X. Y., Zhang, J., Xia, Z. L., Liu, X., Qin, H. J. and Wang, D. W. (2006). Molecular and functional characterization of sulfiredoxin homologs from higher plants. *Cell Research* 16(3): 287-96.

Peremyslov, V. V, Morgun, E. a, Kurth, E. G., Makarova, K. S., Koonin, E. V and Dolja, V. V (2013). Identification of myosin XI receptors in *Arabidopsis* defines a distinct class of transport vesicles. *Plant Cell* 25(8): 3022–38.

Pieterse, C. M. J., Leon-reyes, A., Ent, S. Van Der and Wees, S. C. M. Van (2009). Networking by small-molecule hormones in plant immunity. *Nature Chemical Biology* 5: 308 - 316.

Pieterse, C. M. J., Zamioudis, C., Berendsen, R. L., Weller, D. M., Van Wees, S. C. M.

- and Bakker, P. A. H. M. (2014).** Induced systemic resistance by beneficial microbes. *Annual Review of Phytopathology* 52(1): 47–375.
- Pillotsq, T., Ouzzines, M., Fournel-gigleuxs, S., Lafauries, C., Radominska, A., Burchellii, B., Siest, G. and Magdalou, J. (1993).** Glucuronidation of hyodeoxycholic acid in human liver. *Journal of Biological Chemistry* 268(34): 25636-42.
- Podebrad, F., Heil, M., Leib, S., Geier, B., Beck, T., Mosandl, A., Sewell, A. C. and Böhles, H. (1997).** Analytical approach in diagnosis of inherited metabolic diseases: Maple syrup urine disease (MSUD) – simultaneous analysis of metabolites in urine by enantioselective multidimensional capillary gas chromatography-mass spectrometry. *Journal of High Resolution Chromatography* 20(7): 355–362.
- Poppenberger, B., Berthiller, F., Lucyshyn, D., Sieberer, T., Schuhmacher, R., Krska, R., Kuchler, K., Glössl, J., Luschnig, C. and Adam, G. (2003).** Detoxification of the fusarium mycotoxin deoxynivalenol by a UDP-glucosyltransferase from *Arabidopsis thaliana*. *Journal of Biological Chemistry* 278(48): 47905–47914.
- Puerto-Galan, L., Perez-ruiz, J. M. and Cejudo, F. J. (2015).** The contribution of NADPH thioredoxin reductase C (NTRC) and sulfiredoxin to 2-Cys peroxiredoxin overoxidation in *Arabidopsis thaliana* chloroplasts. *Journal Of Experimental Botany* 66(10): 2957-66.
- Queval, G. and Noctor, G. (2009).** H₂O₂- activated up-regulation of glutathione in *Arabidopsis* involves induction of genes encoding enzymes involved in cysteine synthesis in the chloroplast. *Molecular Plant* 2(2): 344-56.
- Quiel, J. A. and Bender, J. (2003).** Glucose conjugation of anthranilate by the *Arabidopsis* ugt74f2 glucosyltransferase is required for tryptophan mutant blue fluorescence. *Journal of Biological Chemistry* 278(8): 6275–6281.
- Radomska-Pandya, A., Czernik, P. J., Little, J. M., Battaglia, E. And Mackenzie, P. I. (1999).** Structural and functional studies of udp-glucuronosyltransferases. *Drug Metabolism Reviews* 31(4): 817–899.
- Ranty, B., Aldon, D. and Galaud, J.-P. (2006).** Plant calmodulins and calmodulin-related proteins: multifaceted relays to decode calcium signals. *Plant Signaling & Behavior* 1(3): 96–104.
- Rasmussen, J. B., Hammerschmidt, R. and Zook, M. N. (1991).** Systemic induction of salicylic acid accumulation in cucumber after inoculation with *Pseudomonas syringae* pv *syringae*. *Plant Physiology* 97(4): 1342-7.
- Rees, D. C., Johnson, E. and Lewinson, O. (2009).** ABC transporters: The power to change. *Nature reviews. Molecular Cell Biology* 10(3): 218–227.
- Rojas, C. M., Senthil-Kumar, M., Tzin, V. and Mysore, K. S. (2014).** Regulation of primary plant metabolism during plant-pathogen interactions and its contribution to plant defense. *Frontiers in Plant Science* 5: 17.
- Woodward, A. W., Bartel, B. (2005).** Auxin: regulation, action, and interaction. *Annals of Botany* 95(5): 707–735.

- Rivas-San Vicente, M. and Plasencia, J. (2011).** Salicylic acid beyond defence: its role in plant growth and development. *Journal of Experimental Botany* 62(10): 3321–3338.
- Robert-Seilaniantz, A., Navarro, L., Bari, R. and Jones, J. D. G. (2007).** Pathological hormone imbalances. *Current Opinion in Plant Biology* 10(4): 372-9.
- Roden, L. C. and Ingle, R. A. (2009).** Lights, rhythms, infection: the role of light and the circadian clock in determining the outcome of plant – pathogen interactions. *Plant Cell* 21(9): 2546–2552.
- Routaboul, J.-M., Dubos, C., Beck, G., Marquis, C., Bidzinski, P., Loudet, O. and Lepiniec, L. (2012).** Metabolite profiling and quantitative genetics of natural variation for flavonoids in *Arabidopsis*. *Journal of Experimental Botany* 63(10): 3749–3764.
- Roy, S., Roy, S., Kumar, S., Kali, S. and Das, P. (2012).** Functional analysis of light-regulated promoter region of AtPol gene. pp. 411–432. *Planta* 235(2): 411-32.
- Ruzicka, K., Simásková, M., Duclercq, J., Petrásek, J., Zazimalová, E., Simon, S., Friml, J., Van Montagu, M. C. E. and Benková, E. (2009).** Cytokinin regulates root meristem activity via modulation of the polar auxin transport. *Proceedings of the National Academy of Sciences of the United States of America* 106(11): 4284–4289.
- Smith, J. A., Hammerschmidt, R., Fulbright D. W. (1991).** Rapid induction of systemic resistance in cucumber by *Pseudomonas syringae* pv. *syringae*. *Physiological and Molecular Plant Pathology* 38(3): 223–235.
- von Saint Paul, V., Zhang, W., Kanawati, B., Geist, B., Faus-Kessler, T., Schmitt-Kopplin, P. and Schäffner, A. R. (2011).** The *Arabidopsis* glucosyltransferase UGT76B1 conjugates isoleucic acid and modulates plant defense and senescence. *Plant Cell* 23(11): 4124–4145.
- Scalschi, L., Vicedo, B., Camañes, G., Fernandez-Crespo, E., Lapeña, L., González-Bosch, C. and García-Agustín, P. (2013).** Hexanoic acid is a resistance inducer that protects tomato plants against *Pseudomonas syringae* by priming the jasmonic acid and salicylic acid pathways. *Molecular Plant Pathology* 14(4):342–355.
- Schaller, G. E. and Kieber, J. J. (2002).** Ethylene. *The Arabidopsis Book* 1: e0071.
- Scholl, R. L., May, S. T. and Ware, D. H. (2017).** Seed and Molecular Resources for *Arabidopsis*. *Plant Physiology* 124(4): 1477-1480.
- Schröder H. (2010).** Sommerveredelung bei Eichen – eine Erfolgsgeschichte. *AFZ-Der Wald* 5, 16–17.
- Schuster, J. and Binder, S. (2005).** The mitochondrial branched-chain aminotransferase (AtBCAT-1) is capable to initiate degradation of leucine, isoleucine and valine in almost all tissues in *Arabidopsis thaliana*. *Plant Molecular Biology* 57(2): 241–254.
- Seyfferth, C. and Tsuda, K. (2014).** Salicylic acid signal transduction: the initiation of biosynthesis, perception and transcriptional reprogramming. *Frontiers in Plant Science* 5: 697.

- Shah, J., Zeier, J. and Cameron, R. K. (2013).** Long-distance communication and signal amplification in systemic acquired resistance. *Frontiers in Plant Science* 4(30): 1–16.
- Shaked, H., Avivi-Ragolsky, N. and Levy, A. A. (2006).** Involvement of the *Arabidopsis* SWI2/SNF2 chromatin remodeling gene family in DNA damage response and recombination. *Genetics*.173(2): 985–994.
- Shapiguzov, A., Julia, P., Wrzaczek, M. and Kangasjärvi, J. (2012).** ROS-talk – how the apoplast, the chloroplast, and the nucleus get the message through abiotic stress. *Frontiers in Plant Science* 3: 292.
- Sheard, L. B., Tan, X., Mao, H., Withers, J., Ben-nissan, G., Hinds, T. R., Kobayashi, Y., Hsu, F., Sharon, M., Browse, J., He, S. Y., Rizo, J., Howe, G. A. and Zheng, N. (2010).** Jasmonate perception by inositol-phosphate-potentiated COI1–JAZ co-receptor. *Nature* 468(7322): 400–405.
- Shin, L.-J., Lo, J.-C. and Yeh, K.-C. (2012).** Copper chaperone antioxidant Protein1 is essential for copper homeostasis. *Plant Physiology* 159(3): 1099–1110.
- Shitan, N., Bazin, I., Dan, K., Obata, K., Kigawa, K., Ueda, K., Sato, F., Forestier, C. and Yazaki, K. (2003).** Involvement of CjMDR1, a plant multidrug-resistance-type ATP-binding cassette protein, in alkaloid transport in *Coptis japonica*. *Proceedings of the National Academy of Sciences of the United States of America* 100(2): 751–756.
- Simon, C., Langlois-meurinne, M., Didierlaurent, L., Chaouch, S., Bellvert, F., Massoud, K., Garmier, M., Thareau, V., Comte, G., Noctor, G. and Saindrenan, P. (2014).** The secondary metabolism glycosyltransferases UGT73B3 and UGT73B5 are components of redox status in resistance of *Arabidopsis* to *Pseudomonas syringae* pv . *tomato*. *Plant, Cell & Environment* 37(5): 1114-29.
- Singh, H. P., Batish, D. R., Kaur, S., Arora, K. And Kohli, R. K. (2006).** α -Pinene inhibits growth and induces oxidative stress in roots. *Annals of Botany* 98(6): 1261–1269.
- Song, J. T. (2006).** Induction of a salicylic acid glucosyltransferase, AtSGT1, is an early disease response in *Arabidopsis thaliana*. *Molecules and Cells* 22(2): 233–238.
- Song, J. T., Koo, Y. J., Seo, H. S., Kim, M. C., Choi, Y. Do and Kim, J. H. (2008).** Overexpression of AtSGT1, an *Arabidopsis* salicylic acid glucosyltransferase, leads to increased susceptibility to *Pseudomonas syringae*. *Phytochemistry* 69(5): 1128–1134.
- Speiser, A., Haberland, S., Watanabe, M., Wirtz, M. and Dietz, K. (2015).** The significance of cysteine synthesis for acclimation to high light conditions. *Frontiers in Plant Science* 5:776: 1–10.
- Spoel, S. H., Johnson, J. S. and Dong, X. (2007).** Regulation of tradeoffs between plant defenses against pathogens with different lifestyles. *Proceedings of the National Academy of Sciences of the United States of America* 104(47): 18842–18847.
- Spoel, S. H., Koornneef, A., Claessens, S. M. C., Korzelius, J. P., Van Pelt, J. A., Mueller, M. J., Buchala, A. J., Métraux, J.-P., Brown, R., Kazan, K., Van Loon, L. C., Dong, X. and Pieterse, C. M. J. (2003).** NPR1 modulates cross-talk between salicylate- and

- jasmonate-dependent defense pathways through a novel function in the cytosol. *Plant Cell* 15(3): 760–770.
- Staswick, P. E., Serban, B., Rowe, M. and Tiryaki, I. (2005).** Characterization of an arabidopsis enzyme family that conjugates amino acids to indole-3-acetic acid. *Plant Cell* 17(2): 616–627.
- Sun, J., Chen, Q., Qi, L., Jiang, H., Li, S., Xu, Y., Liu, F., Zhou, W., Pan, J., Li, X., Palme, K. and Li, C. (2011).** Jasmonate modulates endocytosis and plasma membrane accumulation of the Arabidopsis PIN2 protein. pp. 360–375. *New Phytologist* 191(2): 360–75.
- Tabata, R., Sumida, K., Yoshii, T., Ohyama, K., Shinohara, H. and Matsubayashi, Y. (2014).** Perception of root-derived peptides by shoot LRR-RKs mediates systemic N-demand signaling. *Science* 6207: 343–346.
- Teng, S., Keurentjes, J., Bentsink, L., Koornneef, M. and Smeekens, S. (2005).** Sucrose-specific induction of anthocyanin biosynthesis in *Arabidopsis* requires the MYB75/PAP1 gene. *Plant Physiology* 139: 1840–1852.
- Teng, S., Wang, L., Srivastava, A. K., Schwartz, C. E. and Alexov, E. (2010).** Structural assessment of the effects of amino acid substitutions on protein stability and protein-protein interaction. *International Journal of Computational Biology and Drug Design* 3(4): 334–349.
- Testa, A., Donati, G., Yan, P., Romani, F., Huang, T. H., Vigano, M. A. and Mantovani, R. (2005).** Chromatin immunoprecipitation (ChIP) on Chip experiments uncover a widespread distribution of NF-Y binding CCAAT sites outside of core promoters. *Journal of Biological Chemistry*. 280: 13606–13615.
- Thakur, M. and Sohal, B. S. (2013).** Role of elicitors in inducing resistance in plants against pathogen infection: a review. *ISRN Biochemistry* 28: 2013
- Thatcher, L. F., Cevik, V., Grant, M., Zhai, B., Jones, J. D. G., Manners, J. M. and Kazan, K. (2016).** Characterization of a JAZ7 activation-tagged *Arabidopsis* mutant with increased susceptibility to the fungal pathogen *Fusarium oxysporum*. *Journal of Experimental Botany* 67(8): 2367–2386.
- Thieme, C. J., Rojas-Triana, M., Stecyk, E., Schudoma, C., Zhang, W., Yang, L., Miñambres, M., Walther, D., Schulze, W. X., Paz-Ares, J., Scheible, W.-R. and Kragler, F. (2015).** Endogenous *Arabidopsis* messenger RNAs transported to distant tissues. *Nature Plants* 1(4): 15025.
- Thompson, A. M. G., Iancu, C. V, Neet, K. E., Dean, J. V and Choe, J. (2017).** Differences in salicylic acid glucose conjugations by UGT74F1 and UGT74F2 from *Arabidopsis thaliana*. *Scientific Reports* 7: 46629.
- Tohge, T., Nishiyama, Y., Hirai, M. Y., Yano, M., Nakajima, J. I., Awazuhara, M., Inoue, E., Takahashi, H., Goodenowe, D. B., Kitayama, M., Noji, M., Yamazaki, M. and Saito, K. (2005).** Functional genomics by integrated analysis of metabolome and transcriptome of Arabidopsis plants over-expressing an MYB transcription factor. *Plant Journal* 42(2): 218–235.

- Tsukagoshi, H. (2012).** Defective root growth triggered by oxidative stress is controlled through the expression of cell cycle-related genes. *Plant Science* 197:30-9
- Umemura, K., Satou, J., Iwata, M., Uozumi, N., Koga, J. and Kawano, T. (2009).** Contribution of salicylic acid glucosyltransferase, OsSGT1 to chemically induced disease resistance in rice plants. *Plant Journal* 57(3): 463-72.
- Vandesompele, J., De Preter, K., Pattyn, F., Poppe, B., Van Roy, N., De Paepe, A. and Speleman, F. (2002).** Accurate normalization of real-time quantitative RT-PCR data by geometric averaging of multiple internal control genes. *Genome Biology* 3(7).
- Vellosillo, T., Martínez, M., López, M. A., Vicente, J., Cascón, T., Dolan, L., Hamberg, M. and Castresana, C. (2007).** Oxylipins produced by the 9-Lipoxygenase pathway in *Arabidopsis* regulate lateral root development and defense responses through a specific signaling cascade. *Plant Cell* 19(3): 831–846.
- Verhage, A., Vlaardingerbroek, I., Raaymakers, C., Dam, N. M. Van and Dicke, M. (2011).** Rewiring of the jasmonate signaling pathway in *Arabidopsis* during insect herbivory. *Frontiers in Plant Science* 26(2):47.
- Verk, M. C. Van, Bol, J. F. and Linthorst, H. J. M. (2011).** WRKY transcription factors involved in activation of SA biosynthesis genes. *BMC Plant Biology* 11: 89.
- Vlot, A. C., Dempsey, D. A. and Klessig, D. F. (2009).** Salicylic acid, a multifaceted hormone to combat disease. *Annual Review of Phytopathology* 47(1): 177–206.
- Vogel-Adghough, D., Stahl, E., Návarová, H. and Zeier, J. (2013).** Pipecolic acid enhances resistance to bacterial infection and primes salicylic acid and nicotine accumulation in tobacco. *Plant Signaling & Behavior* (11): 1–9.
- Wang, D., Pajerowska-mukhtar, K., Culler, A. H., Dong, X. and Carolina, N. (2007).** Salicylic acid inhibits pathogen growth in plants through repression of the auxin signaling pathway. *Current Biology* 17(20): 1784-90.
- Wang, L., Tsuda, K., Truman, W., Sato, M., Nguyen, L. V, Katagiri, F. and Glazebrook, J. (2011).** CBP60g and SARD1 play partially redundant critical roles in salicylic acid signaling. *Plant Journal* 67(6):1029-41.
- Wang, X., Gao, J., Zhu, Z., Dong, X., Wang, X., Ren, G., Zhou, X. and Kuai, B. (2015).** TCP transcription factors are critical for the coordinated regulation of ISOCHORISMATE SYNTHASE 1 expression in *Arabidopsis thaliana*. *Plant Journal*. 82(1):151-62.
- Wang, Y., Zhang, W.-Z., Song, L.-F., Zou, J.-J., Su, Z. and Wu, W.-H. (2008).** Transcriptome analyses show changes in gene expression to accompany pollen germination and tube growth in *Arabidopsis*. *Plant Journal* 148(3): 1201–1211.
- Wasternack, C. and Xie, D. (2010).** The genuine ligand of a jasmonic acid receptor improved analysis of jasmonates is now required. *Plant Signaling & Behavior* 5(4):337-40
- Van Wees, S. C. M. and Glazebrook, J. (2003).** Loss of non-host resistance of *Arabidopsis* NahG to *Pseudomonas syringae* pv. *phaseolicola* is due to degradation products of salicylic

acid. *Plant Journal* 33(4): 733–742.

Wees, S. C. M. Van, Pieterse, C. M. J., Trijssenaar, A., Westende, Y. A. M. Van, Hartog, F. and Loon, L. C. Van (1997). Differential induction of systemic resistance in *Arabidopsis* by biocontrol bacteria. *Molecular Plant-Microbe Interactions* 10(6): 716-24.

Wenkel, S., Turck, F., Singer, K., Gissot, L. and Coupland, G. (2006). CONSTANS and the CCAAT box binding complex share a functionally important domain and interact to regulate flowering of *Arabidopsis*. *Plant Cell* 18(11): 2971-84.

Wildermuth, M., Jones, A. (2009). The role of salicylic acid in *Arabidopsis* root growth. *Conference abstract*. 20th International Conference on *Arabidopsis* Research.

Wildermuth, M. C., Dewdney, J., Wu, G. and Ausubel, F. M. (2001). Isochorismate synthase is required to synthesize salicylic acid for plant defence. *Nature* 414(6863): 562-5.

Willmann, R., Lajunen, H. M., Erbs, G., Newman, M., Kolb, D. and Tsuda, K. (2011). *Arabidopsis* lysin-motif proteins LYM1 LYM3 CERK1 mediate bacterial peptidoglycan sensing and immunity to bacterial infection. *Proceedings of the National Academy of Sciences of the United States of America* 108(49):1 9824-9.

Wind, J., Smekens, S. and Hanson, J. (2010). Sucrose: Metabolite and signaling molecule. *Phytochemistry* 71(14–15): 1610-4.

Wu, C., Li, X., Guo, S. and Wong, S.-M. (2016). Analyses of RNA-Seq and sRNA-Seq data reveal a complex network of anti-viral defense in TCV-infected *Arabidopsis thaliana*. *Scientific Reports* 6.

Wu, Y., Zhang, D., Chu, J. Y., Boyle, P., Wang, Y., Brindle, I. D., De Luca, V. and Després, C. (2012). The *Arabidopsis* NPR1 protein is a receptor for the plant defense hormone salicylic acid. *Cell Reports* 1(6): 639–647.

Yan, Y., Stolz, S., Chételat, A., Reymond, P., Pagni, M., Dubugnon, L. and Farmer, E. E. (2007). A downstream mediator in the growth repression limb of the jasmonate pathway. *Plant Cell* 19(8): 2470.

Yang, Z., He, C., Ma, Y., Herde, M. and Ding, Z. (2017). Jasmonic acid enhances Al-induced root growth inhibition. *Plant Physiology* 173(2): 1420-1433.

Yasuda, M. (2007). Regulation mechanisms of systemic acquired resistance induced by plant activators. *Journal of Pesticide Science* 32: 281-282.

Yin, L., Fristedt, R., Herdean, A., Solymosi, K., Bertrand, M., Andersson, M. X., Mamedov, F., Vener, A. V., Schoefs, B. and Spetea, C. (2012). Photosystem ii function and dynamics in three widely used *Arabidopsis thaliana* accessions. *PLoS ONE*. 7(9): e46206.

Yin, R. (2010). *Arabidopsis* flavonoid glycosylation impacts on phenylpropanoid biosynthesis and plant growth. *Doctoral thesis*.

Yu, H., Zhang, F., Wang, G., Liu, Y. and Liu, D. (2013). Partial deficiency of isoleucine impairs root development and alters transcript levels of the genes involved in branched-chain

amino acid and glucosinolate metabolism in *Arabidopsis*. *Journal of Experimental Botany* 64(2): 599–612.

Zander, M., Chen, S., Imkampe, J., Thurow, C. and Gatz, C. (2011). Repression of the *Arabidopsis thaliana* jasmonic acid/ethylene-induced defense pathway by TGA-interacting glutaredoxins depends on their C-terminal ALWL motif. *Molecular Plant* 5(4): 831–840.

Zander, M., Thurow, C. and Gatz, C. (2014). TGA transcription factors activate the salicylic acid-suppressible branch of the ethylene-induced defense program by regulating ORA59 expression. *Plant Physiology* 165(4): 1671-1683.

Zhang, C., Xie, Q., Anderson, R. G., Ng, G., Seitz, N. C., Peterson, T., McClung, C. R., McDowell, J. M., Kong, D., Kwak, J. M. and Lu, H. (2013). Crosstalk between the circadian clock and innate immunity in *Arabidopsis*. *PLOS Pathogens* 9(6): e1003370.

Zhang, L., Du, L., Shen, C., Yang, Y. and Poovaiah, B. W. (2014). Regulation of plant immunity through ubiquitin-mediated modulation of Ca²⁺ – calmodulin – AtSR1/CAMTA3 signaling. *Plant Journal* 78(2): 269-81.

Zhang, W. (2013). Impact of glycosyltransferase UGT76B1 in *Arabidopsis thaliana* and its substrate isoleucic acid on plant defense. *Doctoral thesis*.

Zhang, X., Chen, Y., Lin, X., Hong, X., Zhu, Y., Li, W., He, W., An, F. and Guo, H. (2013). Adenine phosphoribosyl transferase 1 is a key enzyme catalyzing cytokinin conversion from nucleobases to nucleotides in *Arabidopsis*. *Molecular Plant* 6(5): 1661–1672.

Zhang, Y., Xu, S., Ding, P., Wang, D., Ti, Y., He, J., Gao, M. and Xu, F. (2010). Control of salicylic acid synthesis and systemic acquired resistance by two members of a plant-specific family of transcription factors. *Proceedings of the National Academy of Sciences of the United States of America* 107(42):18220-5.

Zhang, Z. and Baldwin, I. T. (1997). Transport of [2-14 C] jasmonic acid from leaves to roots mimics wound-induced changes in endogenous jasmonic acid pools in *Nicotiana sylvestris*. *Planta* (203) 4: 436–441

Zhao, X., Wang, J., Yuan, J., Wang, X., Zhao, Q., Kong, P. and Zhang, X. (2015). NITRIC OXIDE-ASSOCIATED PROTEIN1 (AtNOA1) is essential for salicylic acid-induced root waving in *Arabidopsis thaliana*. *New Phytologist* 207(1): 211-24.

Zheng, X., Spivey, N. W., Zeng, W., Liu, P.-P., Fu, Z. Q., Klessig, D. F., He, S. Y. and Dong, X. (2012). Coronatine promotes *Pseudomonas syringae* virulence in plants by activating a signaling cascade that inhibits salicylic acid accumulation. *Cell Host & Microbe* 11(6): 587–596.

Zheng, X., Zhou, M., Yoo, H., Pruneda-paz, J. L., Weaver, N., Kay, S. A., Dong, X. (2015). Spatial and temporal regulation of biosynthesis of the plant immune signal salicylic acid. *Proceedings of the National Academy of Sciences of the United States of America* (112)30: 9166–9173.

Zhu, Z., An, F., Feng, Y., Li, P., Xue, L., Mu, A., Jiang, Z. and Kim, J., Lib, W., Zhanga, W., Yua, Q., Donga, Z., Chena, W. Q., Sekic, M., Zhou, J. M., Guoa, H. (2011). Derepression of ethylene-stabilized transcription factors (EIN3 / EIL1) mediates jasmonate and ethylene signaling synergy in *Arabidopsis*. *Proceedings of the National Academy of Sciences of the United States of America* 108(30): 12539–12544.

A

ATCT motif

```
>userseq19682 173nt
+ AAAAAATCTAAACTCGTTATTACATGTTGTAACCCAAA AAAATAAAAA TGAAAAACCG TCGCAAGTGA
- TTTTTTTAGA TTTGAGCAAATAATGTACAA CATTGGGTTT TTTTATTTTACTTTTTGGC AGCGTTCACT
+ TATCGACCTT TCGCCTACTT TCGCAGTCAT GTTGGTGTCT TGACAAAACC CACTGTGGAC GCATATAACC
- ATAGCTGGAA AGCGGATGAA AGCGTGAGTA CAACCACAGA ACTGTTTGG GTGACACCTG CGTATATTGG
+ ACCGGAGGAG TACAGGCCAA AATTTCTATT AT
- TGCATGCTCCGTT TTAAGATAA TA
```

Motifs Found

+ ATCT-motif					
Site Name	Organism	Position	Strand	Matrix score.	sequence function
ATCT-motif	Arabidopsis thaliana	6	+	9	AATCTAATCT part of a conserved DNA module involved in light responsiveness

+ TATA-box					
Site Name	Organism	Position	Strand	Matrix score.	sequence function
TATA-box	Glycine max	20	-	5	TAATA core promoter element around -30 of transcription start
TATA-box	Glycine max	167	-	5	TAATA core promoter element around -30 of transcription start
TATA-box	Brassica oleracea	133	+	6	ATATA core promoter element around -30 of transcription start
TATA-box	Lycopersicon esculentum	45	-	5	TTTTA core promoter element around -30 of transcription start
TATA-box	Arabidopsis thaliana	134	-	4	TATA core promoter element around -30 of transcription start

+ Unnamed_4					
Site Name	Organism	Position	Strand	Matrix score.	sequence function
Unnamed_4	Petroselinum hortense	144	-	4	CTCC
Unnamed_4	Petroselinum hortense	147	-	4	CTCC

B

ATCT motif

```
>userseq19907 167nt
+ AAAAAATCTAAACTCGTTATTACATGTTGTAACCCAAA AAAATAAAAA TGAAAAACCG TCGCAAGTGA
- TTTTTTAGATT TGAGCAAATA AAAGTTGGTT TTTTTATTAT TATTACTCTT TTTTATTTTACTTTTTGGC AGCGTTCACT
+ CTTTTTGCCT ACFTTCGCAC TCATGTTGGT GTCTCGACT AACCTACTGT GGACGCATAT ACCACCGGA
- GGAAAACCGA TGAAAGCGTG AGTACAACCA CAGAGCTGAT TTGGATGACA CCTGCGTATATTGGTGGCCT
+ TGAGTACAAGATAAGTTTC TATTAT
- ACTCATGTCC AATTTCAAGATAA
```

Motifs Found

+ AE-box					
Site Name	Organism	Position	Strand	Matrix score.	sequence function
AE-box	Arabidopsis thaliana	154	-	8	AGAAACTT part of a module for light response

+ ATCT-motif					
Site Name	Organism	Position	Strand	Matrix score.	sequence function
ATCT-motif	Arabidopsis thaliana	4	+	9	AATCTAATCT part of a conserved DNA module involved in light responsiveness

+ CCAAT-box					
Site Name	Organism	Position	Strand	Matrix score.	sequence function
CCAAT-box	Hordeum vulgare	52	-	6	CAACGG MYB1 binding site

+ GT1-motif					
Site Name	Organism	Position	Strand	Matrix score.	sequence function
GT1-motif	Arabidopsis thaliana	149	+	6	GGTTAA light responsive element

+ P-box					
Site Name	Organism	Position	Strand	Matrix score.	sequence function
P-box	Oryza sativa	71	+	7	CCTTTG gibberellin-responsive element

+ TATA-box					
Site Name	Organism	Position	Strand	Matrix score.	sequence function
TATA-box	Glycine max	36	+	5	TAATA core promoter element around -30 of transcription start
TATA-box	Glycine max	161	-	5	TAATA core promoter element around -30 of transcription start
TATA-box	Brassica oleracea	127	+	6	ATATA core promoter element around -30 of transcription start
TATA-box	Glycine max	39	+	5	TAATA core promoter element around -30 of transcription start
TATA-box	Arabidopsis thaliana	128	-	4	TATA core promoter element around -30 of transcription start

Supplementary Figure 2. The analysis of *cis*-regulatory elements of *UGT76B1* promoter region of Col-0 (A), *Ler* (B) and *Ws-4* (C).

Figure continues on the next page

C

```
>userseq20331 153nt
+ AAAAAATTAA CTCGTTTTT TCACCAAAAA ATATTATAAG GGAAACCGTG CAAGTGTATG GCCTTTGCCT
- TTTTAAATF GAGCAAAAA AGTGGTTTTT TATAATATTC CCTTTGGCAC GTTCACATAC CGGAAACGGA
+ ACTTTGCACF CATGTGGTGT TTGACTAACC TACTGTGGAC GCATATAACC ACCGGATGAG TACAAGTAA
- TGAAACGTA GTACACCACA AACTGATTGG ATGACACCTG CGTATATGG TGGCCTACTC ATGTCCAATT
AGTTTTATT AT
- TCAAAAATAA TA
```

Motifs Found

+ GT1-motif

Site Name	Organism	Position	Strand	Matrix score.	sequence	function
GT1-motif	Arabidopsis thaliana	135	+	6	GGTTAA	light responsive element

+ TATA-box

Site Name	Organism	Position	Strand	Matrix score.	sequence	function
TATA-box	Brassica napus	33	+	6	ATTATA	core promoter element around -30 of transcription start
TATA-box	Brassica oleracea	113	+	6	ATATAA	core promoter element around -30 of transcription start
TATA-box	Arabidopsis thaliana	34	-	5	TATAA	core promoter element around -30 of transcription start
TATA-box	Lycopersicon esculentum	144	+	5	TTTTA	core promoter element around -30 of transcription start
TATA-box	Glycine max	32	-	5	TAATA	core promoter element around -30 of transcription start
TATA-box	Arabidopsis thaliana	114	-	4	TATA	core promoter element around -30 of transcription start
TATA-box	Arabidopsis thaliana	35	+	4	TATA	core promoter element around -30 of transcription start
TATA-box	Glycine max	147	-	5	TAATA	core promoter element around -30 of transcription start

Supplementary Figure 2. The analysis of cis-regulatory elements of UGT76B1 promoter region of Col-0 (A), Ler (B) and Ws-4 (C).

Analysis performed by PlantCARE (<http://bioinformatics.psb.ugent.be/webtools/plantcare/html/>) (Lescot *et al.*, 2002).

		(1)	10	20	30	40	50	61	Section 1	
Col-0	(1)	ATGGGAGCTAG	GAAACAAAAC	CCAGTGATCT	TCTCTCCCTT	CCCTTCCCTT	CCCTTCCCTT	CAAGGTCAC		
Ler-0	(1)	ATGGGAGCTAG	GAAACAAAAC	CCAGTGATCT	TCTCTCCCTT	CCCTTCCCTT	CCCTTCCCTT	CAAGGTCAC		
Ler-1_MPI	(1)	ATGGGAGCTAG	GAAACAAAAC	CCAGTGATCT	TCTCTCCCTT	CCCTTCCCTT	CCCTTCCCTT	CAAGGTCAC		
Ler-1_SALK	(1)	ATGGGAGCTAG	GAAACAAAAC	CCAGTGATCT	TCTCTCCCTT	CCCTTCCCTT	CCCTTCCCTT	CAAGGTCAC		
Ws-0	(1)	ATGGGAGCTAG	GAAACAAAAC	CCAGTGATCT	TCTCTCCCTT	CCCTTCCCTT	CCCTTCCCTT	CAAGGTCAC		
Ws-2	(1)	ATGGGAGCTAG	GAAACAAAAC	CCAGTGATCT	TCTCTCCCTT	CCCTTCCCTT	CCCTTCCCTT	CAAGGTCAC		
		(62)	70	80	90	100	110	122	Section 2	
Col-0	(62)	TAAACCCAAT	GTTTCAGCT	CGCCAAAC	ATCTTCTT	CAACAGAGG	CTTCCAT	CACTGTGAT		
Ler-0	(62)	TAAACCCAAT	GTTTCAGCT	CGCCAAAC	ATCTTCTT	CAACAGAGG	CTTCCAT	CACTGTGAT		
Ler-1_MPI	(62)	TAAACCCAAT	GTTTCAGCT	CGCCAAAC	ATCTTCTT	CAACAGAGG	CTTCCAT	CACTGTGAT		
Ler-1_SALK	(62)	TAAACCCAAT	GTTTCAGCT	CGCCAAAC	ATCTTCTT	CAACAGAGG	CTTCCAT	CACTGTGAT		
Ws-0	(62)	TAAACCCAAT	GTTTCAGCT	CGCCAAAC	ATCTTCTT	CAACAGAGG	CTTCCAT	CACTGTGAT		
Ws-2	(62)	TAAACCCAAT	GTTTCAGCT	CGCCAAAC	ATCTTCTT	CAACAGAGG	CTTCCAT	CACTGTGAT		
		(123)	130	140	150	160	170	183	Section 3	
Col-0	(123)	CCACACT	AGTTCAACT	CTCCAACT	CTTCCAAT	TTCCCTCA	TTCA	TTTCGTATCCAT		
Ler-0	(123)	CCACACT	AGTTCAACT	CTCCAACT	CTTCCAAT	TTCCCTCA	TTCA	TTTCGTATCCAT		
Ler-1_MPI	(123)	CCACACT	AGTTCAACT	CTCCAACT	CTTCCAAT	TTCCCTCA	TTCA	TTTCGTATCCAT		
Ler-1_SALK	(123)	CCACACT	AGTTCAACT	CTCCAACT	CTTCCAAT	TTCCCTCA	TTCA	TTTCGTATCCAT		
Ws-0	(123)	CCACACT	AGTTCAACT	CTCCAACT	CTTCCAAT	TTCCCTCA	TTCA	TTTCGTATCCAT		
Ws-2	(123)	CCACACT	AGTTCAACT	CTCCAACT	CTTCCAAT	TTCCCTCA	TTCA	TTTCGTATCCAT		
		(184)	190	200	210	220	230	244	Section 4	
Col-0	(184)	CCCGAT	GCTGTCT	GAACTGA	ACTCCGAT	GTGCAT	GAGATT	CTCCATGACCTCA		
Ler-0	(184)	CCCGAT	GCTGTCT	GAACTGA	ACTCCGAT	GTGCAT	GAGATT	CTCCATGACCTCA		
Ler-1_MPI	(184)	CCCGAT	GCTGTCT	GAACTGA	ACTCCGAT	GTGCAT	GAGATT	CTCCATGACCTCA		
Ler-1_SALK	(184)	CCCGAT	GCTGTCT	GAACTGA	ACTCCGAT	GTGCAT	GAGATT	CTCCATGACCTCA		
Ws-0	(184)	CCCGAT	GCTGTCT	GAACTGA	ACTCCGAT	GTGCAT	GAGATT	CTCCATGACCTCA		
Ws-2	(184)	CCCGAT	GCTGTCT	GAACTGA	ACTCCGAT	GTGCAT	GAGATT	CTCCATGACCTCA		
		(245)	250	260	270	280	290	305	Section 5	
Col-0	(245)	ATTTCAAAGT	GTGGTCT	CCTTTGGT	GATTGCTT	AAAGAA	AGCTTAT	ATCTGAAGAACCAAC		
Ler-0	(245)	ATTTCAAAGT	GTGGTCT	CCTTTGGT	GATTGCTT	AAAGAA	AGCTTAT	ATCTGAAGAACCAAC		
Ler-1_MPI	(245)	ATTTCAAAGT	GTGGTCT	CCTTTGGT	GATTGCTT	AAAGAA	AGCTTAT	ATCTGAAGAACCAAC		
Ler-1_SALK	(245)	ATTTCAAAGT	GTGGTCT	CCTTTGGT	GATTGCTT	AAAGAA	AGCTTAT	ATCTGAAGAACCAAC		
Ws-0	(245)	ATTTCAAAGT	GTGGTCT	CCTTTGGT	GATTGCTT	AAAGAA	AGCTTAT	ATCTGAAGAACCAAC		
Ws-2	(245)	ATTTCAAAGT	GTGGTCT	CCTTTGGT	GATTGCTT	AAAGAA	AGCTTAT	ATCTGAAGAACCAAC		
		(306)	320	330	340	350	366	Section 6		
Col-0	(306)	AGCAGCTT	GTGTGATT	GTGACGCT	CTTTGGT	ACTTCACT	CACGATT	TAACCGAGAAATTC		
Ler-0	(306)	AGCAGCTT	GTGTGATT	GTGACGCT	CTTTGGT	ACTTCACT	CACGATT	TAACCGAGAAATTC		
Ler-1_MPI	(306)	AGCAGCTT	GTGTGATT	GTGACGCT	CTTTGGT	ACTTCACT	CACGATT	TAACCGAGAAATTC		
Ler-1_SALK	(306)	AGCAGCTT	GTGTGATT	GTGACGCT	CTTTGGT	ACTTCACT	CACGATT	TAACCGAGAAATTC		
Ws-0	(306)	AGCAGCTT	GTGTGATT	GTGACGCT	CTTTGGT	ACTTCACT	CACGATT	TAACCGAGAAATTC		
Ws-2	(306)	AGCAGCTT	GTGTGATT	GTGACGCT	CTTTGGT	ACTTCACT	CACGATT	TAACCGAGAAATTC		
		(367)	380	390	400	410	427	Section 7		
Col-0	(367)	AATTTCCCGAGG	ATTGTTCT	CCGAAC	CCGTTAA	CTCAGCTT	TCGTCGCTT	CTCAAAGT		
Ler-0	(367)	AATTTCCCGAGG	ATTGTTCT	CCGAAC	CCGTTAA	CTCAGCTT	TCGTCGCTT	CTCAAAGT		
Ler-1_MPI	(367)	AATTTCCCGAGG	ATTGTTCT	CCGAAC	CCGTTAA	CTCAGCTT	TCGTCGCTT	CTCAAAGT		
Ler-1_SALK	(367)	AATTTCCCGAGG	ATTGTTCT	CCGAAC	CCGTTAA	CTCAGCTT	TCGTCGCTT	CTCAAAGT		
Ws-0	(367)	AATTTCCCGAGG	ATTGTTCT	CCGAAC	CCGTTAA	CTCAGCTT	TCGTCGCTT	CTCAAAGT		
Ws-2	(367)	AATTTCCCGAGG	ATTGTTCT	CCGAAC	CCGTTAA	CTCAGCTT	TCGTCGCTT	CTCAAAGT		
		(428)	438	440	450	460	470	488	Section 8	
Col-0	(428)	TTTCATGTTT	TACGAGAG	AAAGGGT	ATCTTCTT	TACAAGGT	ACACTTT	TGTGACTTTTAT		
Ler-0	(428)	TTTCATGTTT	TACGAGAG	AAAGGGT	ATCTTCTT	TACAAGGT	ACACTTT	TGTGACTTTTAT		
Ler-1_MPI	(428)	TTTCATGTTT	TACGAGAG	AAAGGGT	ATCTTCTT	TACAAGGT	ACACTTT	TGTGACTTTTAT		
Ler-1_SALK	(428)	TTTCATGTTT	TACGAGAG	AAAGGGT	ATCTTCTT	TACAAGGT	ACACTTT	TGTGACTTTTAT		
Ws-0	(428)	TTTCATGTTT	TACGAGAG	AAAGGGT	ATCTTCTT	TACAAGGT	ACACTTT	TGTGACTTTTAT		
Ws-2	(428)	TTTCATGTTT	TACGAGAG	AAAGGGT	ATCTTCTT	TACAAGGT	ACACTTT	TGTGACTTTTAT		
		(489)	499	500	510	520	530	549	Section 9	
Col-0	(489)	ATATCTAGTT	TGCTTCACT	TTTGTGACT	TTTTCT	TGCTTCT	CTCCAT	TGGCAGAGACT		
Ler-0	(489)	ATATCTAGTT	TGCTTCACT	TTTGTGACT	TTTTCT	TGCTTCT	CTCCAT	TGGCAGAGACT		
Ler-1_MPI	(489)	ATATCTAGTT	TGCTTCACT	TTTGTGACT	TTTTCT	TGCTTCT	CTCCAT	TGGCAGAGACT		
Ler-1_SALK	(489)	ATATCTAGTT	TGCTTCACT	TTTGTGACT	TTTTCT	TGCTTCT	CTCCAT	TGGCAGAGACT		
Ws-0	(489)	ATATCTAGTT	TGCTTCACT	TTTGTGACT	TTTTCT	TGCTTCT	CTCCAT	TGGCAGAGACT		
Ws-2	(489)	ATATCTAGTT	TGCTTCACT	TTTGTGACT	TTTTCT	TGCTTCT	CTCCAT	TGGCAGAGACT		
		(550)	550	560	570	580	590	610	Section 10	
Col-0	(550)	AAGGCAGACT	CACCGGT	TCCGGAGCT	TCCGAT	CTTTAGAAT	GAAGGAT	CTTCCATGGTTCC		
Ler-0	(550)	AAGGCAGACT	CACCGGT	TCCGGAGCT	TCCGAT	CTTTAGAAT	GAAGGAT	CTTCCATGGTTCC		
Ler-1_MPI	(550)	AAGGCAGACT	CACCGGT	TCCGGAGCT	TCCGAT	CTTTAGAAT	GAAGGAT	CTTCCATGGTTCC		
Ler-1_SALK	(550)	AAGGCAGACT	CACCGGT	TCCGGAGCT	TCCGAT	CTTTAGAAT	GAAGGAT	CTTCCATGGTTCC		
Ws-0	(550)	AAGGCAGACT	CACCGGT	TCCGGAGCT	TCCGAT	CTTTAGAAT	GAAGGAT	CTTCCATGGTTCC		
Ws-2	(550)	AAGGCAGACT	CACCGGT	TCCGGAGCT	TCCGAT	CTTTAGAAT	GAAGGAT	CTTCCATGGTTCC		
		(611)	611	620	630	640	650	660	671	Section 11
Col-0	(611)	AGACAGAAGT	CCAAGAT	CAGGGGTA	AGTTAC	AGATAGGT	GTGATGAAGT	CACTAAAGTC		
Ler-0	(611)	AGACAGAAGT	CCAAGAT	CAGGGGTA	AGTTAC	AGATAGGT	GTGATGAAGT	CACTAAAGTC		
Ler-1_MPI	(611)	AGACAGAAGT	CCAAGAT	CAGGGGTA	AGTTAC	AGATAGGT	GTGATGAAGT	CACTAAAGTC		
Ler-1_SALK	(611)	AGACAGAAGT	CCAAGAT	CAGGGGTA	AGTTAC	AGATAGGT	GTGATGAAGT	CACTAAAGTC		
Ws-0	(611)	AGACAGAAGT	CCAAGAT	CAGGGGTA	AGTTAC	AGATAGGT	GTGATGAAGT	CACTAAAGTC		
Ws-2	(611)	AGACAGAAGT	CCAAGAT	CAGGGGTA	AGTTAC	AGATAGGT	GTGATGAAGT	CACTAAAGTC		
		(672)	672	680	690	700	710	720	732	Section 12
Col-0	(672)	TTCTCAGGAAT	CATATTT	CAACGCC	ATTGAAGT	CTTTGAA	ACAGAT	CAGCTT	TGATGAAGCC	
Ler-0	(672)	TTCTCAGGAAT	CATATTT	CAACGCC	ATTGAAGT	CTTTGAA	ACAGAT	CAGCTT	TGATGAAGCC	
Ler-1_MPI	(672)	TTCTCAGGAAT	CATATTT	CAACGCC	ATTGAAGT	CTTTGAA	ACAGAT	CAGCTT	TGATGAAGCC	
Ler-1_SALK	(672)	TTCTCAGGAAT	CATATTT	CAACGCC	ATTGAAGT	CTTTGAA	ACAGAT	CAGCTT	TGATGAAGCC	
Ws-0	(672)	TTCTCAGGAAT	CATATTT	CAACGCC	ATTGAAGT	CTTTGAA	ACAGAT	CAGCTT	TGATGAAGCC	
Ws-2	(672)	TTCTCAGGAAT	CATATTT	CAACGCC	ATTGAAGT	CTTTGAA	ACAGAT	CAGCTT	TGATGAAGCC	
		(733)	733	740	750	760	770	780	793	Section 13
Col-0	(733)	GGCATA	GAAATCCC	AGTCCACT	CTTCTGT	TATGGAC	CCCTTTC	CACAGGT	ACGTTTCAGCTT	
Ler-0	(733)	GGCATA	GAAATCCC	AGTCCACT	CTTCTGT	TATGGAC	CCCTTTC	CACAGGT	ACGTTTCAGCTT	
Ler-1_MPI	(733)	GGCATA	GAAATCCC	AGTCCACT	CTTCTGT	TATGGAC	CCCTTTC	CACAGGT	ACGTTTCAGCTT	
Ler-1_SALK	(733)	GGCATA	GAAATCCC	AGTCCACT	CTTCTGT	TATGGAC	CCCTTTC	CACAGGT	ACGTTTCAGCTT	
Ws-0	(733)	GGCATA	GAAATCCC	AGTCCACT	CTTCTGT	TATGGAC	CCCTTTC	CACAGGT	ACGTTTCAGCTT	
Ws-2	(733)	GGCATA	GAAATCCC	AGTCCACT	CTTCTGT	TATGGAC	CCCTTTC	CACAGGT	ACGTTTCAGCTT	
		(794)	794	800	810	820	830	840	854	Section 14
Col-0	(794)	CATCCAGT	AGCTTACT	TGCAC	CAGCAT	GACTTGT	CTCTC	CTGGTT	TAGACAAGCAAGCAAC	
Ler-0	(794)	CATCCAGT	AGCTTACT	TGCAC	CAGCAT	GACTTGT	CTCTC	CTGGTT	TAGACAAGCAAGCAAC	
Ler-1_MPI	(794)	CATCCAGT	AGCTTACT	TGCAC	CAGCAT	GACTTGT	CTCTC	CTGGTT	TAGACAAGCAAGCAAC	
Ler-1_SALK	(794)	CATCCAGT	AGCTTACT	TGCAC	CAGCAT	GACTTGT	CTCTC	CTGGTT	TAGACAAGCAAGCAAC	
Ws-0	(794)	CATCCAGT	AGCTTACT	TGCAC	CAGCAT	GACTTGT	CTCTC	CTGGTT	TAGACAAGCAAGCAAC	
Ws-2	(794)	CATCCAGT	AGCTTACT	TGCAC	CAGCAT	GACTTGT	CTCTC	CTGGTT	TAGACAAGCAAGCAAC	
		(855)	855	860	870	880	890	900	916	Section 15
Col-0	(855)	AAATTC	CGTAAT	CTAC	CGCAAGT	CTTGG	AAGCAT	TGCT	TCGATCGATGAATCTGAAATCTTTG	
Ler-0	(855)	AAATTC	CGTAAT	CTAC	CGCAAGT	CTTGG	AAGCAT	TGCT	TCGATCGATGAATCTGAAATCTTTG	
Ler-1_MPI	(855)	AAATTC	CGTAAT	CTAC	CGCAAGT	CTTGG	AAGCAT	TGCT	TCGATCGATGAATCTGAAATCTTTG	
Ler-1_SALK	(855)	AAATTC	CGTAAT	CTAC	CGCAAGT	CTTGG	AAGCAT	TGCT	TCGATCGATGAATCTGAAATCTTTG	
Ws-0	(855)	AAATTC	CGTAAT	CTAC	CGCAAGT	CTTGG	AAGCAT	TGCT	TCGATCGATGAATCTGAAATCTTTG	
Ws-2	(855)	AAATTC	CGTAAT	CTAC	CGCAAGT	CTTGG	AAGCAT	TGCT	TCGATCGATGAATCTGAAATCTTTG	

Supplementary Figure 3. Alignment of the coding sequence of *UGT76B1* in Col-0, Ws-4 and Ler accession.

Figure continues on the next page.

		Section 16				
	(916)	916	930	940	950	960
Col-0	(916)	GAGATTGCTTGGGGTCTAAGAAACAGCAACCAACCTTTCTATGGTGGTTAGACCCGGTT				
Ler-0	(916)	GAGATTGCTTGGGGTCTAAGAAACAGCAACCAACCTTTCTATGGTGGTTAGACCCGGTT				
Ler-1_MPI	(916)	GAGATTGCTTGGGGTCTAAGAAACAGCAACCAACCTTTCTATGGTGGTTAGACCCGGTT				
Ler-1_SALK	(916)	GAGATTGCTTGGGGTCTAAGAAACAGCAACCAACCTTTCTATGGTGGTTAGACCCGGTT				
Ws-0	(916)	GAGATTGCTTGGGGTCTAAGAAACAGCAACCAACCTTTCTATGGTGGTTAGACCCGGTT				
Ws-2	(916)	GAGATTGCTTGGGGTCTAAGAAACAGCAACCAACCTTTCTATGGTGGTTAGACCCGGTT				
		Section 17				
	(977)	977	990	1000	1010	1020
Col-0	(977)	TAATCCACGGGAAAGAAATGGATCGAGATTCTGCCTAAGGGTTCATCGAAAATCTCGAGGG				
Ler-0	(977)	TAATCCACGGGAAAGAAATGGATCGAGATTCTGCCTAAGGGTTCATCGAAAATCTCGAGGG				
Ler-1_MPI	(977)	TAATCCACGGGAAAGAAATGGATCGAGATTCTGCCTAAGGGTTCATCGAAAATCTCGAGGG				
Ler-1_SALK	(977)	TAATCCACGGGAAAGAAATGGATCGAGATTCTGCCTAAGGGTTCATCGAAAATCTCGAGGG				
Ws-0	(977)	TAATCCACGGGAAAGAAATGGATCGAGATTCTGCCTAAGGGTTCATCGAAAATCTCGAGGG				
Ws-2	(977)	TAATCCACGGGAAAGAAATGGATCGAGATTCTGCCTAAGGGTTCATCGAAAATCTCGAGGG				
		Section 18				
	(1038)	1038	1050	1060	1070	1080
Col-0	(1038)	CCGGGTAAAAATAGTGAAATGGGCACCTCAGCCTGAAGTTTATAGCTCACCGTGCAACAGGC				
Ler-0	(1038)	CCGGGTAAAAATAGTGAAATGGGCACCTCAGCCTGAAGTTTATAGCTCACCGTGCAACAGGC				
Ler-1_MPI	(1038)	CCGGGTAAAAATAGTGAAATGGGCACCTCAGCCTGAAGTTTATAGCTCACCGTGCAACAGGC				
Ler-1_SALK	(1038)	CCGGGTAAAAATAGTGAAATGGGCACCTCAGCCTGAAGTTTATAGCTCACCGTGCAACAGGC				
Ws-0	(1038)	CCGGGTAAAAATAGTGAAATGGGCACCTCAGCCTGAAGTTTATAGCTCACCGTGCAACAGGC				
Ws-2	(1038)	CCGGGTAAAAATAGTGAAATGGGCACCTCAGCCTGAAGTTTATAGCTCACCGTGCAACAGGC				
		Section 19				
	(1099)	1099	1110	1120	1130	1140
Col-0	(1099)	GGATTCTTAACACATTGTGGATGGAACCTCAACACTTGAGGGCATATGTGAAGCTATACCAA				
Ler-0	(1099)	GGATTCTTAACACATTGTGGATGGAACCTCAACACTTGAGGGCATATGTGAAGCTATACCAA				
Ler-1_MPI	(1099)	GGATTCTTAACACATTGTGGATGGAACCTCAACACTTGAGGGCATATGTGAAGCTATACCAA				
Ler-1_SALK	(1099)	GGATTCTTAACACATTGTGGATGGAACCTCAACACTTGAGGGCATATGTGAAGCTATACCAA				
Ws-0	(1099)	GGATTCTTAACACATTGTGGATGGAACCTCAACACTTGAGGGCATATGTGAAGCTATACCAA				
Ws-2	(1099)	GGATTCTTAACACATTGTGGATGGAACCTCAACACTTGAGGGCATATGTGAAGCTATACCAA				
		Section 20				
	(1160)	1160	1170	1180	1190	1200
Col-0	(1160)	TGATATGCAGACCATTCTTTGGGGACCAGAGGGTGAATGCTAGATACATTAAACGATGTTTG				
Ler-0	(1160)	TGATATGCAGACCATTCTTTGGGGACCAGAGGGTGAATGCTAGATACATTAAACGATGTTTG				
Ler-1_MPI	(1160)	TGATATGCAGACCATTCTTTGGGGACCAGAGGGTGAATGCTAGATACATTAAACGATGTTTG				
Ler-1_SALK	(1160)	TGATATGCAGACCATTCTTTGGGGACCAGAGGGTGAATGCTAGATACATTAAACGATGTTTG				
Ws-0	(1160)	TGATATGCAGACCATTCTTTGGGGACCAGAGGGTGAATGCTAGATACATTAAACGATGTTTG				
Ws-2	(1160)	TGATATGCAGACCATTCTTTGGGGACCAGAGGGTGAATGCTAGATACATTAAACGATGTTTG				
		Section 21				
	(1221)	1221	1230	1240	1250	1260
Col-0	(1221)	GAAGATCGGATTGCATTTGGAAAACAAGGTAGAGAGACTAGTGATCGAAAACGCGGTTAGA				
Ler-0	(1221)	GAAGATCGGATTGCATTTGGAAAACAAGGTAGAGAGACTAGTGATCGAAAACGCGGTTAGA				
Ler-1_MPI	(1221)	GAAGATCGGATTGCATTTGGAAAACAAGGTAGAGAGACTAGTGATCGAAAACGCGGTTAGA				
Ler-1_SALK	(1221)	GAAGATCGGATTGCATTTGGAAAACAAGGTAGAGAGACTAGTGATCGAAAACGCGGTTAGA				
Ws-0	(1221)	GAAGATCGGATTGCATTTGGAAAACAAGGTAGAGAGACTAGTGATCGAAAACGCGGTTAGA				
Ws-2	(1221)	GAAGATCGGATTGCATTTGGAAAACAAGGTAGAGAGACTAGTGATCGAAAACGCGGTTAGA				
		Section 22				
	(1282)	1282	1290	1300	1310	1320
Col-0	(1282)	ACACTAATGACGAGCTCGGAAGGGGAAAGAGATCCGCAAGAGGATTATGCCCATGAAGGAAA				
Ler-0	(1282)	ACACTAATGACGAGCTCGGAAGGGGAAAGAGATCCGCAAGAGGATTATGCCCATGAAGGAAA				
Ler-1_MPI	(1282)	ACACTAATGACGAGCTCGGAAGGGGAAAGAGATCCGCAAGAGGATTATGCCCATGAAGGAAA				
Ler-1_SALK	(1282)	ACACTAATGACGAGCTCGGAAGGGGAAAGAGATCCGCAAGAGGATTATGCCCATGAAGGAAA				
Ws-0	(1282)	ACACTAATGACGAGCTCGGAAGGGGAAAGAGATCCGCAAGAGGATTATGCCCATGAAGGAAA				
Ws-2	(1282)	ACACTAATGACGAGCTCGGAAGGGGAAAGAGATCCGCAAGAGGATTATGCCCATGAAGGAAA				
		Section 23				
	(1343)	1343	1350	1360	1370	1380
Col-0	(1343)	CTGTTGAACAATGCCTTAAGCTTGGAGGTTTCATCATTTCCGGAATCTCGAAAACCTTAATTGC				
Ler-0	(1343)	CTGTTGAACAATGCCTTAAGCTTGGAGGTTTCATCATTTCCGGAATCTCGAAAACCTTAATTGC				
Ler-1_MPI	(1343)	CTGTTGAACAATGCCTTAAGCTTGGAGGTTTCATCATTTCCGGAATCTCGAAAACCTTAATTGC				
Ler-1_SALK	(1343)	CTGTTGAACAATGCCTTAAGCTTGGAGGTTTCATCATTTCCGGAATCTCGAAAACCTTAATTGC				
Ws-0	(1343)	CTGTTGAACAATGCCTTAAGCTTGGAGGTTTCATCATTTCCGGAATCTCGAAAACCTTAATTGC				
Ws-2	(1343)	CTGTTGAACAATGCCTTAAGCTTGGAGGTTTCATCATTTCCGGAATCTCGAAAACCTTAATTGC				
		Section 24				
	(1404)	1404	1410	1422		
Col-0	(1404)	TTATATATTGTCTTTCTAA				
Ler-0	(1404)	TTATATATTGTCTTTCTAA				
Ler-1_MPI	(1404)	TTATATATTGTCTTTCTAA				
Ler-1_SALK	(1404)	TTATATATTGTCTTTCTAA				
Ws-0	(1404)	TTATATATTGTCTTTCTAA				
Ws-2	(1404)	TTATATATTGTCTTTCTAA				

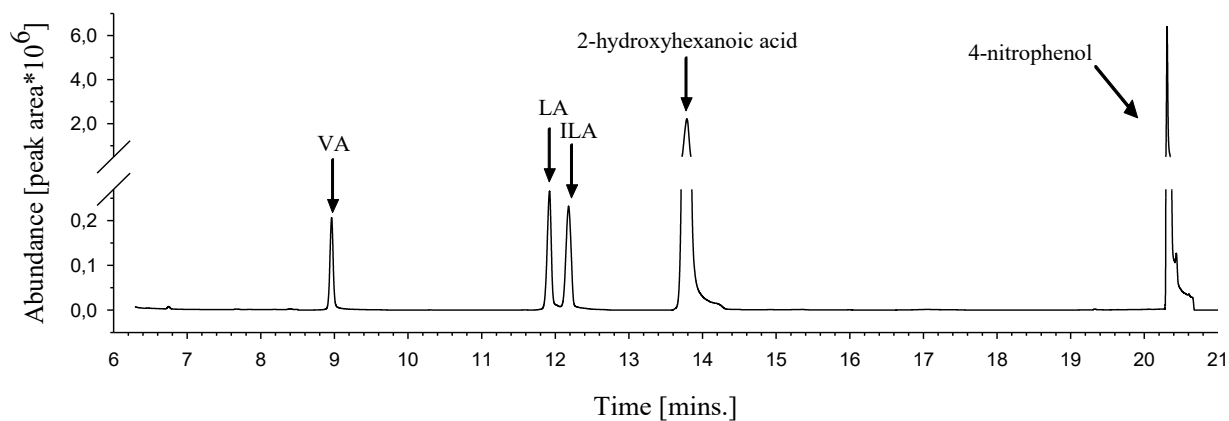
Supplementary Figure 3. Alignment of the coding sequence of *UGT76B1* in Col-0, Ws-4 and Ler accession.

Sequences derived from: <http://1001genomes.org> (02/2016)

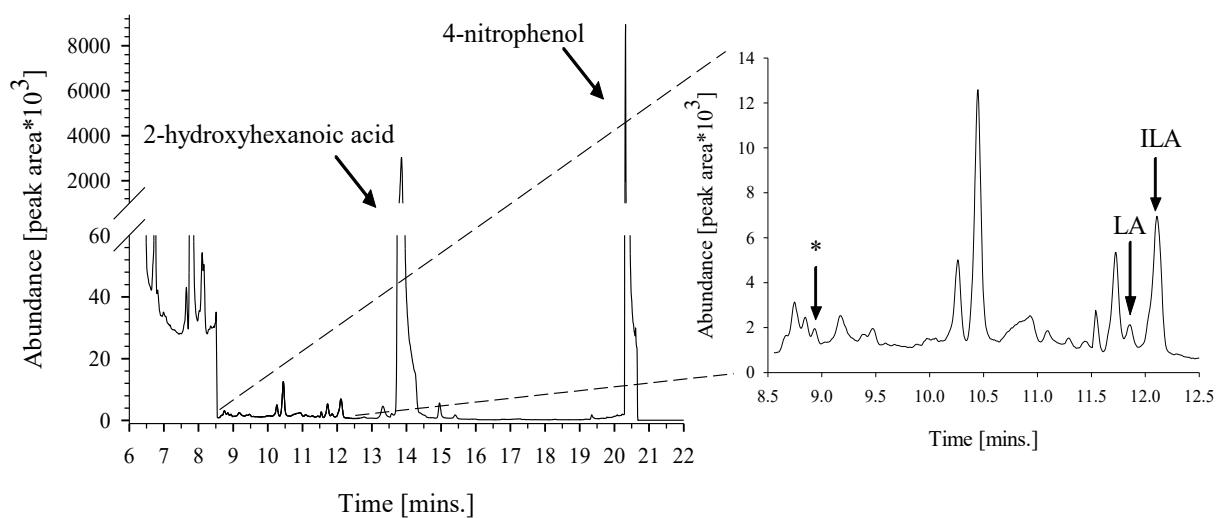
Col-0	(3854)	TCAGAAAGTTGAAAACAAGTACGGCCCTATATCTTGCACCCTACGAAATCACTCTTATGTAGTGCATTGCAAAATGTGCCACGCATGAAAATATATGG	
76b1-WS-F02	(*688)	4001	4100
Col-0	(3954)	GACGGGAAGAACTCGAATGGGAACCTGAGGAACCCGAAAACATTGAAGATATCCTCCATTTAAGAAGGTTGGTACTGATATGATAAAGTATTTCTCCG	
76b1-WS-F02	(*688)	4101	4200
Col-0	(4054)	ATGAACATAATCTGAAGCTCGAAGATGATGCTGTTCTGTGATGCAGAGAAGCTATGTCAAGCATCGCTCTGTCTCAACTCTCGTATTCTACAA	
76b1-WS-F02	(*688)	4201	4300
Col-0	(4154)	TTGCATCCACTGTGATTTTTTCTCCACGAGGTATGTGCTGGTCTTCTTCGAAAATGGATCATGGTGTGCACAAACACACTCTTATCTAGACCCATAT	
76b1-WS-F02	(*688)	4301	4400
Col-0	(4254)	CCTCGAGACAGTTATTATCTCTTGGACTGCCATTTGTCCAGAGGATCCACTGGTTTCAGGTACATATGTTCCATAAGTAATGTAATCCCATCGAA	
76b1-WS-F02	(*688)	4401	4500
Col-0	(4354)	TTGGCATAGATATTCGATGATTTTAGTCCAGATCAITTCCTCAGGAGTATGAACATCCTCTATTTATCTCCACATCCTTCAAAGCAGAAATTCG	
76b1-WS-F02	(*688)	4501	4600
Col-0	(4454)	TTGCCAGGGTTGTGAGAAAGGTGATGAGTCTTACCTGCAGTGTACTATATGCATATTTATCATGTGTTATAAATGGCTACAAATCCAACGGGAGTT	
76b1-WS-F02	(*688)	4601	4700
Col-0	(4554)	AGCTACAAACACGACAAGCATCCTCTTCTCTATGCTATGGAGAGAAAGCAGATGATACGTACTGGTGTGAACATGTGAGAAAAGGTTAATCCAAAGGA	
76b1-WS-F02	(*688)	4701	4800
Col-0	(4654)	ATTGGTCTCACACATGAACATATGTTGTATCACTATCCACTTCATGTCATCTTCGGATCTTCTAGTTATATGAAGCTGGTCCATATTTGATACAA	
76b1-WS-F02	(*688)	4801	4900
Col-0	(4754)	CTATTCCAAATGGAAATCTTCGCAACAGTAACAGCATCGACCCGAATGCACCCGATGGTGTGATCGTGTCCAGTTACATCTACTTCAAACGCAAA	
76b1-WS-F02	(*688)	4901	5000
Col-0	(4854)	CGCGATAAACACCCTGTAACGTTTTCTGCTCTGTGCAATGTTTAGAGGGAGGATGATGGTGTGTAGACATAATGAACTTCTTTGTGTTTATTAAGT	
76b1-WS-F02	(*688)	5001	5100
Col-0	(4954)	TGTTTGTGTTATATCTTTGTGTGTGTGCTTTTTTCAAAGAAATCCGAAACTTGTATCGCCACCCTTAAAGAATGAAATATCTTTGATTTGAT	
76b1-WS-F02	(*688)	5101	5200
Col-0	(5054)	GATTTATCCATCCCTTTTTTTCATTGATATAATTTCTTAAGCCCAAAAAGTGAACAGCTTGACACGTTAARAAGAAAACGAACGCCTGACTCACATA	
76b1-WS-F02	(*688)	5201	5300
Col-0	(5154)	AACAAACCATCTTCTTAACGTAAAGCGCTTAAGAAAACCGAGACCCGATGCACACATATACTTACCCTACTTAGCTCTTTGTAAGTGTGACGA	
76b1-WS-F02	(*688)	5301	5400
Col-0	(5254)	TGTCAAAGGAGCAGAAAGCTATATATGGAGACTTGGATCAATCAGAAGGATAGATGGTGTGATGCTGAAATGCGGGTTTGTCTAATCTCTGTATTTCG	
76b1-WS-F02	(*688)	5401	5500
Col-0	(5354)	GAGAAAGGTGATGAAATGAAGATGAGGGAGTGTGAATCAAGTAGGGAGAAGCTCAAGCAGATGGAGACCACCAAGATTGAGCTGGCGCTTGCT	
76b1-WS-F02	(*688)	5501	5600
Col-0	(5454)	CGTGCCTCTGATGAGTGTATGGCTTAATCTTGTACTGCTCAATCACTTAATAATTTATTTATTTTGGTTTATGGGGTTGGAATTTTTTTAGGGGG	
76b1-WS-F02	(*688)	5601	5700
Col-0	(5554)	TATTTTGTGTTTAAATCTTACAGTAGTCTTAGTTTTAAAAGCTTACTTAGSAGAAAGCACTCATGCAGAGCAGCTTTATCTCCGATCAAACCGGGTTG	
76b1-WS-F02	(*688)	5701	5800
Col-0	(5654)	GACTTGCATAAATGTTTTTTCATATAAACAACACCAAAATTTTATGATATATCATTGCATATATATTTATGATAAAAAATCAACATTATATATACTTTT	
76b1-WS-F02	(*688)	5801	5900
Col-0	(5754)	TATGTACCCTCTCATATAATAGTATAAAAATAATGATATTAATAATAAAAAAATTAACAATAAATTTGTTTTTCCGGCATTACAGCTAAATA	
76b1-WS-F02	(*688)	5901	6000
Col-0	(5854)	TATTTAAATTTTCAAAGTATAATTAATTTGAAAATTTCTATACAAGAATTCATTTTTAATTAGGGCTAAACCCCTTACCAGAGGTAGCCATATAAAT	
76b1-WS-F02	(*688)	6001	6100
Col-0	(5954)	CGGAATGGGTGAATGCAACTTAAGCCGATTATCTTTATTTTTTTTATTTTTTTTATTTTTTTTCTCAATGCTGGAGGATTAATATCATCATATAAATC	
76b1-WS-F02	(*688)	6101	6200
76b1-WS-F05	(1)		
Col-0	(6054)	ATCTTTTTAGAAAGAAAAAATCATCAGAGGTTTAACTATCATCATCGGACATGAGCATGAGGCATAATCTTACGGACAGCAAGCGAATCCTC	
76b1-WS-F02	(*688)		
76b1-WS-F02	(6101)		
76b1-WS-F05	(49)	6201	6300
Col-0	(6154)	GGTTACAGTAACAGGCTCGATTTTTCTGCTCTACACCAACGTAACAATCTGCTCCGGCGACGAACAAACTCTGAGAGTGGATCGAAGCGGCT	
76b1-WS-F02	(*688)		
76b1-WS-F02	(6201)		
76b1-WS-F05	(149)	6301	6373
Col-0	(6254)	CACATCAGAAAACAGAAATCACACGGTCTTGAGCAATGGCTACAGCAACAAACCAACAGGGGAAGCAATA	
76b1-WS-F02	(*688)		

Supplementary Figure 4. Alignment of the 3'-UTR region of *UGT76B1* in Col-0, Ws-4.

Ws-4 and *Ler* demonstrated identical sequence of the 3'-UTR region. Col-0 template sequence derived from: <http://1001genomes.org> (02/2016).

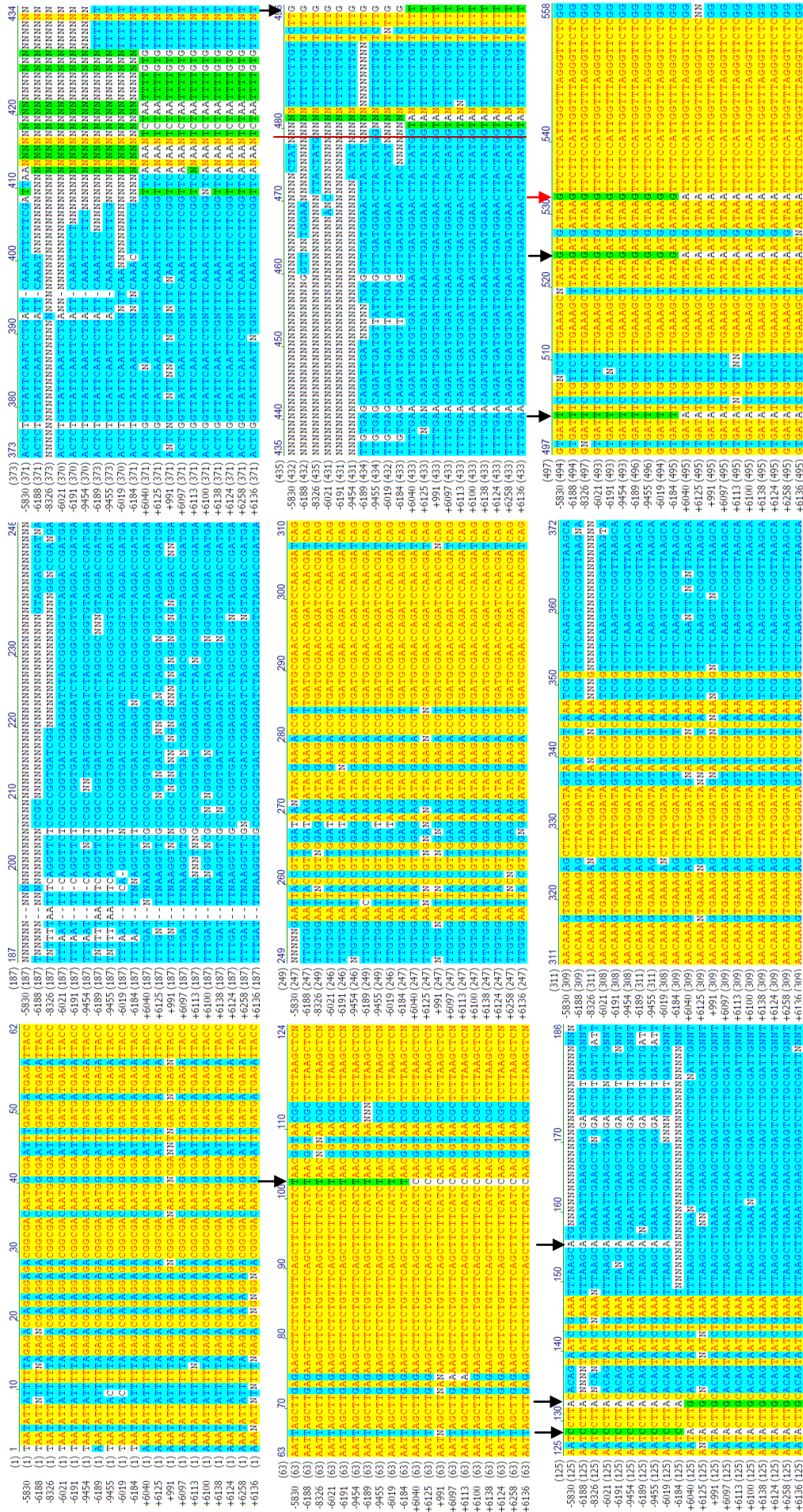


Supplementary Figure 6. SIM chromatogram of VA, LA, ILA, 2-hydroxyhexanoic acid and 4-nitrophenol standards.



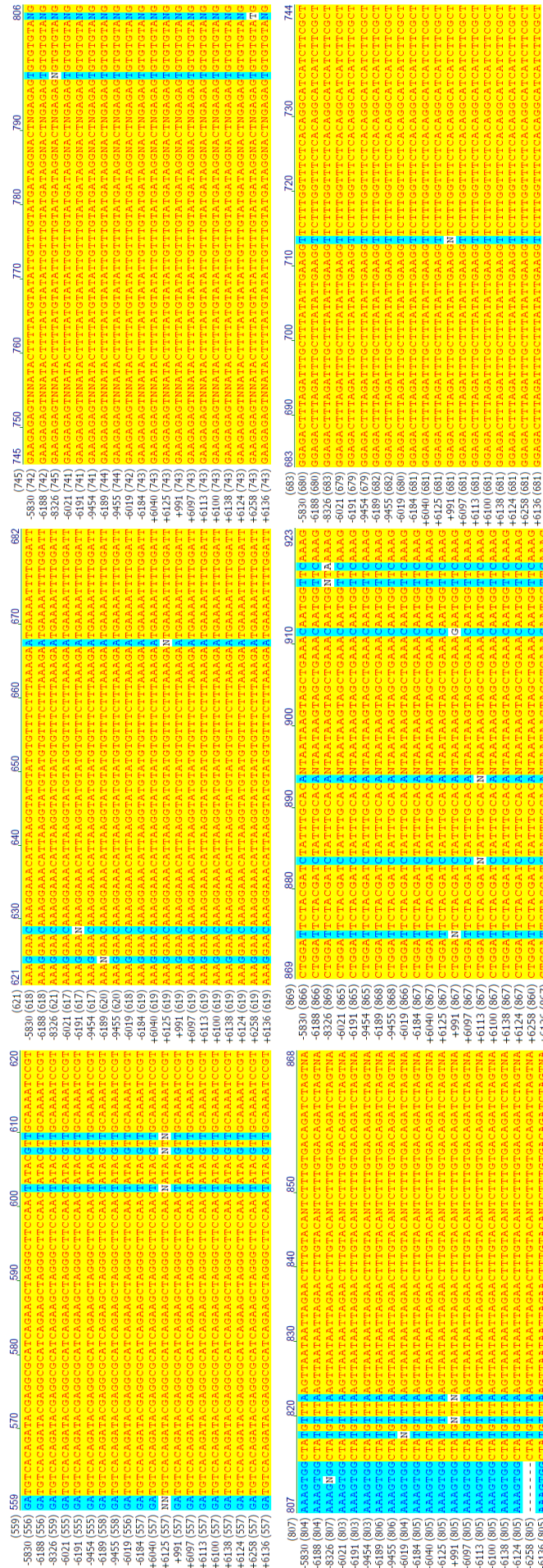
Supplementary Figure 7. SIM chromatogram of LA and ILA in two-week-old *A. thaliana*.

(*) indicates position on the chromatogram where the VA peak should appear.



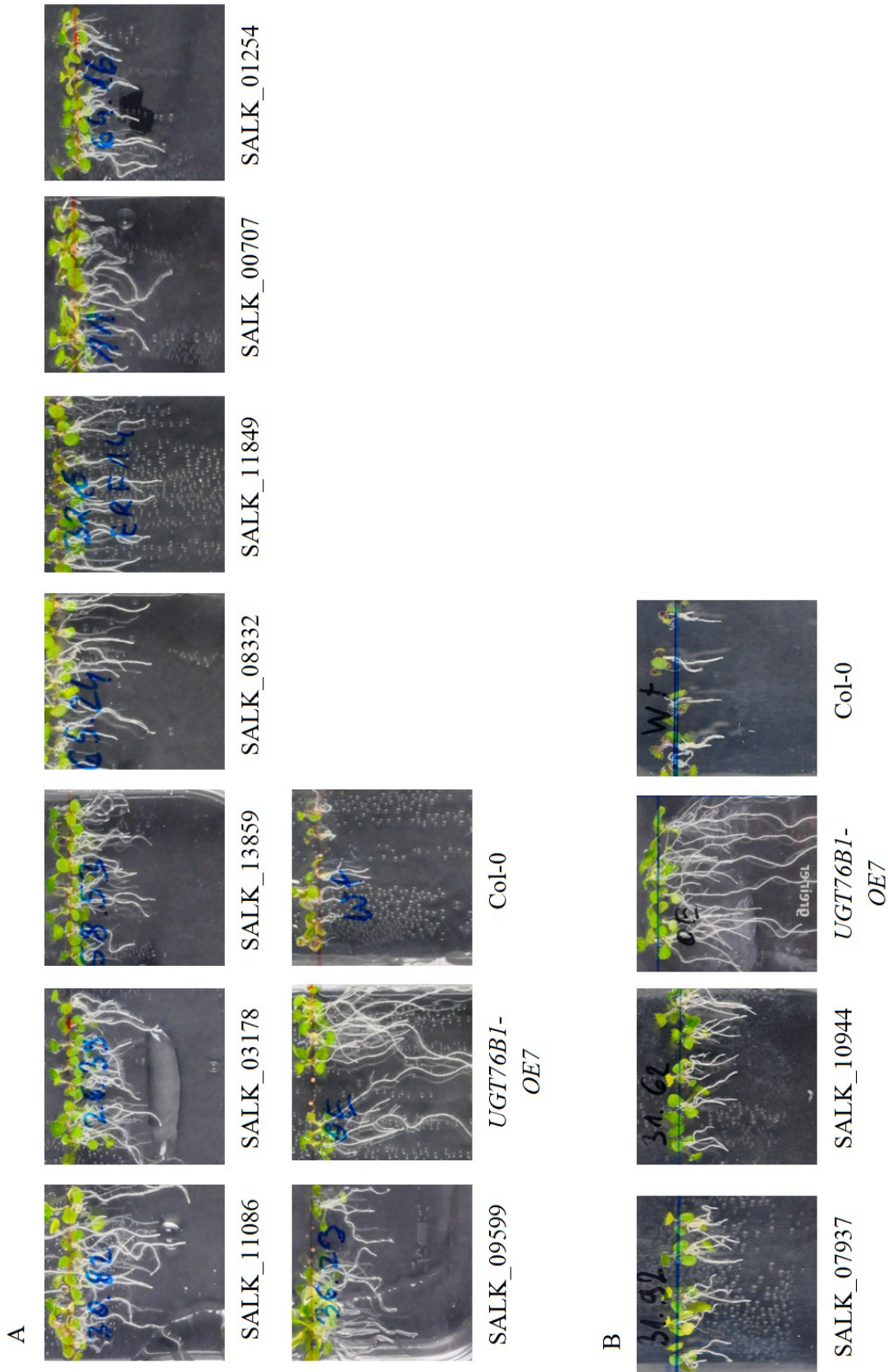
Supplementary Figure 8. Alignment of SRX CDS in ILA top resistant (+) and top susceptible (-) *Arabidopsis* accessions.

Figure continues on the next page.



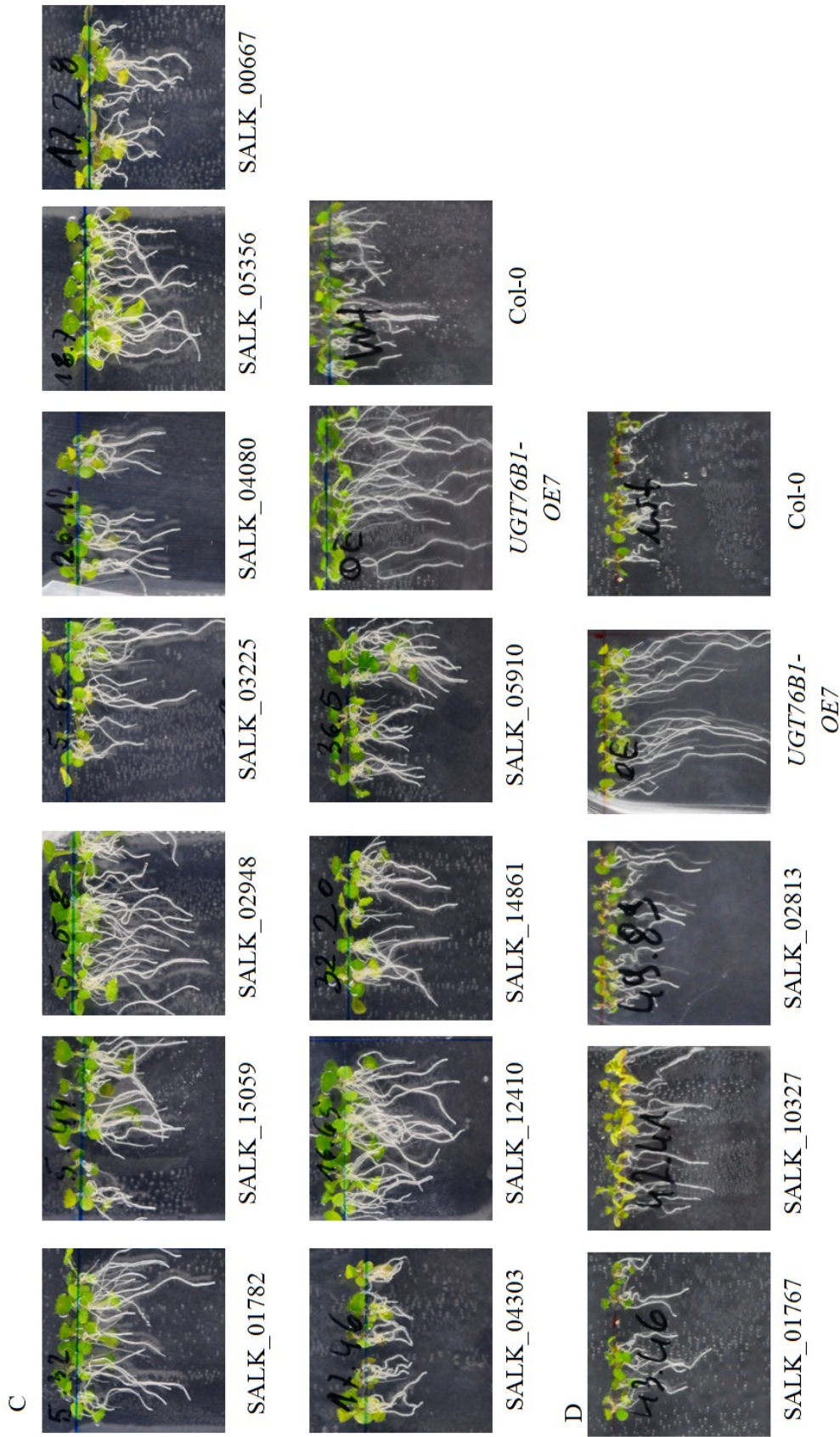
Supplementary Figure 8. Alignment of SRX CDS in ILA top resistant (+) and top susceptible (-) *Arabidopsis* accessions.

The donor splice site marked by the red line is lost due to an A to G substitution (SNP marked with red arrow) in ILA-hypersensitive accessions. Sequences derived from: <http://1001genomes.org> (02/2016).



Supplementary Figure 9. T-DANA insertion lines displaying enhanced root growth resistance in presence of ILA.

Figure continues on the next page.



Supplementary Figure 9. T-DANA insertion lines displaying enhanced root growth resistance in presence of ILA.

Plants have been grown for 10 days in long day conditions (16 h light, 8 h darkness). A, B, C and D were grown separately.

6.2. Supplementary tables**Supplementary Table 1. Swedish *Arabidopsis thaliana* accessions applied in ILA GWAS.**

9454	6174	6092	6913	6145	6077
6200	8256	8306	992	5832	6041
7518	8257	9371	9412	9471	6128
6189	9434	6108	6193	6070	6124
6184	9395	6201	6074	6137	6099
6019	6241	1066	6024	6107	6097
6188	9399	6284	6034	6064	6258
9455	6085	7517	6276	6042	6113
8326	6220	6020	6039	9427	6138
9453	8259	6240	6172	6069	6125
7519	6177	6268	6016	5856	6900
5830	6244	8247	9409	6043	991
6191	6012	6207	6088	5835	6136
6171	6112	9386	6202	9382	6100
6021	1002	6106	8241	6017	6025
9442	6133	6103	6142	6095	6040
9390	5860	6111	6255	997	
9394	6009	6198	8240	6218	
9391	8334	6194	9321	6132	
9470	6974	6199	6126	9476	
6917	8335	6038	5831	6104	
6209	6196	6238	6036	6093	
6203	6231	8249	8351	1435	
6192	6013	8237	6105	6217	
8283	6109	6091	6023	6046	
9433	5865	6096	6098	6115	
6197	8222	6173	6076	6965	
6210	6030	9450	7516	6071	
8369	6180	9421	9388	8231	

Supplementary Table 2. T-DNA insertion mutant lines potentially displaying hypersensitivity to ILA

SALK	AGI	SALK	AGI	SALK	AGI
SALK_000249C	At1g07890	SALK_033423C	At5g49020	SALK_064186C	At3g48180
SALK_000367C	At5g01820	SALK_034227C	At4g30114	SALK_064669C	At2g47540
SALK_000530C	At3g50800	SALK_034800C	At3g55390	SALK_064732C	At5g38150
SALK_001042C	At3g06710	SALK_035104C	At1g13350	SALK_065212C	At5g51510
SALK_001747C	At3g46010	SALK_035238C	At1g68300	SALK_065234C	At5g51130
SALK_003157C	At1g74130	SALK_035324C	At4g18870	SALK_065256C	At1g47128
SALK_003804C	At4g38890	SALK_035445C	At1g18510	SALK_065629C	At1g54510
SALK_003883C	At1g66420	SALK_035886C	At3g28060	SALK_065650C	At1g80490
SALK_004253C	At1g16670	SALK_036004C	At5g37310	SALK_066102C	At4g10400
SALK_006273C	At3g01910	SALK_036544C	At2g33700	SALK_066772C	At4g07915
SALK_006655C	At2g41750	SALK_036910C	At5g24560	SALK_067488C	At5g11820
SALK_007024C	At1g02030	SALK_036979C	At1g41830	SALK_067822C	At2g34730
SALK_007906C	At3g02840	SALK_037371C	At3g61755	SALK_067877C	At5g43455
SALK_008062C	At5g66830	SALK_037550C	At1g78550	SALK_069028C	At5g58990
SALK_008085C	At3g14280	SALK_037627C	At5g12250	SALK_069063C	At5g07820
SALK_008317C	At2g47580	SALK_038523C	At3g20720	SALK_069233C	At4g31680
SALK_008405C	At1g18740	SALK_039003C	At5g01240	SALK_069238C	At1g33110
SALK_008493C	At1g68250	SALK_039033C	At1g22870	SALK_069269C	At1g27320
SALK_008838C	At5g53580	SALK_039183C	At5g21105	SALK_069400C	At1g26190
SALK_009125C	At3g48810	SALK_039514C	At3g02130	SALK_069836C	At1g74210
SALK_009149C	At5g35775	SALK_039832C	At5g23700	SALK_069877C	At4g05050
SALK_009391C	At2g05180	SALK_040835C	At2g34600	SALK_070184C	At3g13330
SALK_009465C	At2g03020	SALK_040854C	At3g23605	SALK_070274C	At4g34400
SALK_009878C	At1g52760	SALK_040891C	At3g22800	SALK_070460C	At5g52950
SALK_010008C	At3g29783	SALK_041347C	At1g67590	SALK_071907C	At2g27820
SALK_010265C	At3g14230	SALK_043616C	At3g22270	SALK_071912C	At5g55570
SALK_010511C	At1g60720	SALK_043730C	At3g28330	SALK_072620C	At1g51750
SALK_010530C	At5g04870	SALK_043961C	At3g11960	SALK_077992C	At3g20362
SALK_010618C	At1g15470	SALK_044163C	At5g03360	SALK_078416C	At2g06255
SALK_010841C	At5g65530	SALK_044797C	At1g18270	SALK_080084C	At5g08580
SALK_010888C	At3g52690	SALK_045940C	At2g28755	SALK_080608C	At2g30140
SALK_010950C	At3g54130	SALK_045948C	At4g35560	SALK_081039C	At5g25850
SALK_011108C	At2g34040	SALK_046119C	At3g25815	SALK_082100C	At1g25320
SALK_011550C	At5g51230	SALK_046165C	At1g73030	SALK_083956C	At4g30133
SALK_011710C	At1g57610	SALK_046205C	At1g03850	SALK_084311C	At4g12990
SALK_011759C	At3g46340	SALK_046451C	At5g42580	SALK_085128C	At4g23210
SALK_011827C	At1g79290	SALK_046588C	At1g13100	SALK_085485C	At2g46440
SALK_011936C	At3g57940	SALK_046603C	At3g56600	SALK_085886C	At2g13570
SALK_012262C	At1g80930	SALK_046958C	At3g10970	SALK_086040C	At5g49050
SALK_012348C	At2g04850	SALK_047091C	At5g20500	SALK_086334C	At3g48590
SALK_012400C	At1g01220	SALK_047200C	At4g04320	SALK_087920C	At5g41910
SALK_012785C	At5g50970	SALK_047534C	At4g39770	SALK_088268C	At1g62430
SALK_012999C	At3g43980	SALK_047797C	At3g21220	SALK_088794C	At4g03500

SALK_013382C	At3g48260	SALK_048079C	At5g54480	SALK_089247C	At3g20865
SALK_013546C	At5g54050	SALK_048133C	At2g38330	SALK_089339C	At1g64350
SALK_014672C	At3g20880	SALK_048602C	At3g53290	SALK_091788C	At3g05525
SALK_015013C	At2g35780	SALK_049965C	At4g17660	SALK_092827C	At2g20010
SALK_015148C	At1g21360	SALK_050231C	At5g62290	SALK_094902C	At5g48680
SALK_015316C	At1g09910	SALK_051265C	At5g60050	SALK_095050C	At1g69020
SALK_015367C	At2g46280	SALK_051316C	At3g13772	SALK_095319C	At1g01960
SALK_016021C	At3g42950	SALK_052079C	At5g17000	SALK_097030C	At1g64490
SALK_016833C	At3g26618	SALK_052138C	At3g53440	SALK_097684C	At3g43670
SALK_017141C	At2g33190	SALK_052305C	At1g75090	SALK_097966C	At5g21960
SALK_017328C	At1g20020	SALK_052447C	At5g03390	SALK_098040C	At1g55680
SALK_018556C	At3g14810	SALK_052517C	At5g58840	SALK_098268C	At4g25070
SALK_018646C	At5g11230	SALK_052654C	At2g46915	SALK_098692C	At2g26900
SALK_018685C	At2g33690	SALK_052716C	At2g14210	SALK_099609C	At3g08690
SALK_019269C	At2g39310	SALK_052903C	At4g22850	SALK_102818C	At5g14890
SALK_020176C	At5g54890	SALK_054406C	At4g38530	SALK_102948C	At1g67420
SALK_020228C	At1g78440	SALK_055070C	At3g44510	SALK_102963C	At5g01450
SALK_020615C	At1g76470	SALK_055217C	At5g43720	SALK_103014C	At1g13980
SALK_020677C	At1g10240	SALK_057261C	At2g19100	SALK_103197C	At5g04700
SALK_020715C	At4g28160	SALK_057940C	At2g41310	SALK_104064C	At1g17070
SALK_021102C	At1g73010	SALK_057946C	At5g30942	SALK_105035C	At1g80610
SALK_022075C	At3g43170	SALK_058186C	At2g05510	SALK_109713C	At3g23910
SALK_022202C	At4g37120	SALK_058192C	At5g55060	SALK_112197C	At5g14920
SALK_022225C	At1g54790	SALK_058483C	At1g78740	SALK_112932C	At5g37930
SALK_022332C	At1g80940	SALK_058561C	At2g41090	SALK_116386C	At2g42640
SALK_022386C	At1g19480	SALK_058794C	At4g16370	SALK_116446C	At4g12570
SALK_022761C	At1g71691	SALK_058830C	At2g35260	SALK_118463C	At5g60850
SALK_022809C	At4g04316	SALK_059037C	At5g63890	SALK_119578C	At5g41520
SALK_023405C	At5g45680	SALK_059074C	At5g03780	SALK_122773C	At1g10090
SALK_023536C	At3g05280	SALK_059126C	At4g02850	SALK_123333C	At1g09010
SALK_023539C	At2g47830	SALK_059522C	At5g04900	SALK_124018C	At1g54770
SALK_024562C	At3g22050	SALK_059655C	At4g01740	SALK_129866C	At3g49960
SALK_025015C	At5g46850	SALK_059700C	At2g34320	SALK_130453C	At1g73240
SALK_025605C	At5g43740	SALK_059858C	At1g04860	SALK_131190C	At1g24420
SALK_025828C	At5g09280	SALK_059958C	At5g41850	SALK_134892C	At1g47310
SALK_026259C	At5g41360	SALK_059964C	At5g37170	SALK_134900C	At4g20700
SALK_026410C	At2g36820	SALK_059964C	At5g37170	SALK_136473C	At2g15840
SALK_026445C	At2g46225	SALK_060204C	At3g42233	SALK_136500C	At1g26200
SALK_026573C	At5g28076	SALK_060776C	At5g12900	SALK_136638C	At3g55290
SALK_026818C	At3g26610	SALK_061305C	At2g35950	SALK_137002C	At5g07740
SALK_027524C	At5g53810	SALK_061309C	At3g29260	SALK_137325C	At5g59830
SALK_027592C	At1g61260	SALK_061391C	At2g36240	SALK_139000C	At2g44800
SALK_027748C	At2g46650	SALK_062605C	At5g47550	SALK_139302C	At1g67890
SALK_028517C	At3g53830	SALK_062797C	At3g29280	SALK_139817C	At1g41710
SALK_029854C	At5g66970	SALK_062905C	At5g03435	SALK_140141C	At1g80210
SALK_029864C	At3g51740	SALK_063109C	At1g16430	SALK_140584C	At4g25120
SALK_031006C	At5g06690	SALK_063355C	At1g49710	SALK_141481C	At1g77570

CURRICULUM VITAE

RAFAŁ PAWEŁ MAKSYM

Date of birth 25th April 1985
Place of birth Gorzów Wielkopolski, Poland
Nationality Poland

Education

- 11/2011 - 02/2018 Ph.D. candidate in Biochemistry**
Ludwig-Maximilians-University, Munich, Germany
Faculty of Chemistry and Pharmacy
Advisor: PD Dr. Anton R. Schäffner, Helmholtz Zentrum München,
Institute for Biochemical Plant Pathology
Research topic: *Arabidopsis* small molecule glucosyltransferase UGT76B1
conjugates both ILA and SA and is essential for the root-driven control of
defense marker genes in leaves
- 11/2011 - 02/2016 HELENA - Helmholtz Graduate School Environmental Health**
- 02/2008 - 06/2008 Semester abroad**
University of Natural Resources and Life Sciences (BOKU), Vienna, Austria
Department of Biotechnology
- 10/2004 - 12/2009 M.Sc. in Biotechnology**
Poznań University of Life Sciences, Poznań, Poland
Faculty of Agronomy
Research topic: Changes induced by abiotic stress in *Nicotiana tabacum*
transcriptome – studies involving cross species hybridization

Research experience

- 01/2010 - 09/2011 Research Assistant**
Institute of Bioorganic Chemistry, Polish Academy of Sciences, Poznań, Poland
- 10/2008 - 12/2009 Research Assistant (Master's thesis project)**
Institute of Bioorganic Chemistry, Polish Academy of Sciences, Poznań, Poland
- 07/2008 - 08/2008 Research Internship**
University of Natural Resources and Life Sciences (BOKU), Vienna, Austria
Department of Agrobiotechnology IFA- Tulln
- 04/2007 - 01/2008 Research Internship**
Centre of Excellence for Nucleic Acid-based Technologies, Institute of Bioorganic Chemistry, Polish Academy of Sciences, Poznań, Poland

Contributions to Scientific Conferences

- 09/2015** **Botaniker Tagung 2015, Freising, Germany**
Presented poster: UGT76B1 and its substrate isoleucic acid (ILA) impact plant defense
- 07/2014** **5th plant NO club meeting, Munich, Germany**
- 03/2014** **Tagung Molekularbiologie der Pflanzen, Dabringshausen, Germany**
Given talk: The small molecule glucosyltransferase UGT76B1 and its substrate isoleucic acid modulates plant pathogen defense

Training

- 09/2016 - 02/2017** Additional qualification in Life Science Management
- 10/2014** Career Opportunities in Biotechnology and Drug Development
- 10/2012 - 12/2012** Professional Discussions in English
- 03/2012 - 04/2012** English for Science and the Laboratory

Scholarships

- 02/2008-06/2008** Socrates/Erasmus Scholarship, University of Natural Resources and Life Sciences (BOKU), Vienna, Austria

Publications

Maksym R. P., Ghirardo A., Zhang W., von Saint Paul V., Lange B., Geist B., Hajirezaei M. R., Schnitzler J. P., Schäffner A. R. (2018). The Defense-Related Isoleucic Acid Differentially Accumulates in *Arabidopsis* Among Branched-Chain Amino Acid-Related 2-Hydroxy Carboxylic Acids. *Front. Plant Sci.* 9: 766

ACKNOWLEDGEMENTS

Firstly, I would like to express my sincere gratitude to my advisor PD Dr. Anton Schäffner for the excellent guidance and continuous support during my PhD study, for his patience, constitutive criticism and careful correction of this thesis. Moreover, his impressive knowledge and scientific enthusiasm inspired me a lot and encouraged me to overcome any difficulties during preparation of this thesis.

I would like to especially acknowledge Prof. Dr. Jörg Durner, my external advisor PD Dr. Dietmar Martin and the members of the examination committee for their willingness to review this work. I am very grateful to Prof. Durner for valuable advices to my projects during the institute seminars and thesis committee meetings.

I would like to give my sincere thanks to Prof. Dr. Jörg-Peter Schnitzler and Dr. Andrea Ghirardo (Research Unit Environmental Simulation, Helmholtz Zentrum München) for providing me the access to the GC-MS instrument. I am indebted to Dr. Andrea Ghirardo for the time-consuming analysis of GC-MS data and optimization of the method. This project would not have been successfully finished without his broad analytical knowledge. I would like to thank Dr. Alexander Christmann (WZW TUM, Freising) for demonstrating how to successfully graft *Arabidopsis* seedlings. I am deeply thankful to Dr. Veronica von Saint Paul and Dr. Wei Zhang for introducing me the UGT76B1 project. Here, I am especially grateful to Dr. Wei Zhang for the guidance and advices during my almost whole work on UGT76B1. I would also like to acknowledge Lucia Gößl for her kind help performing SA and SA glucose conjugates measurements. I am also very grateful to Dr. Elisabeth Georgii for statistical analyses and statistical advices. Birgit Geist and Birgit Lange contributed crucial support in different laboratory issues and advice. Furthermore, I would like to thank Dr. Arthur Korte (GMI Vienna, Austria) for analyzing GWAS data. My thanks are also extended to Eva Rudolf for helping me with modeling of the 3D structure of UGT76B1, as well as Dr. Inonge Gross and Dr. Felicitas Mengel for providing me plant material for GC-MS measurements. Appreciation goes to Dr. Corina Vlot Schuster's group for providing bacterial strains for infection experiments. Moreover, I am really grateful to Evie Bieber for her help during formatting this document.

I wish to extend my sincere gratitude to current and former members of Anton Schäffner's group: Dr. Chen Liu, Dr. Wei Zhang, Dr. Veronica von Saint Paul, Dr. Jin Zhao, Dr. Ming Jin, Dr. Stephan Dräxl, Dr. Malay Das, Dr. Andre Schmiesing, Jessica Lutterbach and Sibylle Bauer. I am really grateful to Dr. Chen Liu for our not only scientific discussions on the way

to the institute and for her great contribution in teaching me Chinese. I would also like to thank my closest neighbours in the office, Dr. Jin Zhao and Dr. Ming Jin for many scientific advices, great atmosphere and borrowing me different items. I am also thankful to Dr. Stephan Dräxl and Dr. Malay Das for excellent advices and interesting scientific and non-scientific discussions. Many thanks to Sibylle Bauer for providing her kind help at the end of my PhD work and for continuing with a great passion some of the projects I have been working on.

I am also deeply thankful to all my colleagues from BIOP and EUS, including: Dr. Werner Heller, Dr. Feng Zhao, Dr. Jeremy Astier, PD Dr. Frank Gaupels, Dr. Christian Lindermayr, Dr. Alexander Mengel, Dr. Katharina Kempkens, Dr. Sanjukta Dey-Irmler, Dr. Finni Häußler, Dr. Ulrike Frank, Dr. Marlies Bichlmeier, Dr. Izabella Kovacs, Dr. Azam Shekariesfahlan, Dr. Izabella Kovacs, Dr. Antonie Bernhard, Dr. Areli Herrera Diaz, Dr. Christian Holzmeister, Dr. Barbro Winkler, Dr. Andreas Albert, Dr. Gitto Kuruthukulangarakoola, Alexandra Ageeva-Kieferle, Elisabeth Pabst, Dörte Mayer, Mary Clancy, Jiangli Zhang, Karoline Stoll, Rosina Ludwig, Elke Mattes, Claudia Knappe, Marion Wenig, Elke Gerstner, Armin Richter, Peter Kary, and all others.

Finally, I want to thank my parents: Hanna, Robert Maksym and grandparents: Barbara, Ludwik Maksym; Teresa, Stanisław Miziniak for their endless support during the last few years. Special thanks also to all my friends here in Germany and in Poland.